Upper Santa Ana River Integrated Model
Summary Report

Part 1 of 5: Text

DRAFT

Prepared For: San Bernardino Valley Municipal Water District

April 29, 2020

GEOSCIENCE Support Services, Inc. | P (909) 451-6650 | F (909) 451-6638
620 Arrow Highway, Suite 2000, La Verne, CA 91750 | Mailing: P.O. Box 220, Claremont, CA 91711
www.gssiwater.com

GEOSCIENCE

THIS REPORT IS RENDERED TO SAN BERNARDINO VALLEY MUNICIPAL WATER DISTRICT AS OF THE DATE HEREOF, SOLELY FOR THEIR BENEFIT IN CONNECTION WITH ITS STATED PURPOSE AND MAY NOT BE RELIED ON BY ANY OTHER PERSON OR ENTITY OR BY THEM IN ANY OTHER CONTEXT. AS DATA IS UPDATED FROM TIME TO TIME, ANY RELIANCE ON THIS REPORT AT A FUTURE DATE SHOULD TAKE INTO ACCOUNT UPDATED DATA.

THIS DOCUMENT HAS BEEN CHECKED FOR COMPLETENESS, ACCURACY, AND CONSISTENCY BY THE FOLLOWING PROFESSIONALS:

____

David Barnes, M.Eng.
Senior Modeler

____

Johnson Yeh, Ph.D., PG, CHG
Principal
CHG No. 422

____

Dennis E. Williams, Ph.D., PG, CHG
President
CHG No. 139

UPPER SANTA ANA RIVER INTEGRATED MODEL

SUMMARY REPORT

CONTENTS

FIGURES

No.	Description	Page
(Inset in Text)		

FIGURES (continued)

FIGURES (continued)

FIGURES (continued)

FIGURES (continued)

FIGURES (continued)

FIGURES (continued)

FIGURES (continued)

FIGURES (continued)

FIGURES (continued)

FIGURES (continued)

FIGURES (continued)

FIGURES (continued)

FIGURES (continued)

FIGURES (continued)

No.	Description
(Attached)	

FIGURES (continued)

FIGURES (continued)

FIGURES (continued)

No.	Description
(Attached)	

FIGURES (continued)

FIGURES (continued)

FIGURES (continued)

FIGURES (continued)

FIGURES (continued)

FIGURES (continued)

FIGURES (continued)

FIGURES (continued)

FIGURES (continued)

FIGURES (continued)

FIGURES (continued)

FIGURES (continued)

FIGURES (continued)

FIGURES (continued)

FIGURES (continued)

FIGURES (continued)

FIGURES (continued)

FIGURES (continued)

FIGURES (continued)

FIGURES (continued)

FIGURES (continued)

FIGURES (continued)

FIGURES (continued)

FIGURES (continued)

FIGURES (continued)

FIGURES (continued)

FIGURES (continued)

FIGURES (continued)

FIGURES (continued)

FIGURES (continued)

FIGURES (continued)

FIGURES (continued)

FIGURES (continued)

FIGURES (continued)

FIGURES (continued)

FIGURES (continued)

FIGURES (continued)

FIGURES (continued)

No.	Description
(Attached)	

TABLES

TABLES (continued)

No. **Description** **Page**

(Inset in Text)

TABLES (continued)

No. *(Inset in Text)*	Description	Page

TABLES (continued)

TABLES (continued)

TABLES (continued)

TABLES (continued)

APPENDICES

Ltr.	Description
(Attached)	
A	Comments and Responses on Draft Technical Memoranda and Model Calibration
B	Database Plan (GEOSCIENCE, March 21, 2018)
C	Meeting Minutes
D	Riparian Vegetation Mapping and Consumptive Water Use – Riparian Subcommittee Meeting Presentation Slides by Aspen Environmental Group (February 7, 2018)
E	Shallow Groundwater and Evapotranspiration Assessment – Riparian Subcommittee Meeting Presentation Slides by Balleau Groundwater, Inc. (February 7, 2018)
F	Evapotranspiration Estimates by Aspen Environmental Group (Draft, December 7, 2017)
G	Technical Memorandum Summarizing the Development of a Unified Upper Santa Ana River Basin Conceptual and Lithologic Model via Integration of Existing Sub-Basin Models (Numeric Solutions, Draft dated March 16, 2018)
H	Individual Model Update: Selected Hydrographs for the Yucaipa Basin Model Calibration Target Wells – 1966 to 2016
I	Individual Model Update: Selected Hydrographs for the San Bernardino Basin Area Model Calibration Target Wells – 1966 to 2016
J	Individual Model Update: Selected Hydrographs for the Rialto-Colton Basin Model Calibration Target Wells – 1966 to 2016
K	Individual Model Update: Selected Hydrographs for the Riverside-Arlington Basin Model Calibration Target Wells – 1966 to 2016
L	Individual Model Update: Selected Hydrographs for the Chino Basin Model Calibration Target Wells – 1966 to 2016
M	Integrated SAR Model: Selected Hydrographs for Target Wells in the Yucaipa Basin Model Area – 1966 to 2016

APPENDICES (continued)

Ltr.	Description
(Attached)	
N	Integrated SAR Model: Selected Hydrographs for Target Wells in the San Bernardino Basin Model Area – 1966 to 2016
O	Integrated SAR Model: Selected Hydrographs for Target Wells in the Rialto-Colton Basin Model Area – 1966 to 2016
P	Integrated SAR Model: Selected Hydrographs for Target Wells in the Riverside-Arlington Basin Model Area – 1966 to 2016
Q	Integrated SAR Model: Selected Hydrographs for Target Wells in the Chino Basin Model Area – 1966 to 2016
R	Riverside North Aquifer Storage & Recovery – Operation & Maintenance Model Technical Memorandum (Draft) by Scheevel Engineering (dated December 16, 2018)
S	Groundwater Level Hydrographs along the Santa Ana River – Scenario Runs

ACRONYMS AND ABBREVIATIONS

Abbrev.	Description
acre-ft/yr	acre-feet per year
amsl	above mean sea level
Aspen	Aspen Environmental Group
BGW	Balleau Groundwater, Inc.
CDA	Chino Basin Desalter Authority
CDFW	California Department of Fish and Wildlife
cfs	cubic feet per second
CGS	California Geological Survey
CIMIS	California Irrigation Management Information System
DEM	digital elevation model
DOGGR	State of California Department of Oil and Gas and Geothermal Resources
DWR	State of California Department of Water Resources
EMWD	Eastern Municipal Water District
ET	evapotranspiration
ETo	reference evapotranspiration
EVMWD	Elsinore Valley Municipal Water District
EROS	Earth Resources Observation and Science
ESPA	EROS Science Processing Architecture
ft	feet

ACRONYMS AND ABBREVIATIONS (continued)

Abbrev.	Description
FTABLE	function table
Geo-Logic	Geo-Logic Associates
GEOSCIENCE	GEOSCIENCE Support Services, Inc.
HCP	Habitat Conservation Plan
HSPF	Hydrological Simulation Program – Fortran
IEUA	Inland Empire Utilities Agency
Integrated SAR Model	Upper Santa Ana River Integrated Model
JCSD	Jurupa Community Services District
ka	thousand years ago
LLWD	Lee Lake Water District
Ma	million years ago
OBMP	Chino Basin Optimum Basin Management Program
OCWD	Orange County Water District
OSR	Operational Storage Requirement
R^2	coefficient of determination
RBFM/NGFM	Refined Basin Flow Model/Newmark Groundwater Flow Model (also known as the SBBA Model)
RIX	Rapid Infiltration and Extraction
RP	regional plant
RPU	Riverside Public Utilities

ACRONYMS AND ABBREVIATIONS (continued)

Abbrev.	Description
RWAP	regional wastewater authority plant
RWQCP	regional water quality control plant
SAR	Santa Ana River
SAWPA	Santa Ana Watershed Project Authority
SBBA	San Bernardino Basin Area (includes the Bunker Hill and Lytle Groundwater Basins)
SCAG	Southern California Association of Governments
SMWC	South Mesa Water Company
SSC	Safe Storage Capacity
SSEBop	Simplified Surface Energy Balance
SSURGO	Soil Survey Geographic
SWM	Stanford Watershed Model
TAC	Technical Advisory Committee
TM	technical memorandum
UCR	University of California, Riverside
USACE	United States Army Corps of Engineers
USEPA	United States Environmental Protection Agency
USFWS	United States Fish and Wildlife Service
USGS	United States Geological Survey
Valley District	San Bernardino Valley Municipal Water District

ACRONYMS AND ABBREVIATIONS (continued)

Abbrev.	Description
WEI	Wildermuth Environmental, Inc.
Western	Western Municipal Water District
WHWC	Western Heights Water Company
WLAM	Waste Load Allocation Model
WRF	water recycling facility
WRP	water reclamation plant
WVWD	West Valley Water District
WWRF	wastewater reclamation facility
WWTP	wastewater treatment plant
YVWD	Yucaipa Valley Water District

UPPER SANTA ANA RIVER INTEGRATED MODEL

SUMMARY REPORT

1.0 EXECUTIVE SUMMARY

1.1 Introduction

GEOSCIENCE Support Services, Inc. (GEOSCIENCE) was tasked with constructing a groundwater flow model for the Upper Santa Ana Valley Groundwater Basin by integrating existing groundwater and surface water models. This model, known as the Integrated SAR Model, was used as a management tool to determine what factors contribute to reduced streamflow in the SAR, and to evaluate potential effects from proposed projects on streamflow and groundwater levels across the basin, including Upper SAR Habitat Conservation Plan (HCP) “Covered Activities”.

The development of the Integrated SAR Model represents a cooperative technical effort involving:

- Representatives of participating parties, including Valley District, Western, IEUA, OCWD, RPU, USGS, USFWS, and the CDFW;
- Representatives of participating parties’ consultants Aspen Environmental Group (Aspen), GEOSCIENCE, Leidos, and Numeric Solutions;
- Technical advisors representing the Balleau Groundwater, Inc. (BGW), Chino Basin Watermaster, ICF, the Santa Ana Regional Water Quality Control Board, the Santa Ana Watershed Project Authority (SAWPA), University of California, Riverside (UCR), U.S. Army Corps of Engineers (USACE), and Wildermuth Environmental, Inc. (WEI).

Collectively, this group represents the Technical Advisory Committee (TAC). Collaboration by these representatives to develop the Integrated SAR Model was achieved through participation at project conference calls, model workshops, and by reviewing and commenting on draft technical memoranda and model files. During the course of this project, individual tasks were summarized in several technical memorandums (TMs). Each draft TM was submitted to the Technical Advisory Committee (TAC) for comment and review. This Summary Report incorporates the material from all previously issued TMs and TAC comments.

Previous groundwater models that were used as a basis for the Integrated SAR Model are the:

- Yucaipa Groundwater Model (GEOSCIENCE, 2017),
- Refined Basin Flow Model/Newmark Groundwater Flow Model (RBFM/NGFM) for the SBBA (GEOSCIENCE, 2009; GEOSCIENCE and Stantec, in progress),
- Rialto-Colton Groundwater Model (GEOSCIENCE, 2015),
- Riverside-Arlington Groundwater Model (WRIME, 2010), and
- Chino Basin Model (WEI, 2015; reconstructed by GEOSCIENCE for this project).

The process of updating and integrating the existing models was summarized in TM No. 1: Model Integration (GEOSCIENCE, 2018a) and is included here as Section 5.0. Since model files were not available for the WEI Chino Basin Model, GEOSCIENCE constructed a separate version of the model based on the approach and data presented in WEI's modeling report (2015). This is discussed in Section 6.0.

Existing watershed models include the:

- Wasteload Allocation Model (WEI, 2009),
- SBBA Riverside Basin Watershed Model (GEOSCIENCE, 2013),
- Yucaipa Watershed Model (GEOSCIENCE, 2014), and
- Wasteload Allocation Model Update (GEOSCIENCE, 2019e).

A watershed model for the Upper SAR Watershed was developed and calibrated from 1966 through 2016 to simulate runoff generated within the watershed and quantify runoff for the Integrated SAR Model (Section 7.0).

Development and calibration of the Integrated SAR Model is discussed in Sections 8.0 and 9.0, respectively. Following model calibration, scenario runs were developed and conducted to assess the hydrologic response of the Upper SAR to various project activities, as presented in Section 10.0. Sections 11.0 and 12.0 of this Summary Report discuss uses and limitations of the Integrated SAR Model, as well as future work.

1.2 Conceptual Model of the Integrated SAR Model

The Upper Santa Ana Valley Groundwater Basin incorporates the Yucaipa, SBBA, Rialto-Colton, Riverside-Arlington, Chino, and Temescal Groundwater Basins. In general, the conceptual geologic models for the six groundwater basins within the Upper Santa Ana Valley Groundwater Basin are similar with respect to the geologic materials present, with minor variations. With respect to geologic history, the Yucaipa, SBBA, and Rialto-Colton basins share similar and overlapping depositional histories due to local tectonics associated with movement along the San Jacinto, San Andreas, and associated faults. Likewise, the Riverside-Arlington, Temescal, and Chino Basins share similar geologic histories. The geologic conceptual model forms the basis for the hydrogeologic conceptual model, which in turn informed the construction of the numerical Integrated SAR Model for the simulation of groundwater flow through the geologic formations.

In order to integrate the existing groundwater models, it was necessary to review the individual conceptual models and identify similarities and differences. It was also necessary to develop an approach for extending model layers – representing geologic units – across existing model boundaries. The hydrogeologic conceptual model provided a framework for identifying geologic units within the Integrated SAR Model domain, identifying sources of inflow and outflow to the groundwater systems, and correlating hydrogeologic units (model layers) between groundwater basins. The hydrogeologic conceptual model of the Integrated SAR Model domain, in combination with the three-dimensional (3-D) lithologic model that was developed for the Integrated SAR Model area, was used to delineate and assign model layers.

1.3 Update of Existing Groundwater Models

Model integration involved updating the existing groundwater flow models (i.e., Yucaipa, SBBA, Rialto-Colton, and Riverside-Arlington Models) with the appropriate resolution, or cell size, and orientation to match that of the Integrated SAR Model. The existing groundwater flow models were also updated so that the hydrologic data covered the model calibration period from January 1966 through December 2016. To complete the model integration process, the unified model layers were applied to the updated groundwater flow models. The individual models were then rerun within the Integrated SAR Model grid to ensure the updated results were consistent with the original existing models. Next, the specified underflow boundary conditions in the individual models were removed and the Integrated SAR Model was run and calibrated without specific underflow across basin boundaries (underflow inflow and outflow across existing model boundaries are simulated by the Integrated SAR Model).

1.4 Construction and Calibration of the Chino Basin Model

In the Chino Basin area of the Integrated SAR Model, existing model files were unavailable. Therefore, a separate version of the Chino Basin Model was constructed and calibrated in the Integrated SAR Model grid. Construction was initially based on available data presented in WEI's model report (2015), but the Chino Basin Model presented herein does differ from the WEI model. Some model parameters and fluxes were developed using different approaches and model parameters were refined through model calibration.

1.4.1 Chino Basin Model Initial Calibration Results

During the Chino Basin Model calibration, model parameters were manually adjusted within acceptable limits until model-generated water levels match historical water level measurements at wells across the model area, thereby reducing residual error. The Chino Basin Model was calibrated using this industry standard "history matching" technique for the period from January 1966 through December 2016. The calibration process used 523,086 water level measurements from 115 calibration target wells from which to match model generated head values against the measured values. Aquifer parameters varied during the model calibration included horizontal and vertical hydraulic conductivity, specific yield, specific storage, horizontal flow barrier conductance, and streambed conductance.

1.5 Upper Santa Ana River Watershed Model

In order to simulate the streamflow more accurately, runoff generated from precipitation within the Upper Santa Ana Valley Groundwater Basin was calculated using a watershed model, which was then included in the Streamflow Package for the Integrated SAR Model. The Upper SAR Watershed Model was developed for the Santa Ana Watershed Project Authority (SAWPA) during the SAR Waste Load Allocation Model (WLAM) Update using the Hydrologic Simulation Program - Fortran (HSPF) computer code (GEOSCIENCE, 2019e). This watershed model was calibrated for the period from October 1, 2006 through September 30, 2016 (Water Year 2007 through 2016) using 2012 land use. For the Integrated SAR Model, the watershed model calibration period was expanded to include the period from January 1966 through December 2016 with additional land use maps from 1963, 1984, 1994, and 2005.

1.5.1 Watershed Model Calibration

The model was calibrated against measured streamflow for the period from January 1, 1966 through December 31, 2016. Streamflow data from three major gaging stations along the SAR were used during the calibration process, including:

- Santa Ana River at E Street,
- Santa Ana River at MWD Crossing, and
- Santa Ana River into Prado Dam.

The results of the Upper SAR Watershed Model calibration are summarized in the following tables.

Table 1-1. Summary of Upper SAR Watershed Model Results – Daily Simulated Streamflow Performance

Gaging Station	Avg. Observed Flow [cfs]	Avg. Model-Simulated Flow [cfs]	Mean Residual [cfs]	Mean Residual as % of Avg. Observed Flow	R^2	Performance
Santa Ana River at E Street	75.4	82.7	-8.2	-11%	0.78	Good
Santa Ana River at MWD Crossing	130.5	133.3	2.1	2%	0.74	Good
Santa Ana River into Prado Dam	273.0	262.7	10.3	4%	0.85	Very Good

Table 1-2. Summary of Upper SAR Watershed Model Results – Monthly Simulated Streamflow Performance

Gaging Station	Avg. Observed Flow [cfs]	Avg. Model-Simulated Flow [cfs]	Mean Residual [cfs]	Mean Residual as % of Avg. Observed Flow	R^2	Performance
Santa Ana River at E Street	75.9	83.3	-8.4	-11%	0.84	Good
Santa Ana River at MWD Crossing	130.5	134.2	1.8	1%	0.85	Very Good
Santa Ana River into Prado Dam	274.7	264.3	10.4	4%	0.94	Very Good

As seen in the tables above, model calibration for the Upper SAR Watershed Model shows good to very good performance at all of the streamflow gages from 1966 to 2016.

1.6 Integrated SAR Model

The Integrated SAR Model domain covers an area of approximately 1,389 square miles (888,768 acres) with a finite-difference grid consisting of 1,642 rows in the northeast to southwest direction and 2,243 columns in the northwest to southeast direction. The grid is rotated at 27° clockwise to be consistent with the previous SBBA, Rialto-Colton, and Yucaipa Models and minimize the number of model cells.

The cell size for the Integrated SAR Model area is 102.5 ft x 102.5 ft – mimicking the high-resolution cell size used in the previous Yucaipa, SBBA, and Rialto-Colton models. This cell size is smaller than those used in the previous Riverside-Arlington Model (164 ft x 164 ft) and Chino Basin Model (200 ft x 200 ft). The purpose of maintaining or enhancing existing model cell size is to preserve the integrity and functionality of each of the five individual groundwater flow models. Following model calibration, any of the individual models may be "de-coupled" from the Integrated SAR Model and be run as a stand-alone model to assess smaller-scale projects within the individual groundwater basins.

Active and inactive model cells of the Integrated SAR Model were assigned according to the designation used by the existing individual models. These active/inactive areas were based on published groundwater basin boundaries and geologic mapping. Active model cells generally represent high-permeability, water-bearing basin fill materials (e.g., alluvium) while inactive, or no-flow, cells represent bedrock or low-permeability, consolidated sedimentary material.

The Integrated SAR Model consists of five model layers:

- Model Layer 1: Shallow river, wash, and axial-channel deposits present in distinct channels, very young and young alluvial deposits, and the upper portion of old and very old alluvial deposits.
- Model Layer 2: Old and very old alluvial deposits and Live Oak Canyon deposits (Yucaipa Basin).
- Model Layer 3: Old and very old alluvial deposits and Live Oak Canyon deposits (Yucaipa Basin).
- Model Layer 4: Old and very old alluvial deposits and Live Oak Canyon deposits (Yucaipa Basin).
- Model Layer 5: Old and very old alluvial deposits, Live Oak Canyon deposits (Yucaipa Basin), and Fernando Group (Chino Basin).

1.6.1 Aquifer Parameters

The original development of aquifer parameters in the individual groundwater models is discussed in the previous modeling reports for each model area. Since the development of a groundwater model for the Chino Basin area was included in the scope of the development of the Integrated SAR Model, the establishment of initial aquifer parameters in this area is outlined in Section 6.0. During the model update and integration process, the aquifer parameters for the previous groundwater models were modified through individual model calibration. These updated values were then used as initial values for the Integrated SAR Model calibration. During model calibration, these initial values were refined through iterative manual adjustments within pre-established upper and lower bounds in order to minimize the residuals between measured and model-calculated groundwater levels.

1.6.2 Recharge and Discharge Terms

Model recharge and discharge components, along with the MODFLOW package used to simulate each water budget term, are summarized in Table 1-3 below.

Table 1-3. Summary of Recharge and Discharge Terms for the Integrated SAR Model

Term		Model Package
Recharge	Recharge from Mountain Front Runoff	Well Package
	Areal Recharge from Precipitation	Recharge Package
	Streambed Percolation	Streamflow Routing Package
	Artificial Recharge	Well Package
	Anthropogenic Return Flow	Well Package and Recharge Package
	Underflow Inflow	Well Package
Discharge	Evapotranspiration	Evapotranspiration Package
	Groundwater Pumping	Well Package
	Rising Water Discharge to Streamflow	Streamflow Routing Package and Drain

1.6.3 Model Calibration

Calibration is the process of adjusting model parameters to produce the best-fit between simulated and observed groundwater system responses. Initial model parameters were based on the updated existing individual models. These values were further adjusted to better match historical observations of groundwater levels and streamflow. The Integrated SAR model calibration consisted of:

- Initial condition simulation (1966), and
- Transient calibration (monthly stress periods from 1966 through 2016).

The Integrated SAR Model was calibrated against 108,502 measurements of groundwater level in 879 calibration wells, as well as streamflow at three gaging stations within the groundwater basin.

1.6.3.1 Initial Condition Simulation

The Integrated SAR Model calibration included an initial condition simulation, or model spin-up period, with model input from January of 1966. The goal of the initial condition model run was to develop a numerically stable initial condition, in good agreement with observed water levels, for the beginning of the transient calibration run. Results of the initial condition simulation are summarized below.

Table 1-4. Summary of Initial Condition Model Simulation Results

Statistic	Integrated SAR Model
Mean Residual	-1.00 ft
Minimum Residual	-73.81 ft
Maximum Residual	223.76 ft
RMSE	38.68 ft
Relative Error	2.2%
R^2	0.99

1.6.3.2 Transient Calibration

The transient calibration run for the Integrated SAR Model covers the period from 1966 through 2016 with monthly stress periods. The goal of the transient model calibration was to produce model-calculated water level and streamflow measurements that match observed water levels and historical streamflow at locations within the model domain. Analysis of model water budget, water level hydrographs, and residuals was conducted after each model calibration run to assess the effects of changes made to model parameters. Parameter values adjusted during the calibration included hydraulic conductivity, storativity/specific storage, specific yield, hydraulic flow barrier conductance, and streambed conductance.

1.6.3.2.1 Groundwater Elevations

The transient model calibration process used 108,502 water level measurements from 879 calibration target wells from which to match model-calculated water levels against observed measurements. Calibration statistics are summarized in the following table.

Table 1-5. Summary of Integrated SAR Model Transient Model Calibration Statistics – All Layers

Statistic	Integrated SAR Model
Mean Residual	-0.98 ft
Minimum Residual	-292.31 ft
Maximum Residual	409.99 ft
RMSE	64.54 ft
Relative Error	1.8%
R^2	0.99

In general, the measured and model-calculated heads compared favorably, and the calibration is further supported by a low relative error 1.8%. In addition, no large changes in the quality of the model calibration are observed between the beginning, middle, and end of the model period.

The model active area is approximately 505 square miles or 322,925 acres. Some areas within the model domain exhibit more error than others. In general, under-simulation of water levels at basin boundaries is more likely. Uncertainty regarding boundary inflows, model layer thickness, and hydraulic properties at the boundaries of the groundwater model also contribute to error at the model boundaries. Another contributing factor to larger residuals in upgradient wells (and also one of the reasons for considering relative error as a calibration metric) is that water levels that exhibit a larger degree of natural variability are also inherently harder to simulate or predict, and are subject to a greater range of natural change and thus, error. Secondly, some water levels may represent pumping conditions or perched conditions, and as such, are not representative of regional groundwater levels. Some differences between model-simulated and measured values are also potentially due to model cell size (102.5 ft by 102.5 ft) being larger than the local scale of observation. Residuals tend to be lower in the center of the basin, where geologic observations are more numerous and regional hydraulic properties and gradients are better defined.

Overall, the calibration results indicate that the standard of calibration achieved in the Integrated SAR Model is suitable for the scale and purpose for which it was developed. Of approximately 108,500 observations, over 41,000 (38%) fell within +/- 20 ft of the observed water level while over 79,000 (73%) fell within +/- 60 ft. Errors were found to be generally randomly distributed in space and time, with the exception of the anomalies noted herein.

The model calibration performance for the individual basin model area is summarized in the following tables.

Table 1-6. Summary of Transient Model Calibration Statistics – Yucaipa Basin Model Area (All Model Layers)

Statistic	Previous Model (GEOSCIENCE, 2017) 1998-2015 Monthly Stress Period	Integrated SAR Model 1966-2016 Monthly Stress Period	
		Individual Model (TM No. 1)	Integrated SAR Model
Mean Residual	5.40 ft	27.51 ft	44.18 ft
Minimum Residual	NA	-264.34 ft	-229.24 ft
Maximum Residual	NA	397.00 ft	360.07 ft
RMSE	64.52 ft	74.27 ft	78.91 ft
Relative Error	2.9%	2.9%	3.1%

Table 1-7. Summary of Transient Model Calibration Statistics – SBBA Model Area (All Model Layers)

Statistic	Previous Model (Stantec and GEOSCIENCE) 1983-2015 Monthly Stress Period	Integrated SAR Model 1966-2016 Monthly Stress Period	
		Individual Model (TM No. 1)	Integrated SAR Model
Mean Residual	11.14 ft	8.61 ft	-25.94 ft
Minimum Residual	NA	-320.86 ft	-292.31 ft
Maximum Residual	NA	362.32 ft	360.17 ft
RMSE	64.16 ft	64.57 ft	64.55 ft
Relative Error	3.5%	3.5%	3.5%

Table 1-8. Summary of Transient Model Calibration Statistics – Rialto-Colton Basin Model Area (All Model Layers)

Statistic	Previous Model (GEOSCIENCE, 2015) 1945-1969 Annual Stress Period, 1970-2014 Monthly Stress Period	Integrated SAR Model 1966-2016 Monthly Stress Period	
		Individual Model (TM No. 1)	Integrated SAR Model
Mean Residual	-6.66 ft	-1.06 ft	19.29 ft
Minimum Residual	NA	-176.99 ft	-113.14 ft
Maximum Residual	NA	351.79 ft	291.28 ft
RMSE	69.40 ft	59.52 ft	53.99 ft
Relative Error	6.2%	5.7%	5.1%

Table 1-9. Summary of Transient Model Calibration Statistics – Riverside-Arlington Basin Model Area (All Model Layers)

Statistic	Previous Model (WRIME 2010) 1965-2007 Monthly Stress Period		Integrated SAR Model 1966-2016 Monthly Stress Period	
	Calibration (1965-2005)	Validation (2006-2007)	Individual Model (TM No. 1)	Integrated SAR Model
Mean Residual	12.10 ft	13.20 ft	-0.37 ft	3.78 ft
Minimum Residual	NA	NA	-63.12 ft	-67.80 ft
Maximum Residual	NA	NA	69.95 ft	81.95 ft
RMSE	16.00 ft	11.80	19.29 ft	22.41 ft
Relative Error	5.0%	5.0%	6.3%	7.8%

Table 1-10. Summary of Transient Model Calibration Statistics – Chino Basin Model Area (All Model Layers)

Statistic	Previous Model (WEI, 2015) 1961-2011 Quarterly Stress Period		Integrated SAR Model 1966-2016 Monthly Stress Period	
	Calibration Wells	Validation Wells	Individual Model (TM No. 1)	Integrated SAR Model
Mean Residual	0.50 ft	-8.64 ft	17.86 ft	1.33 ft
Minimum Residual	-238.56 ft	NA	-244.67 ft	-268.71 ft
Maximum Residual	153.85 ft	NA	673.83 ft	409.99 ft
RMSE	25.38 ft	NA	58.93 ft	33.63 ft
Relative Error	NA	NA	5.2%	3.0%

1.6.3.2.2 Underflow across Basin Boundaries

In contrast to the previous individual groundwater models, the Integrated SAR Model explicitly simulates underflow between adjacent groundwater basins for the first time. Instead of treating boundary inflows between groundwater basins as boundary conditions, the boundaries between adjacent groundwater basins were removed – allowing the groundwater model to solve for underflow across basin boundaries. Groundwater flow across basin boundaries was computed from the cell-by-cell groundwater flow output from the groundwater model simulation, and is summarized in the following table.

Table 1-11. Summary of Underflow across Basin Boundaries

Basin	Underflow [acre-ft/yr]
Underflow from Yucaipa Basin to the SBBA	
Yucaipa Basin Model (GEOSCIENCE, 2017)	3,500
SBBA Model (GEOSCIENCE, 2009)	4,100
Integrated SAR Model	***7,830***
Underflow from Bunker Hill Basin to Rialto-Colton Basin	
SBBA Model (GEOSCIENCE, 2009)	3,800
Rialto-Colton Basin Model (GEOSCIENCE, 2015)	4,000
Integrated SAR Model	***4,700***
Underflow from Lytle Basin to Rialto-Colton Basin	
SBBA Model (GEOSCIENCE, 2009)	2,000
Rialto-Colton Basin Model (GEOSCIENCE, 2015)	14,100
Integrated SAR Model	***14,530***
Underflow from Rialto-Colton Basin to Riverside Basin	
Rialto-Colton Basin Model (GEOSCIENCE, 2015)	17,900
Riverside-Arlington Model (WRIME, 2010)	25,400
Integrated SAR Model	***17,010***
Underflow from Riverside Basin to Chino Basin	
Riverside-Arlington Model (WRIME, 2010)	2,800
Chino Basin Model (GEOSCIENCE, 2018a)	11,300
Integrated SAR Model	***16,260***

1.6.3.2.3 Streamflow

Results of the streamflow calibration at the three gaging stations used for calibration are summarized in the following table. Performance is based on the suggested criteria by Donigian (2002).

Table 1-12. Summary of Integrated SAR Model Results – Monthly Simulated Streamflow Performance

Gaging Station	Avg. Observed Flow [cfs]	Avg. Model-Simulated Flow [cfs]	Mean Residual [cfs]	Mean Residual as % of Avg. Observed Flow	NSE	R^2	Performance
Santa Ana River at E Street	75.9	81.7	-5.8	-8%	0.82	0.84	Good
Santa Ana River at MWD Crossing	130.5	105.3	25.2	19%	0.75	0.81	Good
Santa Ana River into Prado Dam	274.7	286.4	-11.7	-4%	0.81	0.93	Very Good

In general, the model is able to reproduce similar streamflow dynamics seen in observed measurements.

1.6.3.2.4 Water Balance

Groundwater budgets for the individual basin areas summarize all inflow and outflow terms. As outlined previously, inflow terms to the Integrated SAR Model include mountain front runoff, underflow inflow from adjacent groundwater basins, artificial recharge in spreading basins, areal recharge of precipitation, anthropogenic return flow from applied water, and streambed percolation. Discharge terms include groundwater pumping, evapotranspiration from groundwater, and rising water discharge to streamflow. The difference between the total inflow and total outflow equals the change in groundwater storage. The annual change in groundwater storage for each basin area is summarized below.

Table 1-13. Summary of Average Annual Change in Groundwater Storage

Basin	Average Annual Change in Groundwater Storage [acre-ft/yr]
Yucaipa Basin	-1,940
SBBA	-6,240
Rialto-Colton Basin	190
Riverside-Arlington Basin	-3,110
Chino Basin	-16,460
Temescal Basin	-1,350
Prado Basin	20

A water balance was also conducted for Prado Basin, which is included within the area of the Chino and Temescal Basins. During the model calibration period (1966 through 2016), the annual change in groundwater storage for the Prado Basin area is approximately 20 acre-ft/yr.

1.6.3.2.5 Cumulative Change in Groundwater Storage

Many of the basin areas have cumulative change in groundwater storages that respond to changes in hydrologic conditions (i.e., wet and dry periods cause rises and declines in groundwater storage, respectively). Basin response to hydrology is greatest in the SBBA, and generally diminishes in basins with increasing distance from mountain front recharge sources.

It appears that the Integrated SAR Model tends to over-estimate groundwater declines in the SBBA during the latter part of the model simulation period since the model-calculated cumulative change in groundwater storage declines at a faster rate during the last 15 years of simulation than the cumulative change in storage calculated by the groundwater level method. The greater cumulative decline in groundwater storage calculated by the Integrated SAR Model is likely due to the large amount of underflow from Lytle Basin to the Rialto-Colton Basin. This over-estimation in cumulative storage decline can be corrected through future work on the model calibration.

1.7 Predictive Scenarios

Predictive scenarios were run using the calibrated Integrated SAR Model to evaluate the effects of proposed HCP covered activities and other basin management strategies on riparian habitat, groundwater levels, and streamflow. Each model run was developed through collaboration and consultation with the TAC and HCP Team. The general scenario categories include:

- Scenario 1: Evaluate Flow in the SAR and Identify Factors that May be Causing Reduced Flows
- Scenario 2: Evaluate the Proposed HCP Activities with Hydrologic Effects
- Scenario 4: Evaluate Groundwater Management Activities and Changes in Groundwater Pumping

The scenario runs simulate various project effects individually or in combination to assess hydrologic responses in comparison to the baseline (no project) scenario, Scenario 2a. This allowed project impacts to be isolated. For each scenario run, model-predicted flow and groundwater impacts were evaluated, including water level and water budgets for each groundwater basin (e.g., evapotranspiration and underflow across each groundwater basin). In Scenarios 2, 3, and 4, time history of water levels, water budgets and streamflow were compared to a baseline, no project condition simulation to estimate impacts attributable to individual HCP Covered Activities or combinations of HCP Covered Activities. In addition, this information was provided to the Environmental Impact Report (EIR) team for them to establish thresholds of significance.

1.8 Summary

The Integrated SAR Model has combined previous modeling efforts and knowledge base in the Upper Santa Ana Valley Basin into one model. Existing models were updated with the appropriate resolution, or cell size, and orientation to match that of the Integrated SAR Model and were updated with hydrologic data that cover the model calibration period from January 1966 through December 2016. A model for the Chino Basin area was also developed based on the approach outlined by the previous model report (WEI, 2015). Each updated model was rerun individually to ensure the modeling results were consistent with the original existing models. The updated existing models were then incorporated into the Integrated SAR Model domain by developing unified model layers across the groundwater basin, based on the lithologic model of the area and hydrogeologic conceptual understanding. The Integrated SAR Model added key components to the unified numerical model that were absent or not contiguous in previous models to allow the simulation of streamflow and evapotranspiration for the purpose of assessing the effect of various projects on flows and riparian habitat in the Upper SAR.

Calibration of the Integrated SAR Model was conducted with a focus on time-history matching of streamflow and groundwater levels in Upper Santa Ana River. The Integrated SAR Model was successfully calibrated through an initial condition simulation for 1966 and a transient calibration from 1966 through 2016 using monthly stress periods. The calibrated model has a mean residual of -0.98 ft and an RMSE of 64.54 ft. The acceptable model calibration is also reflected by a relative error of 2.2% for the initial condition simulation and 1.8% for the transient calibration. Common modeling practice is to consider a good fit between measured and model-calculated water levels if the relative error is below 10% (Spitz and Moreno, 1996). Calibration is further supported with an R^2 value of 0.99. Results of the flow model calibration indicate that:

- Some areas within the model domain exhibit more error than others. In general, under-simulation of water levels at basin boundaries is more likely due to uncertainty regarding boundary inflows, model layer thickness and hydraulic properties, and the presence of perched groundwater conditions.

- Water level residuals show a generally random distribution in space, with higher residuals in the SBBA and Yucaipa Basin.

- Overall, the calibration results indicate that the standard of calibration achieved in the Integrated SAR Model is suitable for the scale and purpose for which it was developed. Of approximately

108,500 observations, over 41,000 (38%) fell within +/- 20 ft of the observed water level while over 79,000 (73%) fell within +/- 60 ft. Errors were found to be generally randomly distributed in space and time, with the exception of the anomalies noted herein.

- In contrast to the previous individual groundwater models, the Integrated SAR Model explicitly simulates underflow between adjacent groundwater basins for the first time. Model-calculated underflow from Yucaipa Basin to the SBBA averaged 8,180 acre-ft/yr, underflow from Bunker Hill Basin to Rialto-Colton Basin averaged 3,660 acre-ft/yr, underflow from Lytle Basin to Rialto-Colton Basin averaged 13,250 acre-ft/yr, underflow from Rialto-Colton to Riverside Basin averaged 16,490 acre-ft/yr, and underflow from Riverside to Chino Basin averaged 17,280 acre-ft/yr.

- In general, the Integrated SAR Model is able to reproduce similar streamflow dynamics seen in observed measurements. At the E Street gaging station, there is some tendency for the model to over-estimate streamflow later in the calibration and the model appears to slightly under-estimate streamflow at MWD Crossing.

- Many of the basin areas respond to changes in hydrologic conditions (i.e., wet and dry periods cause rises and declines in groundwater storage, respectively). Basin response to hydrology is greatest in the SBBA, and generally diminishes in basins with increasing distance from mountain front recharge sources.

- The Integrated SAR Model tends to over-estimate groundwater declines in the SBBA during the latter part of the model simulation period, likely due to the large amount of underflow from Lytle Basin to the Rialto-Colton Basin. This over-estimation in cumulative storage decline can be corrected through future work on the model calibration.

Model scenarios were conducted to assess the hydrologic response of the Upper SAR to various project activities, including streamflow diversions, recharge basins (new basins and modifications), effluent reductions, and new discharge locations. Specifically, the Integrated SAR Model scenarios evaluate the effects of proposed HCP covered activities and other basin management strategies on riparian habitat, groundwater levels, and streamflow. The scenario runs simulate various project effects individually or in combination to assess hydrologic responses in comparison to a baseline (no project) scenario. For each scenario run, model-predicted flow and groundwater impacts were evaluated, including water level and water budgets for each groundwater basin (e.g., evapotranspiration and underflow across each groundwater basin). Scenario results were compared to a baseline, no project condition simulation to estimate impacts attributable to individual HCP Covered Activities or combinations of HCP Covered Activities. In addition, this information was provided to the Environmental Impact Report (EIR) team for them to establish thresholds of significance.

The Integrated SAR Model was constructed as a management tool for the Upper Santa Ana Valley Basin to assess the effects of various projects, including the Habitat Conservation Plan "Covered Activities." As a management tool, the model is intended to be used to inform the decision-making process. An understanding of the intended uses of the model and limitations and uncertainties associated with modeling results is key to interpreting modeling results and informing the decision-making process.

2.0 INTRODUCTION

The Santa Ana River (SAR) is one of the largest river systems in Southern California – originating in the San Bernardino Mountains of Yucaipa and discharging into the Pacific Ocean in Orange County. Managing flow in the river and the corresponding effect on groundwater levels is important to the many communities that rely on water from the SAR and the groundwater basins associated with it. The Santa Ana River Stipulated Judgement of 1969 established minimum average annual flows at two key areas along the SAR: at the Riverside Narrows and at Prado Dam, the latter representing the division between the upper and lower SAR Groundwater Basins. The Upper Santa Ana Valley Groundwater Basin incorporates the Yucaipa, San Bernardino Basin Area (SBBA)[1], Rialto-Colton, Riverside-Arlington, Chino, and Temescal Groundwater Basins (Figure 1).

There has been an increasing concern within the last few years regarding reduced streamflow in the SAR and the potential effects that approved, outstanding, and proposed wastewater change petitions might have on surface flow and local groundwater levels. Therefore, San Bernardino Valley Municipal Water District (Valley District), in cooperation with Western Municipal Water District (Western), Inland Empire Utilities Agency (IEUA), Orange County Water District (OCWD), Riverside Public Utilities (RPU), the U.S. Geological Survey (USGS), the U.S. Fish and Wildlife Service (USFWS), and the California Department of Fish and Wildlife (CDFW), have tasked GEOSCIENCE Support Services, Inc. (GEOSCIENCE) with constructing a groundwater flow model for the Upper Santa Ana Valley Groundwater Basin by integrating existing groundwater and surface water models. This model, known as the Integrated SAR Model, will be used as a management tool to determine what factors contribute to reduced streamflow in the SAR, and to evaluate potential effects from proposed projects on streamflow and groundwater levels across the basin. These proposed projects include Upper SAR Habitat Conservation Plan (HCP) "Covered Activities", such as the Enhanced Recharge in SAR Basins Project, Riverside North Aquifer Storage and Recovery Project, and several other stormwater capture and recycled water reuse projects along the SAR.

The development of the Integrated SAR Model included the following six tasks:

- Task 1: Model Integration
- Task 2: Flow Model Calibration
- Task 3: Develop and Run Predictive Scenarios
- Task 4: Prepare Draft and Final Report
- Task 5: Project Management, Peer Review, and Meetings
- Task 6: Database Development

[1] The SBBA consists of the Bunker Hill and Lytle Subbasins (see Figure 1).

During the project, individual tasks were summarized in the following technical memorandums (TMs):

- TM No. 1: Model Integration (GEOSCIENCE, 2018a)
- TM No. 2: Calibration Plan (GEOSCIENCE, 2018b)
- TM No. 3: Model Calibration (GEOSCIENCE, 2020a)
- TM No. 4: Major Assumptions of Predictive Scenarios (GEOSCIENCE, 2019a)
- TM No. 4b: Major Assumptions of Management Scenarios that Will Reduce, or Eliminate, Rejected Recharge Upstream and Optimize Storage and Recovery (GEOSCIENCE, 2019b)
- TM No. 5a: Predictive Scenario Results, Part 1 (GEOSCIENCE, 2019c)
- TM No. 5b: Predictive Scenario Results, Part 2 (GEOSCIENCE, 2019d)
- TM No. 5c: Predictive Scenario Results, Part 3 (GEOSCIENCE, 2020b)
- Database Plan (GEOSCIENCE, 2018c)

Each draft TM was submitted to the Technical Advisory Committee (TAC) for comment and review. A summary of comments submitted on the draft TMs, along with GEOSCIENCE responses, is presented in Appendix A. This Summary Report satisfies Task 4 and incorporates the material from TM Numbers 1 through 5c and TAC comments. The final database plan is included as Appendix B.

2.1 Integrated SAR Model Objectives

The main objectives of the Integrated SAR Model were to:

- Develop a tool that will support efforts to conserve and protect riparian habitat and endangered species in the vicinity of the SAR;
- Be able to identify locations of perennial rising or shallow groundwater and assess how these areas might be affected by current and proposed projects;
- Enhance understanding of the HCP baseline condition, including both streamflow and groundwater levels in the Upper SAR region;
- Develop a more certain understanding of how current projects such as groundwater operations amongst the various basins, current operations of Prado Dam and Seven Oaks Dam, and existing practices of various wastewater treatment plants (WWTPs) along the River are currently impacting flow in the SAR and groundwater levels in the area; and
- Predict how proposed projects and mitigation measures addressed in the HCP, and potential projects outside of the HCP, will impact flow in the SAR and groundwater levels in the area – particularly in locations of perennial rising or shallow groundwater.

To achieve these objectives, the Integrated SAR Model was developed from existing groundwater and surface water models of the Upper Santa Ana Valley Groundwater Basin, and calibrated against observed streamflow, groundwater levels, and estimates of evapotranspiration.

2.2 Multi-Agency Cooperative Technical Effort

The development of the Integrated SAR Model represents a cooperative technical effort involving:

- Representatives of participating parties, including Valley District, Western, IEUA, OCWD, RPU, USGS, USFWS, and the CDFW;
- Representatives of participating parties' consultants Aspen Environmental Group (Aspen), GEOSCIENCE, Leidos, and Numeric Solutions;
- Technical advisors representing the Balleau Groundwater, Inc. (BGW), Chino Basin Watermaster, ICF, the Santa Ana Regional Water Quality Control Board, the Santa Ana Watershed Project Authority (SAWPA), University of California, Riverside (UCR), U.S. Army Corps of Engineers (USACE), and Wildermuth Environmental, Inc. (WEI).

Collectively, this group represents the TAC. Collaboration by these representatives to develop the Integrated SAR Model was achieved through participation at project conference calls, model workshops, and by reviewing and commenting on draft technical memoranda and model files. Comments and responses submitted for draft technical memoranda are provided in Appendix A. Reviews and summaries of the July 10, 2019 modeling subcommittee workshop and main conclusions, as well as additional comments provided by the USGS, BGW, WEI, and OCWD are also provided in Appendix A. Meeting minutes from progress calls and model workshops are provided in Appendix C.

2.3 Previous Groundwater and Surface Water Models

Previous groundwater models that were used as a basis for the Integrated SAR Model are the:

- Yucaipa Groundwater Model (GEOSCIENCE, 2017),
- Refined Basin Flow Model/Newmark Groundwater Flow Model (RBFM/NGFM) for the SBBA (GEOSCIENCE, 2009; GEOSCIENCE and Stantec, in progress),
- Rialto-Colton Groundwater Model (GEOSCIENCE, 2015),
- Riverside-Arlington Groundwater Model (WRIME, 2010), and
- Chino Basin Model (WEI, 2015; separate version constructed by GEOSCIENCE for this project).

The previous groundwater models are shown on Figure 2 while the process of updating and integrating the existing models is summarized in Section 5.0. Since model files were not available for the WEI Chino Basin Model, GEOSCIENCE constructed a separate version of the model based on the approach and available data presented in WEI's modeling report (2015). This is discussed in Section 6.0. The individual groundwater models that were incorporated into the Integrated SAR Model are shown on Figure 3.

Existing watershed models include the:

- Wasteload Allocation Model (WEI, 2009),
- SBBA Riverside Basin Watershed Model (GEOSCIENCE, 2013),
- Yucaipa Watershed Model (GEOSCIENCE, 2014), and
- Wasteload Allocation Model Update (GEOSCIENCE, 2019e).

A watershed model for the Upper SAR Watershed was developed and calibrated from 1966 through 2016 to simulate runoff generated within the watershed and quantify runoff for the Integrated SAR Model. The development and calibration of the watershed model is summarized in Section 7.0.

2.4 Model Domain and Model Cell Size for the Integrated SAR Model

The Integrated SAR Model domain covers an area of approximately 1,389 square miles (888,768 acres) with a finite-difference grid consisting of 1,642 rows in the northeast to southwest direction and 2,243 columns in the northwest to southeast direction (Figure 4). The grid is rotated at 27° clockwise to be consistent with the previous SBBA, Rialto-Colton, and Yucaipa Models and minimize the number of model cells.

The cell size for the Integrated SAR Model area is 102.5 ft x 102.5 ft – mimicking the high-resolution cell size used in the previous Yucaipa, SBBA, and Rialto-Colton models. This cell size is smaller than those used in the previous Riverside-Arlington Model (164 ft x 164 ft) and Chino Basin Model (200 ft x 200 ft). The purpose of maintaining or enhancing existing model cell size is to preserve the integrity and functionality of each of the five existing groundwater flow models. Following model calibration, any of the individual models may be "de-coupled" from the Integrated SAR Model and be run as a stand-alone model to assess smaller-scale projects within the individual groundwater basins.

Active and inactive model cells of the Integrated SAR Model were assigned according to the designation used by the existing individual models. These active/inactive areas were based on published groundwater basin boundaries and geologic mapping. Active model cells generally represent high-permeability, water-bearing basin fill materials (e.g., alluvium) while inactive, or no-flow, cells represent bedrock or low-permeability, consolidated sedimentary material. The active model area encompasses approximately 505 square miles (322,925 acres).

2.5 Model Integration Process

Model integration involved updating the existing groundwater flow models (i.e., Yucaipa, SBBA, Rialto-Colton, and Riverside-Arlington Models) with the appropriate resolution, or cell size, and orientation to match that of the Integrated SAR Model. The existing groundwater flow models were also updated so that the hydrologic data covered the model calibration period from January 1966 through December 2016. Each updated model was rerun individually to ensure the modeling results were consistent with the original existing models. The model update process is summarized in Section 5.0. In the Chino Basin area of the Integrated SAR Model, existing model files were unavailable. Therefore, a separate version of the Chino Basin Model was constructed and calibrated in the Integrated SAR Model grid. Construction was initially based on available data presented in WEI's model report (2015), but the Chino Basin Model presented herein does differ from the WEI model. Some model parameters and fluxes were developed using different approaches and model parameters were refined through model calibration. The construction and initial model calibration of the Chino Basin Model is summarized in Section 6.0.

The final step for integrating the individual groundwater flow models was to develop unified model layers for the Integrated SAR Model area. To do so, the geology and hydrology of the individual groundwater basins were evaluated. A lithologic model of the Integrated SAR Model area was also developed from well logs and other available information. The geologic and hydrologic conceptual models and development of model layers for the Integrated SAR Model area is discussed in Sections 3.0 and 4.0.

3.0 GEOLOGIC CONCEPTUAL MODEL OF THE INTEGRATED SAR MODEL

The Upper Santa Ana Valley Groundwater Basin incorporates the Yucaipa, SBBA, Rialto-Colton, Riverside-Arlington, Chino, and Temescal Groundwater Basins (Figure 1). In general, the conceptual geologic models for the six groundwater basins within the Upper Santa Ana Valley Groundwater Basin are similar with respect to the geologic materials present, with minor variations. With respect to geologic history, the Yucaipa, SBBA, and Rialto-Colton basins share similar and overlapping depositional histories due to local tectonics associated with movement along the San Jacinto, San Andreas, and associated faults. Likewise, the Riverside-Arlington, Temescal, and Chino Basins share similar geologic histories. The geologic conceptual model forms the basis for the hydrogeologic conceptual model, which in turn informed the construction of the numerical Integrated SAR Model for the simulation of groundwater flow through the geologic formations.

In order to integrate the existing groundwater models, it was necessary to review the individual conceptual models and identify similarities and differences. It was also necessary to develop an approach for extending model layers, representing geologic units, across existing model boundaries. An overview of the regional geology is discussed below, which provided a framework for identifying geologic units within the Integrated SAR Model domain and correlating hydrogeologic units (model layers) between groundwater basins.

3.1 Geography

The Integrated SAR Model occupies the Upper SAR Watershed in Southern California, which incorporates hills, mountains, and valley areas. The groundwater basins within the model domain are bordered by the San Gabriel Mountains and San Bernardino Mountains to the north and the San Jacinto Mountains to the east (Dutcher and Garrett, 1963; see Figure 1). The Santa Ana Mountains, Chino Hills, and Puente Hills comprise the southwestern and western boundaries of the basin, while the San Jose Hills lie just west of the western model boundary. The Chino and San Bernardino Valleys are separated from the Riverside-Arlington Heights area by the La Loma Hills, Jurupa Mountains, Pedley Hills, and La Sierra Hills. Beyond the Riverside-Arlington Heights area are the Box Springs Mountains and highland area of the El Sobrante de San Jacinto. Moreno Valley, Perris Valley, and Temescal Valley are broad valleys outside of the subject groundwater basins in the eastern portion of the model area. East of the San Bernardino Valley, the model domain includes the Crafton Hills, Yucaipa Valley, and a portion of the San Bernardino Mountains. Elevations in the watershed range from 486 ft at Prado Dam to 11,499 ft in the San Bernardino Mountains near Mt. San Gorgonio. Figure 1 provides a generalized geographic map of the area showing major land features within the model domain. Inset Figure 3-1 below shows the Upper SAR Watershed and the Upper Santa Ana Valley Groundwater Basin. The vertical scale is exaggerated three times to show the relative relief of the watershed area.

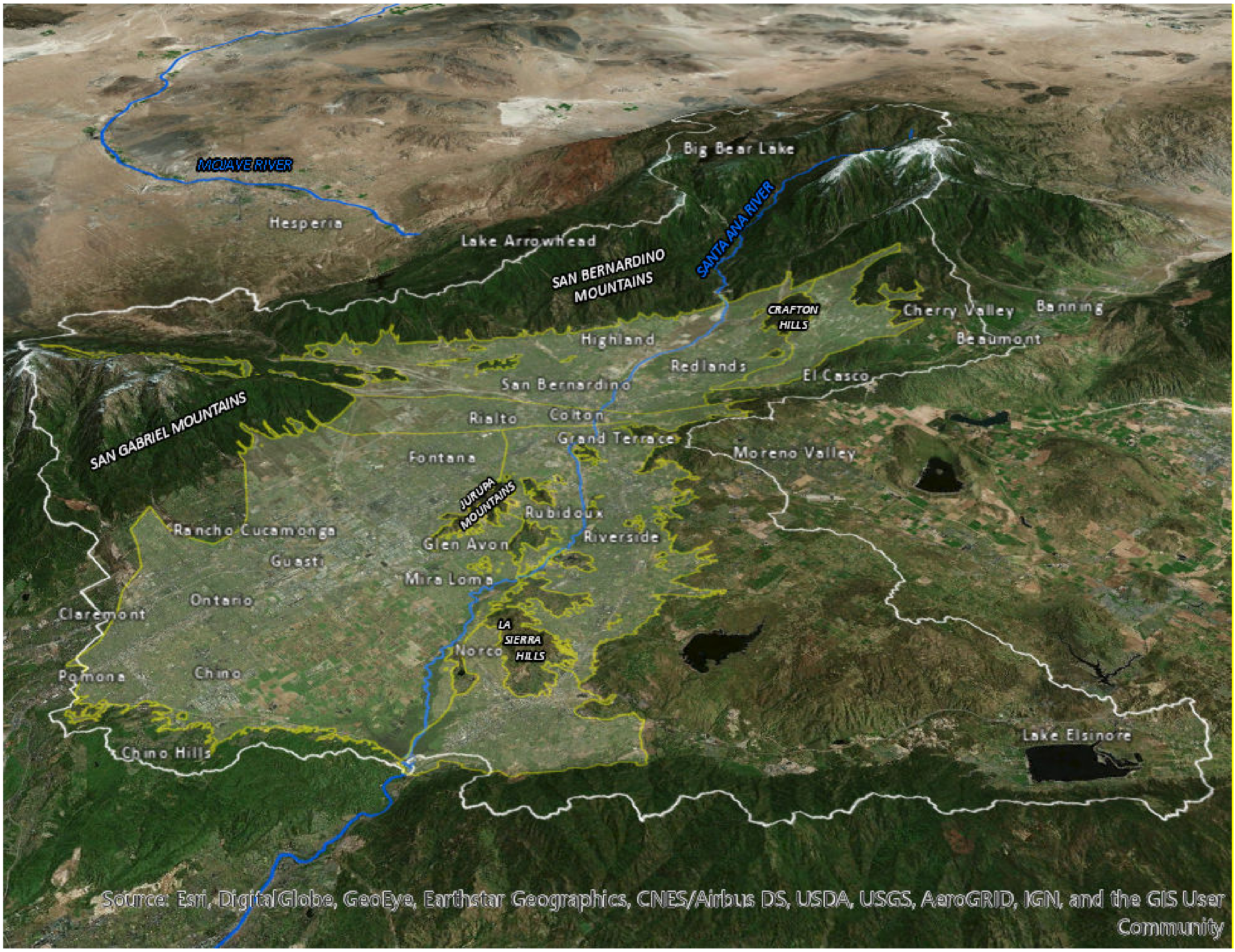

Figure 3-1. Geographic Setting of the Upper SAR Watershed (white line) and Santa Ana Valley Groundwater Basin (yellow line)

3.2 Physiography

The Upper Santa Ana Valley Groundwater Basin overlies one of the most tectonically active regions of California – at the juncture of the Transverse Ranges and the Peninsular Range geomorphic provinces. As described by the California Geological Society (CGS), *"California's geomorphic provinces are naturally defined geologic regions that display a distinct landscape or landform. Earth scientists recognize eleven provinces in California. Each region displays unique, defining features based on geology, faults, topographic relief and climate"* (2002). Some of the features of the Peninsular Ranges Province, which includes the Upper Santa Ana Valley Groundwater Basin, are provided below.

3.2.1 Peninsular Ranges Geomorphic Province

The Upper SAR Watershed lies partly within the Peninsular Ranges Geomorphic Province and partly within the Transverse Ranges Geomorphic Province (Figure 5). The CGS (2002) describes the Peninsular Ranges Province as follows: *"a series of ranges is separated by northwest trending valleys, subparallel to faults branching from the San Andreas Fault. The trend of topography is similar to the Coast Ranges, but the geology is more like the Sierra Nevada, with granitic rock intruding the older metamorphic rocks. The Peninsular Ranges extend into lower California and are bound on the east by the Colorado Desert. The Los Angeles Basin and the island group (Santa Catalina, Santa Barbara, and the distinctly terraced San Clemente and San Nicolas islands), together with the surrounding continental shelf (cut by deep submarine fault troughs), are included in this province."*

In the model domain, the Peninsula Ranges Geomorphic Province is characterized by granitic highland areas such as the Lakeview Mountains, Bernasconi Hills, Box Springs Mountains, Loma Linda Hills, Mt. Rubidoux, Jurupa Mountains, Pedley Hills, and La Sierra Hills. The granitic hills and mountains are separated by flat low-lying alluvial plains and valleys such as Perris Valley, Moreno Valley, Arlington Basin, and Chino Basin (see Figure 5). Within the Peninsula Ranges Geomorphic Province, structural blocks including the Perris Block, San Jacinto Mountains Block, Los Angeles Basin Blocks and a portion of the San Bernardino Basin block underlie the model domain. The Perris Block occupies the major portion of the model domain (Figure 6). Morton and Miller (2006) note that *"the Perris block consists of two distinct parts, a northern and a southern part. Upstream from Corona, the northern part consists of the largely alluvial valley area of the Santa Ana River. Most of the area north of the Santa Ana River is covered by late Pleistocene and Holocene alluvial fan deposits emanating from the high-standing San Gabriel Mountains."* The Chino and Riverside-Arlington groundwater basins underlie the alluviated valleys in the southern part.

Although similar, the boundary of the Peninsula Ranges Geomorphic Province does not coincide with the structural rock assemblage boundaries as defined by Morton and Miller (2006) as the Peninsular Ranges (Rock) Assemblage (refer to Section 3.3.1 for more detail).

3.2.2 Transverse Ranges Geomorphic Province

The CGS (2002) describes the Transverse Ranges Province as follows: *"The Transverse Ranges are an east-west trending series of steep mountain ranges and valleys. The east-west structure of the Transverse Ranges is oblique to the normal northwest trend of coastal California, hence the name 'Transverse.' The province extends offshore to include San Miguel, Santa Rosa, and Santa Cruz islands. Its eastern extension, the San Bernardino Mountains, has been displaced to the south along the San Andreas Fault. Intense north-south compression is squeezing the Transverse Ranges. As a result, this is one of the most rapidly rising* *regions on earth. Great thicknesses of Cenozoic petroleum-rich sedimentary rocks have been folded and faulted, making this one of the important oil producing areas in the United States."*

In the model domain, the Transverse Ranges Geomorphic Province is composed of the San Gabriel Mountains and the San Bernardino Mountains (Figure 5). The boundary of the Transverse Ranges Geomorphic Province and the Mojave Desert Geomorphic Province to the north of the model domain is also shown on Figure 5. The boundaries were digitized from a State-scale geomorphic province map and are therefore not detailed. However, based on the structural rock assemblage distribution assigned by Morton and Miller (2006), the SBBA and Yucaipa Basin lie generally within the Transverse Ranges Geomorphic Province while the Rialto-Colton, Riverside-Arlington, and Chino, and Temescal Basins are located within the Peninsular Ranges Geomorphic Province.

3.3 Geologic Overview

3.3.1 Structural Rock Assemblages

3.3.1.1 Peninsular Ranges Assemblage

Figure 6 shows the distribution of structural assemblages in the model domain area. Morton and Miller (2006) state: *"In the San Bernardino and Santa Ana quadrangles, the Peninsular Ranges Province can be divided into a series of fault-bounded blocks, each of which has a set of uniform characteristics internally."* Figure 6 also shows the boundaries of the internal blocks within the Peninsular Ranges Assemblage. Within the model domain, the Peninsular Ranges Assemblage includes (from west to east) the Los Angeles Basin, Santa Ana Mountains Block, Perris Block, and the San Jacinto Mountains Block. The boundary of the Santa Ana Mountains Block with the Perris Block represents the Elsinore-Chino Fault Zone. The boundary of the Perris Block with the San Jacinto Mountains Block represents the San Jacinto Fault. Groundwater basins are not present in the Santa Ana Mountains Block in the model area. The basement terrane includes Cretaceous granitic rock and Mesozoic or older metasedimentary rock.

3.3.1.2 San Gabriel Mountains Assemblage

The northeastern portion of the model domain is underlain by rocks of the San Gabriel Mountains Assemblage (Figure 6). This assemblage underlies the San Gabriel Mountains north of the Cucamonga and San Jose Faults and is divided into numerous blocks based on the underlying bedrock type. Since the mountainous portions are outside of the active cells of the model, the San Gabriel Mountains Assemblage on Figure 6 only shows the structural blocks for the area between the San Jacinto and San Andreas Fault Zones; namely, the San Bernardino Basin and the Crafton Hills Block. Furthermore, the San Gabriel Mountains Assemblage is divided into rock types above the Vincent Trust Fault and rocks below the Vincent Thrust Fault. According to Morton and Miller (2006), the upper plate suite (including the San

Bernardino Basin) *"consists of a great variety of rocks that includes Proterozoic anorthosite, Proterozoic and Paleozoic gneiss and schist, and Mesozoic granitic rocks"* while the lower plate suite (including the Crafton Hills Block) consists of Cretaceous Pelona Schist.

3.3.2 General Geologic Setting

The Upper SAR Watershed is principally located within the San Bernardino and Santa Ana 30' x 60' quadrangles. In the description which accompanies the geologic map of the San Bernardino and Santa Ana 30' x 60' quadrangles, Morton and Miller (2006) group and subdivide geologic and geomorphic features on the basis of 1) basement rock assemblages, 2) Upper Cretaceous and Tertiary rock distribution, or 3) structural physiographic domains. "Quaternary deposit" is the general description given to surface materials regardless of the type of older rocks that they overlie, with the exception of a few formally-named Pleistocene units. For this study, the geologic units have been grouped into:

1. Holocene and Pleistocene alluvial material,
2. Pleistocene and Plio-Pleistocene sedimentary units, and
3. Early Pliocene to Miocene sedimentary rocks, and Miocene and older undifferentiated bedrock.

Figure 7a shows a generalized geologic map of the model domain and surrounding area while Figure 7b summarizes the specific geologic units within each grouping, as mapped by Morton and Miller (2006) and Matti and others (2015).

3.3.2.1 Miocene and Older Undifferentiated Bedrock

The bedrock area shown on Figure 7a is grouped into Miocene and older consolidated sedimentary, metamorphic, and granitic rock. Units include Paleozoic and Mesozoic metamorphic and granitic rocks such as the Bedford Canyon Formation and Peninsula Ranges batholithic rocks, along with post-batholithic Upper Cretaceous and Paleocene through Miocene sedimentary rock and volcanics. These rocks exhibit very low permeabilities and therefore form the boundaries of the groundwater basins – representing the basement contact for the basin aquifers.

3.3.2.2 Pliocene to Miocene Sedimentary Rocks

The early Pliocene to Miocene marine Puente Formation underlies the Chino Hills and the Puente Hills in the western portion of the model area (see Figure 7a). The formation consists of four members, which are made up of various proportions of consolidated sandstone, conglomerate, shale, and siltstone beds and which are faulted and folded into a broad anticlinal structure along the Chino and Whittier Faults. Although a major source of detritus to the Chino Basin is from the San Gabriel Mountains through smaller streams and from the San Bernardino Mountains and adjacent highlands via the SAR, erosion of the Puente Hills has resulted in the deposition of fine-grained materials in the southern end of the Chino Basin. There are likely clay deposits representing reworked Puente Formation which overlie bedrock in the Chino Basin. In addition, logs made available by the State of California Department of Oil and Gas and Geothermal Resources (DOGGR) note Puente Formation at depth in the Chino Basin.

Southeast of the Upper Santa Ana Valley Groundwater Basin, there are surface exposures of late Miocene to middle Pleistocene deposits (Matti et al., 2015). Described from oldest to youngest, these sedimentary deposits consist of the Mt. Eden Formation and the San Timoteo Formation. Mt. Eden alluvial sediments originated from the erosion of crystalline bedrock from the nearby Peninsular Ranges, while limestone and mudrock within the Mt. Eden deposits are the result of periodic aquatic depositional environments. Figure 7a shows the limited extent of the Mt Eden Formation at the eastern end of the San Timoteo Badlands.

In contrast to the Peninsular Ranges source of the Mt. Eden Formation, the overlying San Timoteo Formation’s conglomeratic, sandy, and muddy deposits originated from San Gabriel Mountains-type crystalline rocks, with paleocurrent evidence indicating a southeasterly direction of deposition (Matti et al, 2015).

The Miocene Puente Formation and Mt. Eden Formation, along with the Plio-Pleistocene San Timoteo Formation, exhibit very low permeability and, for the most part, outcrop outside of the groundwater basin boundaries. At depth within the groundwater basin boundaries, they form the effective base of the groundwater basins.

3.3.2.3 Pleistocene Sedimentary Units

Following initial activity of the San Jacinto Fault around 1.2 million years ago (Ma), deposition of the San Timoteo Formation ceased and alluvial deposition of the sedimentary deposits of Live Oak Canyon began from a different depositional provenance. Sediments of the sedimentary deposits of Live Oak Canyon are sourced from both San Gabriel Mountains- and San Bernardino Mountains-type crystalline rocks, with paleocurrent indicators suggesting south-southwest directions of deposition (Matti et al., 2015). Recent mapping of the contact between the sedimentary deposits of Live Oak Canyon and the San Timoteo Formation in the El Casco 7.5 Minute Quadrangle suggests that the shift in depositional source in this region indicates significant changes in paleogeography and paleotopography – most recently related to activity along the San Jacinto Fault and uplift of the San Timoteo Badlands (Matti et al., 2015). The sedimentary deposits of Live Oak Canyon are permeable and represent the basal sedimentary unit throughout much of the Yucaipa Basin.

3.3.2.4 Holocene and Pleistocene Deposits

Holocene and Pleistocene deposits immediately underlie the groundwater basins. These deposits include young alluvial channel and alluvial fan deposits as well as older alluvial channel and fan deposits. Figure 7b provides a summary of the types of deposits included as Holocene and Pleistocene deposits. Since Pleistocene time, these deposits have been primarily sourced from highland areas surrounding the groundwater basins, such as the San Gabriel Mountains and San Bernardino Mountains. These deposits can be very permeable and are the primary source of groundwater in all of the basins, with the exception of the Yucaipa Groundwater Basin.

3.3.3 Structural Geology

The Integrated SAR Model incorporates one of the most tectonically active regions of California. Active faults – including the San Andreas and San Jacinto Faults – cross the model domain, along with numerous associated subsidiary faults formed as a result of the regional tectonic regime. The individual groundwater basins within the Upper Santa Ana Valley Groundwater Basin are either separated by faults (i.e., SBBA, and Rialto-Colton Basins, Rialto-Colton and Chino Basins, and the SBBA and Riverside-Arlington Basins), or they are separated by bedrock highlands (i.e., Riverside-Arlington and Chino Basins). The major northwest-trending faults include the San Andreas, Rialto-Colton, Loma Linda, San Jacinto, Banning, Chino, and Elsinore-Chino Faults (refer to Figure 6).

3.3.3.1 San Bernardino Basin Area and Yucaipa Basin

The advent of movement along the San Jacinto Fault around 1.2 million years before present has played a major role in the depositional history as well as the distribution of the lithologic units in the model area. The boundary of the northern portion of the San Jacinto Mountains Block of the Peninsular Ranges Assemblage underlies the San Timoteo Badlands but does not include the Crafton Hills or Yucaipa Valley and is bounded on the west by the San Jacinto Fault (Figure 6). The San Timoteo Badlands is an area of uplift and erosional dissection that has formed as a result of late Quaternary uplift along a restraining bend in the San Jacinto Fault (Kendrick et al., 2002). The Upper SAR Watershed includes San Timoteo Canyon. The watershed divide is located just east of where State Highway 60 passes through the Badlands. In addition, a portion of the Perris Block in the southeastern model domain is outside of the Upper SAR Watershed. Here, the Perris Block is a highland area underlain by shallow bedrock and Pleistocene paleochannels (DWR, 1955). The area is drained by the San Jacinto River and Salt Creek, which flow into Railroad Canyon Reservoir and then into Lake Elsinore.

The southern San Bernardino Mountains form the northern boundary of the Upper Santa Ana Valley Groundwater Basin – specifically along the SBBA and Yucaipa Groundwater Basins. These basins are composed of multiple fault blocks that achieved their current configuration as a result of transpressional deformation along the San Andreas Fault. The SBBA is present within the San Bernardino Basin (or San Bernardino Valley) block (see Figure 6).

Kenney (2011) reports that *"the San Bernardino Valley fault block (SBVFB) is defined as the crust bounded by the San Jacinto fault zone to the southwest, the San Andreas fault zone to the northeast, and the Crafton Hills fault zone to the southeast. All of these fault zones are considered active. The SBVFB is likely experiencing counter-clockwise block rotations associated with right-lateral motion on the San Andreas and San Jacinto fault zones. Extension is also occurring in the San Bernardino Valley likely associated with a transfer of slip from the San Andreas to the San Jacinto Fault zone in the region which has resulted in the valley tectonically dropping down and development of the extensional Crafton Hills fault zone consisting of a series of dominantly normal faults"*. Pliocene through Quaternary sedimentary material has been deposited in the down-dropped extensional San Bernardino Valley and Yucaipa Basin. Faulting and deposition of alluvial materials has occurred at the same time – with detritus from the San Bernardino Mountains filling in the down-dropped basin created from tectonic extension between the San Andreas and San Jacinto Faults. The greatest thickness of groundwater aquifer material is in the San Bernardino Valley, east of the San Jacinto Fault. The base of the aquifer in the SBBA and the Yucaipa Basin area is composed of Pleistocene and potentially Plio-Pleistocene consolidated sediments (Danskin et al., 2006). These sediments have likely been deformed from the tectonic processes that created both groundwater basins.

Geologic mapping conducted for determining the location of potential groundwater barriers in relation to SAR groundwater recharge basins located near the San Bernardino Mountain front noted that mid-Pleistocene units were faulted in the area of the western alluvial highlands, near the apex of the SAR (GEOSCIENCE, 2012). The mid-Pleistocene units exhibit an approximate 25-degree dip toward the southwest, which indicates that tilting and possibly folding has occurred in the area since the middle to late Pleistocene. This suggests that similar-aged sediments buried beneath the groundwater basin may also be tilted with the overlying material resting unconformably over the tilted strata. Kendrick and others (2002) have suggested the presence of at least three paleosols in the late Pleistocene stratigraphic section of the San Timoteo Badlands, represented by the time period 43-67 thousand years before present (ka). The presence of small thin clay units represents periods of topographic stability – enough to allow the development of surface soils. For the most part, paleosols are noted on driller's logs. However, if thick enough, they might be noted as a clay unit. These layers would not be continuous in the subsurface, since they are likely interrupted by paleo-channels like their modern counterparts.

Based on the existence of groundwater barriers farther west in the SBBA and Yucaipa Groundwater Basins, active faulting along the San Jacinto Fault and associated faults and along the faults that make up the

Crafton Hills Horst and Graben Complex appears to extend to near-surface elevations. Since tectonic subsidence in the SBBA is on-going, Pleistocene deposits may have experienced some degree of deformation. Therefore, they may not be in the original position they were deposited in. Areas where deformation of the underlying units at depth is likely were considered during the model calibration process.

3.3.3.2 Chino, Temescal, Rialto-Colton, and Riverside-Arlington Basins

The surface traces of the Elsinore, Chino, and Whittier Faults are present along the eastern portion of the Santa Ana Mountains Block (Figure 6). The boundary between the Perris Block and the Santa Ana Mountains Block is placed east of the Chino Fault, within the Chino Groundwater Basin, and coincident with the Elsinore Fault in Temescal Basin.

The Chino Basin contains a relatively thin sequence of Los Angeles Basin Tertiary rocks, including petroleum producing units (French, 1999). This portion of the Chino Groundwater Basin (west of the Perris Block) is underlain by a down-dropped fault block – between the Chino Fault on the west and an unnamed fault or possibly a depositional contact to the east (Morton and Miller, 2006). As reported in the Chino Basin Groundwater Model report, "*According to Durham and Yerkes (1964), this sequence reaches a total stratigraphic thickness of more than 24,000 feet in the Puente Hills and is down-warped more than 8,000 feet below sea level in the Prado Dam area. Wherever mapped, these strata are folded and faulted and, in most places, dip from 20 to 60 degrees*" (WEI, 2015). The folded tertiary sediments at depth are overlain by Quaternary sediments in the upper 300-500 ft.

The Perris Block in the Chino Groundwater Basin is underlain by shallow bedrock. The northeastern portion of the Perris Block contains the Rialto-Colton Groundwater Basin (Paulinski, 2012). The eastern boundary of the Perris Block and Peninsular Ranges Assemblage coincides with the San Jacinto Fault Zone and the eastern boundary of the Rialto-Colton Groundwater Basin. The structural geology and stratigraphy in the Rialto-Colton Groundwater basin is similar to the Chino Basin, as it lies within the Perris Block. This area consists of granitic basement rock, overlain by consolidated sedimentary rock of Plio-Pleistocene age, overlain by Pleistocene to Holocene alluvial fan and channel deposits.

4.0 HYDROLOGIC CONCEPTUAL MODEL

Equally important to the development of the Integrated SAR Model is the conceptual understanding of the Upper Santa Ana Valley Groundwater Basin hydrologic system. This includes surface water, groundwater, and the interaction between them.

4.1 Sources of Inflow and Outflow (Recharge and Discharge)

Identifying sources of inflow and outflow to the Upper Santa Ana Valley Groundwater Basin was key in determining where and how to simulate recharge and discharge in the Integrated SAR Model. In general, sources of inflow to the groundwater basin include ungaged and gaged runoff from the surrounding watershed areas, underflow inflow from neighboring mountain blocks and groundwater basins, precipitation, and applied water. This translates to recharge from mountain front runoff, the direct infiltration of precipitation, percolation from streamflow, artificial recharge, return flow, and underflow inflow. Sources of outflow/discharge chiefly consist of surface water flow out of the groundwater basin (including the contribution from rising groundwater), evapotranspiration, and groundwater pumping. These main physical sources are discussed briefly in the following sections.

Methods of simulating recharge and discharge terms (i.e., “flux” terms) in the Upper SAR Groundwater Basin vary between the individual existing groundwater flow models. A summary of how the individual models handled recharge and discharge terms in previous studies is provided in the following sections, along with the approach used for the Integrated SAR Model. Model packages for simulating flux terms in the Integrated SAR Model are summarized in Table 2-3 below. Recharge and discharge terms are also shown on Figure 9. Simulation of recharge and discharge terms in the Integrated SAR Model is discussed in Section 6.3.

4.1.1 Mountain Front Runoff

While crystalline bedrock is typically assumed to have a negligible contribution to groundwater flow, the numerous faults and fractures present in the low-permeability bedrock surrounding the Upper Santa Ana Valley Groundwater Basin allow the mountain block to represent a significant source of recharge. Recharge from mountain front runoff includes both recharge from ungaged surface runoff and subsurface inflow, and is assumed to occur along the contact between upgradient outcrops of bedrock and downgradient alluvial materials. Recharge from mountain front runoff include contributions from the San Gabriel Mountains, San Bernardino Mountains, Shandin Hills, Crafton Hills, the Badlands, Box Springs Mountain, Jurupa Mountains, Pedley Hills, Yucaipa Hills (east of the Yucaipa Basin), La Sierra Hills, El Sobrante de San Jacinto, Santa Ana Mountains, and Chino Hills (Figure 8).

Each of the individual models that make up the Integrated SAR Model include assumptions for recharge from mountain front runoff, based on previous studies. These estimates, which are detailed in the individual model reports, were included in the Integrated SAR Model. Simulation of recharge from mountain front runoff in the existing groundwater flow models is summarized in Table 4-1 below.

Table 4-1. Simulation of Recharge from Mountain Front Runoff in Individual Groundwater Flow Models

Yucaipa Model (GEOSCIENCE, 2017)	SBBA Model (Stantec and GEOSCIENCE)	Rialto-Colton Model (GEOSCIENCE, 2015)	Riverside-Arlington Model (WRIME, 2010)	Chino Model (GEOSCIENCE)
Well Package	Well Package	Well Package	Well Package	Well Package

The recharge from mountain front runoff used by the existing groundwater flow models was incorporated into the Integrated SAR Model and simulated with MODFLOW's Well Package. During the model calibration period from January 1966 through December 2016, recharge from mountain front runoff averaged 43,290 acre-ft/yr (Figure 9). The USGS is currently working on the California Basin Characteristic Model (BCM; Flint and Flint, 2014), which could help refine the estimation of mountain front recharge for future iterations of the Integrated SAR Model.

4.1.2 Precipitation

The Upper Santa Ana Valley Groundwater Basin is generally characterized by a typical Mediterranean climate of hot, dry summers and short, mild, moist winters. Daily precipitation data are available from a multitude of precipitation gaging stations within the Integrated SAR Model boundary (Figure 10). One of the most complete sets of daily precipitation data is from the San Bernardino County Hospital Station. Annual rainfall and a cumulative departure from mean annual precipitation at this gage is provided as Figure 11. As shown, the mean annual precipitation is approximately 15.7 inches. The cumulative departure curve illustrates when there have been periods of dry (below average) or wet (above average) hydrology. On this figure, a positive slope for the cumulative departure curve indicates wet hydrology while a negative slope indicates dry hydrology.

Precipitation within the surrounding watershed area contributes to gaged and ungaged mountain front runoff, while precipitation within the groundwater basin contributes to recharge from the direct infiltration of precipitation and local runoff, which contributes to streamflow. The amount of runoff from precipitation was calculated by the surface water model (refer to Section 8.3.3 for quantification of this inflow term). Simulation of areal recharge from precipitation in the existing groundwater flow models is summarized in Table 4-2 below.

Table 4-2. Simulation of Areal Recharge from Precipitation in Individual Groundwater Flow Models

Yucaipa Model (GEOSCIENCE, 2017)	SBBA Model (Stantec and GEOSCIENCE)	Rialto-Colton Model (GEOSCIENCE, 2015)	Riverside-Arlington Model (WRIME, 2010)	Chino Model (GEOSCIENCE)
Recharge Package	Recharge Package	Recharge Package	Well Package	Recharge Package

Areal recharge from precipitation in the existing groundwater flow models was incorporated into the Integrated SAR Model and simulated with MODFLOW's Recharge Package. For the model calibration period, areal recharge averages 51,970 acre-ft/yr (Figure 12).

4.1.3 Streamflow

Streamflow provides a considerable amount of recharge to the Upper Santa Ana Valley Groundwater Basin by conveying water from surrounding mountainous areas (where the greatest concentration of precipitation falls) to the groundwater basin; allowing the water to become recharge through streambed infiltration in unlined channels. In general, the amount of recharge depends on the channel lining type (lined vs. unlined), conductance of the streambed materials, streambed geometry, water levels in the surrounding groundwater system, and amount of streamflow in the channel.

As shown in Table 4-3 below, all of the individual groundwater flow models except for the Riverside-Arlington Groundwater Model use the MODFLOW Streamflow Routing Package to simulate streambed percolation. The Streamflow Routing Package assigns recharge to stream cells that are sequentially numbered in the downstream direction. The downward leakage of streamflow, or streambed percolation, is calculated as a function of the hydraulic conductivity of the streambed, the wetted perimeter of the streambed, the length of the stream reach, the underlying groundwater head, stream stage, and streambed thickness. Model input for the routing package includes stream inflow, stream channel geometry, and streambed conductance.

Table 4-3. Simulation of Streambed Percolation in Individual Groundwater Flow Models

Yucaipa Model (GEOSCIENCE, 2017)	SBBA Model (Stantec and GEOSCIENCE)	Rialto-Colton Model (GEOSCIENCE, 2015)	Riverside-Arlington Model (WRIME, 2010)	Chino Model (GEOSCIENCE)
Streamflow Routing Package	Streamflow Routing Package	Streamflow Routing Package	River Package	Streamflow Routing Package

Since the River Package used in the existing Riverside-Arlington Groundwater Model is unable to quantify the amount of streamflow in the SAR, it was converted to the Streamflow Routing Package in the Integrated SAR Model. Also, in order to improve the accuracy of streamflow in the Integrated SAR Model, and therefore streambed percolation, runoff generated from precipitation within the watershed boundary was calculated by the HSPF watershed model. This runoff, in turn, was simulated in the groundwater model using the Streamflow Routing Package. In order to address changes in river channel geometry, historical streamflow was evaluated to identify high flow periods. For these specific years (1967, 1969, 1978, 1979, 1980, 1983, 1993, 1995, 1998, and 2005), the width of the channels and streambed conductance was adjusted to account for the higher flows and greater wetted area.

Contributions to streamflow in the groundwater basin include inflow from the surrounding watershed, local runoff, wastewater discharges, and rising groundwater discharge to surface water. In addition to evapotranspiration and infiltration, reduction in streamflow is caused by surface water diversions.

4.1.3.1 Inflow from the Surrounding Watershed

The majority of streamflow in the Upper Santa Ana Valley Groundwater Basin originates as runoff from neighboring mountain areas. Streamflow from the surrounding watershed area enters the groundwater basin in the SAR and its tributaries. This flow includes outflow from Seven Oaks Dam. Daily historical data from gages are available for major creeks entering the groundwater basin (Figure 13). However, some ungaged surface water inflow from the watershed area enters the groundwater basin through minor tributaries or tributaries that do not have suitable gages for the quantification of stream inflow. Runoff from these areas was calculated by the surface water model (refer to Section 8.3.3 for quantification of this inflow term).

4.1.3.2 Local Runoff

Local runoff from precipitation and applied water represents a contribution to streamflow within the groundwater basin. The amount of runoff generated depends not only on the amount of water applied at the surface (through precipitation, irrigation, or other), but also on topography, soil type, and land use. In general, steeper areas with less permeable soil coverage and greater impervious area due to development generate more runoff. Runoff generated within the groundwater basin was also calculated by the surface water model (refer to Section 8.3.3 for quantification of this inflow term).

4.1.3.3 Wastewater Discharges

Wastewater discharge from POTWs represents a significant source of streamflow. Points of discharge are shown on Figure 14. Daily and/or monthly data for permitted discharges are available from these POTWs. During the model calibration period from 1966 through 2016, wastewater discharges averaged 87,750 acre-ft/yr (Figure 15). As shown on the figure, wastewater discharges have decreased within the last 10 years or so due to water conservation programs.

4.1.3.4 Rising Groundwater Discharge to Streamflow

A stream gains or loses water depending on the relative head in the stream and in the underlying aquifer. When the head in the stream is higher than the head in the aquifer, the stream loses water to the aquifer; when the head in the stream is lower than the head in the aquifer, the stream gains water from the aquifer. In natural systems, the amount of rising water fluctuates depending on groundwater elevations relative to stream stage. Understanding this interchange of water between the stream and the aquifer was one of the key issues driving the development of the Integrated SAR Model.

Areas of historically high groundwater levels causing groundwater to discharge to streamflow within the Upper Santa Ana Valley Groundwater Basin are known to be present in San Timoteo Canyon, at the Riverside Narrows, and at Prado Dam (Figure 16). In addition, rising water was observed in Warm Creek until the early 1990s (Danskin et al., 2005). The Streamflow Routing Package used for the Integrated SAR Model calculates the amount of water lost to surface flow in the form of rising water discharge to streamflow (refer to Section 8.3.9 for quantification of this outflow term).

4.1.3.5 Diversions

Streamflow, including dry-weather and storm flows, is occasionally diverted for artificial recharge in spreading basins or for other reuse purposes. These diversions, which are available from the agencies diverting the water, reduce the available amount of streamflow that contributes to recharge from streambed percolation.

4.1.4 Artificial Recharge

Artificial groundwater recharge in the Upper Santa Ana Valley Groundwater Basin is achieved through the spreading of water at recharge basins located in the Yucaipa, SBBA, Rialto-Colton, and Chino Groundwater Basins (Figure 17). This artificial recharge may include not only the surface water diversions discussed above, but also recycled and imported water. Simulation of artificial recharge in the existing groundwater flow models is summarized in Table 4-4 below.

Table 4-4. Simulation of Artificial Recharge in Individual Groundwater Flow Models

Yucaipa Model (GEOSCIENCE, 2017)	SBBA Model (Stantec and GEOSCIENCE)	Rialto-Colton Model (GEOSCIENCE, 2015)	Riverside-Arlington Model (WRIME, 2010)	Chino Model (GEOSCIENCE)
Well Package	Well Package	Well Package	-	Well Package

In the Integrated SAR Model, artificial recharge volumes were simulated using the Well Package. Spreading records are available from operating agencies and averaged 53,930 acre-ft/yr for the model calibration period from 1966 through 2016 (Figure 18). As shown on Figure 18, the volume of artificial recharge in spreading basins increases during the last 25 years due to an increase in recharge programs.

4.1.5 Anthropogenic Return Flow

Water applied at the surface can become runoff (if applied in excess of infiltration capacity or irrigation requirements) or can be consumed by evapotranspiration (ET). In addition, it can become groundwater recharge through deep percolation. Anthropogenic return flow refers to the amount of water that returns to the aquifer after application of water to the land surface in the form of irrigation, or from leaks in water and sewer lines. This includes the use of groundwater, recycled water, and imported water. Each of the individual models that make up the Integrated SAR Model include assumptions for anthropogenic return flow, based on previous studies. These estimates, which are detailed in the individual model reports, were included in the Integrated SAR Model. Simulation of return flow in the existing groundwater flow models is summarized in Table 4-5 below.

Table 4-5. Simulation of Return Flow in Individual Groundwater Flow Models

Yucaipa Model (GEOSCIENCE, 2017)	SBBA Model (Stantec and GEOSCIENCE)	Rialto-Colton Model (GEOSCIENCE, 2015)	Riverside-Arlington Model (WRIME, 2010)	Chino Model (GEOSCIENCE)
Recharge Package & Well Package	Well Package	Recharge Package	Well Package	Recharge Package & Well Package

In the Integrated SAR Model, return flow was simulated using the Well and Recharge Packages. During the model calibration period from January 1966 through December 2016, anthropogenic return flow averaged 79,580 acre-ft/yr (Figure 19).

4.1.6 Underflow Inflow

Underflow inflow to the Upper Santa Ana Valley Groundwater Basin from upgradient groundwater basin areas occurs in San Timoteo Canyon, along the southwestern edge of the SBBA (Danskin et al., 2006; updated SBBA Model by GEOSCIENCE and Stantec, in progress). However, because the northern boundary of the Chino Basin area in the Integrated SAR Model starts below the Redhill Fault (refer to Figure 6), underflow inflow (including contributions from the upgradient groundwater basin area and mountain front recharge) at this point was incorporated into the Integrated SAR Model. Underflow was initially based on the methodology outlined in the Chino Basin Model report (WEI, 2015) and adjusted during model calibration. Locations of underflow inflow are shown on Figure 20. Underflow inflow volumes were modified during model calibration (refer to Section 8.3.6 for quantification of this inflow term).

4.1.7 Evapotranspiration

ET includes the consumption of surface and groundwater through evaporation and transpiration by plants. In general, groundwater ET decreases with decreasing groundwater elevation and is the highest in areas where groundwater level elevations approach or exceed the ground surface. The simulation of ET in the existing groundwater flow models is summarized in Table 4-6 below.

Table 4-6. Simulation of Evapotranspiration in Individual Groundwater Flow Models

Yucaipa Model (GEOSCIENCE, 2017)	SBBA Model (Stantec and GEOSCIENCE)	Rialto-Colton Model (GEOSCIENCE, 2015)	Riv-Arlington Model (WRIME, 2010)	Chino Model (GEOSCIENCE)
ET Package	ET Package	ET Package	-	ET Package

As shown, MODFLOW's ET Package is used in all of the existing groundwater flow models. This was the same method of simulating ET used in the Integrated SAR Model. The ET Package simulates the effects of plant transpiration and direct evaporation in removing water from the saturated zone. Input values include data on maximum ET rate, ET surface, and extinction depth.

Since the model was utilized to evaluate potential changes in groundwater elevations in areas where groundwater-dependent riparian habitat occurs, it was crucial to ensure the model-simulated water levels in riparian areas are as accurate as possible. Such riparian habitat typically depends on the presence of groundwater at relatively shallow depths, or rising groundwater (in some cases, ten to fifteen feet or less below ground surface). In order to incorporate the general water requirements of riparian vegetation in the Integrated SAR Model, Aspen evaluated riparian vegetation coverage and estimated consumptive use based on published ET rates. In addition, BGW conducted a separate assessment of ET using a thermal based energy balance approach as a means of providing a basis for peer review of the hydrologic budget for the Integrated SAR Model. These two methods of estimating ET were presented at the January 30, 2018 model workshop and February 7, 2018 riparian vegetation subcommittee meeting (see Appendices D and E). The two estimation methods are briefly summarized in the following sections.

4.1.7.1 Aspen Riparian Vegetation Mapping and Consumptive Water Use

Aspen mapped the extent of riparian vegetation along the SAR and defined riparian vegetation types throughout the model calibration period (January 1966 through December 2016) at approximately 10-year intervals. The riparian vegetation was then divided into categories. While habitat assessments often require more detailed vegetation types, coarser categories were chosen for this work because of the scale and limited historical data on vegetation distribution. The vegetation categories were largely based on categories recommended by Maddock and others (2012) and include:

- **Deep-rooted riparian**: deep-rooted drought-intolerant phreatophytes that rely on shallow groundwater for establishment, growth, and transpiration (e.g., cottonwood, willow);
- **Giant reed**: fast-growing, tall, perennial grass found in wetland areas (e.g., Arundo);

- **Obligate wetland**: plants requiring standing water or saturated soils near the surface (e.g., cattail, tule, bulrush);
- **Managed wetland**: wetland areas managed and maintained for wildlife habitat;
- **Open water**;
- **Shallow-rooted riparian**: shallow-rooted drought-intolerant phreatophytes that rely on shallow groundwater for establishment, growth, and transpiration (e.g., cocklebur, curly dock, deer grass);
- **Transitional riparian**: species that, although not strictly dependent on a high water table, have water requirements that generally exceed the surrounding environment. Typically found along the outer edges of riparian systems (e.g., sycamore); and
- **Unvegetated sandy wash**.

The vegetation coverages in the Integrated SAR Model domain are provided on Figures 21 through 26. Monthly ET estimates for the different vegetation categories were derived from a literature search of available published ET rates. When available, local ET rates were used. However, ET rates for some riparian vegetation categories (e.g., shallow-rooted riparian and transitional riparian) were difficult to find. In these cases, ET rates from agricultural data (i.e., irrigated crops) were substituted. The literature review conducted by Aspen was summarized in a separate TM entitled “Evapotranspiration Estimates,” provided here as Appendix F. Estimated ET rates are shown in Figure 4-1 below.

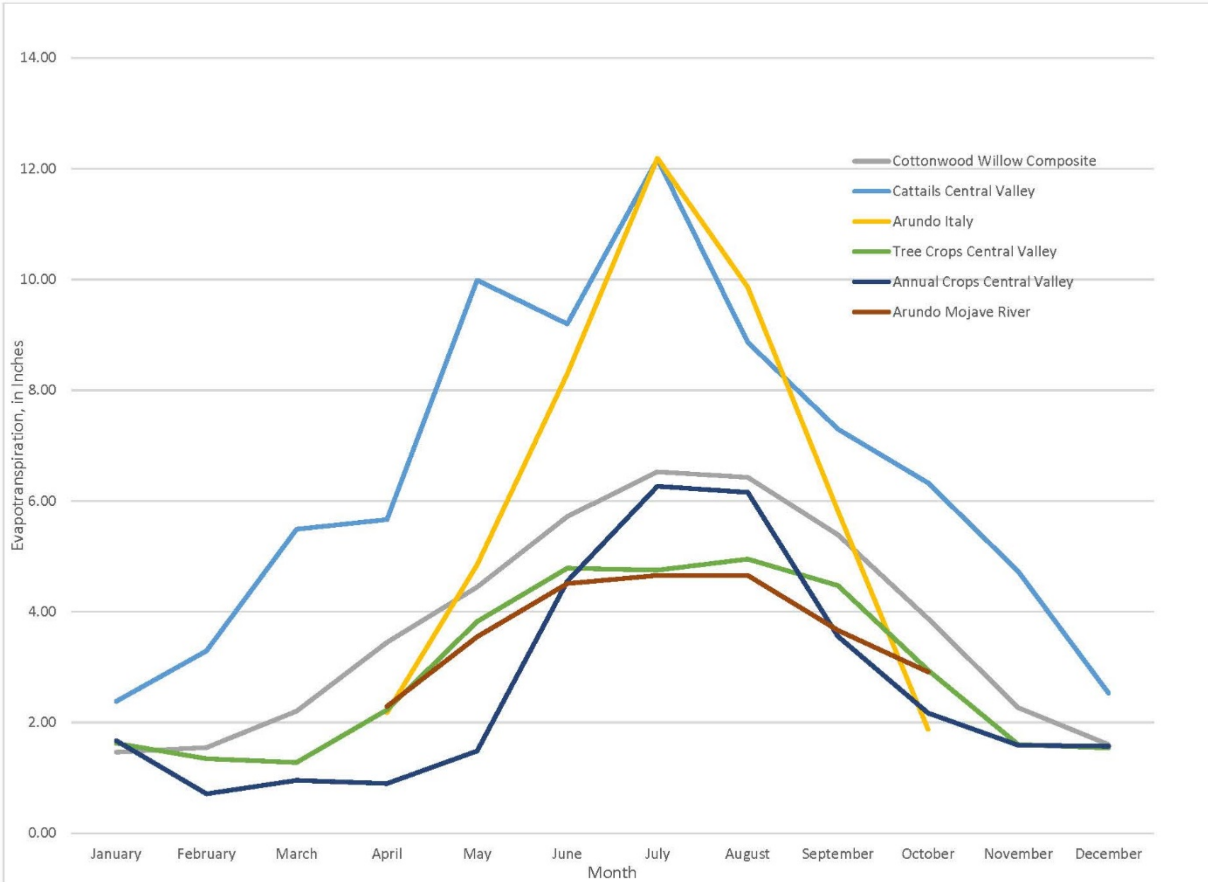

Figure 4-1. Evapotranspiration for Various Vegetation Types

The annual consumptive use of riparian vegetation was then determined by multiplying the acreage for each vegetation type by the literature-derived ET rate for that category.

4.1.7.2 Shallow Groundwater and Evapotranspiration Assessment by BGW

BGW estimated ET from riparian vegetation within the Integrated SAR Model area through an operational Simplified Surface Energy Balance (SSEBop). This thermal based approach estimates ET by applying a temperature relationship between “wet” areas (i.e., cool, high latent heat flux, high evapotranspiration) and “dry” areas (hot, high sensible heat flux, low ET) to remotely-sensed surface temperature data. Fractional ET (ET divided by reference ET (ETo)) from different times can be used to obtain seasonal and yearly ET amounts. Remotely sensed thermal and vegetation index data from the USGS Earth Resources Observation and Science (EROS) Science Processing Architecture (ESPA) system, along with California Irrigation Management Information System (CIMIS) meteorological data including ETo, air temperature, and solar radiation, were used for the analysis. ET in the shallow groundwater area of the Integrated SAR

Model (water level less than 20 ft deep) was estimated from 1986 through 2016 (with the exclusion of 2012), based on available data. This area of shallow groundwater is also shown on Figures 21 through 26.

BGW also compared the SSEBop estimated ET to the ET estimates from Aspen (refer to slide 59, Appendix E). The ET estimates by Aspen fall within the range of historical variability derived from BGW's SSEBop estimates.

4.1.7.3 Riparian Areas

As shown on Figures 21 through 26, the riparian areas delineated to support the simulation of ET in the Integrated SAR Model include the vegetated areas mapped by Aspen and WEI (2017), as well as the extent of shallow groundwater (i.e., groundwater less than 20 ft below ground surface) delineated by BGW in the Chino and Riverside-Arlington area, Matti and Carson (1991) in the SBBA, and existing modeling in the Yucaipa Basin (GEOSCIENCE). The riparian area throughout the model calibration period is summarized in the following tables.

Table 4-7. Riparian Area – Integrated SAR Model

Area	1960 - 1965	1976 - 1977	1985 - 1988	1996 - 1999	2004* - 2006	2015 - 2016
	[acres]					
Aspen Riparian Vegetation Area in Chino Basin and Riverside-Arlington Basin						
Deep-Rooted Riparian	369	1,814	4,611	4,068	2,424	4,573
Giant Reed	0	6	528	1,002	285	488
Obligate Wetland	79	0	2	41	9	32
Managed Wetland	0	0	537	493	479	477
Open Water	50	49	289	451	62	557
Shallow-Rooted Riparian	62	665	60	275	308	167
Transitional Riparian	433	106	931	676	232	1,119
Unvegetated Sandy Wash	46	0	278	357	25	93
Subtotal	*1,039*	*2,640*	*7,236*	*7,363*	*3,824*	*7,506*
WEI (2017) Riparian Vegetation Area in Chino Basin and Riverside-Arlington Basin (additional area not included in Aspen's mapping)						
Subtotal	*769*	*805*	*629*	*634*	*1,302*	*736*
BGW Shallow Groundwater Area in Chino Basin (additional area not included in Aspen's or WEI's mapping)						
Subtotal	*10,559*	*9,049*	*5,629*	*4,026*	*7,616*	*5,049*
Matti and Carlson (1991) Shallow Groundwater Area in the SBBA						
Subtotal	*12,714*	*12,714*	*12,714*	*12,714*	*12,714*	*12,714*
GEOSCIENCE (2017) Shallow Groundwater Area in Yucaipa Basin						
Subtotal	*282*	*282*	*282*	*282*	*282*	*282*
TOTAL	**25,363**	**25,490**	**26,490**	**25,019**	**25,738**	**26,287**

* Note: Aspen mapping for 2004 had reduced spatial coverage upstream of Prado Basin. In these areas, zone mapping from 1996/98 was applied.

Table 4-8. Riparian Area – Prado Basin

Area	1960 - 1965	1976 - 1977	1985 - 1988	1996 - 1999	2004* - 2006	2015 - 2016
	[acres]					
Aspen Riparian Vegetation Area in Prado Basin						
Deep-Rooted Riparian	369	1,814	2,693	2,662	2,424	2,723
Giant Reed	0	6	170	397	285	294
Obligate Wetland	79	0	2	18	9	8
Managed Wetland	0	0	537	493	479	477
Open Water	50	49	109	230	62	441
Shallow-Rooted Riparian	62	665	60	275	308	151
Transitional Riparian	433	106	630	222	232	146
Unvegetated Sandy Wash	46	0	22	13	25	3
Subtotal	*1,039*	*2,640*	*4,223*	*4,310*	*3,824*	*4,243*
WEI (2017) Riparian Vegetation Area in Prado Basin (additional area not included in Aspen's mapping)						
Subtotal	*769*	*805*	*628*	*634*	*1,302*	*736*
BGW Shallow Groundwater Area in Prado Basin (additional area not included in Aspen's or WEI's mapping)						
Subtotal	*4,974*	*3,458*	*2,173*	*2,022*	*2,123*	*1,973*
TOTAL	**6,782**	**6,903**	**7,024**	**6,966**	**7,249**	**6,952**

* Note: Aspen mapping for 2004 had reduced spatial coverage upstream of Prado Basin. In these areas, zone mapping from 1996/98 was applied.

As shown in the tables above, riparian habitat generally increases throughout the simulation period. The vegetation is likely responding to an increase in water availability (due to reduced agricultural diversions and increased discharges from upstream users) and timing of flows in the SAR and its tributaries. Inflow to Prado Dam increased and reached a high in the 1990s, but has generally decreased since 2005.

4.1.7.4 Maximum Evapotranspiration Demand

By using the acreages tabulated above and applying the literature-derived ET rate for each vegetation category, the annual consumptive use of riparian vegetation can be approximated. Where no specific type of vegetation is specified, the coverage was assigned the properties of deep-rooted riparian vegetation. Estimated ET demands are summarized in the following tables.

Table 4-9. Maximum Evapotranspiration Demand – Integrated SAR Model

Maximum Evapotranspiration Demand	1960 - 1965	1976 - 1977	1985 - 1988	1996 - 1999	2004 - 2006	2015 - 2016
	[acres]					
Aspen Riparian Vegetation Area in Chino Basin and Riverside-Arlington Basin						
Deep-Rooted Riparian	1,562	7,681	19,526	17,226	10,264	19,367
Giant Reed	0	30	2,551	4,842	1,374	2,359
Obligate Wetland	346	0	7	179	40	139
Managed Wetland	0	0	2,124	1,952	1,895	1,888
Open Water	199	194	1,144	1,786	247	2,203
Shallow-Rooted Riparian	290	3,095	280	1,281	1,433	780
Transitional Riparian	1,560	383	3,352	2,432	837	4,026
Unvegetated Sandy Wash	36	0	220	282	20	74
Subtotal	*3,993*	*11,383*	*29,206*	*29,980*	*16,110*	*30,836*
WEI (2017) Riparian Vegetation Area in Chino Basin and Riverside-Arlington Basin (additional area not included in Aspen's mapping)						
Subtotal	*3,255*	*3,410*	*2,662*	*2,684*	*5,516*	*3,119*
BGW Shallow Groundwater Area in Chino Basin (additional area not included in Aspen's or WEI's mapping)						
Subtotal	*44,716*	*38,323*	*23,838*	*17,050*	*32,255*	*21,381*
Matti and Carlson (1991) Shallow Groundwater Area in the SBBA						
Subtotal	*53,843*	*53,843*	*53,843*	*53,843*	*53,843*	*53,843*
GEOSCIENCE (2017) Shallow Groundwater Area in Yucaipa Basin						
Subtotal	*1,192*	*1,192*	*1,192*	*1,192*	*1,192*	*1,192*
TOTAL	**106,999**	**108,151**	**110,741**	**104,749**	**108,916**	**110,371**

Table 4-10. Maximum Evapotranspiration Demand – Prado Basin

Maximum Evapotranspiration Demand	1960 - 1965	1976 - 1977	1985 - 1988	1996 - 1999	2004 - 2006	2015 - 2016
	[acres]					
Aspen Riparian Vegetation Area in Prado Basin						
Deep-Rooted Riparian	1,562	7,680	11,404	11,273	10,264	11,530
Giant Reed	0	31	821	1,918	1,374	1,421
Obligate Wetland	346	0	9	79	40	34
Managed Wetland	0	0	2,125	1,951	1,895	1,888
Open Water	199	194	431	910	247	1,745
Shallow-Rooted Riparian	290	3,095	280	1,281	1,433	704
Transitional Riparian	1,560	383	2,268	799	837	526
Unvegetated Sandy Wash	36	0	17	10	20	2
Subtotal	*3,993*	*11,383*	*17,355*	*18,221*	*16,110*	*17,850*
WEI (2017) Riparian Vegetation Area in Prado Basin (additional area not included in Aspen's mapping)						
Subtotal	*3,231*	*3,409*	*2,659*	*2,635*	*5,457*	*3,084*
BGW Shallow Groundwater Area in Prado Basin (additional area not included in Aspen's or WEI's mapping)						
Subtotal	*21,063*	*14,644*	*9,202*	*8,564*	*8,990*	*8,355*
TOTAL	**28,287**	**29,436**	**29,216**	**29,420**	**30,557**	**29,289**

It is important to note that this method of estimating ET, along with the estimations produced by BGW, should yield ET rates that are greater than those calculated by the Integrated SAR Model. This is because these estimates include consumptive use by riparian vegetation from surface water, soil moisture, and groundwater. The Integrated SAR Model, on the other hand, only accounts for ET from the saturated aquifer system (i.e., at or below the water table).

4.1.8 Groundwater Pumping

Groundwater pumping represents the primary source of discharge from the Upper Santa Ana Valley Groundwater Basin. The simulation of pumping in the existing groundwater flow models is summarized in Table 4-11 below.

Table 4-11. Simulation of Groundwater Pumping in Individual Groundwater Flow Models

Yucaipa Model (GEOSCIENCE, 2017)	SBBA Model (Stantec and GEOSCIENCE)	Rialto-Colton Model (GEOSCIENCE, 2015)	Riv-Arlington Model (WRIME, 2010)	Chino Model (GEOSCIENCE)
Multi-Node Well Package	Well Package	Multi-Node Well Package	Well Package	Well Package

Groundwater pumping from the individual groundwater models was compiled and simulated in the Integrated SAR Model using the Multi-Node Well (MNW2) Package. This package is used to simulate injection and production volumes for wells screened across multiple model layers. This allows the simulated injection and production from model layers to be proportioned based on the relative saturated screen length within each model layer and the hydraulic conductivity of each model layer.

The locations of pumping wells are shown on Figure 27 (entire Integrated SAR Model area) and Figure 28 (Prado Basin area). During the model calibration period from 1966 through 2016, groundwater pumping averaged 473,110 acre-ft/yr (Figure 29). The majority of this pumping occurred in the Chino Basin and the SBBA, where pumping totaled 181,180 acre-ft/yr and 182,200 acre-ft/yr, respectively. While overall groundwater pumping increased slightly in the latter half of the calibration period, the distribution among types of groundwater pumping changed dramatically – with a shift from primarily agricultural pumping to primarily municipal pumping.

4.2 Hydrostratigraphy

Previous modeling has conceptualized the groundwater basins in a similar way. In general, the groundwater basins are filled with unconsolidated and poorly-consolidated sediments, which compose the valley-fill aquifers and are considered to be the more permeable part of the groundwater system. Igneous and metamorphic rocks underlying and surrounding the valley-fill aquifers are assumed to be poorly permeable and form the bedrock surface in all of the individual groundwater basins. Older sedimentary rocks that fill the Yucaipa Basin and bound the southwestern edge of the SBBA and southern boundary of the Chino Basin are more consolidated and assumed to be less permeable and transmit smaller amounts of water. While these consolidated sedimentary deposits in the Yucaipa Basin and Temescal Basin may be able to provide significant quantities of water to wells that penetrate them, they were not simulated in this version of the Integrated SAR Model. The correlation of the hydrogeologic units with the geologic units described in the previous sections is summarized in Table 1.

4.2.1 Development of Unified Model Layers

The geologic conceptual model was used to help define and unify model layers across individual model boundaries. In addition, a three-dimensional (3-D) lithologic model was developed for the Integrated SAR Model area to better identify the physical extents, thickness, continuity, and lithology of the geologic units across the model domain. Existing lithologic models covered the SBBA, Rialto-Colton, and Riverside-Arlington Basins. For the Yucaipa, Chino, and Temescal Basins, Numeric Solutions used lithologic data from driller's logs, geophysical logs, published cross-sections, and other available data sources to define crystalline bedrock and consolidated sedimentary rock elevations and estimate the lithology at each cell of a 3-D mesh. The process of developing the Unified Upper SAR Lithologic Model along with the lithologic modeling assumptions are described in Appendix G. Lithologic cross-sections through the Integrated SAR Model are provided as Figures 30 through 34.

The geologic conceptual model was then used in combination with the 3-D lithologic model to unify the model layers across the Integrated SAR Model domain. The correlation of geologic units to existing hydrogeologic units was adjusted, where needed, to allow for the correlation of hydrogeologic units across individual model boundaries.

Assignment of groundwater model layers (shown on Table 1 in the third column under each basin) was made based on the following considerations:

- Hydrogeologic units from the model documentation for each individual groundwater basin.
- Geologic units. If a hydrogeologic unit consists of multiple geologic units, distribution of the geologic units were reflected in hydraulic conductivity values assigned in the model. For example, higher hydraulic conductivity zones were used for the shallow river, wash, and channel deposits.
- Head differences measured in multi-depth monitoring wells used to define the base of the top model layer. As an example, if there were no differences in water levels measured from a well screened 40-50 ft deep and a well screened 90-100 ft deep, the base of the top model layer was assigned as at least 100 ft deep.
- Historical water table used to assign the base of Model Layer 1 to ensure layer saturation and minimize numerical instability problems (especially in the northwestern portion of the San Bernardino Basin Area, Rialto-Colton Basin, and Chino Basin).
- Consolidation. For the purpose of this version of the Integrated SAR Model, geologic units of sedimentary consolidated rocks (including the San Timoteo Formation, Mt. Eden, and Puente Formation) and Miocene and Older consolidated sedimentary, metamorphic, and granitic rocks (undifferentiated) were not included since they have very low permeability.

Of the seven model layers presented in Table 1, only the upper five were modeled in the Integrated SAR Model. The individual model layers are described in further detail in Section 8.1.3.

5.0 UPDATE OF EXISTING GROUNDWATER MODELS

5.1 Yucaipa Basin Model Update

5.1.1 Existing Yucaipa Basin Model

The Yucaipa Basin Model was developed by GEOSCIENCE in 2017 for Yucaipa Valley Water District (YVWD). The model was constructed for the unconsolidated sediments of the Yucaipa Groundwater Basin and consists of five model layers:

- Layer 1 – Younger and Older Alluvium
- Layers 2 through 5 – San Timoteo Formation

The Yucaipa Basin Model was constructed using MODFLOW-NWT, a block-centered, finite-difference groundwater flow code developed by the USGS (Niswonger el al., 2011). The USGS MODFLOW-NWT is a Newton-Raphson formulation of MODFLOW-2005 and represents an improved solution for unconfined groundwater-flow problems.

The groundwater flow model grid covers an area of approximately 125 square miles (80,000 acres) with a finite-difference grid consisting of 469 rows in the northeast-to-southwest direction (i-direction) and 710 columns in the northwest-to-southeast direction (j-direction), for a total of 332,990 cells per layer, or 1,664,950 cells total. Each model cell of the Yucaipa Groundwater Model represents an area of 102.5 ft x 102.5 ft (see Figure 35). The model grid is rotated 27^{o} clockwise.

Recharge and discharge components in the Yucaipa Groundwater Model include the following terms:

- Recharge:
  - Recharge from Mountain Front Runoff
  - Areal Recharge from Precipitation
  - Return Flow from Applied Water (Anthropogenic Return Flow)
  - Artificial Recharge
  - Streambed Percolation
- Discharge:
  - Groundwater Pumping
  - Evapotranspiration
  - Rising Water Discharge to Streamflow
  - Underflow Outflow to San Timoteo Canyon
  - Underflow Outflow to the SBBA

Boundary conditions for the Yucaipa Basin Model are shown on Figure 36. A complete description of each recharge and discharge term included in the Yucaipa Basin Model, along with measured and estimated values, can be found in the existing model report (GEOSCIENCE, 2017).

The Yucaipa Basin Model was calibrated from January 1998 through December 2015 using a monthly stress period. The acceptable model calibration is reflected by a low relative error of 2.9% and ability to reflect observed temporal trends in monitored wells. Common modeling practice is to consider a good fit between measured and model-calculated water levels if the relative error is below 10% (Spitz and Moreno, 1996).

5.1.2 Update of the Yucaipa Basin Model

The existing Yucaipa Basin Model already has the same orientation and cell size as the Integrated SAR Model. Therefore, the boundary conditions and other model features were transferred directly to the Integrated SAR Model domain.

Since the existing Yucaipa Basin Model was only calibrated from January 1998 through December 2015, the model recharge and discharge terms were updated monthly from January 1966 through December 1997 and January 2016 through December 2016 to create a data set that covered the entire Integrated SAR Model calibration period.

5.1.3 Updated Yucaipa Basin Model Results

After the model input files were updated, the Yucaipa Basin Model was rerun. Model-calculated water levels were compared to observed water levels from calibration target wells. Water level calibration target wells for the Yucaipa Basin Model are shown on Figure 37 while selected hydrographs for the Yucaipa Basin Model are provided in Appendix H.

Figure 38 shows a scatter plot of measured versus model-calculated water levels. As can be seen, most of the points are clustered around a diagonal line (representing where measured water levels match model-calculated water levels). This reflects a good match between measured and model-calculated water levels. There is also good correlation between the existing Yucaipa Basin Model and Updated Yucaipa Basin Model, indicating that the model update and incorporation into the Integrated SAR Model domain was successful.

Water level residual statistics are summarized in the table below.

Table 5-1. Water Level Residual Statistics – Yucaipa Basin Model

Residual Statistic	Previous Model (GEOSCIENCE, 2017) (1998-2015)	Updated Yucaipa Basin Model		
		(1998-2015)	(1966-1997, 2016)	(1966-2016)
Mean Residual[1] [ft]	5.40	21.68	36.86	27.51
Standard Deviation [ft]	64.52	77.97	66.88	74.27
Relative Error[2]	2.9%	3.5%	2.7%	2.9%

[1]Residual = measured water level minus model-calculated water level

[2]Relative Error = standard deviation of the residuals divided by the observed water level range

As shown in the table above, the Updated Yucaipa Basin Model has a relative error of 2.9% for the period from 1966 through 2016, which is the same as the relative error for the existing Yucaipa Basin Model. This is a further indication that the Updated Yucaipa Basin Model was incorporated successfully into the Integrated SAR Model domain.

The average annual groundwater budgets for the Updated Yucaipa Basin Model during the period from 1966 through 2016 are provided on Figure 39. As shown, the basin storage decreases by an average of 2,570 acre-ft/yr from 1966 to 2016. The cumulative change in groundwater storage is also shown on Figure 40. The change in groundwater storage shows a very muted response to changes in hydrologic conditions, as indicated by the cumulative departure from mean precipitation at the San Bernardino County Hospital Precipitation Station.

5.2 SBBA Model Update

5.2.1 Existing SBBA Model

The Refined Basin Flow Model/Newmark Groundwater Flow Model (RBFM/NGFM), also known as the SBBA Model, is a five-layered model that was developed by GEOSCIENCE in 2009 for Valley District. It is currently being updated by GEOSCIENCE and Stantec. The model layers consist of:

- Layer 1 – Upper Confining Member and Upper Water-Bearing Zone;
- Layer 2 – Middle Confining Member;
- Layer 3 – Middle Water-Bearing Zone;
- Layer 4 – Lower Confining Member; and
- Layer 5 – Lower Water-Bearing Zone.

The SBBA Model was originally constructed with MODFLOW-2000. During current work with Stantec, the computer code was updated with MODFLOW-NWT. The model area covers approximately 253 square miles (161,811 acres). The SBBA Model consists of 470 rows in the northeast-to-southwest direction (i-direction) and 1,427 columns in the northwest-to-southeast direction (j-direction), for a total of 3,353,450 cells (see Figure 41). Each model cell is 102.5 ft x 102.5 ft and the model grid is rotated at 27^{o} clockwise.

Recharge and discharge components in the SBBA Model include the following terms:

- Recharge:
  - Recharge from Mountain Front Runoff
  - Areal Recharge from Precipitation
  - Return Flow from Applied Water
  - Artificial Recharge
  - Streambed Percolation
  - Underflow Inflow from Yucaipa Basin
- Discharge:
  - Groundwater Pumping
  - Evapotranspiration
  - Underflow Outflow to Rialto-Colton Basin

Boundary conditions for the SBBA Model are shown on Figure 42. A complete description of each recharge and discharge term included in the SBBA Model can be found in the existing model report (GEOSCIENCE, 2009).

The SBBA Model was calibrated from January 1983 through December 2015 with a monthly stress period. The acceptable model calibration is reflected by a low relative error of 3.5%.

5.2.2 Update of the SBBA Model

The existing SBBA Model already has the same orientation and cell size as the Integrated SAR Model. Therefore, the boundary conditions and other model features were transferred directly to the Integrated SAR Model domain.

During the model update process, the SBBA Model recharge and discharge terms (calibrated from January 1983 through 2015) were updated monthly from January 1966 through December 1982 and January 2016 through December 2016 to create a data set that covered the entire Integrated SAR Model calibration period.

5.2.3 Updated SBBA Model Results

After the model input files were updated, the SBBA Model was rerun. Model-calculated water levels were compared to observed water levels from calibration target wells. Water level calibration target wells for the SBBA Model are shown on Figure 43 while selected hydrographs for the SBBA Model are provided in Appendix I.

Figure 44 shows a scatter plot of measured versus model-calculated water levels. As can be seen, most of the points are clustered around a diagonal line, which reflects a good match between measured and model-calculated water levels.

Water level residual statistics are summarized in the table below.

Table 5-2. Water Level Residual Statistics – SBBA Model

Residual Statistic	Previous Model (Stantec and GEOSCIENCE)	Updated SBBA Model		
	(1983-2015)	(1983-2015)	(1966-1982, 2016)	(1966-2016)
Mean Residual[1] [ft]	11.14	11.14	-14.12	8.61
Standard Deviation [ft]	64.16	64.16	63.85	64.57
Relative Error[2]	3.5%	3.5%	3.8%	3.5%

[1]Residual = measured water level minus model-calculated water level

[2]Relative Error = standard deviation of the residuals divided by the observed water level range

As shown in the table above, the Updated SBBA Model has a relative error of 3.5% for the period from 1966 through 2016, which is the same as the relative error for the existing SBBA Model. While the residual statistics indicate an acceptable level of model integration, additional calibration was conducted on the Updated SBBA Model to improve performance in this area.

The average annual groundwater budgets for the Updated SBBA Model during the period from 1966 through 2016 are provided on Figure 45. As shown, the basin storage decreases by an average of 1,410 acre-ft/yr from 1966 to 2016. The cumulative change in groundwater storage is also shown on Figure 46. The change in groundwater storage shows a marked response to changes in hydrologic conditions, as indicated by the cumulative departure from mean precipitation at the San Bernardino County Hospital Precipitation Station.

5.3 Rialto-Colton Basin Model Update

5.3.1 Existing Rialto-Colton Basin Model

The Rialto-Colton Basin Groundwater Model was developed in 2015 by GEOSCIENCE for Valley District, West Valley Water District (WVWD), Goodrich, City of Rialto and City of Colton. The model was created to simulate flow and solute transport in the unconsolidated to consolidated sediments of the Rialto-Colton Groundwater Basin and consists of seven distinct model layers:

- Layer 1 – River Channel Deposits;
- Layer 2 – Upper Water-Bearing Unit;
- Layer 3 – Middle Water-Bearing Unit Shallow Zone (Intermediate Aquifer or B Aquifer);
- Layer 4 – Middle Water-Bearing Unit Upper Deep Zone (BC Aquitard or Perching Layer);
- Layer 5 – Middle Water-Bearing Unit Lower Deep Zone (Upper Regional Aquifer or C Aquifer);
- Layer 6 – Lower Water-Bearing Unit (Lower Regional Aquifer); and
- Layer 7 – Consolidated Deposits.

The Rialto-Colton Basin Model was constructed using MODFLOW-NWT. The model covers an area of approximately 97 square miles (62,280 acres) with a finite-difference grid consisting of 278 rows in the northeast to southwest direction and 938 columns in the northwest to southeast direction for a total of 260,764 cells per layer, or 1,825,348 cells total. Each model cell represents an area of approximately 102.5 ft x 102.5 ft (see Figure 47). The model grid is rotated 27° clockwise.

Recharge and discharge components in the Rialto-Colton Basin Model area include the following terms:

- Recharge:
  - Underflow Inflow from SBBA (Lytle Basin – see Figure 1)
  - Underflow Inflow from SBBA (Bunker Hill Basin – see Figure 1)
  - Artificial Recharge of Imported Water
  - Ungaged Runoff and Subsurface Inflow from the San Gabriel Mountains
  - Ungaged Runoff and Subsurface Inflow from the Badlands
  - Anthropogenic Return Flow
  - Areal Recharge from Precipitation
  - Streambed Percolation from the SAR and Warm Creek
  - Percolation from Irrigation Canal
- Discharge:
  - Groundwater Pumping

- Evapotranspiration
- Underflow Outflow to North Riverside Basin
- Underflow Outflow to Chino Basin

Boundary conditions for the Rialto-Colton Basin Model are shown on Figure 48. A complete description of each recharge and discharge term included in the Rialto-Colton Basin Model, along with measured and estimated values, can be found in the existing model report (GEOSCIENCE, 2015).

The Rialto-Colton Basin flow model was successfully calibrated through a steady state calibration for 1945 and a transient calibration from 1945 through 2014. The transient calibration uses annual stress periods from 1945 through 1969 and monthly stress periods from 1970 through 2014. The acceptable model calibration is reflected by a relative error of 4.3% for the steady state calibration and 6.2% for the transient calibration period.

5.3.2 Update of the Rialto-Colton Basin Model

The existing Rialto-Colton Basin Model already has the same orientation and cell size as the Integrated SAR Model. Therefore, the boundary conditions and other model features were transferred directly to the Integrated SAR Model domain.

In addition, since the existing Rialto-Colton Basin Model calibration period spans from January 1945 through December 2014, the model recharge and discharge terms only had to be updated monthly from January 2015 through December 2016 to create a data set that covered the entire Integrated SAR Model calibration period. The recharge and discharge terms for 1966 through 1969 were also changed from annual stress periods to monthly stress periods.

5.3.3 Updated Rialto-Colton Basin Model Results

After the model input files were updated, the Rialto-Colton Basin Model was rerun. Model-calculated water levels were compared to observed water levels from calibration target wells. Water level calibration target wells for the Rialto-Colton Basin Model are shown on Figure 49 while selected hydrographs for the Rialto-Colton Basin Model are provided in Appendix J.

Figure 50 shows a scatter plot of measured versus model-calculated water levels. As can be seen, most of the points are clustered around a diagonal line, which reflects a good match between measured and model-calculated water levels. There is also good correlation between the existing Rialto-Colton Basin Model and Updated Rialto-Colton Basin Model, indicating that the model update and incorporation into the Integrated SAR Model domain was successful.

Water level residual statistics are summarized in the table below.

Table 5-3. Water Level Residual Statistics – Rialto-Colton Basin Model

Residual Statistic	Previous Model (GEOSCIENCE, 2015) (1945-2014)	Updated Rialto-Colton Basin Model		
		(1966-2014)	(2015-2016)	(1966-2016)
Mean Residual[1] [ft]	-6.66	-0.92	-2.71	-1.06
Standard Deviation [ft]	69.40	60.48	46.56	59.52
Relative Error[2]	6.2%	5.8%	4.6%	5.7%

[1]Residual = measured water level minus model-calculated water level
[2]Relative Error = standard deviation of the residuals divided by the observed water level range

As shown in the table above, the Updated Rialto-Colton Basin Model has a relative error of 5.7% for the period from 1966 through 2016, which is better than but comparable to the relative error of 6.2% for the existing Rialto-Colton Basin Model. This is a further indication that the Updated Rialto-Colton Basin Model was incorporated successfully into the Integrated SAR Model domain.

The average annual groundwater budgets for the Updated Rialto-Colton Basin Model during the period from 1966 through 2016 are provided on Figure 51. As shown, the basin storage decreases by an average of 2,620 acre-ft/year from 1966 to 2016. The cumulative change in groundwater storage is also shown on Figure 52. The change in groundwater storage shows a slightly delayed response to changes in hydrologic conditions, as indicated by the cumulative departure from mean precipitation at the San Bernardino County Hospital Precipitation Station. In addition, while the average change in groundwater storage is negative, the groundwater in storage at the end of the Integrated SAR Model simulation period (2016) is approximately equal to the starting groundwater storage in 1966.

5.4 Riverside-Arlington Basin Model Update

5.4.1 Existing Riverside-Arlington Basin Model

The Riverside-Arlington Basin Model was developed by WRIME in 2010 for Western. It is a three layer model consisting of the following:

- Layer 1 – Coarse Alluvium and River Channel Deposits;
- Layer 2 – Upper Alluvium; and

- Layer 3 – Lower Alluvium.

The Riverside-Arlington Basin Model was constructed using the MODFLOW-2000 computer code and covers an area of approximately 95.5 square miles (61,120 acres). The model grid consists of 300 rows in the northwest-to-southeast direction (i-direction) and 609 columns in the southwest-to-northeast direction (j-direction), for a total of 182,700 cells per model layer (see Figure 53). Each model cell represents an area of 164 ft x 164 ft, and the entire grid is rotated 51° counterclockwise.

Recharge and discharge components in the Riverside-Arlington Basin Model area include the following terms:

- Recharge:
  - Recharge from Mountain Front Runoff
  - Deep Percolation of Precipitation and Applied Water (Recharge from Areal Precipitation and Anthropogenic Return Flow)
  - Underflow Inflow from SBBA (Bunker Hill Basin – see Figure 1)
  - Underflow Inflow from Rialto Basin
  - Streambed Percolation
  - Recharge from RIX Percolation

- Discharge:
  - Groundwater Pumping
  - Pumping from RIX
  - Underflow Outflow to Chino Basin
  - Underflow Outflow to Hole Lake Area
  - Underflow Outflow to Temescal Basin at Arlington Narrows
  - Rising Water Discharge to Streamflow

Boundary conditions for the Riverside-Arlington Basin Model are shown on Figure 54. A complete description of each recharge and discharge term included in the Riverside-Arlington Basin Model, along with measured and estimated values, can be found in the existing model report (WRIME, 2010).

The Riverside-Arlington Basin Model was calibrated from January 1965 through December 2007 using a monthly stress period and included a validation period from January 2006 through December 2007. The acceptable model calibration is reflected by a low relative error of 5% for both the model calibration and validation periods.

5.4.2 Update of the Riverside-Arlington Basin Model

The existing Riverside-Arlington Basin Model has a different orientation and cell size than the Integrated SAR Model. Therefore, in order to incorporate the existing model into the Integrated SAR Model domain, the boundary conditions and other model features were transferred to a grid rotated at 27° clockwise with a cell size of 102.5 ft x 102.5 ft.

Since the existing Riverside-Arlington Basin Model was only calibrated from January 1965 through December 2007, the model recharge and discharge terms were updated monthly from January 2008 through December 2016 to create a data set that covered the entire Integrated SAR Model calibration period.

5.4.3 Updated Riverside-Arlington Basin Model Results

After the model input files were updated, the Riverside-Arlington Basin Model was rerun. Model-calculated water levels were compared to observed water levels from calibration target wells. Water level calibration target wells for the Riverside-Arlington Basin Model are shown on Figure 55 while selected hydrographs for the Riverside-Arlington Basin Model are provided in Appendix K.

Figure 56 shows a scatter plot of measured versus model-calculated water levels. As can be seen, most of the points are clustered around a diagonal line, which reflects a good match between measured and model-calculated water levels. There is also good correlation between the existing Riverside-Arlington Basin Model and Updated Riverside-Arlington Basin Model, indicating that the model update and incorporation into the Integrated SAR Model domain was successful.

Water level residual statistics are summarized in the table below.

Table 5-4. Water Level Residual Statistics – Riverside-Arlington Basin Model

Residual Statistics	Previous Model (WRIME 2010)		Updated Riverside-Arlington Basin Model			
	Calibration (1965-2005)	Validation (2006-2007)	(1966-2005)	(2006-2007)	(2008-2016)	(1966-2016)
Mean Residual[1] [ft]	12.10*	13.20*	1.91	6.94	-7.14	-0.37
Standard Deviation [ft]	16.00	11.80	17.55	12.29	22.29	19.29
Relative Error[2]	5.0%	5.0%	5.8%	4.5%	8.6%	6.3%

[1]Residual = measured water level minus model-calculated water level

[2]Relative Error = standard deviation of the residuals divided by the observed water level range

*Value represents mean absolute residual

As shown in the table above, the Updated Riverside-Arlington Basin Model has a relative error of 6.3%, which is slightly higher than but comparable to the existing model relative error. This is a further indication that the Updated Riverside-Arlington Basin Model was incorporated successfully into the Integrated SAR Model domain.

The average annual groundwater budgets for the Updated Riverside-Arlington Basin Model during the period from 1966 through 2016 are provided on Figure 57. As shown, the basin storage decreases by an average of 2,090 acre-ft/yr from 1966 to 2016. The cumulative change in groundwater storage is also shown on Figure 58. The change in groundwater storage shows a muted response to changes in hydrologic conditions, as indicated by the cumulative departure from mean precipitation at the San Bernardino County Hospital Precipitation Station.

6.0 CONSTRUCTION AND CALIBRATION OF THE CHINO BASIN MODEL

6.1 Model Construction

Unlike the other previous groundwater models, model files for the existing Chino Basin Model were not available. Therefore, a Chino Basin model component was constructed for the Integrated SAR Model based on information provided in the 2013 Chino Basin Groundwater Model Update Report (WEI, 2015), data from the Chino Basin Watermaster and entities within the groundwater basin, and the lithologic model developed for the Chino Basin area. Available information was digitized and assembled in a GIS database.

The Chino Basin Model is located in the southwest portion of the Integrated SAR Model, and the lower left corner is coincident with that of the integrated model domain. The Chino Basin Model consists of three layers, representing:

- Layer 1 – Shallow Aquifer;
- Layer 2 – Upper Deep Aquifer; and
- Layer 3 – Lower Deep Aquifer.

The Chino Basin Model was constructed using MODFLOW-2000 and covers an area of approximately 536 square miles (342,958 acres). The finite-difference grid consists of 1,292 rows in the northeast to southwest direction and 1,100 columns in the northwest to southeast direction for a total of 1,421,220 cells per layer, or 4,263,600 cells total. Each model cell represents an area of 102.5 ft x 102.5 ft (see Figure 59). The model grid is rotated 27° clockwise.

Recharge and discharge components in the Chino Basin Model area include the following fluxes:

- Recharge:
  - Areal Recharge from Precipitation and Anthropogenic Return Flow
  - Artificial Recharge
  - Underflow Inflow from Chino Hills, Six Basins, Cucamonga Basin, Rialto-Colton Basin, Jurupa Mountains, Pedley Hills, and La Sierra Hills
  - Underflow Inflow from North Riverside Basin, Arlington Narrows, Riverside Narrows, and Santa Ana Mountains
  - Streambed Percolation

- Discharge:
  - Groundwater Pumping (Pool 1: Agricultural)

- Groundwater Pumping (Pool 2 & 3: Non-Agricultural and Appropriator)
- Groundwater Pumping (Chino Basin Desalter Authority; CDA)
- Evapotranspiration
- Rising Water Discharge to Streamflow

Locations of boundary fluxes were spatially located in the model grid and volumetric fluxes were distributed to model cells of each boundary type. The locations of model boundary conditions for the Chino Basin Model are shown on Figure 60.

6.1.1 Aquifer Parameters

6.1.1.1 Layer Elevations

Land surface elevation, as determined from digital elevation models (DEMs) for the 7.5” topographic quadrangles which cover the Chino Basin Model area, were used as the top of Model Layer 1. The top of Model Layers 2 and 3 were considered the bottom of Model Layers 1 and 2, respectively. The bottom elevation of Model Layer 3 is considered the effective base of the aquifer system. Delineation of the boundaries between the model layers was based on previous published cross-sections and model layer designations (WEI, 2015), as well as the lithologic model constructed for the Chino Basin. Model layer thicknesses for the Chino Basin Model are shown on Figure 61.

6.1.1.2 Hydraulic Conductivity

Hydraulic conductivities for each of the three model layers were developed from the lithologic model. The approach to estimate an initial horizontal hydraulic conductivity distribution was a thickness-weighted average of hydraulic conductivities of each lithologic type. Horizontal hydraulic conductivity was computed using the equation:

$$F_1 K_1 + F_2 K_2 + \ldots\ldots + F_n K_n$$

Where:

F = the fraction of each model cell of a given lithologic type,
K = the average estimated hydraulic conductivity for that lithologic type.

This approach utilized fifteen different lithologic types. The hydraulic conductivity of each lithologic type was estimated based on literature ranges (Halford and Kuniansky, 2002) and adjusted using a best-fit approach to match pumping test data from the Chino Basin. A zonal calibration was conducted and hydraulic conductivities were manually adjusted in each calibration zone to fit observed water levels in the model domain. The resulting horizontal and vertical hydraulic conductivities for each layer are presented in Figure 62 and 63, respectively. As shown, vertical hydraulic conductivity decreases significantly towards the center of the model domain in the vicinity of the Riley Barrier and Central Avenue fault.

6.1.1.3 Storativity

Both specific yield and specific storage values were used in the Chino Basin Model. The type of storativity value used depended on the nature of the model layer through time (i.e., unconfined or confined). Specific yield and specific storage values were estimated initially and final parameter values were based on zonal calibration to measured water level data. The distribution of model storage parameters is presented on Figures 64 and 65 for specific yield and storativity, respectively.

6.1.1.4 Horizontal Flow Barriers

The Central Avenue Fault, Riley Barrier, and the west branch of the Rialto-Colton Fault were modeled with the Horizontal Flow Barrier Package by assigning a lower hydraulic conductivity value to the conductance term between model cells along the fault trace. The locations of the horizontal flow barriers in the Chino Basin Model are shown on Figure 66.

6.1.2 Recharge and Discharge Terms

6.1.2.1 Underflow Inflow

Subsurface boundary inflows consist of groundwater underflow into the Chino Basin Model domain from adjacent groundwater basins and from mountain front recharge processes. Subsurface boundary inflows were simulated using specified flux and general head boundaries. The locations of subsurface boundary inflows are shown on Figure 67. Subsurface boundary inflow volumes simulated with specified flux boundaries are shown by location and volume on Figure 68. Subsurface boundary inflow from Chino Hills, Six Basins, Cucamonga Basin, Rialto-Colton Basin, Jurupa Mountains and Pedley Hills, and La Sierra Hills was simulated by assigning a specified flux through the Well Package. Subsurface boundary inflow from Riverside Basin, Riverside Narrows, Arlington Narrows, and the Santa Ana Mountains was simulated by using general head boundaries, which calculate the amount of underflow based on the water level gradient across the boundary. Water levels and water level hydrographs in the vicinity of the general head boundaries were used to establish water levels for each general head boundary.

6.1.2.2 Artificial Recharge

Artificial recharge data were compiled from three sources. IEUA provided monthly recharge data by artificial recharge basin from 2005 to 2016. The Chino Basin Watermaster provided similar monthly recharge data from 1978 to 2016. Artificial recharge data was also estimated prior to 1978 as part of the WEI Chino Basin Groundwater Model and was available in an annual format (WEI, 2015). Recycled, imported, and storm water recharge were compiled for each spreading basin. Recharge locations are shown on Figure 69 while recharge volumes are reported on Figure 70. Monthly recharge volumes were simulated in the groundwater model as specified fluxes using the MODFLOW Well Package.

6.1.2.3 Areal Recharge from Precipitation and Anthropogenic Return Flow

Areal recharge from precipitation and anthropogenic return flow is a primary inflow to the Chino Basin groundwater model and is composed of the deep percolation of precipitation, return flows from agricultural, municipal and supplemental water supplies, and leakage from the municipal pipe network and from septic tanks. Areal recharge from precipitation was estimated using model results from the surface water model for each individual subbasin in the groundwater model domain (refer to Section 7.0). Recharge zones for the groundwater model were based on the subbasin delineation from this surface water model and are shown on Figure 71.

Municipal return flows, leakage from the pipe network, and leakage from septic tanks were estimated for each recharge zone corresponding to a surface water model subbasin. Agricultural return flows were accounted for by applying a net return flow of 34% for agricultural wells in Model Layer 1. Municipal return flows were estimated as ten percent of municipal production in each recharge zone (assuming 50% outdoor water usage and 20% return flow). Supplemental return flow was estimated following the same methodology used for municipal return flows. Leakage from the municipal pipe network was assumed to be 2% of municipal pumping, and was distributed by recharge zone. Septic tank return flow was estimated based on volumes reported in the WEI 2013 Chino Basin Model Update (WEI, 2015).

As shown on Figure 72, areal recharge from precipitation totaled approximately 20,430 acre-ft/yr on average, or approximately 12% of average rainfall in the Chino Basin. Recharge from return flow averaged approximately 54,960 acre-ft/yr, as shown on Figure 73.

6.1.2.4 Streambed Percolation

Streambed percolation was simulated in the groundwater model using the Streamflow Routing Package. The location of simulated streamflow segments is presented on Figure 74 and include the SAR, Chino Creek, Mill Creek, and Temescal Wash. Recycled water discharge was also incorporated into the streamflow package. The streambed hydraulic conductivity was estimated and adjusted during the model calibration process.

6.1.2.5 Groundwater Pumping

Groundwater pumping data were collected from the Chino Basin Watermaster and municipal water providers within the active model area. Since Watermaster records of agricultural pumping are incomplete through the early 2000s, agricultural pumping was updated to reflect the pumping reported by WEI in the Chino Basin Model report (WEI, 2015). Information on well total depth and screened interval was used to determine which model layer pumping was occurring from. Where groundwater pumping occurred from multiple model layers, groundwater pumping was assigned to those layers based on the model layer transmissivity and screen information. The model incorporates data from a total of 1,425 pumping wells in the Chino Basin – the locations of which are shown on Figure 75. The volume of groundwater pumping by type is shown on Figure 76. During the model calibration period (1966 through 2016), groundwater pumping in the Chino Basin area has shifted from being primarily agricultural to mostly municipal.

6.1.2.6 Evapotranspiration

Consumptive use by riparian vegetation in the Chino Basin Model was simulated using the MODFLOW Evapotranspiration Package and based on the riparian vegetation mapping and consumptive use estimates developed by Aspen and BGW (refer to Section 4.1.7). Each vegetation group was assigned a maximum monthly evapotranspiration rate by stress period and an extinction depth at which evapotranspiration processes cease. Evapotranspiration extinction depths for riparian plant functional groups were developed from literature values (Maddock et al., 2012).

Six periods (1965, 1977, 1988, 1996, 2004, 2015) were used to assign coverages of the different riparian vegetation types. Additional riparian vegetation extent was also mapped for 1960, 1977, 1985, 1999, 2006, and 2016 for the Annual Report of the Prado Basin Habitat Sustainability Committee – Water Year 2015/2016 (WEI, 2017). The locations of riparian vegetation over the model calibration period are shown on Figures 77 through 82. These areas of riparian vegetation were added to the model. Where no vegetation type classification was available, the properties of deep-rooted riparian vegetation were assumed. In general, the riparian vegetated area increases throughout the study period.

6.1.2.7 Rising Water Discharge to Streamflow

A stream gains or loses water depending on the relative head in the stream and in the underlying aquifer. When the head in the stream is higher than the head in the aquifer, the stream loses water to the aquifer;

when the head in the stream is lower than the head in the aquifer, the stream gains water from the aquifer. The amount of water lost by the groundwater system to streamflow through rising water is a model-calculated value. The location of rising water discharge to streamflow in the Chino Basin Model is shown on Figure 83.

6.2 Initial Model Calibration

Model calibration is the process of adjusting the model parameters to produce the best-fit between simulated and observed groundwater system responses. During the Chino Basin Model calibration, model parameters were manually adjusted within acceptable limits until model-generated water levels match historical water level measurements at wells across the model area, thereby reducing residual error. The Chino Basin Model was calibrated using this industry standard “history matching” technique for the period from January 1966 through December 2016. The aquifer parameters varied during the model calibration included horizontal and vertical hydraulic conductivity, specific yield, specific storage, horizontal flow barrier conductance, and streambed conductance.

6.2.1 Water Levels

The calibration process used 523,086 water level measurements from 115 calibration target wells from which to match model generated head values against the measured values, including water level targets adjacent to the Chino Creek, Mill Creek, and Prado Basin from IEUA Prado Basin Habitat Sustainability Project wells. If a target well was screened in multiple layers, the target was assigned to the shallowest screened layer. Target wells used for model flow calibration are shown on Figure 84. Water level elevations in the Chino Basin generally slope from north-northeast to south-southwest, as groundwater flows from source areas towards discharge in the SAR and its tributaries.

Figure 85 shows a scatter plot of measured versus model-calculated water levels. As can be seen, most of the points are clustered around a diagonal line (representing where measured water levels match model-calculated water levels). This reflects a good match between measured and model-calculated water levels.

Table 6-1. Summary of Chino Basin Model Calibration - Water Level Statistic

Parameter	Statistic
Mean Residual[1]	17.86 ft
Standard Deviation	58.93 ft
Relative Error[2]	5.2%

[1]Residual = measured water level minus model-calculated water level
[2]Relative Error = standard deviation of the residuals divided by the observed water level range

The good calibration is further supported by a low relative error of 5.2%, which is well below the relative error of 10% (Spitz and Moreno, 1996). Appendix L shows selected hydrographs for the Chino Basin Model calibration from 1966 through 2016. In general, the model-calculated water levels match well with the measured water levels. However, an average residual of 17.86 ft indicates model-simulated water levels are generally lower than observed water levels in the model. Additional work was conducted during calibration of the Integrated SAR Model to improve model calibration in this area. The improved final Chino Basin calibration is presented in Section 9.3.1.5.

6.2.2 Streamflow

Model-calculated streamflow at Prado Dam was also compared with observed streamflow at the SAR below Prado Dam Gaging Station. A scatter plot of measured versus model-simulated monthly streamflow is shown on Figure 86 while a hydrograph at this location is shown on Figure 87. In general, model-simulated streamflow shows a good correlation with observed values. An R^2 value of 0.84 and average residual of -4.5 cfs for monthly streamflow (1.6% of the observed mean monthly streamflow) was computed for the model calibration period.

6.2.3 Change in Groundwater Storage

The water budgets for the Chino Basin Model calibration period (1966 through 2016) are presented on Figure 88. As shown, the calibration period shows a higher annual total outflow than total inflow, resulting in an annual average change in groundwater storage of approximately -16,540 acre-ft/yr. This is evidenced by generally declining water levels throughout Chino Basin over the model simulation period. The cumulative change in annual groundwater storage is also shown on Figure 89. Like many of the other models, the change in groundwater storage responds to changes in hydrologic conditions recorded at the San Bernardino County Hospital Precipitation Station, but shows an overall declining trend.

7.0 UPPER SANTA ANA RIVER WATERSHED MODEL

In order to simulate the streamflow more accurately, runoff generated from precipitation within the Upper Santa Ana Valley Groundwater Basin was calculated using a watershed model, which was then included in the Streamflow Package for the Integrated SAR Model. The Upper SAR Watershed Model (see Figure 90) was developed for SAWPA during the SAR Waste Load Allocation Model (WLAM) Update using the Hydrologic Simulation Program - Fortran (HSPF) computer code (GEOSCIENCE, 2019e). This watershed model was calibrated for the period from October 1, 2006 through September 30, 2016 (Water Year 2007 through 2016) using 2012 land use. For the Integrated SAR Model, the watershed model calibration period was expanded to include the period from January 1966 through December 2016 with additional land use maps from 1963, 1984, 1994 and 2005. The following sections discuss the development and calibration of the watershed model.

7.1 Watershed Model Computer Code

The watershed model for the Upper Santa Ana Valley Groundwater Basin was developed using HSPF. HSPF is a successor to the FORTRAN version of the Stanford Watershed Model (SWM). The SWM evolved over the period from approximately 1956 through 1966. Work in 1974 resulted in the widely available codes developed for and with support of the United States Environmental Protection Agency (EPA). HSPF is a comprehensive and physically based watershed model that can simulate all water cycle components with a time step of less than one day. Figure 91 is a schematic diagram showing the water cycle components simulated by the HSPF.

7.2 Watershed Model Development

The Upper SAR Watershed area was divided into 526 sub-watersheds (see Figure 92). Delineation of the sub-watersheds was based on topography, drainage pattern, type of stream channel, and location of streamflow gaging stations. Each sub-watershed consists of a stream segment and either pervious, impervious, or a combination both land surfaces. Sub-watersheds, or elements, are areas that are assumed to have similar hydrogeologic characteristics. They were created for the Upper SAR Watershed with the US EPA BASINS 4.1 program. The program segments the watershed into several sub-watersheds and stream reaches using a delineation tool and a USGS 10-meter-by-10-meter DEM, as well as user-specified outlet locations. The location of these outlets was based on change in channel type (e.g., lined, unlined, etc.) and geography.

7.3 Data Requirements for the Watershed Model

Watershed hydrologic modeling requires a variety of data to characterize the water balance and hydrologic processes that occur in a watershed. These data include:

- Land surface elevations,
- Soil types,
- Land use,
- Precipitation,
- Evaporation,
- Stream Channel Characteristics,
- Discharges, and
- Streamflow.

Sources of data were included in Database Plan for the Integrated SAR Model (Appendix B). The following sections briefly describe the types of input data.

7.3.1 Land Surface Elevations

Land surface elevations were obtained by using a USGS 10-meter-by-10-meter DEM in ESRI ArcMap 10. The DEMs are used to evaluate surface water runoff patterns, and in turn to delineate the watershed and sub-watershed boundaries.

7.3.2 Soil Types

Soil type and distribution affects infiltration, surface runoff, interflow, groundwater storage, and deep groundwater losses. Information on both type and distribution of soil types in the study area is available from an ESRI shapefile of Soil Survey Geographic (SSURGO) Database hydrologic soil group information (Soil Survey Staff et al., 2011) (see Figure 93). There are four basic types of soils under this classification system (Group A through D), which are based on soil texture and properties. SSURGO describes each type as the following:

- Group A soils have a high infiltration rate (low runoff potential) when thoroughly wet. They consist mainly of deep, well drained to excessively drained sands or gravelly sands and have a high rate of water transmission. This would be sand, loamy sand, or sandy loam types of soils.
- Group B soils have a moderate infiltration rate when thoroughly wet. They consist mainly of moderately deep or deep, moderately drained soils that have moderately fine texture to

moderately coarse texture and have a moderate rate of water transmission. This includes the silt loam and loam soils.

- Group C soils have a slow infiltration rate when thoroughly wet. They consist mainly of soils having a layer that impedes the downward movement of water or soils of moderately fine texture or fine texture. They have a slow rate of water transmission. The predominant soil in this group is a sandy clay loam.
- Group D soils have a very slow infiltration rate (high runoff potential) when thoroughly wet. They consist chiefly of clays that have a high shrink-swell potential, soils that have a high water table, soils that have a claypan or clay layer at or near the surface, and soils that are shallow over nearly impervious material. Therefore, they have a very slow rate of water transmission. This includes clay loam, silty clay loam, sandy clay, silty clay or clay type soils. Bedrock is also included in this group due to its very low infiltration rate.

A relative infiltration rate is associated with each soil group, ranging from soils with a high infiltration rate characteristic of coarser sediments (Group A) to a very low infiltration rate characteristic of finer grained materials (Group D). Each sub-watershed is given an average infiltration index based on the percentage of the various soil types within its borders. The infiltration rate was assigned initially based on the calculated infiltration index and adjusted during model calibration.

7.3.3 Land Use

Land use and development affect how water enters or leaves a system by altering infiltration, surface runoff, location, degree of evapotranspiration, and where water is applied in the form of irrigation. Since the model calibration period covers the period from January 1, 1966 through December 31, 2016, land use maps from 1963, 1984, 1993, 2005, and 2012 (Figures 94 through 98) were used to locate and designate areas as being pervious or impervious within the model boundary during the simulation periods 1966-1975, 1976-1986, 1987-1996, 1997-2006, and 2007-2016, respectively. Six main land use categories were used for the purpose of identifying perviousness:

- Agriculture/Golf Course/Parks,
- Commercial/Industrial/Public Facility,
- Open Space/Dry Agriculture/Water Body,
- Residential Low Density,
- Residential Medium Density, and
- Residential High Density.

The land use category determines to what degree areas are pervious or impervious. Even urban areas are assumed to have a percentage of perviousness associated with them (i.e., landscaping). The assumed pervious percentages for the different land use categories are presented in the table below (Aqua Terra, 2005).

Table 7-1. Assumed Pervious Percentages for Land Use

Land Use Category	% Pervious
Agriculture/Golf Courses/Parks	100
Open Space/Dry Agriculture/Water	100
Commercial/Industrial/Public Facilities	20
Residential Low Density	90
Residential Medium Density	50
Residential High Density	40

7.3.4 Precipitation

Precipitation adjustment factors were assigned to each sub-watershed. These factors were used to determine average daily precipitation values for each sub-watershed based on the precipitation recorded at selected stations in the Upper SAR Watershed area. Nineteen (19) precipitation stations were chosen for the calculation of the adjustment factors. Locations of these stations are shown on Figures 10 and 99.

The process of calculating the precipitation adjustment factors for each sub-watershed involved the following steps:

- An average annual precipitation value was calculated for each sub-watershed based on isohyetal contours of gridded PRISM historical average annual precipitation in the SAR Ana River Watershed area (see Figure 99).
- The average annual precipitation value from the isohyetal contours was noted for each precipitation station.
- The average annual precipitation values within each sub-watershed were compared to the average precipitation at each precipitation station. The station with an average annual precipitation value closest to that at individual sub-watersheds in the vicinity was used to assign daily values (typically coinciding with Theissen polygon boundaries).

- A precipitation adjustment factor was then calculated by dividing the average annual precipitation value for each sub-watershed by the average precipitation value of the station that was designated as being the closest match in terms of long-term average precipitation (from PRISM isohyetal contours). Precipitation adjustment factors and designated precipitation stations are also shown on Figure 99.
- Historical daily precipitation values for each station were then multiplied by the precipitation adjustment factor to determine daily precipitation within each sub-watershed.

7.3.5 Evapotranspiration

ET is included in the HSPF modeling process using the following methodology:

- Monthly average ETo was collected for California Irrigation Management Information System (CIMIS) ETo Zones 6, 9, and 14 (refer to Figure 100 for zone locations).
- Hourly ET rates were collected from CIMIS stations at the University of California, Riverside (UC Riverside #44; data available from 6/2/1985) and Pomona (Pomona #78; data available from 3/14/1989), located in CIMIS Zones 6 and 9, respectively. The locations of these evaporation stations are also shown on Figure 100. Assumed values for missing hourly data were calculated based on average daily ET at that station or interpolated from recordings on either side of the missing data.
- Adjustment factors were developed for ETo Zones 6 and 9 based on average annual ET rates and data from the CIMIS ET stations. The adjustment factor is equal to the ETo Zone average annual ET divided by the CIMIS station average annual ET.
- The adjustment factors were then used to apply hourly ET rates from the CIMIS station in a given zone to each sub-watershed within that same zone (ET for a given sub-watershed = corresponding ETo Zone CIMIS station hourly ET x adjustment factor). Hourly ET rates were also developed for sub-watersheds within CIMIS ETo Zone 14 based on the monthly average reference ET for that zone. For CIMIS Zone 14, daily evapotranspiration values were assumed to be constant within each month.

For years prior to CIMIS station readings, CIMIS monthly zonal ETo values were used. Daily evapotranspiration values were assumed to be constant within each month.

7.3.6 Streamflow

External inflow into the Integrated SAR Model area is primarily represented by streamflow from tributaries flowing into the Upper Santa Ana Valley Groundwater Basin. The amount of streamflow was quantified based on daily historical gaged data. Figure 101 shows the location of these gaging stations, including Cucamonga, Lytle, Cajon, Devil Canyon, East Twin, City, Plunge, Mill, Carbon, and Santiago Creeks. Streamflow from Seven Oaks Dam outflow (i.e., Santa Ana Canyon) to the SAR was also one of the external sources for the Upper SAR Watershed Model. These discharges were accounted for in the gaged streamflow at the downstream Santa Ana River near Mentone, CA gage. Ungaged streamflow entering the groundwater basin (primarily in the Yucaipa Basin area) was also calculated by the watershed model.

7.3.7 Stream Channel Characteristics

Stream channel characteristics (e.g., lined or unlined) were used to determine the degree to which streamflow is able to infiltrate in stream reaches within the model area. The type of stream channel for each stream reach segment was analyzed to determine the hydraulic behavior through the use of an FTABLE (hydraulic table). FTABLEs determine the infiltration volume of stream reaches by using the HSPF BMP Toolkit created by the USEPA, which takes into account the lining type, slope, Manning's Roughness Coefficient (used for flow calculations), and the length of the stream reach. Each sub-watershed was assigned model parameter values based on the available data in the area.

7.3.8 Wastewater Discharge

Wastewater discharge from wastewater facilities within the model area includes the Beaumont Wastewater Treatment Plant (WWTP), YVWD Henry N. Wochholz Regional Water Recycling Facility (WRF), San Bernardino Water Reclamation Plant (WRP), Rialto WWTP, Colton WWTP, San Bernardino/Colton Rapid Infiltration and Extraction (RIX) Facility, Hole Lake, Riverside Regional Water Quality Control Plant (RWQCP), Western Riverside County Wastewater Authority Plant (RWAP), Eastern Municipal Water District's (EMWD's) Region-Wide Water Recycling System, Elsinore Valley Municipal Water District (EVMWD) Regional Wastewater Reclamation Facility (WWRF), Lee Lake Water District (LLWD) WWTP, City of Corona WWTP, IEUA Regional Plants (RPs), and IEUA's Carbon Canyon WRF (see Figure 14). Additional discharges tributary to the SAR, such as discharges from OCWD's turnout OC-59, were also included in the watershed model.

7.4 Watershed Model Calibration

7.4.1 Calibration Process

Model calibration is a trial-and-error process which consists of iteratively adjusting model parameters, within acceptable ranges, until the model provides a reasonable match between the model-simulated and measured data. Proper calibration is important in order to reduce uncertainty in the model results (Engel et al., 2007). The accuracy of data simulated by the calibrated model is evaluated using the techniques recommended by the one of authors for HSPF (Donigian, 2002).

The model was calibrated against measured streamflow for the period from January 1, 1966 through December 31, 2016. Streamflow data from three major gaging stations along the SAR (see Figure 101 for locations) were used during the calibration process, including:

- Santa Ana River at E Street,
- Santa Ana River at MWD Crossing, and
- Santa Ana River into Prado Dam.

Model calibration was performed in accordance with guidelines provided by the USEPA (2000). The major parameters adjusted during calibration of the Upper SAR Watershed Model included the following:

- Lower zone nominal soil moisture storage,
- Upper zone nominal soil moisture storage,
- Interception storage,
- Interflow inflow parameter,
- Base groundwater recession,
- Fraction of groundwater inflow to deep recharge,
- Fraction of remaining ET from baseflow,
- ET by riparian vegetation,
- Lower zone ET parameter, and
- Function tables (FTABLE) which include physical information (shape, depth, width, slope, length, Manning Factor, and materials), and infiltration rates for reaches of each sub-watershed.

7.4.2 Calibration Criteria

As mentioned above, the Upper SAR Watershed Model was calibrated against measured streamflow at three gaging stations for the period from January 1, 1966 through December 31, 2016. The qualitative calibration results are shown as:

- Hydrographs of measured and model-simulated daily streamflow;
- Hydrographs of measured and model-simulated monthly streamflow;
- Scatterplots of measured versus model-simulated daily streamflow; and
- Scatterplots of measured versus model-simulated monthly streamflow.

In addition to the qualitative calibration results listed above, the quantitative R-squared values between the measured and model-simulated streamflow values were examined in accordance with the performance criteria suggested by Donigian (2002). Streamflow residuals were also evaluated.

7.4.3 Streamflow Calibration Results

Figures 102 through 104 show scatterplots of measured and model-simulated daily streamflow for each gaging station for the period from January 1, 1966 to December 31, 2016. In a perfect calibration, all points (observed along the x-axis and model-simulated along the y-axis) would fall on the diagonal line with a R-squared value of 1. Greater deviation of points from the diagonal line corresponds with lower the R-squared values and poorer model calibration performance. Figures 105 through 107 show scatterplots of measured and model-simulated monthly streamflow for each gaging station for the period from January 1966 through December 2016.

The following table summarizes calibration performance criteria from Donigian (2002), which were used for the Upper SAR Watershed Model calibration.

Table 7-2. Watershed Model Calibration Performance Criteria

Type of Flow Data	R^2 (Goodness-of-Fit)	Calibration Performance
Daily Flow	$R^2 < 0.60$	Poor
	$0.60 < R^2 < 0.70$	Fair
	$0.70 < R^2 < 0.80$	Good
	$R^2 > 0.80$	Very Good
Monthly Flow	$R^2 < 0.65$	Poor
	$0.65 < R^2 < 0.75$	Fair
	$0.75 < R^2 < 0.85$	Good
	$R^2 > 0.85$	Very Good

The results of the Upper SAR Watershed Model calibration are summarized in the following tables.

Table 7-3. Upper SAR Watershed Model Results – Daily Simulated Streamflow Performance

Gaging Station	Avg. Observed Flow [cfs]	Avg. Model-Simulated Flow [cfs]	Mean Residual [cfs]	Mean Residual as % of Avg. Observed Flow	R^2	Performance
Santa Ana River at E Street	75.4	82.7	-8.2	-11%	0.78	Good
Santa Ana River at MWD Crossing	130.5	133.3	2.1	2%	0.74	Good
Santa Ana River into Prado Dam	273.0	262.7	10.3	4%	0.85	Very Good

Table 7-4. Upper SAR Watershed Model Results – Monthly Simulated Streamflow Performance

Gaging Station	Avg. Observed Flow [cfs]	Avg. Model-Simulated Flow [cfs]	Mean Residual [cfs]	Mean Residual as % of Avg. Observed Flow	R^2	Performance
Santa Ana River at E Street	75.9	83.3	-8.4	-11%	0.84	Good
Santa Ana River at MWD Crossing	130.5	134.2	1.8	1%	0.85	Very Good
Santa Ana River into Prado Dam	274.7	264.3	10.4	4%	0.94	Very Good

As seen in the table above, model calibration for the Upper SAR Watershed Model shows good to very good performance at all of the streamflow gages from 1966 to 2016.

Hydrographs showing model-simulated and measured daily streamflow for the three gaging stations from January 1, 1966 through December 31, 2016 were plotted to evaluate model calibration performance (see Figures 108 through 110). As shown, there are similar temporal dynamics in both model-simulated and measured daily streamflow at the three gaging stations. Figures 111 through 113 also show similar temporal dynamics in both model-simulated and measured monthly streamflow. At E Street, following the cessation of treated wastewater discharge at San Bernardino Municipal Water Reclamation Facility, zero flow events become more common.

8.0 INTEGRATED SAR MODEL DEVELOPMENT

8.1 Model Conceptualization

A conceptual model is the basis for building the structure of a groundwater model so that it best represents the hydrogeologic system. The conceptual model for the Upper Santa Ana Valley Groundwater Basin was based on known and interpreted physical and hydrologic characteristics of the groundwater system, as presented in Sections 3.0 and 4.0.

8.1.1 Model Codes and Stress Periods

The Integrated SAR Model was constructed using MODFLOW, a block-centered, modular finite-difference groundwater flow code. Widely used and highly versatile, it was developed by the USGS (McDonald and Harbaugh, 1988) for the purpose of modeling both saturated and unsaturated groundwater flow. Specifically, the Newton formulation of the MODFLOW-2005 computer code, known as MODFLOW-NWT, was used for the Integrated SAR Model. The Newton-Raphson solver included in the MODFLOW-NWT code is well suited for solving problems involving drying and rewetting nonlinearities of the unconfined groundwater flow equation (Niswonger et al., 2011).

MODFLOW is modular in the sense that a standard format has been established for the interface between each module of the program, as well as the common variables that must be accessible to all modules. The modules or packages used include Basic (BAS), Evapotranspiration (EVT), Streamflow Routing (STR), Upstream Weighting (UPW), Recharge (RCH), Newton Solver (NWT), Horizontal Flow Barrier (HFB), Multi-Node Well 2 (MNW2), Well (WEL), and General-Head Boundary (GHB). The input data for the MODFLOW-NWT modules was based on a monthly basis (i.e., monthly stress periods) from January 1966 through December 2016. The monthly stress periods provide the ability to model the seasonal aspects of fluxes such as areal recharge, return flow, pumping, mountain front runoff, underflow, and streambed percolation.

The pre- and post-processors used to manipulate model input and output data arrays include the following:

- Geographical Information System (GIS);
- Groundwater Vistas; and
- Proprietary software developed by GEOSCIENCE.

The GIS software used was ESRI ArcMap 10.5. Groundwater Vistas, which was developed by Environmental Simulations, Inc. (1999), is a Windows graphical user interface for 3-D groundwater flow and transport modeling. FORTRAN source codes, custom-developed by GEOSCIENCE, were used to prepare MODFLOW model input data for the well and recharge packages and hydraulic conductivities.

8.1.2 Model Grids and Cells

The Integrated SAR Model domain covers an area of approximately 1,320 square miles (843,000 acres) with a finite-difference grid consisting of 1,642 rows in the northeast to southwest direction and 2,243 columns in the northwest to southeast direction (Figure 4). The active model area encompasses approximately 505 square miles (322,925 acres). The grid is rotated at 27° clockwise to be consistent with the previous SBBA, Rialto-Colton, and Yucaipa Models and minimize the number of model cells.

The cell size for the Integrated SAR Model area is 102.5 ft x 102.5 ft (Figure 4) – mimicking the high-resolution cell size used in the previous Yucaipa, SBBA, and Rialto-Colton Models. This cell size is smaller than those used in the previous Riverside-Arlington Model (164 ft x 164 ft) and Chino Basin Model (200 ft x 200 ft). The purpose of maintaining or enhancing existing model cell size was to preserve the integrity and functionality of each of the five existing groundwater flow models. Following model calibration, any of the individual models may be "de-coupled" from the Integrated SAR Model and be run as a stand-alone model to assess smaller-scale projects within the individual groundwater basins.

8.1.3 Model Layers

The individual groundwater basins within the larger Upper Santa Ana Valley Groundwater Basin contain a series of unconsolidated to semi-consolidated alluvial deposits, river and stream deposits, and interbedded sands and clays underlain by consolidated bedrock. The stratigraphic units in the Basins do not always form well-defined aquifers and containing units, so they had to be separated into water bearing units for modeling purposes.

As mentioned previously, the hydrogeologic conceptual model was used in combination with the 3-D lithologic model to delineate unified model layers across individual basin boundaries. The correlation of geologic units to existing hydrogeologic units was adjusted, where needed, to allow for the correlation of hydrogeologic units across model boundaries. Of the seven model layers presented in Table 1, only the upper five were modeled in the Integrated SAR Model. All of the layers in the Integrated SAR Model are hydraulically connected. Cross-sections showing the division of model layers are provided as Figures 114 through 119. The assignment of model layers based on the geology and hydrogeology is summarized in the table below.

Table 8-1. Model Layers of the Integrated SAR Model

Model Layer	Geologic Unit(s)	Description
1	Shallow river, wash, and axial-channel deposits present in distinct channels, very young and young alluvial deposits, and the upper portion of old and very old alluvial deposits	This is the top model layer, which receives streambed percolation, and deep percolation from precipitation and artificial recharge. The aquifer system of this layer provides groundwater for pumping and riparian consumptive use. This layer extends from land surface to approximately 100-200 ft deep along the Santa Ana River up to 1,000 ft deep in areas with deeper water levels. It transmits high amount of groundwater flow in the permeable Shallow river, wash and channel deposits. Upper Confining Member in the SBBA is included in this model layer.
2	Old and very old alluvial deposits and Live Oak Canyon deposits (Yucaipa Basin)	This layer consists of sediments underlying Model Layer 1 and ranges in thickness from 5 ft in the Chino Basin area and around the model edges up to 600 ft in the Calimesa area in the southern part of the Yucaipa Basin. The aquifer system of this layer provides groundwater for pumping in most of the individual basins. However, in the central part of the SBBA, this layer includes a layer of low permeability, interbedded silt, clay, and sand that can reach thicknesses of 300 ft (i.e., Middle Confining Member).
3	Old and very old alluvial deposits and Live Oak Canyon deposits (Yucaipa Basin)	This layer consists of sediments underlying Model Layer 2 and ranges in thickness from 5 ft in the central and northeastern model areas up to 1,300 ft in the Calimesa area in the southern part of the Yucaipa Basin. The aquifer system of this layer provides groundwater for pumping in most of the individual basins. However, in the upper portion of the Rialto-Colton Basin, this layer includes low permeability, fine-grained sediments ranging in thickness from a few ft up to 80 ft (i.e., BC Aquitard). In the Chino Basin, this layer represents low permeability, interbedded silt, clay, and sand ranging in thickness from a few ft in the eastern portion up to 400 ft in the western portion of the Chino Basin.
4	Old and very old alluvial deposits and Live Oak Canyon deposits (Yucaipa Basin)	This layer consists of sediments underlying Model Layer 3 and ranges in thickness from 5 ft in the southern central portion and northeastern model areas up to 1,400 ft in the Calimesa area in the southern part of the Yucaipa Basin. The aquifer system of this layer provides groundwater for pumping in each of the individual basins.

Model Layer	Geologic Unit(s)	Description
5	Old and very old alluvial deposits, Live Oak Canyon deposits (Yucaipa Basin), and Fernando Group (Chino Basin)	This layer consists of sediments underlying Model Layer 4 and ranges in thickness from 5 ft in the southern central portion and northeastern model areas to over 1,400 ft in the Calimesa area in the southern part of the Yucaipa Basin. The aquifer system of this layer provides groundwater for pumping in each of the individual basins.
6	Consolidated sedimentary rocks, including the San Timoteo Formation and Mt. Eden deposits (Yucaipa Basin) and Puente Formation (Chino Basin)	This layer consists of consolidated sedimentary rock underlying Model Layer 5. While not modeled, this layer ranges in thickness from 5 ft in the southern central portion and northeastern model areas up to 1,200 ft in the western Chino Basin area. The materials that form this layer are less permeable and generally form the basal layer of the overlying, more permeable aquifer layers. This layer was not simulated in this version of the Integrated SAR Model.
7	Granitic and metamorphic rock, including the Bedford Canyon Formation and Peninsula Ranges batholithic rocks.	This layer consists of crystalline granitic and metamorphic rock underlying Model Layer 6. The materials that form this layer are less permeable and constitute the basement complex for the individual groundwater basins. This layer was not simulated in this version of the Integrated SAR Model.

The base elevations of each model layer were determined from the lithologic model developed using lithologic data from geophysical borehole logs and driller's logs (Figure 120 through 124). During the model construction process, the thickness and extent of Model Layer 1 was increased to reflect the more permeable river-channel deposits present across the individual groundwater basins, allow the model to mimic groundwater transport through these materials (both horizontally across the landscape and vertically), account for shallow groundwater interaction with the river and ET, and to avoid dry cell problems (when the water table falls below the bottom of the model layer). The final model layer thicknesses for each layer in the Integrated SAR Model are shown in Figure 125.

8.1.4 Boundary Conditions

A boundary condition is any external influence or effect that acts either as a source or sink, adding or removing water from the groundwater flow system. They are used to simulate the model's interaction with the surrounding regional system. The boundary conditions used in the model include no-flow, general-head, stream, and well (specified flux) (see Figure 126).

Active and inactive model cells are assigned based on basin boundaries established during previous modeling. However, during the model integration process, active cells were connected between the Arlington and Temescal Basins just southeast of the junction between Interstate 15 and State Highway 91 to reflect the continuation of surface alluvial deposits between the two basins. The no-flow cells assigned to the non-alluvial or low permeability bedrock portions of the model area are depicted as gray on model figures. A general-head boundary, shown in dark red on Figure 126, was used in the Riverside-Arlington Basin to represent groundwater discharge to Hole Lake (WRIME, 2010). Stream cells (shown in blue) were used to simulate recharge from streambed percolation. Well, or specified flux, boundary conditions were used to represent several features in the Integrated SAR Model, including mountain front recharge (shown in purple on Figure 126), pumping wells (shown in bright red), and underflow inflow from upgradient groundwater basin areas (shown in khaki green).

8.2 Aquifer Parameters

Various aquifer parameters are necessary to simulate groundwater flow. The original development of aquifer parameters in the individual groundwater models is discussed in the previous modeling reports for each model area (refer to Section 2.3 for documentation references). Since the development of a groundwater model for the Chino Basin area was included in the scope of the development of the Integrated SAR Model, the establishment of initial aquifer parameters in this area is outlined in Section 6.0. During the model review process, BGW compared aquifer characteristics of the WEI Chino Basin Model and the calibrated SAR model in the Chino Basin area. The results of that analysis are provided in Appendix A.

During the model update and integration process, the aquifer parameters for the previous groundwater models were modified through individual model calibration. These updated values were then used as initial values for the Integrated SAR Model calibration. During model calibration, these initial values were refined through iterative manual adjustments within pre-established upper and lower bounds in order to minimize the residuals between measured and model-calculated groundwater levels. The calibrated aquifer parameters for the Integrated SAR Model are provided in the following sections and summarized in Table 2.

8.2.1 Horizontal Hydraulic Conductivity

The calibrated horizontal hydraulic conductivity values are shown for each model layer on Figure 127. In general, higher values of horizontal hydraulic conductivity were assigned along the SAR and its tributaries. In these areas, the calibrated horizontal hydraulic conductivity generally ranges from approximately 100 to 450 ft/day. Lower values of horizontal hydraulic conductivity represent the Newmark/Muscoy plume area in the SBBA (Layer 2), the perched layer in the Rialto-Colton Basin (Layer 3), and the confining layer in the southwestern Chino Basin (Layer 3). In these low permeability zones, the calibrated horizontal hydraulic conductivity ranges from less than 10 ft/day to approximately 25 ft/day.

8.2.2 Vertical Hydraulic Conductivity

In the Integrated SAR Model, flow from one model layer to another is controlled by the vertical hydraulic conductivity. Figure 128 shows the spatial distribution of the calibrated vertical hydraulic conductivity values for each model layer in the Integrated SAR Model. Patterns in the distribution of the vertical hydraulic conductivity values generally reflect those seen in the horizontal hydraulic conductivity distribution. Higher values of vertical hydraulic conductivity, ranging from 0.1 to over 5 ft/day, are generally found along the SAR, while lower values of vertical hydraulic conductivity, ranging from less than 0.001 to 0.1 ft/day, are found in the Newmark/Muscoy plume area in the SBBA (Layer 2), the perched layer in the Rialto-Colton Basin (Layer 3), and the confining layer in the southwestern Chino Basin (Layer 3).

8.2.3 Specific Yield

Specific yield, or secondary storage coefficient, is used in unconfined aquifers while storativity is used for confined aquifers. The Integrated SAR Model is set up so that either may be used. This means that values for the primary (storativity) and secondary storage coefficients are provided and the model uses the appropriate value based on whether the aquifer is confined or unconfined. Spatial distributions of specific yield are shown on Figure 129. In the Integrated SAR Model, specific yield ranges from less than 0.05 to 0.35.

8.2.4 Storativity

Storativity (S) is also referred to as the primary storage coefficient. In confined aquifers, storativity is equal to the specific storage (Ss) times the aquifer thickness (b):

$$S = Ss \times b$$

Storativity values from the preexisting individual groundwater models were used initially in the Integrated SAR Model and further refined through calibration. However, since MODFLOW-NWT uses specific storage, the storativity values were divided by the Integrated SAR Model layer thickness in preparation for model input. The storativity for Model Layers 2 through 5, which ranges from 1×10^{-6} to 5×10^{-3}, are shown on Figure 130.

8.2.5 Horizontal Flow Barriers

The location and extent of the faults in the Integrated SAR Model is consistent with previous models. The presence of faults has important implications on groundwater flow because faults are often low permeability features that can restrict the movement of groundwater. In all of the previous models in the Upper Santa Ana Valley Groundwater Basin, faults in were designated as horizontal flow barriers (HFBs) by evaluating water levels on either side of a fault, and were modeled using the HFB Package by assigning a hydraulic conductance value to the boundary of the barrier.

Two new HFBs were added for the Integrated SAR Model to explicitly simulate the underflow flux between groundwater basins. These HFBs coincide with former groundwater model boundaries representing Barrier E and the San Jacinto fault (northeast border of Rialto-Colton Basin with the SBBA), and the Rialto-Colton Fault (southwest border of Rialto-Colton Basin with Chino and Riverside-Arlington Basins). The locations of the HFBs are shown on Figure 131.

An initial hydraulic flow barrier calibration was conducted varying conductance across hydraulic flow barrier segments across a broad range of feasible values. Model calibration statistics, and in particular, water levels immediately adjacent to basin boundaries and the underflow water budget were assessed to establish baseline values for the HFB Package. These values were further refined during an iterative calibration process with other model parameters, as discussed in Section 9.0.

8.3 Model Recharge and Discharge Terms

Model recharge and discharge components, along with the MODFLOW package used to simulate each water budget term, are summarized in Table 8-2 below.

Table 8-2. Recharge and Discharge Terms for the Integrated SAR Model

Term		Model Package
Recharge	Recharge from Mountain Front Runoff	Well Package
	Areal Recharge from Precipitation	Recharge Package
	Streambed Percolation	Streamflow Routing Package
	Artificial Recharge	Well Package
	Anthropogenic Return Flow	Well Package and Recharge Package
	Underflow Inflow	Well Package
Discharge	Evapotranspiration	Evapotranspiration Package
	Groundwater Pumping	Well Package
	Rising Water Discharge to Streamflow	Streamflow Routing Package and Drain

The relative contributions of recharge and discharge terms are shown on Figures 132 and 133, respectively. Simulation of each recharge and discharge term in the Integrated SAR Model is discussed in the following sections.

8.3.1 Recharge from Mountain Front Runoff

Recharge from mountain front runoff occurs along the boundaries of the groundwater basin, where the model boundary abuts the mountain front, as shown on Figure 8. In the Integrated SAR Model, recharge from mountain front runoff is simulated using the Well Package, through which specified inflows are assigned to the groundwater model domain in model layers 1 and 2 representing the shallow aquifer. The amount of mountain front recharge assigned to the model area was based on previous modeling work and methodologies vary between existing models (refer to previous modeling reports for additional information). During the model calibration period from 1966 through 2016, mountain front runoff averaged 43,290 acre-ft/yr (Figure 9).

8.3.2 Areal Recharge from Precipitation

Areal recharge, or direct infiltration of precipitation, was applied to the uppermost active model layer of the Integrated SAR Model using the Recharge package. Total volumes of areal recharge are shown in Figure 12. Total annual average areal recharge from precipitation totaled 51,970 acre-ft/yr. The method of estimation varies by groundwater basin, and is consistent with the approach used in each individual groundwater basin model.

8.3.3 Streambed Percolation

Streambed percolation was simulated by the Integrated SAR Model using the Streamflow Routing Package. The Streamflow Routing Package routes tributary inflows through the stream network shown on Figure 126, and simulates streambed percolation based on streamflow, streambed conductance, and groundwater level. Tributary inflow locations include both gaged inflows in the upstream areas of the SBBA, and ungaged inflows in the upstream areas of the Yucaipa Basin – where tributary inflows were estimated with the watershed model. During the model calibration period, tributary inflow from outside of the groundwater basin (including gaged and ungaged flow) averaged 258,050 acre-ft/yr (Figure 134).

Additional sources of inflow to the Streamflow Routing Package include runoff generated within the groundwater basin and recycled water discharge. Runoff generated within the groundwater basin was calculated by the Upper SAR Watershed Model. This runoff is shown on Figure 135 by basin area, and averages 75,330 acre-ft/yr during the model calibration period. Locations of recycled water discharge along the stream network are shown on Figure 14. Discharge from these facilities averaged 87,750 acre-ft/yr from 1966 through 2016 (Figure 15).

Three gaging stations within the groundwater basin (shown on Figure 101) were used to adjust streambed conductance and calibrate the Integrated SAR Model. The streamflow calibration is discussed in additional detail in the Model Calibration section of this report (Section 9.3.3). Model-calculated recharge from streambed percolation averages 242,640 acre-ft/yr for the model calibration period from 1966 through 2016 (Figure 136).

8.3.4 Artificial Recharge

Artificial groundwater recharge occurs in spreading basins throughout the Integrated SAR Model domain. The locations are shown on Figure 17. Recycled, imported, and stormwater recharge data were collected based on monthly measurements and estimates from various water agencies and compiled for each spreading basin location. The total annual average volume of artificial recharge is 53,930 acre-ft/yr, as shown in Figure 18. Chino Basin and SBBA areas make up 18,790 acre-ft/yr and 21,880 acre-ft/yr of that total, respectively. The volumes of artificial recharge were simulated using the Well Package.

8.3.5 Anthropogenic Return Flow

Anthropogenic return flow refers to the amount of water that returns to the aquifer after application of water to the land surface in the form of irrigation, or from leaks in water lines, sewer lines and septic systems. Volumes of anthropogenic return flow used in the Integrated SAR Model are consistent with the methodologies used in the individual groundwater models, which varies by model (refer to previous modeling reports for additional information). The total annual average return flow from applied water totals 79,580 acre-ft/yr from 1966 through 2016 (Figure 19).

8.3.6 Underflow Inflow

In areas where the model boundary does not immediately border the mountain front, water flows into the model domain as underflow from adjacent groundwater basins (Figure 20; refer to Section 4.1.6). Methods for estimating underflow were based on the approaches used by the individual groundwater models. During model calibration, underflow along the northern boundary of the Chino Basin Model area was increased based on the undersimulation bias of computed water levels in this region of the Integrated SAR Model domain. The undersimulation bias in water level residuals was most apparent along the northern model boundary, indicating potential additional underflow across the boundary. The calibrated underflow inflow is shown on Figure 137 and averaged 34,630 acre-ft/yr for the model calibration period from 1966 through 2016. The majority of underflow occurred along the northern Chino Basin boundary.

8.3.7 Evapotranspiration

ET from a groundwater system generally decreases with decreasing groundwater elevation, and is at its highest in areas where groundwater elevations approach or exceed land surface. ET is simulated in the Integrated SAR Model using the Evapotranspiration Package. In a given model cell, ET ranges from the maximum ET rate at land surface to zero at a specified ET extinction depth. The outflow from ET depends on the proximity of the water table to land surface and the type of riparian vegetation present in the area.

Riparian vegetation extent and ET rates were based on the riparian vegetation mapping and consumptive use estimates developed by Aspen and BGW (including mapped coverages from WEI and others; refer to Section 4.1.7). Riparian vegetation mapping was conducted at five different times throughout the model simulation period. Each mapping was used to classify riparian vegetation up to the midpoint stress period with the next riparian vegetation mapping time. These riparian vegetation mappings were used to establish ET zones in the groundwater model. Each ET zone represents a vegetation group and was assigned a maximum monthly ET rate per stress period and an extinction depth at which ET processes cease.

ET extinction depths for riparian plant functional groups were developed from literature values (Maddock et al., 2012). The extinction depths ranged from a minimum of 3.28 ft (1 meter) up to almost 20 ft, depending on the type of riparian vegetation present, as summarized in the table below. The majority of vegetation in the model simulation area was deep rooted riparian vegetation, as shown in Table 4-7.

Table 8-3. Evapotranspiration Extinction Depths

Vegetation Type/Classification		Extinction Depth [ft]
Aspen Classification	Deep-rooted riparian	16.40
	Shallow-rooted riparian	4.92
	Transitional riparian	20.00
	Obligate wetland	3.28
	Open water	3.28
	Unvegetated sandy wash	3.28
	Giant Reed	3.28
	Managed Wetland	3.28
Additional Riparian Zones	Chino Riparian (WEI mapping)	16.40
	Riparian (BGW Shallow Groundwater Area)	16.40
	SBBA Riparian (Matti and Carson)	16.40
	Yucaipa Riparian (Geoscience)	16.40
	No ET	3.28

ET was computed from the cell-by-cell groundwater flow output for the entire model domain, as well as for Prado Basin alone (to allow for a comparison with existing work completed in the Prado Basin area). The outflows from the groundwater system due to ET throughout the model area and within Prado Basin are shown on Figures 138 and 139, respectively, for the model calibration period from 1966 through 2016. ET from the entire Integrated SAR Model area averages 30,330 acre-ft/yr while ET from the Prado Basin averages 15,960 acre-ft/yr. ET stabilizes during the later portions of the simulation period. Vegetation coverage remains similar in overall acreage, and baseflows at MWD Crossing have increased due to RIX operations. Seasonal variations in ET are shown in Figure 140. ET peaks in the hotter summer months and reaches a minimum over the winter months.

Values of model-calculated ET described above are lower than the maximum values in Tables 4-9 and 4-10, which were estimated by acreage and maximum ET rate as an upper bound. In Prado Basin, the model-calculated average ET value is approximately half of the maximum ET demand computed. As mentioned above, the maximum ET method assumes that the entire acreage is evapotranspiring at a maximum rate, while the model accounts for groundwater elevation and the component of ET from the groundwater system.

8.3.8 Groundwater Pumping

Groundwater pumping represents the largest source of discharge from the Integrated SAR Model. Pumping data for 2,643 wells were assembled for the calibration period from 1966 to 2016. The locations of pumping wells are shown on Figure 27 while annual pumping rates are shown on Figure 28. Pumping records were obtained from the existing individual models and updated for the Integrated SAR Model calibration period, as described in Section 5.0 (and Section 6.0 for the Chino Basin Model). During the model calibration period, groundwater pumping averaged 473,110 acre-ft/yr in the Integrated SAR Model domain. Monthly pumping from individual wells was assigned to model cells and layers using the Well Package. For wells screened in multiple aquifers, a portion of the well's total production was apportioned to each aquifer according to the screened interval of the well and hydraulic conductivity of the screened area.

8.3.9 Rising Water Discharge to Streamflow

Groundwater outflow from the Integrated SAR Model also occurs as rising water discharge to streamflow at San Timoteo Canyon, Riverside Narrows, and Prado Dam. Rising water occurs as groundwater gradients push groundwater to the surface at topographic lows or geologic contacts. Groundwater becomes surface water outflow when it reaches the land surface. Outflow values from the Integrated SAR Model are simulated using the Drain Package and the Streamflow Routing Package. The rising water discharge represents a model-calculated value, since the outflow is dependent upon the groundwater elevation at the drain boundary and the conductance of the drain. In San Timoteo Canyon, rising water discharge averaged 2,190 acre-ft/yr from 1966 through 2015 (Figure 141). During the same period, rising water at Riverside Narrows and Prado Dam averaged 10,300 acre-ft/yr and 16,650 acre-ft/yr, respectively (Figures 142 and 143). Total average rising water discharge to streamflow during the model calibration period is 29,140 acre-ft/yr (Figure 144).

9.0 INTEGRATED SAR MODEL CALIBRATION

Model calibration was conducted in accordance with the finalized flow model calibration plan, which was developed through discussions with TAC in model workshops, project status updates, and through the incorporation of comments from draft technical memoranda (see Appendix A).

9.1 Model Calibration Process

Calibration is the process of adjusting model parameters to produce the best-fit between simulated and observed groundwater system responses. Initial model parameters were based on the updated existing individual models. These values were further adjusted to better match historical observations of groundwater levels and streamflow. The Integrated SAR model calibration consisted of:

- Initial condition simulation (1966), and
- Transient calibration (monthly stress periods from 1966 through 2016).

The following trial-and-error model calibration approach was used:

1. Initial parameters were established based on parameter values from the updated individual groundwater models. The Integrated SAR Model was run to establish baseline values for the calibration metrics listed in the following section.
2. Model calibration was analyzed based on the metrics below. Areas of under- or over-estimation of water level were identified. Areas in which to improve model calibration were also identified.
3. Calibration was conducted, focusing on HFB parameterization and streambed conductance, to establish baseline parameters for the HFB and Streamflow Routing Packages. A wide range of values were tested to identify sensitivity and establish suitable baseline parameters.
4. Step 2 was repeated.
5. Calibration, primarily of hydraulic conductivity, was conducted in an iterative manner; with updates and refinements to HFB and streambed conductance.
6. Step 2 was repeated. After every model run, calibration metrics were assessed. Changes that improved calibration and did not adversely affect model calibration in other areas of the model were retained.
7. Steps 5 and 6 were repeated, iteratively improving model calibration based on the metrics below.

To account for the length of the transient calibration period and differences in data accuracy, calibration was reviewed through time, with additional importance placed on more recent data, as well as model performance over the more recent time period.

9.1.1 Calibration Targets

The Integrated SAR Model was calibrated against 108,502 measurements of groundwater level in 879 calibration wells, as well as streamflow at three gaging stations within the groundwater basin. Target wells for each model area are summarized in Tables 3 through 7 while streamflow gaging stations are summarized in Table 8.

While all target wells were used for the groundwater flow model calibration, some recent water level measurements were removed from Prado Basin monitoring wells because of increased sampling frequency. These shallow wells are located near the SAR and were included because the provide important control near the river. However, water level measurements at these wells were down-sampled to monthly measurement intervals in order to reduce bias on residual statistics generated to evaluate model calibration.

9.1.2 Calibration Criteria

The calibration process was conducted in general accordance of the guidelines documented in “Standard Guide for Comparing Ground-Water Flow Model Simulations to Site-Specific Information” (ASTM, 1993), “Standard Guide for Calibrating a Ground-Water Flow Model Application” (ASTM, 1996) and “Guidelines for Evaluating Ground-Water Flow Models” (Reilly and Harbaugh, 2004). This includes establishing calibration targets, identifying calibration parameters, using history matching, and using both qualitative and quantitative criteria to evaluate model performance.

During model calibration, hydraulic properties were manually altered and the results of each change were measured against qualitative and quantitative calibration metrics with the goal of reducing the difference between observed and simulated groundwater levels. Qualitative and quantitative measures of model calibration were used to determine whether changes to model parameters improved or worsened the model calibration.

Qualitative and quantitative measures of model calibration include:

- Hydrographs of observed versus model-simulated groundwater levels
- Scatterplots of observed versus model-simulated groundwater levels

- Spatial and temporal distribution of groundwater level residuals[2]
- Hydrographs of observed versus model-simulated streamflow
- Water balance
- Residual statistics, including:
    - Root Mean Square Error (RMSE): Root mean square error provides a measure of the spread of the residuals. Model calibration seeks to minimize RMSE and generally, a lower RMSE indicates a calibration closer to the observed data. Note: the RMSE is the same as the standard deviation of the residuals.
    - Mean Residual: Average of the residuals. Mean residual can help to identify bias in model-simulated versus observed water level data. Calibration seeks to minimize mean residual.
    - Relative Error: Relative error is the standard deviation of the residuals or RMSE normalized by the range of observed groundwater levels. Calibration seeks to minimize relative error.
    - R^2: Indicates the "goodness of fit" between measured and model-simulated values. For a perfect calibration, all points (observed along the x-axis and model-simulated along the y-axis) would fall on the diagonal line (regression line) with a R^2 value of 1. A greater deviation of points from the diagonal line corresponds with lower R^2 values and poorer model calibration performance. Streamflow was examined in accordance with the R^2 performance criteria suggested by Donigian (2002).
- Histograms of groundwater level residuals

During discussions of model calibration, the TAC agreed that not all data used for model calibration should be given the same consideration. This is due to the relative increase in data availability in more recent years as well as the general tendency towards increasing measurement accuracy and reliability with time. Rather than incorporating a formal weighting technique into the model calibration, a visual approach was used for the Integrated SAR Model. During the model calibration process, more emphasis was placed on the model's ability to reproduce observed measurements over a more recent period (i.e., 1991 through 2016), as well during very wet and very dry hydrologic conditions. This visual evaluation of model calibration was facilitated by TAC feedback during progress meetings.

[2] Residual = measured water level minus model-calculated water level. Negative residual values indicate model over-estimation, positive residual values indicate model under-estimation.

9.1.3 Updates to the Calibration following Peer Review

Calibration of the Integrated SAR Model was reviewed by the TAC, who provided feedback. Additional calibration was preformed to address areas identified by the TAC for improvement. Key changes to the calibration included:

- Updates to the Streamflow-Routing Package and refinements to calibration along the SAR. The spatial discretization of the SFR package was refined to make each model cell a reach. This resolved issues with elevation errors at intermediate locations along the longer stream reaches. Additional calibration along the Santa Ana River was conducted, given the importance of model performance along it.
- Storativity was updated based on TAC comments. Some values of storativity were updated following changes in the thickness of the model, particularly the subdivision of Layer 1 in Chino Basin into two layers. Also, values outside typical ranges of storativity were identified and corrected.
- The location of the ET boundary was updated in eastern Chino Basin following a review of areal imagery indicating developed instead of riparian land cover.
- Additional calibration of hydraulic conductivity was conducted following feedback from the TAC regarding areas of focus.

9.2 Initial Condition Simulation Results

The Integrated SAR Model calibration included an initial condition simulation, or model spin-up period, with model input from January of 1966. The goal of the initial condition model run was to develop a numerically stable initial condition, in good agreement with observed water levels, for the beginning of the transient calibration run. The initial condition was developed using a trial-and-error approach as described by Danskin and others (2006). Parameter values updated during the process included hydraulic conductivity, streambed conductance, hydraulic flow barrier conductance, and the convergence criteria of the solver. Changes to these parameters were made in tandem with updates to the transient groundwater model.

The initial condition simulation was conducted with water level measurements from 100 target wells (see Figure 145 for well locations). Model-simulated groundwater elevations for 1966 are shown on Figure 146. A graphical comparison between measured and model-simulated heads for the initial condition simulation is shown on Figure 147 and summarized in the table below. In Figure 147, the closer the heads fall on the straight line, the better the match.

Table 9-1. Initial Condition Model Simulation Statistics

Statistic	Integrated SAR Model
Mean Residual	-1.00 ft
Minimum Residual	-73.81 ft
Maximum Residual	223.76 ft
RMSE	38.68 ft
Relative Error	2.2%
R^2	0.99

Relative error of the residuals (i.e., standard deviation of the residuals divided by the observed head range) was also calculated to evaluate the model calibration quantitatively. Common modeling practice is to consider a good fit between historical and model predicted data if the relative error is below 10% (Spitz and Moreno, 1996; Environmental Simulations, Inc., 1999). As seen in the table above, the relative error for the 100 target wells is 2.2%, which is well below the recommended error of 10%. The spatial distributions of water level residuals for the initial condition run are shown on Figures 148 through 151 for Model Layers 1 through 4 (no target wells were screened in Model Layer 5). As shown, the majority of water level observations in 1966 fall in Layer 1 of the groundwater model.

Numerical accuracy problems are often derived from inappropriate model grid spacing, time steps, and closure criteria for convergence. The global budget error measures numerical accuracy and is calculated as the difference of total inflows and total outflows divided by the average of the total inflows and outflows. The Integrated SAR Model initial condition simulation run has a global budget error of 0.01%. In general, a global budget error of less than 1% is considered acceptable.

9.3 Transient Calibration Results

The transient calibration run for the Integrated SAR Model covers the period from 1966 through 2016 with monthly stress periods. The goal of the transient model calibration was to produce model-calculated water level and streamflow measurements that match observed water levels and historical streamflow at locations within the model domain. Analysis of model water budget, water level hydrographs, and residuals was conducted after each model calibration run to assess the effects of changes made to model parameters. Parameter values adjusted during the calibration included hydraulic conductivity, storativity/specific storage, specific yield, hydraulic flow barrier conductance, and streambed conductance.

9.3.1 Groundwater Elevations

The transient model calibration process used 108,502 water level measurements from 879 calibration target wells, shown on Figure 152, from which to match model-calculated water levels against observed measurements. Figure 153 shows a scatter plot of measured versus model-calculated water levels in all model layers of the Integrated SAR Model for the calibration period. Calibration statistics are also summarized in the following table.

Table 9-2. Integrated SAR Model Transient Model Calibration Statistics – All Layers

Statistic	Integrated SAR Model
Mean Residual	-0.98 ft
Minimum Residual	-292.31 ft
Maximum Residual	409.99 ft
RMSE	64.54 ft
Relative Error	1.8%
R^2	0.99

The graphical comparison between measured and model-predicted heads for the transient calibration shows the groundwater level measurements mainly clustered around the straight line. In general, the measured and model-calculated heads compared favorably, and the calibration is further supported by a low relative error 1.8% and R^2 of 0.99. Residuals from the Integrated SAR Model calibration were also broken out by time period to evaluate model performance during the first ten years of model simulation (1966 through 1975; Figure 154), middle ten years (1987 through 1996; Figure 155), and last ten years (2007 through 2016; Figure 156). The RMSE varies from 58 to 72 ft. Mean residual remains under ~12 ft in all three time periods. No large changes in the quality of the model calibration are observed between the three different time periods. Model performance during these three periods is summarized below.

Table 9-3. Transient Model Calibration Statistics – 1966 to 1975, 1987 to 1996, and 2007 to 2016

Statistic	First 10 Years 1966-1975	Middle 10 Years 1987-1996	Last 10 Years 2007-2016
Mean Residual	2.95 ft	8.98 ft	-12.58 ft
Minimum Residual	-131.25 ft	-292.31 ft	-216.70 ft
Maximum Residual	249.93 ft	360.17 ft	409.99 ft
RMSE	58.27 ft	71.45 ft	61.65 ft
Relative Error	2.0%	2.0%	1.8%
R^2	0.99	0.99	0.99

Figures 157 through 161 show the spatial distribution of average residuals for the model calibration period (1966 through 2016) by model layer. Some areas within the model domain exhibit more error than others. Figure 157 shows a random distribution of model residuals in Layer 1, with the exception of wells at higher elevation near basin boundaries – where model errors are larger. In general, under-simulation of water levels at basin boundaries is more likely. Uncertainty regarding boundary inflows, model layer thickness, and hydraulic properties at the boundaries of the groundwater model also contribute to error at the model boundaries. Another contributing factor to larger residuals in upgradient wells (and also one of the reasons for considering relative error as a calibration metric) is that water levels that exhibit a larger degree of natural variability are also inherently harder to simulate or predict, and are subject to a greater range of natural change and thus, error. Secondly, some water levels may represent pumping conditions or perched conditions, and as such, are not representative of regional groundwater levels. Some differences between model-simulated and measured values are also potentially due to model cell size (102.5 ft by 102.5 ft) being larger than the local scale of observation. Residuals tend to be lower in the center of the basin, where geologic observations are more numerous and regional hydraulic properties and gradients are better defined. Additional explanation of areas where the model has trouble matching observed water levels is provided by-basin in the following sections. In general, the model calibration was conducted at a regional scale, and localized changes at individual model cells were not performed adjacent to individual wells to improve calibration at a particular well.

Residuals were also plotted for stress periods exhibiting dry hydrologic conditions (September of 1990; Figure 162) and wet hydrologic conditions (March of 1983; Figure 163). Water level residuals show a generally random distribution in space, with higher residuals in the SBBA and Yucaipa Basin, similar to the overall spatial distribution of model residuals. In the SBBA, the model appears slightly more likely to underestimate groundwater levels in wet years.

Figure 164 shows the temporal residual plot for all observations in the Integrated SAR Model with time. No overall bias or skew is visible in the plot with time, indicating a random distribution of residuals through time. In general, the number of observations increases in the mid-1980s, as more groundwater observations are recorded. The plot of temporal residuals is another indication that model error does not significantly increase during wet or dry hydrologic periods. The standard deviation of model residuals decreases or converges with time on the residual plot.

A histogram of water level residuals for the Integrated SAR Model is presented as Figure 165. The residuals are bell-shaped with 38% of the model residuals falling between +/- 20 ft and 73% between +/- 60 ft, indicating model-simulated water levels are in general agreement with observed water levels.

Measured water levels were compared to model-calculated water level contours for dry and wet hydrologic conditions in Figures 166 through 175. Model-calculated conditions were compared to observations to determine if simulated gradients matched observations under different hydrologic conditions. Average vertical movement of water was plotted as well and is shown on Figure 176.

Overall, the calibration results indicate that the standard of calibration achieved in the Integrated SAR Model is suitable for the scale and purpose for which it was developed. Of 108,502 observations, over 41,000 fell within +/- 20 ft of the observed water level while over 79,000 fell within +/- 60 ft. Errors were found to be generally randomly distributed in space and time, with the exception of the anomalies noted herein. A description of the model calibration for the individual basin model areas is provided in the following sections.

9.3.1.1 Yucaipa Basin

The Yucaipa Basin Model (GEOSCIENCE, 2017) was updated to maintain consistency with the conceptual geologic model layers provided by the USGS. This update to the conceptual model required a recalibration of model hydraulic properties in the Yucaipa Basin to match observed groundwater levels, since the different layer thicknesses affected the transmissivities. During model calibration, an overestimation bias in the middle and downstream portions of the groundwater basin was addressed by adjusting the hydraulic conductivity distribution and HFB conductance.

Scatterplots for measured versus model-calculated water levels in the Yucaipa Basin for 93 target wells from 1966 through 2016 are shown on Figure 177 for all model layers and on Figures 178 through 182 for Layers 1 through 5. Calibration statistics for all model layers in the Yucaipa Basin Model area are presented below.

Table 9-4. Transient Model Calibration Statistics – Yucaipa Basin Model Area (All Model Layers)

Statistic	Previous Model (GEOSCIENCE, 2017) 1998-2015 Monthly Stress Period	Integrated SAR Model 1966-2016 Monthly Stress Period	
		Individual Model (Section 5.1)	Integrated SAR Model
Mean Residual	5.40 ft	27.51 ft	44.18 ft
Minimum Residual	NA	-264.34 ft	-229.24 ft
Maximum Residual	NA	397.00 ft	360.07 ft
RMSE	64.52 ft	74.27 ft	78.91 ft
Relative Error	2.9%	2.9%	3.1%
R^2	NA	NA	0.96

Some water levels in the Yucaipa Basin appear to represent localized perched water level conditions or areas of low transmissivity at the margins of the groundwater basin. These areas are visible in the spatial distribution of water level residuals shown on Figures 157 through 161.

The temporal distribution of water level residuals in the Yucaipa Basin is shown on Figure 183 while a histogram of water level residuals is shown on Figure 184. The histogram reveals that model water level residuals are bell-shaped, but skewed slightly towards model over-estimation of groundwater levels. This is primarily due to slight over-simulation towards the end of the model simulation period, as evidenced by the temporal distribution of residuals plot in Figure 183. 22% of model water level residuals fall between +/- 20 ft while 57% of water level residuals fall between +/- 60 ft, indicating overall agreement with observed water levels.

Selected water level hydrographs for the Yucaipa Basin model area are shown on Figure 185. As shown, model-calculated water levels match observed water levels generally, with an undersimulation bias, with the exception of a several wells at the margins of the groundwater basin. Here, the model-calculated water levels are generally lower than the observed water levels. Additional hydrographs for the Yucaipa Basin are presented as Appendix M.

9.3.1.2 SBBA

Water level calibration in the SBBA was assessed with 48,610 observations from 287 calibration wells. Scatterplots of measured versus model-calculated water levels in the SBBA from 1966 through 2016 are shown on Figure 186 for all model layers and on Figures 187 through 191 for Layers 1 through 5. Calibration statistics for all model layers in the SBBA Model area are presented below.

Table 9-5. Transient Model Calibration Statistics – SBBA Model Area (All Model Layers)

Statistic	Previous Model (Stantec and GEOSCIENCE) 1983-2015 Monthly Stress Period	Integrated SAR Model 1966-2016 Monthly Stress Period	
		Individual Model (Section 5.2.3)	Integrated SAR Model
Mean Residual	11.14 ft	8.61 ft	-25.94 ft
Minimum Residual	NA	-320.86 ft	-292.31 ft
Maximum Residual	NA	362.32 ft	360.17 ft
RMSE	64.16 ft	64.57 ft	64.55 ft
Relative Error	3.5%	3.5%	3.5%
R^2	NA	NA	0.96

The temporal distribution of water level residuals in the SBBA is shown on Figure 192. No major temporal trends in bias are observed in the plot, as evidenced by model residual distribution maintaining a similar distribution about the x-axis of the plot through time. A higher number of water level observations are present after 1983. No significant response to wet and dry hydrologic periods is observed in the residual plot, indicating that the groundwater model is capturing trends and responses in the groundwater system under differing hydrologic conditions.

A histogram of water level residuals in the SBBA is presented as Figure 193. The residuals are bell-shaped and 61% of model residuals fall between +/- 60 ft of observed water levels. The histogram shows a slight skew towards over-estimation of groundwater levels primarily at lower groundwater elevations. This is also reflected in the mean residual of -25.94 ft.

Hydrographs for selected wells within the SBBA are presented on Figures 194a and 194b. During the model calibration process, an undersimulation bias along the SAR was addressed by adjusting streambed conductance values along the stream network. Following calibration, general agreement with water levels and water level trends is observed through time. Additional hydrographs for the SBBA are presented as Appendix N.

9.3.1.3 Rialto-Colton Basin

Model calibration in the Rialto-Colton Basin was assessed with 26,297 water level observations from 333 calibration wells. Scatterplots of measured versus model-calculated water levels in the Rialto-Colton Basin from 1966 through 2016 are shown on Figure 195 for all model layers and on Figures 196 through 200 for

Layers 1 through 5. Calibration statistics for all model layers in the Rialto-Colton Model area are presented below.

Table 9-6. Transient Model Calibration Statistics – Rialto-Colton Basin Model Area (All Model Layers)

Statistic	Previous Model (GEOSCIENCE, 2015) 1945-1969 Annual Stress Period, 1970-2014 Monthly Stress Period	Integrated SAR Model 1966-2016 Monthly Stress Period	
		Individual Model (Section 5.3.3)	Integrated SAR Model
Mean Residual	-6.66 ft	-1.06 ft	19.29 ft
Minimum Residual	NA	-176.99 ft	-113.14 ft
Maximum Residual	NA	351.79 ft	291.28 ft
RMSE	69.40 ft	59.52 ft	53.99 ft
Relative Error	6.2%	5.7%	5.1%
R^2	NA	NA	0.97

In Model Layer 1, some water levels are under-estimated in the headwater portion of the basin, as shown in the spatial distribution plot on Figure 157. These observations may represent perched conditions in the shallow aquifer. These outliers are also observed on the temporal residual plot on Figure 201. Excluding these observations, model residuals are otherwise grouped closely about the x-axis in the temporal residual plot, and do not show any significant trends in bias with time, indicating that the groundwater model is capturing trends in groundwater levels in differing hydrologic conditions.

A histogram of water level residuals in the Rialto-Colton Basin is shown as Figure 202. Residuals are randomly distributed about zero and 63% of model water level residuals fall between +/- 20 ft, indicating a good match between observed and simulated groundwater levels.

Selected hydrographs for the Rialto-Colton Basin are presented on Figure 203. Water level hydrographs show general agreement with groundwater levels and trends in groundwater levels. Additional hydrographs for the Rialto-Colton Basin are presented as Appendix O.

9.3.1.4 Riverside-Arlington Basin

Model calibration in the Riverside-Arlington Basin was assessed with 6,643 water level observations from 55 calibration wells. Scatterplots of measured versus model-calculated water levels in the Riverside-Arlington Basin from 1966 through 2016 are shown on Figure 204 for all model layers and on Figures 205 through 209 for Layers 1 through 5. Calibration statistics for all model layers in the Riverside-Arlington Model area are presented below.

Table 9-7. Transient Model Calibration Statistics – Riverside-Arlington Basin Model Area (All Model Layers)

Statistic	Previous Model (WRIME 2010) 1965-2007 Monthly Stress Period		Integrated SAR Model 1966-2016 Monthly Stress Period	
	Calibration (1965-2005)	Validation (2006-2007)	Individual Model (Section 5.4.3)	Integrated SAR Model
Mean Residual	12.10 ft	13.20 ft	-0.37 ft	3.78 ft
Minimum Residual	NA	NA	-63.12 ft	-67.80 ft
Maximum Residual	NA	NA	69.95 ft	81.95 ft
RMSE	16.00 ft	11.80	19.29 ft	22.41 ft
Relative Error	5.0%	5.0%	6.3%	7.8%
R^2	NA	NA	NA	0.90

The scatterplots of observed versus model-calculated water levels in Figure 204 shows good agreement between observed and simulated water levels, with an RMSE of 24.85 ft. Greater scatter in the upper right portion of the scatterplot indicates relatively larger error at higher observed groundwater elevations.

The temporal distribution of water level residuals in the Riverside-Arlington Basin is shown on Figure 210. No major temporal trends in residuals are apparent, which is another indication that the groundwater model is capturing trends in groundwater levels under differing hydrologic regimes.

A histogram plot of residuals is presented as Figure 211. Residuals are randomly distributed about zero in a bell shape, with 63% falling between +/- 20 ft.

Selected water level hydrographs for the Riverside-Arlington Basin are shown in Figure 212. Additional hydrographs for the Riverside-Arlington Basin are presented as Appendix P.

9.3.1.5 Chino and Temescal Basins

Scatterplots for measured versus model-calculated water levels in the Chino and Temescal Basins for 111 target wells from 1966 through 2016 are shown on Figure 213 for all model layers and on Figures 214 through 218 for Layers 1 through 5. Calibration statistics for all model layers in the Chino Basin Model area are presented below.

Table 9-8. Transient Model Calibration Statistics – Chino Basin Model Area (All Model Layers)

Statistic	Previous Model (WEI, 2015) 1961-2011 Quarterly Stress Period		Integrated SAR Model 1966-2016 Monthly Stress Period	
	Calibration Wells	Validation Wells	Individual Model (Section 6.2.1)	Integrated SAR Model
Mean Residual	0.50 ft	-8.64 ft	17.86 ft	1.33 ft
Minimum Residual	-238.56 ft	NA	-244.67 ft	-268.71 ft
Maximum Residual	153.85 ft	NA	673.83 ft	409.99 ft
RMSE	25.38 ft	NA	58.93 ft	33.63 ft
Relative Error	NA	NA	5.2%	3.0%
R^2	NA	NA	NA	0.93

Water level calibration in the Chino and Temescal Basins shows general agreement in most areas of the groundwater basin. In the scatterplots of observed versus model-calculated water levels, most water level pairs fall along the diagonal axis of the plot and do not show significant bias towards under- or over-simulation of observed water levels. Two USGS multilevel observation wells in the northeast corner of the model domain account for the points in the upper-right corner of the scatterplot that fall off the diagonal (Figure 213). The wells lie immediately adjacent to a fault boundary and observed water levels in this location tend to be one to two hundred feet higher than the adjacent regional groundwater surface.

The temporal distribution of water level residuals in the Chino and Temescal Basins is shown on Figure 219 while a histogram of water level residuals is shown on Figure 220. In Figure 219, temporal trends in residuals are absent from the plot, indicating that the model is not developing bias as the simulation progressed through differing hydrologic conditions. Water levels are randomly distributed in a bell shape about zero, and 68% fall between +/- 20 ft.

Selected water level hydrographs for target wells in the Chino and Temescal Basins are shown on Figures 221a and 221b. Additional hydrographs for the Chino Basin model area are presented as Appendix Q.

9.3.1.6 Prado Basin Area

Scatterplots for measured versus model-calculated water levels in the Prado Basin area for 10 target wells from 1966 through 2016 are shown on Figure 222 for all model layers. Temporal distribution of water level residuals are shown on Figure 223. A histogram of water level residuals is shown in Figure 224 and selected hydrographs in the Prado Basin Area in Figure 225. Calibration statistics for all model layers in the Prado Basin area are presented below.

Table 9-9. Transient Model Calibration Statistics – Prado Basin Area (All Model Layers)

Statistic	Integrated SAR Model 1966-2016 Monthly Stress Period
Mean Residual	0.68 ft
RMSE	5.70 ft
Relative Error	11.6%
R^2	0.89

The model calibration in the Prado Basin area has an RMSE of 5.70 feet, which is lower than Chino Basin overall, indicating a close match to observed water levels in the Prado Basin area.

9.3.1.7 Water Level Profile

A water level profile parallel to the SAR is presented for Layer 1 as Figure 226 under dry hydrologic conditions (represented by September 1990) and as Figure 227 under wet hydrologic conditions (represented by March 1983).

9.3.2 Underflow across Basin Boundaries

In contrast to the previous individual groundwater models, the Integrated SAR Model explicitly simulates underflow between adjacent groundwater basins for the first time. Instead of treating boundary inflows between groundwater basins as boundary conditions, the boundaries between adjacent groundwater basins were removed – allowing the groundwater model to solve for underflow across basin boundaries.

Groundwater flow across basin boundaries was computed from the cell-by-cell groundwater flow output from the groundwater model simulation. Figures showing flux across basin boundaries are presented graphically in Figures 228 through 232 and summarized in the following table.

Table 9-10. Underflow across Basin Boundaries

Basin	Underflow [acre-ft/yr]
Underflow from Yucaipa Basin to the SBBA	
Yucaipa Basin Model (GEOSCIENCE, 2017)	3,500
SBBA Model (GEOSCIENCE, 2009)	4,100
Integrated SAR Model	***7,830***
Underflow from Bunker Hill Basin to Rialto-Colton Basin	
SBBA Model (GEOSCIENCE, 2009)	3,800
Rialto-Colton Basin Model (GEOSCIENCE, 2015)	4,000
Integrated SAR Model	***4,700***
Underflow from Lytle Basin to Rialto-Colton Basin	
SBBA Model (GEOSCIENCE, 2009)	2,000
Rialto-Colton Basin Model (GEOSCIENCE, 2015)	14,100
Integrated SAR Model	***14,530***
Underflow from Rialto-Colton Basin to Riverside Basin	
Rialto-Colton Basin Model (GEOSCIENCE, 2015)	17,900
Riverside-Arlington Model (WRIME, 2010)	25,400
Integrated SAR Model	***17,010***
Underflow from Riverside Basin to Chino Basin	
Riverside-Arlington Model (WRIME, 2010)	2,800
Chino Basin Model (GEOSCIENCE, Section 6.0)	11,300
Integrated SAR Model	***16,260***

9.3.3 Streamflow

The Integrated SAR Model streamflow calibration was assessed in tandem with the groundwater level calibration after each iteration or model run. Streamflow calibration was conducted based on analysis of streamflow at three gaging stations within the groundwater basin, as well as shallow groundwater wells in the vicinity of the stream network. The three gaging stations used for the model calibration include: SAR at E Street, SAR at MWD Crossing, and SAR inflow to Prado Dam (see Figure 101 for gaging station locations). Streambed conductance was adjusted by reach to improve R^2 values at the gaging stations and calibrate to groundwater level observations in the vicinity of the stream network. Nash-Sutcliffe Efficiency (NSE) was also computed.

Results of the streamflow calibration at the three gaging stations are shown on Figures 233 through 235 and summarized in the following table. Performance is based on the suggested criteria by Donigian (2002; see Table 7-2).

Table 9-11. Integrated SAR Model Results – Monthly Simulated Streamflow Performance

Gaging Station	Avg. Observed Flow [cfs]	Avg. Model-Simulated Flow [cfs]	Mean Residual [cfs]	Mean Residual as % of Avg. Observed Flow	NSE	R^2	Performance
Santa Ana River at E Street	75.9	81.7	-5.8	-8%	0.82	0.84	Good
Santa Ana River at MWD Crossing	130.5	105.3	25.2	19%	0.75	0.81	Good
Santa Ana River into Prado Dam	274.7	286.4	-11.7	-4%	0.81	0.93	Very Good

Hydrographs of observed and model-calculated monthly streamflow are provided as Figures 236 through 238. In general, the model is able to reproduce similar streamflow dynamics seen in observed measurements. At the E Street gaging station, there is some tendency for the model to over-estimate streamflow later in the calibration (Figure 236). The model also appears to slightly under-estimate streamflow at MWD Crossing (Figure 237). The decrease in baseflow at E Street gaging station, and the corresponding increase in flow at MWD Crossing is consistent with the shift of wastewater discharge to the RIX discharge from the San Bernardino Municipal Water Reclamation Facility discharge.

9.3.4 Water Balance

As outlined previously in this report, inflow terms to the Integrated SAR Model include mountain front runoff, underflow inflow from adjacent groundwater basins, artificial recharge in spreading basins, areal recharge of precipitation, anthropogenic return flow from applied water, and streambed percolation. Discharge terms include groundwater pumping, evapotranspiration from groundwater, and rising water discharge to streamflow. Groundwater budgets for the individual basin areas are shown on Figures 239 through 244 and summarized in Tables 9 through 14. The difference between the total inflow and total outflow equals the change in groundwater storage. The annual change in groundwater storage for each basin area is summarized below.

Table 9-12. Average Annual Change in Groundwater Storage

Basin	Average Annual Change in Groundwater Storage [acre-ft/yr]
Yucaipa Basin	-1,940
SBBA	-6,240
Rialto-Colton Basin	190
Riverside-Arlington Basin	-3,110
Chino Basin	-16,640
Temescal Basin	-1,350

A water balance was also conducted for Prado Basin, which is included within the area of the Chino and Temescal Basins. This water balance is shown on Figure 245. During the model calibration period (1966 through 2016), the annual change in groundwater storage for the Prado Basin area is approximately 450 acre-ft/yr.

9.3.5 Cumulative Change in Groundwater Storage

Cumulative annual change in groundwater storage for the individual basin areas are provided on Figures 246 through 251. The spatial distribution of change in groundwater storage is shown in Figure 252. The cumulative departure from mean annual precipitation at the San Bernardino County Hospital Station is also shown on the figures. Many of the basin areas respond to changes in hydrologic conditions (i.e., wet and dry periods cause rises and declines in groundwater storage, respectively). Basin response to hydrology is greatest in the SBBA (Figure 247), and generally diminishes in basins with increasing distance from mountain front recharge sources.

From Figure 247, it appears that the Integrated SAR Model tends to over-estimate groundwater declines in the SBBA during the latter part of the model simulation period. As shown on the figure, the model-calculated cumulative change in groundwater storage declines at a faster rate during the last 15 years of simulation than the cumulative change in storage calculated by the groundwater level method. The greater cumulative decline in groundwater storage calculated by the Integrated SAR Model is likely due to the large amount of underflow from Lytle Basin to the Rialto-Colton Basin. This over-estimation in cumulative storage decline can be corrected through future work on the model calibration.

10.0 PREDICTIVE SCENARIOS

10.1 Description of Model Scenarios

Model scenarios assess the hydrologic response of the Upper SAR to various project activities, including streamflow diversions, recharge basins (new basins and modifications), effluent reductions, and new discharge locations. Specifically, the Integrated SAR Model scenarios evaluate the effects of proposed HCP covered activities and other basin management strategies on riparian habitat, groundwater levels, and streamflow. Each model run was developed through collaboration and consultation with the TAC and HCP Team. The list of scenario runs developed by the TAC is summarized in Table 16. As shown, the general scenario categories include:

- Scenario 1: Evaluate Flow in the SAR and Identify Factors that May be Causing Reduced Flows
- Scenario 2: Evaluate the Proposed HCP Activities with Hydrologic Effects
- Scenario 4: Evaluate Groundwater Management Activities and Changes in Groundwater Pumping

The scenario runs simulate various project effects individually or in combination to assess hydrologic responses in comparison to the baseline (no project) scenario, Scenario 2a. For each scenario run, model-predicted flow and groundwater impacts were evaluated, including water level and water budgets for each groundwater basin (e.g., evapotranspiration and underflow across each groundwater basin). In Scenarios 2 and 4, time history of ET, water levels, streamflow, rising water, and water budgets were compared to a baseline, no project condition simulation to estimate impacts attributable to individual HCP Covered Activities or combinations of HCP Covered Activities. In addition, this information was provided to the Environmental Impact Report (EIR) team for them to establish thresholds of significance.

10.2 HCP Covered Activities

HCP Covered Activities modeled in the predictive scenarios represent those activities which have been identified as having an impact on the hydrologic system in the Upper Santa Ana Valley Groundwater Basin. These activities were provided by ICF and the HCP Hydrology TAC, and include streamflow diversions, recharge basins (new basins and modifications), effluent reductions, and new discharge locations. An overview of these projects is shown on Figure 253. The covered activities are briefly discussed below, by basin.

10.2.1 HCP Covered Activities in the San Bernardino Basin Area (SBBA)

The HCP activities in the SBBA are summarized in Table 10-1, below, and shown on Figures 254 through 257. Figures showing the location of the projects and annual project impacts are indicated in the two right-hand columns of the following table.

Table 10-1. HCP Activities in the San Bernardino Basin Area (SBBA)

Project ID	Activity	Type	Figure	
			Location	Impact
CD.4	Mill Creek Diversion Project	Stormwater Capture	254	258
EV.4.01 - 4.03	Sterling Natural Resource Center (SNRC)	Recycled Water	254, 259	260
VD.2.01	Cajon Creek	Stormwater Capture	256	261
VD.2.02	Cable Creek	Stormwater Capture	256	262
VD.2.03	Lytle Creek	Stormwater Capture	257	263
VD.2.05	City Creek	Stormwater Capture	254	264
VD.2.06	Plunge Creek – Basin 1	Stormwater Capture	254	265
VD.2.07	Cajon-Vulcan 1	Stormwater Capture	255,257	266
VD.2.08	Vulcan 2	Stormwater Capture	255,257	267
VD.2.09	Lytle-Cajon	Stormwater Capture	257	268
VD.2.10	Plunge Creek – Basin 2	Stormwater Capture	254	269
VD.2.11	Devil Creek	Stormwater Capture	255	270
VD.2.12	Waterman Basin Spreading Grounds	Stormwater Capture	255	271
VD.2.13	Twin Creek Spreading Grounds	Stormwater Capture	255	272
VD.3	Enhanced Recharge Project	Stormwater Capture	254	273

10.2.1.1 CD.4: Mill Creek Diversion Project

The Mill Creek Spreading Facilities are located 3 miles south of Seven Oaks Dam on Mill Creek (see Figure 254). Planned improvements to the diversion headworks will increase the diversion flow capacity and improve reliability at the Mill Creek Spreading Facilities, resulting in the capture and recharge of additional flows along Mill Creek. Currently, the North Canal inlet restricts capacity to 55 cfs. A new North Canal Inlet structure will allow for 210 cfs to be diverted. Collectively, new construction and improvements to existing facilities are anticipated to yield an increase in average annual capture of 7,960 acre-feet (af; Figure 258). This recharge estimation is based on previous stormwater flow and capture analysis conducted by GEOSCIENCE (2016).

10.2.1.2 EV.4.01-4.03: Sterling Natural Resource Center

The SNRC project involves the construction of treatment facility to produce tertiary treated water in compliance with California Code of Regulations Title 22 recycled water quality requirements for unrestricted use. The location of the proposed facility is shown in Figure 254 and detailed in Figure 259. Treated water would be discharged to City Creek during low flow conditions to enhance recharge and discharged to Redlands Basin during high flow conditions. The project involves the construction of treated water conveyance to discharge locations at City Creek and Redlands Basin. According to recent modeling work conducted by GEOSCIENCE (in progress), the project would discharge an average of 8,950 afy in City Creek and Redlands Basin, while also resulting in reduced flow to the Rapid Infiltration and Extraction (RIX) treatment facility (Figure 260). Of this discharge, approximately 1,520 afy will be recharged at Redlands Basin. The remaining 7,430 afy will be discharged to City Creek where it is expected that 7,150 afy will percolate in City Creek and the remaining 280 afy will flow into the SAR. Since this section of the SAR is typically dry, discharge that flows into the SAR will likely percolate before it can contribute to streamflow.

10.2.1.3 VD.2.01: Cajon Creek

The Cajon Creek project would construct a new diversion berm, conveyance and recharge basins providing a diversion capacity of 500 cfs along Cajon Creek (see Figure 256). Four recharge basins with a storage volume of 129.4 af will be constructed along with a sand diversion berm along Cajon Creek. Based on previous stormwater flow and capture analysis (GEOSCIENCE, 2016), the new recharge basins will provide an estimated additional recharge of 1,120 afy (Figure 261).

10.2.1.4 VD.2.02: Cable Creek

The Cable Creek project (see Figure 256) would construct an inflatable rubber dam diversion, three recharge basins totaling 37.9 wetted acres, and a diversion inlet structure with a 500 cfs capacity. The perimeter berms around the ponds will be approximately 10 ft tall and provide a storage volume of 281 af. Based on previous stormwater flow and capture analysis (GEOSCIENCE, 2016), the new recharge basin will provide an additional average annual recharge of 2,420 afy (Figure 262).

10.2.1.5 VD.2.03: Lytle Creek

The diversion and basin system project in Lytle Creek would be located north-west of the CEMEX screening plant (see Figure 257). CEMEX is planning to construct a berm that could isolate the basin area currently open to flows from Lytle Creek. The proposed project would construct a diversion berm in channel, along with a basin inlet structure and piping to a series of cells within the CEMEX basin area. The cell berms would be approximately 15 feet high and create a storage volume of 460 af. The forebay area pooling water would create an additional 223 af of storage. Based on previous stormwater flow and capture analysis (GEOSCIENCE, 2016), the project is estimated to improve groundwater recharge in this basin by an average of 3,620 afy (Figure 263).

10.2.1.6 VD.2.05: City Creek

The diversion and recharge basin project along City Creek would consist of a rubber dam diversion berm and nine recharge basins constructed south-west from Baseline Avenue (see Figure 254). The proposed basin layout will consist of perimeter berms approximately 10 ft in height with a storage volume of 254 af. The inlet structure will have a diversion capacity of 500 cfs. Based on previous stormwater flow and capture analysis (GEOSCIENCE, 2016), the anticipated average annual additional recharge from the City Creek project is estimated to be 4,600 af (Figure 264).

10.2.1.7 VD.2.06: Plunge Creek – Basin 1

The diversion and recharge basin project at Plunge Creek site 1 (see Figure 254) would construct a rubber dam diversion to an 8-ft deep basin with a storage volume of 40 af. The diversion inlet structure will have a diversion capacity of 250 cfs. Based on previous stormwater flow and capture analysis (GEOSCIENCE, 2016), the anticipated increase in annual recharge is 900 af at the Plunge Creek site 1 (Figure 14). The inflatable rubber dam has dimensions of 165 ft long by 8 ft tall and was selected due to the frequent and high flow rates predicted to occur at the site.

10.2.1.8 VD.2.07: Cajon-Vulcan 1

The Cajon Creek/Vulcan 1 site is an existing 115-ft deep aggregate mining pit, shown on Figure 4 or Figure 6. The proposed project would construct a sand diversion berm across the entire width of Cajon Creek which would divert flows up to 500 cfs. In addition to the 3,000-ft long sand diversion berm, a 500 cfs diversion inlet structure and a surface water bypass structure would be constructed. The bypass structure would allow for downstream flows below 500 cfs, if desired, without washing out the berm. Based on previous stormwater flow and capture analysis (GEOSCIENCE, 2016), the average annual additional recharge anticipated from the City Creek project is estimated to be 490 af (Figure 266).

10.2.1.9 VD.2.08: Vulcan 2

The Vulcan 2 project would divert flows in the Devil Creek Diversion Channel (see Figure 255 or Figure 257). The channel delivers flows from Devil Creek and Cable Creek into Cajon Creek. The recharge basin location is an unimproved site planned for future aggregate mining. An inflatable rubber dam would be constructed in the diversion channel and divert water to four recharge basins with a storage volume of 383 af. The diversion capacity would be 750 cfs. Based on previous stormwater flow and capture analysis (GEOSCIENCE, 2016), this project would result in an average annual increase in recharge of 2,450 afy (Figure 267).

10.2.1.10 VD.2.09: Lytle-Cajon

The Lytle-Cajon Basin project would construct an in-channel recharge basin system in the Lytle Creek wash downstream of the Baseline Road/Lytle Creek Wash crossing (see Figure 257). Eight (8) flow-through basins would be constructed in-series with 8- to 10-ft berms constructed with native creek material. The storage volume of the basins would be 244 af. Based on previous stormwater flow and capture analysis (GEOSCIENCE, 2016), the average annual recharge volume would be approximately 2,910 afy (Figure 268).

10.2.1.11 VD.2.10: Plunge Creek-Basin 2

The Plunge Creek Basin 2 project is located west of the 210 Freeway/Plunge Creek crossing (see Figure 254). The project includes the construction of 10.7 acres of basin, the construction of an inflatable rubber dam to divert water, and a 350 cfs diversion capacity. The project is adjacent to the southernmost basin of the City Creek Site (VD.2.05). For operational flexibility, a transfer pipe could connect the two basins. The 10.7 acres of basin would be divided into two cells totaling 66 af of storage volume. Based on previous stormwater flow and capture analysis (GEOSCIENCE, 2016), the additional average annual recharge from this project is anticipated to be 2,210 afy (Figure 269).

10.2.1.12 VD.2.11: Devil Creek

The Devil Creek site improvements would include an inflatable armored dam (Obermeyer Spillway Gate) diversion across Devil Creek (see Figure 255) to increase the diversion rate capacity and divert low flows. Two additional recharge cells as well as improvements to existing basins would allow the capture of greater volumes, realizing a diversion capacity of 500 cfs. The storage volume of the proposed basins would be 242 af. Based on previous stormwater flow and capture analysis (GEOSCIENCE, 2016), the project would increase the average annual recharge at the site by approximately 1,910 afy (Figure 270).

10.2.1.13 VD.2.12: Waterman Basin Spreading Grounds

The Waterman Basin Spreading Grounds site (see Figure 255) attenuates storm flows in Waterman Creek with a radial diversion structure. The improvements to the site include a 35-ft long by 8-ft tall armored inflatable dam (Obermeyer Spillway Gate) across Waterman Creek to improve diversion capacity. The existing basins provide a storage volume of 180 af. Additional improvements to the Waterman Basin site would include refurbishment of two radial gate systems, three inner-basin surface transfer structures and ten low-level outlets/drains. The improvements to the site would improve diversion capacity to as high as 1,000 cfs. Based on previous stormwater flow and capture analysis (GEOSCIENCE, 2016), the project is anticipated to increase recharge by an annual average of approximately 1,420 af (Figure 271).

10.2.1.14 VD.2.13: Twin Creek Spreading Grounds

The Twin Creek Spreading Grounds site (see Figure 255) would be improved by reconstructing and armoring berms between each basin, adding low level outlets/drains to each basin, and re-grading to restore infiltration rates and drainage. Based on previous stormwater flow and capture analysis (GEOSCIENCE, 2016), the proposed improvements are estimated to yield an increase in annual average recharge of 3,310 afy (Figure 272).

10.2.1.15 VD.3: Enhanced Recharge Project

The Enhanced Recharge Project is located on the SAR with diversion facilities downstream of Seven Oaks Dam (Figure 254). The existing facilities have a capacity to divert up to 195 cfs from the SAR. Phase 1a improvements include modifications to the Cuttle Weir, sediment management facilities, and construction of the Plunge Pool Pipeline. Phase 1b improvements would construct 25 recharge basins in two phases, along with conveyance for diverted water to the new recharge basins. Based on previous stormwater flow and capture analysis (GEOSCIENCE, 2016), the increased diversion capacity of 500 cfs will allow additional stormwater diversions of approximately 3,720 afy (Figure 273; 17,400 afy under baseline conditions (195 cfs capacity) and 21,120 afy under HCP covered activity (500 cfs capacity)). The diversion for the HCP covered activity is approximately 15,820 afy above San Bernardino Valley Water Conservation District (SBVWCD) seasonal water rights[3] (5,300 afy under both baseline conditions and HCP covered activity).

10.2.2 HCP Covered Activities in Rialto-Colton and Riverside-Arlington Basins

The HCP activities in the Rialto-Colton and Riverside-Arlington Basins are summarized in Table 10-2, below, and shown on Figures 257 and 274 through 276. Figures showing the location of the projects and annual project impacts are indicated in the two right-hand columns of the following table.

[3] SBVWCD seasonal licenses include:

- License 2831 – 8,300 af from January 1 through May 31
- License 2832 – 2,100 af from October 1 through December 31

Table 10-2. HCP Activities in the Rialto-Colton and Riverside-Arlington Basins

Project ID	Activity	Type	Figure	
			Location	Impact
Rial.1	Rialto Wastewater Treatment Plant Reuse Project	Recycled Water	274	277
RPU.5	Riverside North Aquifer Storage and Recovery Project	Stormwater Capture	274	278a, 278b
RPU.8*	Riverside Basin Recharge Project	Stormwater Capture	274,275	279
RPU.10	Santa Ana River Sustainable Parks and Tributaries Water Reuse Project	Recycled Water	274,275	280, 281
VD.1	Cactus Basin Recharge Project	Stormwater Capture	257	282
WD.1	SBMWD Recycled Water Project	Recycled Water	274	283
West.3*	Recycled Water Live Stream Discharge	Recycled Water	276	284
West.6*	Arlington Basin Water Quality Improvement Project	Stormwater Capture	276	285

* Surface Hydrology not connected to main stem of the SAR, but need to evaluate habitat effect(s) for covered species.

10.2.2.1 Rial.1: Rialto Wastewater Treatment Plant Reuse Project

The Rialto Wastewater Treatment Plant Reuse Project would reduce the amount of treated effluent discharged to the Rialto Channel, which then flows to the SAR (see Figure 274). The effluent discharge reduction is anticipated to occur in two phases. Phase 1 would reduce the average discharge from 9.3 cfs to 7 cfs, a reduction of approximately 1,390 afy (Figure 277). Phase 2 would reduce the average discharge from 7 cfs to 5 cfs, for a total reduction of 4.3 cfs. A Rialto Channel improvement design would also create an inset channel to provide habitat for native species. For the purposes of this modeling exercise, the Integrated SAR Model scenarios only evaluated the impacts of Phase 1. Phase 2 may be modeled at a later time.

10.2.2.2 RPU.5: Riverside-North Aquifer Storage and Recovery Project

The Riverside-North Aquifer Storage and Recovery Project (RNASR) would create in-channel and off-channel recharge facilities along the SAR in proximity to the confluence of the SAR and Warm Creek (see Figure 274). An inflatable rubber dam system constructed in segments would pool water for in-channel recharge in an area of 24 acres. Off-channel recharge basins would be constructed, along with diversion structure with a capacity of 250 cfs in the levee wall. The off-channel recharge facility would consist of up to five individual recharge basins. The inflatable rubber dam would be deployed when flows in the river were less than 4,000 cfs. An in-channel recharge capacity of 36 cfs is anticipated, while off-channel capacity is estimated at 250 cfs. Recharge from this project was modeled by Scheevel Engineering (2018;

see Appendix R). The project is anticipated to recharge approximately 5,930 afy of stormwater without upstream HCP covered activities (Figure 278a) and 6,110 afy with all upstream HCP covered activities (Figure 278b).

10.2.2.3 RPU.8: Riverside Basin Recharge Project

RPU plans to construct new recharge basins and/or repurpose existing flood control basins to recharge additional stormwater, imported water, and water diverted from the Riverside North Aquifer Storage and Recovery Project. Four basins considered for the recharge project include Columbia, Marlborough, Spring Brook, and Van Buren basins (see Figures 274 and 275). This project is anticipated to increase stormwater recharge at the four sites, collectively, by 1,460 afy (Figure 279).

10.2.2.4 RPU.10: Santa Ana River Sustainable Parks and Tributaries Water Reuse Project

The SAR Sustainable Parks and Tributaries Water Reuse Project would redistribute effluent resulting in a discharge reduction at Riverside Regional Water Quality Plant (RWQCP; see Figures 274 and 275). The project would install 52,000 ft of pipeline to deliver tertiary treated recycle water from RWQCP to RPU customers and proposed Upper SAR HCP Santa Ana sucker mitigation sites along existing tributaries. The project would reduce discharge at RWQCP by 12,650 afy (Figure 280), providing 4,930 afy for tributary in-stream flows (Figure 281) and 7,730 afy for use by RPU.

10.2.2.5 VD.1: Cactus Basin Recharge Project

The Cactus Basin Recharge Project would involve improvements to the existing Cactus Basins, which are located along the Rialto Channel in the Rialto-Colton Basin (see Figure 257). Storm flow and additional runoff would be recharged at Cactus Basins 1, 2, 3, and 3a. Potential stormwater recharge at Cactus Basins 1-3 was estimated by CWE (2018), which is expected to average 1,360 afy (Figure 282).

10.2.2.6 WD.1: SBMWD Recycled Water Project

The City of San Bernardino Municipal Water Department (SBMWD) plans to develop a recycled water project that would permanently reduce the amount of treated effluent discharged from the RIX facility into the SAR (see Figure 274). Phase 1 of the effluent reduction would reduce effluent discharge by 5 MGD, a 5,600 afy reduction in flow to RIX (Figure 283). A Phase 2 reduction could occur in the future if the HCP demonstrates USFWS success criteria are met or exceeded. Phase 2 would reduce effluent discharge by an additional 3,622 afy. For the purposes of this modeling exercise, the Integrated SAR Model scenarios only evaluated the impacts of Phase 1. Phase 2 may be modeled at a later time.

10.2.2.7 West.3: Recycled Water Live Stream Discharge

Western currently has no ability to discharge excess recycled water at the Western Water Recycling Facility. If excess recycled water is available, it passes through the distribution system, is retreated at Western Riverside Regional Wastewater Authority treatment plant and discharged to Prado Basin. Therefore, a new emergency discharge point would discharge directly into the Mockingbird Creek drainage (see Figure 276). The discharge is anticipated to average 200 afy (Figure 284).

10.2.2.8 West.6: Arlington Basin Water Quality Improvement Project

Western plans to construct new artificial recharge basins at sites in the vicinity of the Arlington Desalter in the City of Riverside. The Victoria site and other potential sites (Figure 276) would be used to recharge stormwater from Mockingbird Reservoir. It is anticipated that this activity would divert an average of 300 afy of stormwater and involve the additional recharge of 1,850 afy from other sources (imported or recycled water). The total volume of additional recharge is 2,150 afy (Figure 285).

10.2.3 HCP Covered Activities in the Chino Basin

The HCP activities in Chino Basin are summarized in Table 10-3, below, and shown in Figures 286 through 291. Figures showing the location of the projects and annual project impacts are indicated in the two right-hand columns of the following table.

Table 10-3. HCP Activities in the Chino Basin

Project ID	Activity	Type	Figure	
			Location	Impact
IEUA.1.01	Wineville Basin	Stormwater Capture	288, 289	292
IEUA.1.02	Lower Day Basin	Stormwater Capture	286	293
IEUA.1.03	San Sevaine Basin Cells 1-5	Stormwater Capture	286	294
IEUA.1.04	Victoria Basin Improvements	Stormwater Capture	286	295
IEUA.1.05	Montclair Basin Cells 1-4	Stormwater Capture	287, 289	296
IEUA.1.06	Jurupa Basin	Stormwater Capture	288	297
IEUA.1.07	Declez Basin	Stormwater Capture	288, 289	298
IEUA.1.08	CSI Basin	Stormwater Capture	288	299
IEUA.1.09	Ely Basin	Stormwater Capture	287, 289	300
IEUA.1.10	RP3 Basin	Stormwater Capture	288	301
IEUA.1.11	Turner Basin	Stormwater Capture	287	302
IEUA.1.12	East Declez Basin	Stormwater Capture	288, 289	303
IEUA.3.01	Cucamonga Creek Dry-Weather Flow Diversion to Regional Water Recycling Plant No. 1 Project	Dry-Weather Flow Capture	287, 289	304
IEUA.3.02	Cucamonga Creek at Interstate 10 Dry-Weather Flow Diversion to Regional Water Recycling Plant No. 1 Project	Dry-Weather Flow Capture	287, 289	305
IEUA.3.03	Chino Creek at Chino Hills Parkway Dry-Weather Flow Diversion to Carbon Canyon Water Recycle Facility Project	Dry-Weather Flow Capture	290	306
IEUA.3.04	Day Creek at Wineville Basin Outflow Diversion to Regional Water Recycling Plant No. 1 Project	Dry-Weather Flow Capture	288, 289	307
IEUA.3.05	San Sevaine Creek Diversion to Regional Water Recycling Plant No. 1 Project	Dry-Weather Flow Capture	288, 289	308
IEUA.3.06	Lower Deer Creek Diversion to Regional Water Recycling Plant No. 5 Project	Dry-Weather Flow Capture	289	309
IEUA.4	Inland Empire Utilities Agency Regional Wastewater Treatment Expansion	Recycled Water	287, 289, 290, 291	310
West.13	Western Riverside County Regional Wastewater Treatment Plant Enhancement and Expansion	Recycled Water	291	311

10.2.3.1 IEUA.1.01: Wineville Basin

Wineville Flood Control Basin (Figures 288 or 289) would be repurposed to serve as a flood control and recharge basin. Improvements to the basin will be made, including the installation of a pneumatic gate to raise the storage elevation in the basin by 9 ft. Stormwater recharge values were developed by WEI and provided by Chino Basin Watermaster (CBWM). Total stormwater recharge, including that from enhanced stormwater recharge at Wineville Basin, Jurupa Basin (IEUA.1.06), and RP3 Basin (IEUA.1.10), will increase by an average of 3,430 afy (see Figure 39 for recharge at Wineville Basin).

10.2.3.2 IEUA.1.02: Lower Day Basin

The Lower Day Basin (Figure 286) currently captures stormwater flows with a rubber dam diversion. A new diversion downstream of the current diversion, and improvements to the existing rubber dam, would create an additional 163 af of storage volume. Based on recharge estimates developed by WEI and provided by CBWM, this project would generate an additional annual average recharge of 1,240 afy (Figure 293).

10.2.3.3 IEUA.1.03: San Sevaine Basin Cells 1-5

San Sevaine Basins 1-5 recharge water and provide flood control on San Sevaine Creek and Etiwanda Channel (Figure 286). An inlet structure for Basins 1-3 and a pump station in Basin 5 would allow recirculation of water from Basin 5 back up to Basins 1-3, which offer higher percolation rates. Based on recharge estimates developed by WEI and provided by CBWM, the improvements would yield an estimated average increased annual recharge of 880 afy (Figure 294).

10.2.3.4 IEUA.1.04: Victoria Basin Improvements

Victoria Basin (Figure 286) is a recharge and flood control basin owned by San Bernardino County Flood Control District (SBCFCD) and operated by IEUA. It captures flow from Etiwanda Creek channel and from San Sevaine Channel. A mid-level outlet to the basin would be abandoned to create more storage volume and improve recharge. Based on recharge estimates developed by WEI and provided by CBWM, the project would realize an additional average annual recharge of 90 afy (Figure 295).

10.2.3.5 IEUA.1.05: Montclair Basin Cells 1-4

Montclair Basins (Figure 287) are located on San Antonio Creek, which is tributary to Chino Creek, and ultimately terminates at the SAR near Prado Dam. Low level drains between Basins 1 and 2 and 2 and 3 would be constructed to improve flow between the basins. Basin 4 may be deepened to improve storage. New inlet structures for Basins 2 and 3 would also be constructed. Based on recharge estimates developed by WEI and provided by CBWM, the improvements to the basins would yield an additional annual recharge of 150 afy (Figure 296).

10.2.3.6 IEUA.1.06: Jurupa Basin

Jurupa Basin is a flood control basin owned by SBCFCD (Figure 288 or 289). The improvements to Jurupa Basin, which functions currently as a storage reservoir, would be to increase the pump station capacity from Jurupa Basin to RP3 Basins from 20 cfs to 40 cfs. The improvements would allow more stormwater to be diverted to RP3 Basins for recharge. The yield from the Jurupa Basin improvements is combined with Wineville Basin (IEUA.1.01) and the RP3 Basins (IEUA1.10). Based on recharge estimates developed by WEI and provided by CBWM, the additional average annual recharge from these three projects combined is 3,430 afy. No recharge occurs at the Jurupa Basin location (Figure 297).

10.2.3.7 IEUA.1.07: Declez Basin

Declez Basin (Figure 288 or 289) is owned by SBCFCD and operated by IEUA. Improvements to the basin would include replacing an embankment with a dam and installing a gate on the low-level drain. These improvements would increase the storage volume and recharge function of the basin. Based on recharge estimates developed by WEI and provided by CBWM, the estimated additional annual average recharge at Declez Basin would be 330 afy (Figure 298).

10.2.3.8 IEUA.1.08: CSI Basins

The CSI Basin (Figure 288) improvement project is a basin deepening project to increase storage volume and recharge. The proposed improvements would deepen the existing basin in its current footprint by ten feet. The other infrastructure at the basin would remain. Based on recharge estimates developed by WEI and provided by CBWM, the improvement in average annual recharge is estimated to be 120 afy from San Sevaine Creek (Figure 299).

10.2.3.9 IEUA.1.09: Ely Basin

Ely Basin (Figure 287 or 289) is operated as a recharge and flood control facility by IEUA and owned by SBCFCD and Chino Basin Water Conservation District (CBWCD). The proposed improvements would excavate the basin and increase the drainage area to enable additional recharge of stormwater from West Cucamonga Creek. Based on recharge estimates developed by WEI and provided by CBWM, the additional anticipated average annual recharge as a result of the improvements would be 250 afy (Figure 300).

10.2.3.10 IEUA.1.10: RP3 Basin

RP3 Basin (Figure 288) consists of four recharge basins operated for recharge, habitat mitigation, and flood control purposes on Declez Channel by IEUA. The proposed improvements to RP3 include a new recharge basin and improvements to inlet structures. The result would be additional storage and improved recharge of stormwater. The yield of the RP3 Basin project is combined with Wineville Basin (IEUA1.01) and Jurupa Basin (IEUA1.06). Based on recharge estimates developed by WEI and provided by CBWM, these projects would collectively provide an additional 3,430 afy of average annual recharge (see Figure 301 for recharge at RP3 Basin).

10.2.3.11 IEUA.1.11: Turner Basin

Turner Basin (Figure 287) serves a water recharge and flood control purpose on Cucamonga and Deer Creeks, which flow into the basin from the north and east. Based on recharge estimates developed by WEI and provided by CBWM, raising the spillway of Turner Basin 2 would result in additional storage volume and an additional annual average recharge of 30 afy (Figure 302).

10.2.3.12 IEUA.1.12: East Declez Basin

The East Declez Basin (Figure 288 or 289) project involves the construction of a new basin to accept stormwater from a new drop inlet in Declez Channel. A new 54-inch pipeline will convey stormwater from the new inlet to the recharge basin. In addition, stormwater from Jurupa Basin would be pumped to the Declez Channel though a 60 cfs pump station that would be constructed. These proposed activities would result in an increased storage of 300 af. Based on recharge estimates developed by WEI and provided by CBWM, an additional average annual recharge of 330 afy is anticipated for this project (Figure 303).

10.2.3.13 IEUA.3.01: Cucamonga Creek Dry-Weather Flow Diversion to Regional Water Recycling Plant No. 1 Project

This Cucamonga Creek Dry-Weather Flow Diversion project is a dry-weather flow diversion project which would divert water from Cucamonga Creek (Figure 289) to IEUA's Regional Water Recycling Plant No. 1 (RP-1). An average combined diversion with the Cucamonga Creek at Interstate 10 Dry-Weather Flow Diversion to RP-1 Project (IEUA.3.02) and the Lower Deer Creek Diversion to Regional Water Recycling Plant No. 5 (RP-5) Project (IEUA.3.06) would total 600 afy (see Figure 304 for diversions from Cucamonga Creek). The water would be treated to Title 22 Groundwater Replenishment – Surface Application standards and utilized for direct non-potable reuse or groundwater replenishment.

10.2.3.14 IEUA.3.02: Cucamonga Creek at Interstate 10 Dry-Weather Flow Diversion to Regional Water Recycling Plant No. 1 Project

This Cucamonga Creek Dry-Weather Flow Diversion project is a dry-weather flow diversion project which would divert water from Cucamonga Creek at Interstate-10 (Figure 287) to RP-1. An average combined diversion from this project along with IEUA 3.01 and 3.06 would total 600 afy (see Figure 305 for diversions at Interstate 10). The water would be treated to Title 22 Groundwater Replenishment –Surface Application standards and utilized for direct non-potable reuse or groundwater replenishment.

10.2.3.15 IEUA.3.03: Chino Creek at Chino Hills Parkway Dry-Weather Flow Diversion to Carbon Canyon Water Recycle Facility Project

The Chino Creek at Chino Hills Parkway dry-weather flow diversion project would divert dry-weather flows from Chino Creek (Figure 290) to Carbon Canyon Water Recycling Facility (CCWRF). The project would divert 140 afy of dry-weather flows to be treated for reuse or groundwater replenishment in IEUA's recycled water system (Figure 306).

10.2.3.16 IEUA.3.04: Day Creek at Wineville Basin Outflow Diversion to Regional Water Recycling Plant No. 1 Project

The Day Creek at Wineville Basin project (Figure 288 or 289) would involve the diversion of outflows from Wineville Basin to Day Creek for subsequent Title 22 treatment at RP-1. The project would capture 390 afy from Day Creek for reuse in IEUA's recycled water system (Figure 307).

10.2.3.17 IEUA.3.05: San Sevaine Creek Diversion to Regional Water Recycling Plant No. 1 Project

The San Sevaine Creek Diversion (Figure 288 or 289) would divert an average annual amount of water from San Sevaine Creek of 670 afy (Figure 308). The water would be diverted to RP-1 for Title 22 treatment and reuse in IEUA's recycled water system.

10.2.3.18 IEUA.3.06: Lower Deer Creek Diversion to Regional Water Recycling Plant No. 5 Project

The Lower Day Creek Diversion (Figure 289) would divert water from Lower Day Creek to RP-5. An average combined diversion from this project along with IEUA 3.01 and 3.02 would total 600 afy (see Figure 309 for diversions from Lower Deer Creek).

10.2.3.19 IEUA.4: Inland Empire Utilities Agency Regional Wastewater Treatment Expansion

This project involves maximizing the reuse of 13.8 cfs (7.4 mgd) of effluent flow (i.e., discharges) from IEUA's regional water recycling plants (RWRPs). This project would increase the reuse of local recycled water within IEUA's service area and reduce effluent flow discharges from the RWRPs to Prado Lake, Chino Creek, and Cucamonga Creek (Figures 287, 289, 290, and 291) during the cooler shoulder and winter months (i.e., November through March). Effluent would be reduced by approximately 9,860 afy (combined), as shown on Figure 310. Summer flows would remain at current levels.

This HCP covered activity was developed later in the modeling process. While a model run was made to determine project impacts (Scenario 2c.8; see Section 10.15), other scenarios that were already completed were not rerun to incorporate this additional project. This includes Scenarios 2b.1, 2b.2, and 2b.3 (all project scenarios under varying hydrologic assumptions), Scenario 2c.7 (IEUA baseflow reduction activities), and Scenario 2e.2 (all IEUA activities).

10.2.3.20 West.13: Western Riverside County Regional Wastewater Treatment Plant Enhancement and Expansion

The ultimate goal of the Western Riverside Regional Wastewater Treatment Plant Enhancement and Expansion (Figure 291) is to reduce the discharge of effluent to the SAR to zero. The water would be treated and used within the service area instead of discharged to the SAR. This would reduce the amount of discharge from the Western Riverside County Regional Wastewater Authority (WRCRWA) treatment plant by 10,080 afy (Figure 311).

10.3 Scenario 1: Evaluate Flow in the SAR and Identify Factors that May be Causing Reduced Flows

Scenario 1 evaluates flow in the SAR and uses a water budget analysis of the calibrated groundwater model to identify factors that may be causing reduced flows. The following approach was used to identify significant hydrologic changes that occurred during the calibration period:

1. Evaluate changes in: a) the contribution of various sources of flow, including sources or diversions of flow, b) the river "footprint", or areas of shallow groundwater (e. g., less than 10 ft bgs)[4], and c) gaining or losing stream segments throughout the calibration period from 1966 through 2016.

   A water budget analysis was conducted for the SAR through time to assess the relative magnitude of various sources of inflow to the river, including gaged and ungaged inflows from outside the

[4] Since riparian vegetation is largely dependent on shallow groundwater, change in areas of model-calculated shallow groundwater was used as a proxy to identify areas with potential changes in riparian vegetation.

groundwater basin, local runoff generated from precipitation within the groundwater basin, wastewater discharge, other non-tributary discharges (including imported water deliveries to the surface water system, Arlington Desalter discharge, and discharge from groundwater pumped in the SBBA), and rising water from the groundwater system. The river "footprint" was also assessed to identify gaining and losing reaches through time.

2. Identify changes in water source(s) that have the greatest impact on river flows, if any.

   Results from Item 1 were used to identify what change in water source had the greatest impact on river flow, if any.

10.3.1 Hydrologic Base Period

Scenario 1 was conducted using the final calibration run of the Integrated SAR Model (calibration period from January 1966 through December 2016). This period includes wet, dry, and average hydrological conditions, as shown on Figure 11.

10.3.2 Water Budget Analysis

Water budget analysis was used to assess the stream water budget, similar to methods used for the groundwater basin as a whole. The SAR was considered the control volume, and sources of inflow and outflow were identified and assessed. Sources of inflow to the SAR include tributary inflow from outside the groundwater basin, runoff generated within the groundwater basin, rising groundwater discharge to surface flow, and surface water discharge. Outflow consists of streambed percolation (Figure 312).

10.3.2.1 Sources of Inflow

Sources of inflow to the SAR were assessed both in terms of overall inflow and relative contribution to inflow as a percentage of overall flow. Precipitation drives tributary inflow and runoff generated within the groundwater basin, and trends in both these terms are difficult to assess because these fluxes are highly variable year-to-year – reflecting changes in rainfall. The ten-year average volumes and relative contribution of various sources of inflow to the SAR are summarized in the following tables presented in Figures 313 and 314, respectively, with the cumulative departure from mean precipitation shown along the top of each chart.

Table 10-4. Average Annual Inflow to the Santa Ana River

Hydrologic Period	Annual Average Precipitation	Tributary Inflow from Outside of the Groundwater Basin	Runoff from Within the Groundwater Basin	Surface Water Discharge	Rising Water	TOTAL
	[inch/year]	[afy]				
1966-1975	14.9	232,880	49,720	38,850	28,360	349,810
1976-1985	19.0	327,700	81,720	63,350	29,560	502,330
1986-1995	16.6	262,770	93,470	95,000	29,420	480,660
1996-2005	14.7	286,190	87,590	126,780	28,090	528,650
2006-2015	12.1	194,490	65,660	113,600	24,020	397,770
1966-2016	15.4	258,060	75,330	87,750	27,770	448,910

Table 10-5. Relative Sources of Inflow to the Santa Ana River

Hydrologic Period	Annual Average Precipitation	Tributary Inflow from Outside of the Groundwater Basin	Runoff from Within the Groundwater Basin	Surface Water Discharge	Rising Water	TOTAL
	[inch/year]	[afy]				
1966-1975	14.9	67%	14%	11%	8%	100%
1976-1985	19.0	65%	16%	13%	6%	100%
1986-1995	16.6	55%	19%	20%	6%	100%
1996-2005	14.7	54%	17%	24%	5%	100%
2006-2015	12.1	49%	17%	29%	6%	100%
1966-2016	15.4	57%	17%	20%	6%	100%

Trends in ten-year averages of tributary inflow and local runoff are a result of wet and dry hydrologic periods and changes in basin physiography, including flood control infrastructure (notably, Seven Oaks Dam) and urbanization, which tends to contribute to higher runoff. Ten-year average tributary inflow ranges from approximately 328,000 afy during the wet hydrologic period from 1976 through 1985 to approximately 195,000 afy during the drought period from 2006 through 2015. That difference in flow from tributary inflow is larger than the contribution of any other source during any other period in the analysis (Tables 10-4 and 10-5) and highlights the primary role tributary inflow has in the hydrology of the

Upper SAR. The relative contribution of tributary inflow to the overall water budget decreases over the calibration period as a result of dry hydrologic conditions in the latter two ten-year periods, increased recycled water discharges that grow over the period to make up a significant portion of inflow, and possibly some reduction in tributary inflow downstream of Seven Oaks Dam.

The most prominent trend in Figure 314 and Table 10-5 is the increase in contribution from recycled water discharge to streamflow. Over the simulation period, contribution from recycled water discharge to streamflow increases from 11% (38,850 afy) of total inflow for the period from 1966 through 1976 to 29% (113,600 afy) of total inflow for the period from 2006 through 2015. The rising contribution of recycled water to streamflow decreases the seasonality of low flows and increases percolation downstream of discharge locations. Reduced seasonality in depth to water in the vicinity of the stream is observed in simulated groundwater levels as a result of this shift to more regular sources of inflow.

Rising water makes up 5-8% of overall streamflow and in most of the ten-year periods was around 28,000 afy. In the most recent ten-year period (2006 through 2015), rising water fell to approximately 24,000 afy, corresponding to the decade with the lowest rainfall (12.1 inches per year on average; see Figure 313).

Inflows are balanced by streambed percolation and outflow from the basin at Prado Dam. The terms are also highly hydrologically driven, with high amounts of runoff and streambed percolation occurring during wet years (Figures 313 and 314).

10.3.2.2 River Footprint

Based on previous work conducted by Aspen for the estimation of riparian water use/evapotranspiration, areas with depth to groundwater of less than ten feet were used as an approximation of the river footprint. The river footprint was plotted through time. Snapshots during the month of September at ten year intervals are shown on Figure 315 while the footprint under dry and wet hydrologic conditions is shown on Figure 316. Initially, the footprint extends into Temescal along Temescal Creek. The footprint shrinks in this area through the simulation period toward Prado Basin and the Santa Ana River. Elsewhere, shallow groundwater expands outward toward the recycled water discharges along Chino Creek. The overall footprint in the Prado Basin area remains relatively consistent elsewhere.

10.3.2.3 Gaining and Losing Stream Reaches through Time

Gaining and losing reaches are presented on Figures 317 through 322 under average hydrologic conditions and in ten-year increments. Similar to the analysis conducted for sources of inflow, ten-year averages are presented for streambed percolation as well. These figures identify gaining and losing reaches through time, and changes in the magnitude and direction of surface water/groundwater interaction. Gaining reaches are present in San Timoteo, near MWD Crossing and Prado Basin. Some reaches between MWD Crossing and E Street gaging station change between gaining and losing reaches through time depending on hydrology, recycled water discharge, and groundwater levels adjacent to the SAR. Overall however, while the magnitude of losing reaches changes through time, the pattern of gaining and losing reaches through time is consistent.

10.3.3 Impacts on River Flows

The two major persistent trends identified by assessing the sources of inflow are:

1) Precipitation drives tributary inflow and local runoff, which support higher streambed percolation and runoff at Prado Dam during wet years, but also result in lower streamflow during periods of extended drought, such as the period from 2006 through 2015. The SAR is driven primarily by tributary inflows from outside the groundwater basin.

A large increase in recycled water discharge occurs over the course of the simulation period from 1966 through 2016. The location and lack of seasonality in the discharge create more uniform inflow the SAR, and tend to promote higher streambed percolation and groundwater levels downstream of discharge locations. Figure 323 shows changes in streambed percolation in selected SAR reaches. In particular, changes in streambed percolation as a result of the cessation of discharge at the San Bernardino Water Reclamation Plant (WRP) and transfer of discharge to the Rapid Infiltration and Extraction (RIX) facility in the mid-1990s can be discerned.

10.4 Scenario 2a: Baseline Model Run

Scenario 2a is a baseline condition model run with no HCP activities implemented. This run serves as a benchmark for comparison with project condition scenario runs. Water balance and water level results are compared to this baseline run to isolate the hydrologic effects of each projector combined projects. Scenario 2a assumptions are discussed in detail below.

10.4.1 Hydrologic Base Period

The hydrologic base period for Scenarios 2 through 4[5], which will be used as a basis for the amount of precipitation that falls on the model area and surrounding watersheds during the simulation period, is from January 1966 through December 1990. As shown on Figure 11, this period includes wet, dry, and

[5] Scenarios 2b.2 and 2b.3 represent all project conditions under two different climate change alternatives.

average hydrological conditions. This period also corresponds to the period identified by the HCP Hydrology TAC as the HCP base period.

10.4.2 Recharge and Discharge Terms

Recharge and discharge (flux) assumptions are presented in the following section for Scenario 2a, the baseline condition simulation. Figures showing fluxes for the predictive model period also show fluxes from the model calibration period for comparison with historical hydrology.

10.4.2.1 Recharge from Mountain Front Runoff

The location of mountain front recharge is shown on Figure 324. Inflow from mountain front runoff is applied to the model following the same approach used for the model calibration. Recharge from mountain front runoff is dependent on the hydrology and is based on historical conditions (i.e., HCP base period from 1966 through 1990). In Chino Basin, in order to maintain consistency with assumptions made in Scenario 1A from the CBWM Storage Framework report (WEI, 2018), the average mountain front runoff from 1966 through 2016 (calibration run) was applied. In the SBBA, Rialto-Colton, and Riverside-Arlington Basins, the average annual recharge for the scenario run is different than the calibration period due to the difference in the averaging period. Annual recharge from mountain front runoff, which averaged 47,630 afy under baseline (Scenario 2a) conditions, is presented in Figure 325.

10.4.2.2 Underflow Inflow

Underflow inflow occurs along portions of the Chino Basin and SBBA (Figure 326). Annual underflow inflow is presented in Figure 327 under calibration and baseline (Scenario 2a) conditions. In Chino Basin, historical average underflow inflow was used to match assumptions made in the Storage Framework baseline Scenario 1A (WEI, 2018). In the SBBA, historical hydrology was duplicated for the predictive period. The historical annual average underflow in the Integrated SAR model is 34,630 afy. The annual average underflow inflow for the baseline model run (Scenario 2a) is 34,980 afy.

10.4.2.3 Areal Recharge from Precipitation

Areal recharge from precipitation is based on historical conditions and applied with the same approach used for the model calibration. Where the calibrated Integrated SAR Model used land use to determine areal recharge, the individual models and HSPF model were rerun with the most recent land use (2012) and historical rainfall from the HCP base period (1966-1990) to determine areal recharge under baseline (Scenario 2a) conditions. This approach was used for the Chino Basin and Yucaipa Basin. In Riverside-Arlington Basin, the California Department of Water Resources (DWR) Integrated Water Flow Model

Demand Calculator (IDC) model was rerun with the latest land use and HCP base period hydrology to determine areal recharge under baseline conditions. Empirical relationships with HCP base period hydrology were used in the Rialto-Colton Basin and the SBBA Basins. The annual areal recharge from precipitation, which averaged 43,190 afy under baseline (Scenario 2a) conditions, is presented in Figure 328.

10.4.2.4 Return Flow from Applied Water

Return flow from applied water was computed based on the approach used in the calibrated model for each basin. For example, Yucaipa Basin, anthropogenic return flows at parks and golf courses were updated based on the average return flow over the last 5 years of the simulation period. In the SBBA, return flows from applied water were based on relationships to water use over the calibration period. In Rialto-Colton Basin, the empirical relationship to municipal groundwater pumping was updated based on baseline pumping projections. These relationships were extrapolated over the HCP base period based on the pumping projection. In Riverside-Arlington Basin, the DWR IDC model was used to determine return flows. In Chino Basin, an approach based on water use was used to estimate return flows from applied water. This approach was updated based on the pumping projection discussed in Section 10.4.2.10. Annual return flow from applied water is shown in Figure 329 and averaged 67,150 afy under baseline (Scenario 2a) conditions.

10.4.2.5 Artificial Recharge

Artificial recharge projections for recharge basins not included in the HCP Covered Activities are available from urban water management plans (UWMPs) for agencies servicing the model area. A list of UWMPs is provided in Table 10-6, below. UWMPs were used in Yucaipa Basin to establish estimated additional recharge for Wilson Creek Spreading Grounds. In Chino Basin, projections of stormwater diversions under no-project (baseline) conditions and using 1966-1990 hydrology were developed by WEI and provided to GEOSCIENCE by CBWM. Imported water and recycled water recharge in Chino Basin under baseline conditions are consistent with the Scenario 1A assumptions in the CBWM Storage Framework report (WEI, 2018). In the SBBA, recharge of SWP water was determined and distributed amongst recharge basins using an allocation model spreadsheet incorporating SWP reliability (DWR, 2015). In Rialto-Colton Basin, all artificial recharge activities are associated with HCP activities, so were not included in the baseline simulation. During the calibration period, recharge activities at Linden Basin and Cactus Basin No. 2 accounted for the 790 afy annual average artificial recharge. In Riverside-Arlington Basin, non-HCP RIX activities were used to establish the baseline condition recharge of 30,800 afy. Locations of artificial recharge are shown on Figure 330 while annual volumes of artificial recharge are presented in Figure 331 under model calibration and baseline (Scenario 2a) conditions. Artificial recharge averaged 122,560 afy under baseline conditions.

Table 10-6. Available Resources for Water Projections

Agency	Resource
Chino Basin Desalter Authority	2015 UWMP (Karen E. Johnson, 2016)
Chino Hills, City of	2015 UWMP (City of Chino Hills, 2016)
Chino, City of	2015 UWMP (City of Chino, 2016)
Colton, City of	2015 San Bernardino Valley Regional UWMP (WSC, 2016)
Corona, City of	2015 UWMP (KWC Engineers, 2016)
Cucamonga Valley Water District	2015 UWMP (CivilTec, 2016)
East Valley Water District	2015 San Bernardino Valley Regional UWMP (WSC, 2016)
Eastern Municipal Water District	2015 UWMP (RMC, 2016)
Fontana Water Company	2015 UWMP (West Yost Associates, 2017)
Jurupa Community Services District	2015 UWMP (A.A. Webb, 2016)
Loma Linda, City of	2015 San Bernardino Valley Regional UWMP (WSC, 2016)
Marygold Mutual Water Company	2015 San Bernardino Valley Regional UWMP (WSC, 2016)
Monte Vista Water District	2015 UWMP (MVWD, 2016)
Muscoy Mutual Water Company	2015 San Bernardino Valley Regional UWMP (WSC, 2016)
Norco, City of	2015 UWMP (City of Norco, 2016)
Ontario, City of	2015 UWMP (Ontario Municipal Utilities Company, 2016)
Other/Private	2015 San Bernardino Valley Regional UWMP (WSC, 2016), 2013 Recharge Master Plan Update (WEI, 2012)
Redlands, City of	2015 San Bernardino Valley Regional UWMP (WSC, 2016)
Rialto, City of	2015 San Bernardino Valley Regional UWMP (WSC, 2016)
Riverside Highland Water Company	2015 San Bernardino Valley Regional UWMP (WSC, 2016)
Riverside Public Utilities	2015 UWMP (WSC, 2016)
Rubidoux Community Services District	2015 UWMP (K&S, 2016)
San Bernardino, City of	2015 San Bernardino Valley Regional UWMP (WSC, 2016)
Terrace Water Company	2015 San Bernardino Valley Regional UWMP (WSC, 2016)
Valley District	2015 San Bernardino Valley Regional UWMP (WSC, 2016)
West Valley Water District	2015 San Bernardino Valley Regional UWMP (WSC, 2016)
Western Municipal Water District	2015 UWMP (RMC, 2016)
Yucaipa Valley Water District	2015 San Bernardino Valley Regional UWMP (WSC, 2016)

10.4.2.6 Streambed Percolation

Streambed percolation is calculated by the Streamflow Routing Package of MODFLOW based on streamflow, groundwater levels, and the calibrated streambed conductance. Contributions to streamflow consist of tributary inflow from the surrounding watershed areas, runoff generated within the groundwater basin, and discharges to streamflow from POTWs and other dischargers. Streamflow entering the model area from outside of the groundwater basin is based on historical data from gaged streamflow, where available, or calculated runoff from the watershed model. Runoff generated within the groundwater basin is based on the runoff calculated by the watershed model using 2012 land use and under historical 1966-1990 hydrologic conditions. Discharges to streamflow from POTWs are based on the current discharges provided by the individual agencies, except for changes in discharge included in HCP Covered Activities. The locations of surface water discharge are shown on Figure 332 and summarized annually in Figure 333 for the calibration period (1966-2016) and baseline conditions (Scenario 2a, 1966-1990). For the baseline scenario run, surface water discharge averaged 108,740 afy.

10.4.2.7 Tributary Inflow from Outside the Groundwater Basin

Tributary inflow from outside the groundwater basin for the baseline scenario was updated using the HSPF surface water model with 2012 land use and historical HCP base period hydrology. Outflow from the Seven Oaks Dam during the calibrated model period was based on gauged inflow. For the predictive model period, HSPF surface water model output was used at this location. Inflows to the Yucaipa Basin were also based on updated HSPF model output. Other inflows were based on historical hydrology. The locations of tributary inflow are shown on Figure 334. Annual average tributary inflow to during the baseline period is 220,410 afy, as shown on Figure 335.

10.4.2.8 Runoff Generated Within the Groundwater Basin

Runoff generated within the groundwater basin is calculated by the HSPF model rerun with historical hydrology (1966-1990) and the most recent (2012) land use. Runoff generated within the groundwater basin during predictive model period under baseline (Scenario 2a) conditions averaged 78,260 afy (Figure 336).

10.4.2.9 Evapotranspiration

Evapotranspiration (ET) is a model-calculated value dependent on simulated groundwater level below land surface throughout the model run. The ET Package was updated using the most recent vegetation zones. Maximum ET rates and extinction depths for these vegetation zones remained the same as those developed in collaboration with the Riparian Subcommittee during the development of the calibrated model. The location of ET areas is shown on Figure 337. ET under calibration and baseline (Scenario 2a) conditions is shown on Figure 338 for the entire Integrated SAR Model area and on Figure 339 for the Prado Basin. For the baseline scenario, ET averaged 29,650 afy and 15,600 afy for the SAR Model area and Prado Basin, respectively. Monthly ET for the entire Integrated SAR Model area and Prado Basin area is also provided on Figures 340 and 341, respectively.

10.4.2.10 Groundwater Pumping

Groundwater pumping projections were developed through a multi-step process and refined in consultation with water agencies in the groundwater model area. In general, UWMPs, which are listed in Table 10-6, were reviewed in detail and information regarding increased potable water demand was tabulated. The demand increase projections are based on population estimates and per capita water use estimates by water use type for each water agency. Ratios of increase were established for water agencies based on potable water demand increases. These increases were checked against the water supply section to determine whether additional groundwater pumping would be used to meet the projected increase in water demand. Groundwater pumping projections were subsequently updated based on input from water agencies and TAC members. The groundwater pumping projections were circulated amongst regional and retail water agencies in the basin to solicit additional input. The spatial distribution of pumping amongst water agency wells was established based on the average pumping distribution from the last five years of data available.

The location of groundwater pumping is shown on Figure 342 while annual groundwater pumping during the calibration period and under baseline conditions is shown on Figure 343. Under baseline conditions, total pumping averaged 500,650 afy.

In Yucaipa Basin, groundwater pumping remains within the safe yield of the basin. Conjunctive use and imported water supplies, as well as additional utilization of recycled water, are anticipated to meet additional demand in the future. Projected pumping for the baseline scenario in Yucaipa is tabulated in Table 18. The annual average groundwater pumping during the calibration period (1966-2016) was 9,210 afy while the annual average under baseline (Scenario 2a) conditions for the predictive model period (1966-1990) is 9,630 afy.

In SBBA, a water source allocation spreadsheet was used to determine groundwater pumping. Demand was met first with available surface water – a function of historical hydrology. Groundwater pumping met the increased demand if surface water was not available to do so. Pumping for the SBBA is tabulated in Table 18. In the SBBA, the annual average pumping during the baseline model run (Scenario 2a) is 194,520 afy. Historical annual average pumping during the calibration period (1966-2016) was 178,610 afy.

In the Rialto-Colton Basin, an iterative review and modeling process was completed to adjust the pumping volumes to comply with the 1961 Decree. The 1961 Decree determines pumping rights based on Spring-High water level in three index wells: Rialto-4, WVWD-11, and WVWD-16. Pumping rights are reduced if the Index water level is below a threshold level of 969.7 ft by 1%/ft. A portion of the water rights are not subject to reduction. Table 18 shows the 1961 Decree Adjusted pumping developed by running the groundwater model iteratively and adjusting the groundwater pumping within the 1961 Decree boundary. Under baseline conditions, pumping in Rialto-Colton Basin averaged 24,050 afy.

In Riverside-Arlington, pumping projections follow the UWMP approach. The average annual pumping during the baseline model run is 92,940 afy. The historical average annual pumping during the calibration period (1966-2016) was 72,160 afy.

In Chino Basin, groundwater pumping projections developed by WEI for the CBWM Storage Framework Scenario 1A baseline condition were used to be consistent with prior modeling (WEI, 2018). The pumping projections assume the implementation of 2010 and 2013 Recharge Master Plan Update (RMPU) projects by 2021. Chino Basin pumping by water agency is shown in Table 18. Annual average groundwater pumping in Chino Basin under baseline (Scenario 2a) conditions is 165,900 afy over the predictive model period (1966-1990), while historical pumping averaged 181,180 afy over the calibration period (1966-2016).

10.4.2.11 Rising Water Discharge to Streamflow

Rising water discharge to streamflow is a model-calculated value. In the predictive model scenarios, streamflow or drain package parameters remain the same as those determined in the calibrated model. General locations of rising water in the model area are shown on Figure 344. Rising water for Scenario 2a averaged 25,140 afy, as presented on Figure 345.

10.4.3 Results

10.4.3.1 Evapotranspiration

A summary of annual ET for Scenario 2a is provided on Figure 338 for the entire Integrated SAR Model area and on Figure 339 for the Prado Basin. As shown, an annual average ET of 29,650 afy occurs during the baseline period (hydrology 1966 through 2016) across the entire model area while 15,600 afy of ET occurs in the Prado Basin area. Each subsequent scenario run is compared against the values from the Scenario 2a baseline model run.

10.4.3.2 Groundwater Levels

Scenario 2a baseline model water levels along the SAR are provided in Appendix S. In Rialto-Colton Basin, water levels during the baseline Scenario 2a run are stable or decline slightly over the predictive model period. In Riverside-Arlington, water levels in the vicinity of the SAR are steady. In Chino Basin, water levels in the PB wells (shallow wells proximal to the SAR) are also steady – showing a slight seasonal variation due to ET.

10.4.3.3 Streamflow

Average annual streamflow for the baseline model period is summarized in Table 19. During the baseline model period, average annual tributary inflow decreases slightly versus the calibrated model period due to operations and diversions at the Seven Oaks Dam.

10.4.3.4 Rising Water

Rising water that contributes to streamflow was also calculated by the model. The amount of rising water for the scenario runs is summarized in Table 20. As shown, rising water in Yucaipa, Riverside-Arlington, and Prado Basins averaged 1,100 afy, 9,870 afy, and 14,170 afy during the baseline model run, respectively.

10.4.3.5 Average Annual Water Budgets

Average annual water budgets for the baseline (Scenario 2a) are shown in Figures 346 through 352 for each groundwater basin and Prado. Scenario 2a water budgets are presented along with the values for the calibration period from 1966-2016.

10.5 Scenario 2b.1: All HCP Covered Activities (Hydrology 1966 – 1990)

Scenario 2b.1 evaluated the effect of all HCP covered activities. During this run, all of the HCP covered activities listed in Table 17 were implemented under HCP base period hydrology (i.e., hydrology from 1966 through 1990). However, as discussed in Section 10.2.3.19, since IEUA.4 was developed so much later in the modeling process, Scenario 2b.1 (which was already completed at the time) was not rerun to incorporate this additional project.

10.5.1 HCP Covered Activities Implemented

Each activity is briefly described in Section 10.2 of the report. All stormwater diversions and recharge, dry-weather flow diversions, and/or effluent discharge reductions/redistributions associated with each of these activities were implemented. Please note, the covered activity IEUA.4 (Inland Empire Utilities Agency Regional Wastewater Treatment Expansion) was developed later in the modeling process. As such, scenarios that were already completed (including Scenario 2b.1) were not rerun to incorporate this additional project. Recharge and discharge terms not affected by the HCP activities remained the same as those in the baseline simulation, which were described in Section 10.4.2.

10.5.1.1 Surface Water Diversion

HCP activities that involve stormwater diversion divert streamflow into artificial recharge basins during wet months. In the case of dry-weather flow projects, surface water diverted to water treatment facilities for reuse during dry months. The annual change in surface water diversion under Scenario 2b.1, compared to baseline conditions, is shown in Figure 353. The annual average increase in surface water diversion from the baseline (Scenario 2a) was 48,540 afy. The largest increases occurred in SBBA, where an additional 32,010 afy of stormwater was diverted and recharged. In Rialto-Colton, an additional 6,110 afy was diverted by HCP activities. In Chino Basin, an additional surface water diversion of 8,660 afy occurred from HCP activities.

10.5.1.2 Artificial Recharge

Annual change in artificial recharge for Scenario 2b.1 (Figure 354), compared to baseline conditions, includes increases in recharge from stormwater diversion, recycled water, and imported water. The primary increases are related to the stormwater increases described in the section above. Other increases come from imported and recycled water recharge in HCP activities. The total annual average increase in artificial recharge over the simulation period is 51,480 afy.

10.5.1.3 Surface Water Discharge

Annual change in surface water discharge as a result of all HCP covered activities is shown in Figure 355. In the SBBA, wastewater discharge increases by 11,070 afy due to activities associated with the SNRC. In Riverside-Arlington, wastewater discharge was reduced by 11,870 afy as a result of the SNRC and other reductions to RIX discharge. Declines at the RWQCP and WRCRWA discharge locations account for the 22,730 afy decrease in surface water discharge in the Chino Basin.

10.5.2 Results

10.5.2.1 Evapotranspiration

ET across the entire Integrated SAR Model area under Scenario 2b.1 conditions is summarized in Figure 356. The change in ET for the entire model area, compared to baseline conditions, is shown on Figure 357 while seasonal ET is shown on Figure 358. The total ET, change in ET, and seasonal ET for Prado Basin under Scenario 2b.1 conditions is shown on Figures 359, 360, and 361, respectively. Increases in ET occur in the SBBA due to higher groundwater levels as a result of increases in groundwater storage. Overall, ET in the Integrated SAR Model decreases slightly from 29,650 afy under baseline conditions to 28,880 afy under Scenario 2b.1 conditions.

10.5.2.2 Groundwater Levels

Groundwater level hydrographs for selected wells are provided in Appendix S. Water levels under Scenario 2b.1 conditions are displayed next to those calculated under baseline conditions for wells along the SAR. In Rialto-Colton Basin, water levels near the SAR are approximately 20 to 25 ft higher than Scenario 2a water levels at the end of the predictive model period, and are stable or have increased slightly overall, reflecting an increase in groundwater storage. The difference between water levels in the two scenarios along the SAR in Riverside-Arlington Basin is small. In Chino Basin, water levels along the SAR remain fairly stable during the calibration, baseline, and Scenario 2b.1 model runs and reflect seasonal changes in ET. Scenario 2b.1 water levels in shallow Prado Basin monitoring wells (see PB-2 and PB-7) coincide with baseline (Scenario 2a) water levels.

10.5.2.3 Streamflow

The distribution of monthly streamflow in the Santa Ana River at E St., MWD Crossing, and Prado Dam under Scenario 2a and Scenario 2b.1 is shown on Figures 362 through 365. Average annual streamflow is summarized in Table 19. HCP covered activities influence streamflow through diversion and recharge of stormwater and dry-weather flows or through effluent reductions and redistributions. Changes in streamflow and groundwater levels also influence streambed percolation, as the distribution of in-channel recharge changes when groundwater is diverted in headwaters for recharge.

At E St., diversions reduce average flow from 54 cfs to 50 cfs, a decline of 4 cfs. At MWD Crossing, average flow is reduced from 93 cfs to 71 cfs, a decline of 22 cfs. At Prado Dam, average flow is reduced from 269 cfs to 206 cfs, a reduction of 63 cfs. Decreases in streamflow are observed across the range of monthly streamflow rates at MWD Crossing and at Prado Dam (Figures 364 and 365). This is seen in the shift downward and to the left of the Scenario 2b.1 exceedance probability curve compared to the baseline Scenario 2a exceedance probability curve.

10.5.2.4 Rising Water

Rising water that contributes to streamflow was also calculated by the model. The amount of rising water for the scenario runs is summarized in Table 20 and presented on Figure 366. As shown, rising water in Yucaipa and Riverside-Arlington Basins increases under Scenario 2b.1 by 40 afy and 100 afy, respectively, compared to baseline (Scenario 2a) conditions. In Prado Basin, rising water decreases by 1,230 afy with the implementation of all HCP covered activities.

10.5.2.5 Average Annual Water Budgets

Average annual water budgets under Scenario 2b.1 conditions are shown in Figures 367 through 373 for each groundwater basin and Prado. Diversion and recharge are offset by decreases in streambed percolation, particularly in the upper watershed where channels are dry, and recharge is relocated to artificial recharge basins where it may have otherwise infiltrated in-channel. Also, net streambed percolation decreases due to increases in gaining stream reaches in response to increased artificial recharge. Artificial recharge is increased by a total of 51,480 afy within the five groundwater basins if all HCP covered activities are implemented. This results in increases in groundwater storage in the SBBA, where artificial recharge increases by approximately 32,150 afy (Figure 368). In Chino Basin, the decline in groundwater storage lessens to -2,650 afy under Scenario 2b.1 conditions, as compared to the baseline (Figure 371).

10.6 Scenario 2b.2: All HCP Activities (2030 Climate Change)

10.6.1 General Assumptions

Scenario 2b.2 assesses the effects of simulated 2030 climate conditions with the implementation of all HCP Covered Activities. The 2030 climate conditions were developed based on Sustainable Groundwater Management Act (SGMA) Climate Change Technical Advisory Group (CCTAG) Guidance. The CCTAG reviewed ensemble climate simulations to develop change factors for precipitation and evapotranspiration (DWR, 2018). The climate change factors were downscaled to the Variable Infiltration Capacity (VIC) land surface model grid by the CCTAG. Each VIC grid cell contains a change factor which varies by month and location. For the groundwater modeling conducted here-in, these change factors have been applied to past HCP base period hydrology (1966 to 1990) to develop updated boundary conditions reflective of future climate. The VIC grid cells were referenced to the MODFLOW model grid, and change factors were applied based on the grid cell each MODFLOW model grid cell fell within. A map of VIC grid cells and how those overlap with the study area is included in Figure 374.

Adjustments to average monthly precipitation at the San Bernardino County Hospital Station based on the climate change factors is shown on Figure 375. Average annual and monthly climate change factors for each groundwater basin are shown in Figures 376 to 385. For 2030 climate change, the average precipitation climate change factor shows a reduction in precipitation of 3 to 5 percent. In the summer months, increases in precipitation are anticipated. However, these months have little precipitation, so these increases do not correspond to large increases in rainfall amount. Decreases during October through December account for the primary reduction in overall precipitation (Figure 375). Tributary inflow and runoff were also reduced by an average climate change factor for each groundwater basin.

Evapotranspiration change factors are shown in Figures 388 through 405. ET is anticipated to increase approximately 5% in the 2030 climate change guidance. The ET change factors show greater uniformity than the precipitation factors, which are more variable.

10.6.2 HCP Covered Activities Implemented

Scenario 2b.2 applies all HCP Covered Activities, which are described in detail in Section 10.2, and include stormflow and dry-weather diversion projects and baseflow reduction activities. The activities implemented are the same as those implemented in Scenario 2b.1 (Section 10.5).

10.6.2.1 Surface Water Diversion

Scenario 2b.2 assumes the implementation of all HCP Covered Activities. Surface water diversion activities include stormflow diversions and dry-weather flow diversion projects that direct streamflow into spreading grounds, recharge basins, or in the case of dry-weather flow diversions to water treatment facilities. The annual average increase in surface water diversion as compared to the Scenario 2a baseline averages 48,540 afy in Scenario 2b.2 (Figure 353). The majority of diversion, 32,010 afy, occurs in SBBA as a result of stormwater recharge projects. Increase in surface water diversion averages 8,660 afy in Chino Basin as a result of dry-weather flow and stormwater diversion projects.

10.6.2.2 Artificial Recharge

Artificial recharge of diverted stormwater occurs in spreading grounds and recharge basins. The average increase in artificial recharge for Scenario 2b.2 is 51,480 afy, assuming implementation of all HCP Covered Activities (Figure 354). In SBBA, the average increase in artificial recharge is 32,150 afy of the total. In Rialto-Colton, an increase of 5,310 afy occurs. In Riverside-Arlington, an increase of 7,160 afy results. In Chino Basin, an increase in artificial recharge of 6,860 afy occurs as a result of the stormwater diversion and recharge.

10.6.2.3 Surface Water Discharge

In the SBBA, SNRC and associated activities increase recycled water discharge by 11,070 afy (Figure 355). In Riverside-Arlington, wastewater discharge was reduced by 11,870 afy due to implementation of SNRC and other reductions to RIX discharge. Declines at the RWQCP and WRCRWA discharge locations result in a 22,730 afy decrease in discharge in the Chino Basin.

10.6.3 Results

Results from Scenarios 2b.2 and 2b.3 can be interpreted against Scenario 2a: Baseline and Scenario 2b.1: All HCP Covered Activities. Comparing results against Scenario 2b.1 isolates the effect of climate change in the results, while comparing against the Scenario 2a: Baseline results yields the net change of All HCP Covered Activities and climate change.

10.6.3.1 Evapotranspiration

Evapotranspiration results for Scenario 2b.2 are shown in Figures 400 to 405. Potential evapotranspiration rates have increased by approximately 5%. This increase due to climate change results in a 320 afy increase in ET in Prado Basin as compared to Scenario 2b.1. However, the implementation of all HCP Covered Activities under 2030 climate change conditions results in an overall decline of -640 afy in groundwater ET in Prado Basin, compared to baseline (Scenario 2a). Total ET in Scenario 2b.2 is 29,630 afy, which is 20 afy less than the Scenario 2a: Baseline Scenario. This reflects a decrease in ET as a result of the implementation of all HCP Covered Activities, and an offsetting increase as a result of warmer projected future temperatures in 2030. Seasonal distribution of ET for the entire model and for Prado only is shown in Figures 402 and 405 respectively. Figures 403 and 404 show annual and annual change in Prado Basin ET.

10.6.3.2 Groundwater Levels

Groundwater level hydrographs for wells along the SAR are provided in Appendix S. Water levels are compared to baseline conditions, with water levels for each well location shown alongside the project condition hydrographs and historical water level observations. Starting upstream, at Airport No.2, water levels are projected to be approximately 20 -30 ft higher than Scenario 2a: Baseline water levels as a result of additional recharge due to implementation of HCP Covered Activities. Downstream, at 1S/4W20H03, water levels are also higher than 2a: Baseline levels by approximately 10-20 ft throughout the simulation period. Moving farther downstream, at Well #28, water levels are coincident with Scenario 2a: Baseline water levels. In Chino Basin, at PB-1_2, water levels are slightly higher than baseline due to recharge activities.

10.6.3.3 Streamflow

Streamflow results reflect the combination of all HCP Activities, including stormwater diversion and recharge, and baseflow reduction activities. The effect of climate change alone is visible in the difference between Scenario 2b.2 streamflow results and those from Scenario 2b.1. Average streamflow at Prado is reduced by 5 cfs at Prado as a result of climate change hydrology (Table 19) – from 206 cfs in Scenario 2b.1 to 201 cfs under Scenario 2b.2 conditions.

Exceedance probability plots for model-simulated streamflow at E. St, MWD Crossing and Prado Dam are shown in Figures 407 through 409. Low flows increased slightly at E. St. as a result of recharge activities, but this is offset by reductions in higher flows shown in Figure 407. Decreases occur across flow ranges at MWD Crossing and Prado in Figures 408 and 409.

10.6.3.4 Rising Water

In Scenario 2b.2, rising water is reduced due to reduced mountain front runoff, streambed percolation, and areal recharge from precipitation. Rising water is tabulated in Table 20 and shown on Figure 410. Reductions in rising water occur in Riverside-Arlington and Prado, as compared to Baseline conditions. Rising water is also lower in all three locations than that expected under Scenario 2b.1 conditions (All HCP Covered Activities). Rising water is 40 afy lower in Yucaipa, 180 afy lower in Riverside-Arlington, and 440 afy lower at Prado due to projected 2030 climate change.

10.6.3.5 Average Annual Water Budgets

Average annual water budgets for Scenario 2b.2 are shown in Figures 367 to 373. Results for Scenarios 2a, 2b.1, 2b.2 and 2b.3 are presented alongside one another to allow for comparison amongst varying scenarios. In the SBBA, Scenario 2b.2 (2030 climate change conditions) causes a decrease in groundwater storage of 2,620 afy over Scenario 2b.1 conditions. This is due to reductions in inflow to the groundwater system in mountain front runoff, streambed percolation, and areal recharge from precipitation. A reduction in underflow inflow from Yucaipa is also observed. Likewise, reductions in mountain front runoff, streambed percolation, and underflow inflow in Rialto-Colton Basin are observed. These reductions due to 2030 climate change result in lower underflow outflow and change in groundwater storage. In Riverside-Arlington Basin, the results of 2030 climate change are visible in reduced mountain front runoff and areal recharge from precipitation. Under Scenario 2b.2 conditions, rising water is lower and ET is elevated, as compared with Scenario 2b.1. Also, change in groundwater storage is decreased. In Chino Basin, 2030 climate change reduces areal recharge from precipitation and mountain front runoff. ET increases in Chino Basin from 19,900 afy to 20,410 afy due to warmer temperatures predicted in the 2030 climate change scenario. Change in Chino Basin groundwater storage decreases from -2,650 afy under Scenario 2b.1 conditions to -3,740 afy with 2030 climate change due to reduced inflows and increased outflows.

10.7 Scenario 2b.3: All HCP Activities (2070 Climate Change)

10.7.1 General Assumptions

Scenario 2b.3 assesses the effects of simulated 2070 climate conditions with the implementation of all HCP Covered Activities. As with the 2030 climate change scenario, Scenario 2b.3, climate change conditions were developed based on climate change factors developed by the SGMA CCTAG. Adjustments to average monthly precipitation at the San Bernardino County Hospital Station based on the climate change factors is shown on Figure 375. Average annual and monthly precipitation change factors for each groundwater basin are shown in Figures 376 to 387. For 2070 climate change, the average precipitation climate change factor shows a reduction in precipitation of 4 to 6 percent. In the summer months, increases in precipitation are anticipated. However, these months have little precipitation, so these increases do not correspond to large increases in rainfall amount. Decreases during October through December account for the primary reduction in overall precipitation (Figure 375). Tributary inflow and runoff were also reduced by an average climate change factor for each groundwater basin.

Evapotranspiration change factors are shown in Figures 388 through 399. ET is anticipated to increase approximately 10% in the 2070 climate change guidance. The ET change factors show greater uniformity than the precipitation factors, which are more variable.

10.7.2 HCP Covered Activities Implemented

Scenario 2b.3 applies all HCP Covered Activities. The activities are described in detail in Section 10.2, and include stormflow and dry-weather diversion projects and baseflow reduction activities. The activities implemented are the same as those implemented in Scenario 2b.1 (Section 10.5).

10.7.2.1 Surface Water Diversion

Scenario 2b.3 assumes the implementation of all HCP Covered Activities. Surface water diversion activities include stormflow diversions and dry-weather flow diversion projects that direct streamflow into spreading grounds, recharge basins, or in the case of dry-weather flow diversions to water treatment facilities. The annual average increase in surface water diversion as compared to the Scenario 2a baseline averages 48,540 afy in Scenario 2b.3 (Figure 353). The majority of diversion, 32,010 afy, occurs in SBBA as a result of stormwater recharge projects. Increase in surface water diversion averages 8,660 afy in Chino Basin as a result of dry-weather flow and stormwater diversion projects.

10.7.2.2 Artificial Recharge

Artificial recharge of diverted stormwater occurs in spreading grounds and recharge basins. The average increase in artificial recharge for Scenario 2b.3 is 51,480 afy, assuming implementation of all HCP Covered Activities (Figure 354). In SBBA, the average increase in artificial recharge is 32,150 afy of the total. In Rialto-Colton, an increase of 5,310 afy occurs. In Riverside-Arlington, an increase of 7,160 afy results. In Chino Basin, an increase in artificial recharge of 6,860 afy occurs as a result of the stormwater diversion and recharge.

10.7.2.3 Surface Water Discharge

In the SBBA, SNRC and associated activities increase recycled water discharge by 11,070 afy. In Riverside-Arlington, wastewater discharge was reduced by 11,870 afy due to implementation of SNRC and other reductions to RIX discharge (Figure 355). Declines at the RWQCP and WRCRWA discharge locations result in a 22,730 afy decrease in discharge in the Chino Basin.

10.7.3 Results

Results from Scenarios 2b.2 and 2b.3 can be interpreted against Scenario 2a: Baseline and Scenario 2b.1: All HCP Covered Activities. Comparing results against Scenario 2b.1 isolates the effect of climate change in the results, while comparing against the Scenario 2a: Baseline results yields the net change of All HCP Covered Activities and climate change.

10.7.3.1 Evapotranspiration

Evapotranspiration results for Scenario 2b.3 are shown in Figures 411 to 416. Potential evapotranspiration rates have increased by approximately 10%. This increase due to climate change results in a 650 afy increase in ET in Prado Basin as compared to Scenario 2b.1. However, the implementation of all HCP Covered Activities under 2070 climate change conditions results in an overall decline of -310 afy in groundwater ET in Prado Basin, compared to baseline (Scenario 2a). Total ET in Scenario 2b.3 is 30,380 afy, which is 730 afy more than Scenario 2a: Baseline Scenario. While there is a general decrease in ET as a result of implementing all HCP Covered Activities, it is not enough to offset the increase as a result of warmer projected temperatures for 2070. Seasonal distribution of ET for the entire model and for Prado only is shown in Figures 413 and 416 respectively. Figures 414 and 415 show annual and annual change in Prado Basin ET.

10.7.3.2 Groundwater Levels

Groundwater level hydrographs for wells along the SAR are provided in Appendix S. Water levels are compared to baseline conditions, with water levels for each well location shown alongside the project condition hydrographs and historical water level observations. Groundwater elevations in these wells under Scenario 2b.3 (2070 climate change) conditions generally exhibit the same trends as those predicted under Scenario 2b.2 (2030 climate change) conditions, though water levels are slightly lower.

10.7.3.3 Streamflow

Streamflow results reflect the combination of all HCP Activities, including stormwater diversion and recharge, and baseflow reduction activities. The effect of climate change alone is visible in the difference between Scenario 2b.3 streamflow results and those from Scenario 2b.1. Average streamflow at Prado is reduced by 9 cfs at Prado as a result of climate change hydrology (Table 19) – from 206 cfs in Scenario 2b.1 to 197 cfs under Scenario 2b.3 conditions.

Exceedance probability plots for model-simulated streamflow at E. St, MWD Crossing and Prado Dam are shown in Figures 418 through 420. As with Scenario 2b.2, low flows increased slightly at E. St. as a result of recharge activities, but this is offset by reductions in higher flows shown in Figure 418. Decreases occur across flow ranges at MWD Crossing and Prado in Figures 419 and 420.

10.7.3.4 Rising Water

In Scenario 2b.3, rising water is reduced due to reduced mountain front runoff, streambed percolation, and areal recharge from precipitation. Rising water is tabulated in Table 20 and shown on Figure 421. Reductions in rising water occur in Yucaipa, Riverside-Arlington, and Prado, as compared to Baseline conditions. Rising water is also lower in all three locations than that expected under Scenario 2b.1 conditions (All HCP Covered Activities). Rising water is 80 afy lower in Yucaipa, 260 afy lower in Riverside-Arlington, and 790 afy lower at Prado due to projected 2070 climate change.

10.7.3.5 Average Annual Water Budgets

Average annual water budgets for Scenario 2b.3 are shown in Figures 367 to 373. Results for Scenarios 2a, 2b.1, 2b.2 and 2b.3 are presented alongside one another to allow for comparison amongst varying scenarios. In the SBBA, Scenario 2b.3 (2070 climate change conditions) causes a decrease in groundwater storage of 4,990 afy over Scenario 2b.1 conditions. This is due to reductions in inflow to the groundwater system in mountain front runoff, streambed percolation, and areal recharge from precipitation. A reduction in underflow inflow from Yucaipa is also observed. Likewise, reductions in mountain front runoff, streambed percolation, and underflow inflow in Rialto-Colton Basin are observed. These reductions due to 2070 climate change result in lower underflow outflow and change in groundwater storage. In Riverside-Arlington Basin, the results of 2070 climate change are visible in reduced mountain front runoff and areal recharge from precipitation. Under Scenario 2b.3 conditions, rising water is lower and ET is elevated, as compared with Scenario 2b.1. Also, change in groundwater storage is decreased. In Chino Basin, 2070 climate change reduces areal recharge from precipitation and mountain front runoff. ET increases in Chino Basin from 19,900 afy to 20,890 afy due to warmer temperatures predicted in the 2070 climate change scenario. Change in Chino Basin groundwater storage decreases from -2,650 afy under Scenario 2b.1 conditions to -5,380 afy with 2070 climate change due to reduced inflows and increased outflows.

10.8 Scenario 2c.1: SNRC, San Bernardino Baseflow Reduction Activities, and Rialto Baseflow Reduction

10.8.1 HCP Covered Activities Implemented

Scenario 2c runs implement various combinations of baseflow reduction activities to assess the effects of each or combinations of projects. Scenario 2c.1 implements effluent discharge reduction at RIX from the SNRC (including additional recharge in City Creek and Redlands Basin), Clean Water Factory, and the Rialto Wastewater Treatment Plant Reuse Project. These projects are shown on Figure 422 and summarized in Table 10-7 below. The activities are described in Table 17 and in Section 10.2.

Table 10-7. HCP Activities (Scenario 2c.1)

Project ID	Activity	Type
EV.4.01 - 4.03	Sterling Natural Resource Center	Effluent Discharge Reduction / Recharge
WD.1	SBMWD Recycled Water Project	Effluent Discharge Reduction
Rial.1	Rialto Wastewater Treatment Plant Reuse Project	Discharge Reduction

10.8.1.1 Surface Water Diversion

No changes in surface water diversion were implemented in this scenario.

10.8.1.2 Artificial Recharge

As shown on Figure 423, artificial recharge in the SBBA increases by 870 afy under Scenario 2c.1 conditions as a result of recycled water recharge in Redlands Basins from the SNRC. This recharge would be diverted to Redlands Basins during high flow events in City Creek to optimize recharge.

10.8.1.3 Surface Water Discharge

In Scenario 2c.1, wastewater discharge in the SBBA would increase by 8,080 afy due to SNRC activities (Figure 424). A portion (4,700 afy) of this discharge percolates in City Creek. The remainder would flow to the SAR and likely percolate there since this segment of the river is typically dry. The City of Rialto and RIX reductions as a result of SNRC, SBMWD Recycled Water Project, and Rialto Wastewater Treatment Plant Reuse Project would reduce effluent discharge by 17,350 afy in the Riverside-Arlington Basin. The annual average reduction in effluent discharge is 9,270 afy.

10.8.2 Results

10.8.2.1 Evapotranspiration

ET across the entire Integrated SAR Model area under Scenario 2c.1 conditions is summarized in Figure 425. The change in ET for the entire model area, compared to baseline conditions, is shown on Figure 426 while seasonal ET is shown on Figure 427. The total ET, change in ET, and seasonal ET for Prado Basin under Scenario 2c.1 conditions is shown on Figures 428, 429, and 430, respectively. A decrease in effluent discharge in Riverside-Arlington led to a reduction in evapotranspiration in that groundwater basin. ET in other groundwater basins was not affected by the activities covered in Scenario 2c.1.

10.8.2.2 Groundwater Levels

Groundwater level hydrographs for selected wells are provided in Appendix S. Water levels under Scenario 2c.1 conditions are displayed next to those calculated under baseline conditions for wells along the SAR. Groundwater levels in Rialto-Colton and in Riverside-Arlington decline slightly under Scenario 2c.1 due to effluent redistribution and effluent discharge reductions. In Chino Basin, water levels adjacent to the SAR remained unaffected and were coincident with baseline (Scenario 2a) water levels.

10.8.2.3 Streamflow

The distribution of monthly streamflow in the Santa Ana River at E St., MWD Crossing, and Prado Dam under Scenario 2a and Scenario 2c.1 is shown on Figures 431 through 434. Average annual streamflow is summarized in Table 19. Reductions in effluent discharge resulted in lower average discharges at MWD Crossing and Prado Dam. At E St., streamflow increases very slightly as shown in the exceedance plot in Figure 432. At MWD Crossing, streamflow decreases by 25 cfs, from 103 cfs to 78 cfs. A similar decrease is observed at Prado Dam.

10.8.2.4 Rising Water

The amount of rising water for the scenario runs is summarized in Table 20. As shown, rising water in Yucaipa Basin is unaffected by Scenario 2c.1 since the activities are located downgradient. In the Riverside-Arlington and Prado Basins, rising water under Scenario 2c.1 conditions decreases by 1,320 afy and 30 afy, respectively, compared to baseline (Scenario 2a) conditions.

10.8.2.5 Average Annual Water Budgets

The annual water budgets for Scenario 2c.1 are shown on Figures 436 through 442 for each groundwater basin and Prado.

10.9 Scenario 2c.2: SNRC and San Bernardino Baseflow Reduction Activities

10.9.1 HCP Covered Activities Implemented

Scenario 2c.2 implements the SNRC activities and Clean Water Factory. These activities are shown on Figure 443 and summarized in Table 10-8 below. The activities are described in Table 17 and in Section 10.2.

Table 10-8. HCP Activities (Scenario 2c.2)

Project ID	Activity	Type
EV.4.01 - 4.03	Sterling Natural Resource Center	Effluent Discharge Reduction / Recharge
WD.1	SBMWD Recycled Water Project	Effluent Discharge Reduction

10.9.1.1 Surface Water Diversion

No increases in stormwater diversion would occur with Scenario 2c.2.

10.9.1.2 Artificial Recharge

As shown on Figure 444, artificial recharge in the SBBA increases 870 afy in Scenario 2c.2 as a result of recycled water recharge in Redlands Basins from the SNRC. This recharge would be diverted to Redlands Basins during high flow events in City Creek as in Scenario 2c.1.

10.9.1.3 Surface Water Discharge

As in Scenario 2c.1, wastewater discharge in the SBBA would increase by 8,080 afy under Scenario 2c.2 conditions in response to SNRC activities (Figure 445). A portion (4,700 afy) of this discharge percolates in

City Creek. The remainder would flow to the SAR and likely percolate there since this segment of the river is typically dry. RIX reductions as a result of the SNRC and SBMWD Recycled Water Project would reduce effluent discharge by 15,970 afy in the Riverside-Arlington Basin. The annual average reduction in effluent discharge would be 7,890 afy.

10.9.2 Results

10.9.2.1 Evapotranspiration

ET across the entire Integrated SAR Model area under Scenario 2c.2 conditions is summarized in Figure 446. The change in ET for the entire model area, compared to baseline conditions, is shown on Figure 447 while seasonal ET is shown on Figure 448. The total ET, change in ET, and seasonal ET for Prado Basin under Scenario 2c.2 conditions is shown on Figures 449, 450, and 451, respectively. A decrease in effluent discharge in Riverside-Arlington led to a reduction in evapotranspiration in that groundwater basin. ET in other groundwater basins was not affected. Results from Scenario 2c.2 closely resemble the results from Scenario 2c.1. The difference between Scenarios 2c.1 and 2c.2 is that the 1,390 afy effluent reduction from the Rialto Wastewater Treatment Plant Reuse Project was not simulated in this scenario.

10.9.2.2 Groundwater Levels

Groundwater level hydrographs for selected wells are provided in Appendix S. Water levels under Scenario 2c.2 conditions are displayed next to those calculated under baseline conditions for wells along the SAR. Results from Scenario 2c.2 closely resemble results from Scenario 2c.1. Groundwater levels in Rialto-Colton and in Riverside-Arlington declined slightly due to the implementation of Scenario 2c.2 effluent redistribution and effluent discharge reductions. In Chino Basin, water levels adjacent to the SAR remained unaffected and were coincident with the baseline Scenario 2a water levels.

10.9.2.3 Streamflow

The distribution of monthly streamflow in the Santa Ana River at E St., MWD Crossing, and Prado Dam under Scenario 2a and Scenario 2c.2 is shown on Figures 452 through 455. Average annual streamflow is summarized in Table 19. Reductions in effluent discharge resulted in lower average discharges at MWD Crossing and Prado Dam. Streamflow increases very slightly at E St., as shown in the exceedance plot in Figure 453. At MWD Crossing, streamflow decreased by 23 cfs, from 103 cfs to 80 cfs. A similar decrease was observed at Prado Dam. The absence of the Rialto Wastewater Treatment Plant Reuse Project discharge reduction (-1,390 afy of effluent discharge) resulted in a 2 cfs difference in streamflow at MWD Crossing and at Prado Dam compared to Scenario 2c.1.

10.9.2.4 Rising Water

The amount of rising water for the scenario runs is summarized in Table 20. As shown, rising water in Yucaipa Basin is relatively unaffected by Scenario 2c.2 since the activities are located downgradient. In the Riverside-Arlington and Prado Basins, rising water under Scenario 2c.2 conditions decreases by 1,240 afy and 30 afy, respectively, compared to baseline (Scenario 2a) conditions.

10.9.2.5 Average Annual Water Budgets

The annual water budgets for Scenario 2c.2 are shown on Figures 436 through 442 for each groundwater basin and Prado.

10.10 Scenario 2c.3: Rialto Baseflow Reduction

10.10.1 HCP Covered Activities Implemented

Scenario 2c.3 implements Rialto Wastewater Treatment Plant Reuse Project activities alone, as summarized in Table 10-9 below. This activity is also shown on Figure 457 and is described in Table 17 and in Section 10.2.

Table 10-9. HCP Activities (Scenario 2c.3)

Project ID	Activity	Type
Rial.1	Rialto Wastewater Treatment Plant Reuse Project	Discharge Reduction

10.10.1.1 Surface Water Diversion

No increases in stormwater diversion would occur under Scenario 2c.3 conditions.

10.10.1.2 Artificial Recharge

No increases in artificial recharge would occur under Scenario 2c.3 conditions.

10.10.1.3 Surface Water Discharge

In Scenario 2c.3, Rial.1 is implemented by itself. Effluent discharge reduction would occur in the Riverside-Arlington Basin. The annual average reduction in effluent discharge to the SAR would be 1,390 afy (Figure 458).

10.10.2 Results

10.10.2.1 Evapotranspiration

ET across the entire Integrated SAR Model area under Scenario 2c.3 conditions is summarized in Figure 459. The change in ET for the entire model area, compared to baseline conditions, is shown on Figure 460 while seasonal ET is shown on Figure 461. The total ET, change in ET, and seasonal ET for Prado Basin under Scenario 2c.3 conditions is shown on Figures 462, 463, and 464, respectively. As shown, the implementation of the Rialto Wastewater Treatment Plant Reuse Project does not affect ET.

10.10.2.2 Groundwater Levels

Groundwater level hydrographs for selected wells are provided in Appendix S. Water levels under Scenario 2c.3 conditions are displayed next to those calculated under baseline conditions for wells along the SAR. Groundwater levels under Scenario 2c.3 conditions were coincident with Scenario 2a baseline groundwater levels.

10.10.2.3 Streamflow

The distribution of monthly streamflow in the Santa Ana River at E St., MWD Crossing, and Prado Dam under Scenario 2a and Scenario 2c.3 is shown on Figures 465 through 468. Average annual streamflow is summarized in Table 19. Reductions in effluent discharge resulted in lower average discharges at MWD Crossing and Prado Dam. At MWD Crossing, streamflow decreased by 3 cfs, from 103 cfs to 100 cfs. A similar decrease is observed at Prado Dam. No change in streamflow was observed at E St., which is upstream of the decreases in effluent discharge.

10.10.2.4 Rising Water

The amount of rising water for the scenario runs is summarized in Table 20 and shown on Figure 469. As shown, rising water in Yucaipa and Prado Basins is unaffected by Scenario 2c.3. In the Riverside-Arlington Basin, rising water under Scenario 2c.3 conditions decreases by 20 afy, compared to baseline (Scenario 2a) conditions.

10.10.2.5 Average Annual Water Budgets

The annual water budgets for Scenario 2c.3 are shown on Figures 436 through 442 for each groundwater basin and Prado.

10.11 Scenario 2c.4: SNRC Only

10.11.1 HCP Covered Activities Implemented

Scenario 2c.4 applies effluent discharge reduction at RIX from implementation of the SNRC (including additional recharge in City Creek and Redlands Basin). This project is shown on Figure 470 and summarized in Table 10-10 below. The activity is described in Table 17 and in Section 10.2.

Table 10-10. HCP Activities (Scenario 2c.4)

Project ID	Activity	Type
EV.4.01 - 4.03	Sterling Natural Resource Center	Recycled Water

10.11.1.1 Surface Water Diversion

No changes in surface water diversion were implemented in this scenario.

10.11.1.2 Artificial Recharge

Artificial recharge increases by 8,670 afy as a result of SNRC operations, with an average of 7,150 afy additional recharge in City Creek downstream of the discharge point during low flow conditions and an average of 1,520 afy diverted and recharged in Redlands Basin during high flow conditions to allow for increased recharge. Increases in artificial recharge as a result of this project are shown in Figure 471.

10.11.1.3 Surface Water Discharge

In the SBBA, an increase in surface water discharge of 280 afy at the confluence of City Creek and the SAR is anticipated under Scenario 2c.4 conditions. Reductions at RIX as a result of SNRC operation would reduce effluent discharge by 8,950 afy in the Riverside-Arlington Basin (Figure 472). This reduction at RIX, minus the 280 afy anticipated to flow to the SAR, becomes artificial recharge in City Creek and Redlands Basin as described above.

10.11.2 Results

10.11.2.1 Evapotranspiration

ET for the entire Integrated SAR Model domain for Scenario 2c.4 is summarized in Figure 473. The change in ET for the entire model area, compared to baseline conditions, is shown on Figure 474 while seasonal ET is shown on Figure 475. As shown, ET in the entire model area decreased by approximately 290 afy as compared to baseline (Scenario 2a) conditions. The majority of this decrease (270 afy) occurred in the

Riverside-Arlington Basin during the summer months as the result of reduced effluent discharge from RIX. ET in the SBBA also increased by 30 afy as the result of SNRC artificial recharge operations. The total ET under Scenario 2c.4 conditions for Prado Basin is shown on Figure 476. Figures 477 and 478 show the change in ET in Prado, compared to baseline conditions, and seasonal ET in Prado, respectively. In Prado, the decreased discharge in Riverside-Arlington led to a reduction in evapotranspiration of approximately 50 afy.

10.11.2.2 Groundwater Levels

Groundwater level hydrographs for wells along the SAR are provided in Appendix S. Water levels are compared to baseline conditions, with water levels for each well location shown alongside the project condition hydrographs. Water levels in Chino Basin adjacent to the SAR remained unaffected by the changes in the location of recycled water discharge in the upper watershed. Water levels were slightly lower during dry periods at Well #28 in Riverside-Arlington Basin as a result of the reduction in discharge at RIX. This is also consistent with the slight reduction in ET in Riverside-Arlington Basin observed in the ET results (Figure 95), as discussed in the previous section.

10.11.2.3 Streamflow

Average streamflow at the main SAR gaging station locations (E St., MWD Crossing, and at Prado Dam) is shown on Figure 479 under baseline (Scenario 2a) and Scenario 2c.4 conditions. The distributions of monthly streamflow in the SAR at E St., MWD Crossing, and Prado Dam under Scenario 2a and Scenario 2c.4 conditions are shown on Figures 480 through 482. Average annual streamflow is summarized in Table 19. The reduced discharge of 8,950 afy at RIX results in an observed reduction in streamflow of 11 to 12 cfs at MWD Crossing and at Prado Dam. At E St., streamflow increases very slightly as observed in the exceedance probability plot in Figure 480 and Table 19. This increase is due to a small amount of flow reaching the SAR in the SBBA below City Creek.

10.11.2.4 Rising Water

The amount of rising water for the scenario runs is summarized in Table 20 and shown annually on Figure 483. Rising water in Yucaipa Basin is unaffected by Scenario 2c.4 since the activities are located downgradient of the basin. In the Riverside-Arlington and Prado Basins, rising water under Scenario 2c.4 conditions decreases by 700 afy and 20 afy, respectively, compared to baseline (Scenario 2a) conditions.

10.11.2.5 Average Annual Water Budgets

Average annual water budgets under Scenario 2c.4 conditions are shown in Figures 484 through 490 for each groundwater basin and Prado. Operation of the SNRC increases groundwater storage in the SBBA by nearly 6,000 afy in response to the combined increase in artificial recharge and streambed percolation of nearly 7,000 afy. The rise in groundwater in this area also leads to increased ET and underflow to Rialto-Colton Basin (Figure 486). Downgradient, decreases in discharge from RIX cause a reduction in streambed percolation from RIX – leading to a slight decrease in groundwater storage in the Riverside-Arlington Basin.

10.12 Scenario 2c.5: Santa Ana River Sustainable Parks and Tributaries Water Reuse Project

10.12.1 HCP Covered Activities Implemented

Scenario 2c.5 implements the SAR Sustainable Parks and Tributaries Water Reuse Project. This activity is shown on Figure 491 and summarized in Table 10-11 below. The activity is described in Table 17 and in Section 10.2.

Table 10-11. HCP Activities (Scenario 2c.5)

Project ID	Activity	Type
RPU.10	SAR Sustainable Parks and Tributaries Water Reuse Project	Recycled Water

10.12.1.1 Surface Water Diversion

No increases in stormwater diversion would occur with Scenario 2c.5.

10.12.1.2 Artificial Recharge

No increases in artificial recharge would occur under Scenario 2c.5 conditions.

10.12.1.3 Surface Water Discharge

The SAR Sustainable Parks and Tributaries Water Reuse Project would reduce discharge at the Riverside Regional Water Quality Control Plant (RWQCP) by 12,650 afy. Of this, 4,930 afy will be redistributed to four proposed Santa Ana Sucker mitigation sites upstream, along existing tributaries (see Figure 492).

10.12.2 Results

10.12.2.1 Evapotranspiration

ET for the entire Integrated SAR Model domain for Scenario 2c.5 is summarized in Figure 493. The change in ET for the entire model area, compared to baseline conditions, is shown on Figure 494 while seasonal ET is shown on Figure 495. As shown, ET in the entire model area decreased by approximately 230 afy as compared to baseline (Scenario 2a) conditions. The majority of this decrease occurred in Prado Basin during the summer months as the result of reduced effluent discharge from the RWQCP. ET in Riverside-Arlington Basin increased slightly by 10 afy as the result of the transfer of recycled water from the downstream location to Santa Ana Sucker mitigation sites upstream. The total ET under Scenario 2c.5 conditions for Prado Basin is shown on Figure 496. Figures 497 and 498 show the change in ET in Prado, compared to baseline conditions, and seasonal ET in Prado, respectively.

10.12.2.2 Groundwater Levels

Groundwater level hydrographs for selected wells are provided in Appendix S. Overall, water levels show little sensitivity to Scenario 2c.5 activities at monitoring locations within Prado Basin and upstream in Riverside-Arlington Basin, even though ET in Prado Basin is reduced.

10.12.2.3 Streamflow

Average streamflow at the main SAR gaging station locations (E St., MWD Crossing, and at Prado Dam) is shown on Figure 499 under baseline (Scenario 2a) and Scenario 2c.5 conditions. The distributions of monthly streamflow in the SAR at E St., MWD Crossing, and Prado Dam under Scenario 2a and Scenario 2c.5 conditions are shown on Figures 500 through 502. Average annual streamflow is summarized in Table 19. Reductions in effluent discharge resulted in lower average discharges at MWD Crossing and Prado Dam. As a result of transfers and reductions in discharge at RWQCP, streamflow increases at MWD Crossing by 4 cfs and decreases by 13 cfs at Prado Dam (Figure 503, Table 19). Increases are prominent in the lower right portion of the exceedance probability plot at MWD Crossing in Figure 501 due to the new discharge locations upstream of MWD Crossing increasing low flows in the SAR. Reductions in discharge at RWQCP result in lower flows at Prado Dam, as seen in the exceedance plot (Figure 502).

10.12.2.4 Rising Water

Rising water for each scenario run is summarized in Table 20 and shown annually on Figure 503. In Scenario 2c.5, rising water decreases slightly in Prado Basin (30 afy) and increases slightly in Riverside-Arlington Basin as a result of the reduction and relocation of recycled water discharge. Rising water in Yucaipa Basin is relatively unaffected by Scenario 2c.5 since the activities are located downgradient. In the Riverside-Arlington and Prado Basins, rising water under Scenario 2c.5 conditions increases by 20 afy and decreases by 30 afy, respectively, compared to baseline (Scenario 2a) conditions.

10.12.2.5 Average Annual Water Budgets

Average annual water budgets under Scenario 2c.5 conditions are shown in Figures 504 through 510 for each groundwater basin and Prado. The reduction of discharge from the RWQCP at the edge of Chino Basin and relocation of a portion of that discharge to habitat locations in upstream Riverside-Arlington Basin cause a reduction of streambed percolation and ET in Chino Basin and slight increases in streambed percolation and ET in Riverside-Arlington Basin. This corresponds to a decrease in groundwater storage in Chino Basin (80 afy compared to baseline conditions; Figure 508) and a slight increase in groundwater storage in Riverside-Arlington Basin (30 afy compared to baseline conditions; Figure 507).

10.13 Scenario 2c.6: Western Riverside County Regional Wastewater Treatment Plant Enhancement and Expansion

10.13.1 HCP Covered Activities Implemented

Scenario 2c.6 implements the Western Riverside County Regional Wastewater Treatment Plant Enhancement and Expansions project, as summarized in Table 10-12 below. These activities are shown on Figure 511 and described in Table 17 and Section 10.2.

Table 10-12. HCP Activities (Scenario 2c.6)

Project ID	Activity	Type
West.13	Western Riverside County Regional Wastewater Treatment Plant Enhancement and Expansions	Recycled Water

10.13.1.1 Surface Water Diversion

No increases in stormwater diversion would occur under Scenario 2c.6 conditions.

10.13.1.2 Artificial Recharge

No increases in artificial recharge would occur under Scenario 2c.6 conditions.

10.13.1.3 Surface Water Discharge

In Scenario 2c.6, a discharge reduction at the Western Riverside County Regional Wastewater Authority (WRCRWA) treatment plant of 10,080 afy would occur (Figure 512). The water would be treated and used within the service area instead of discharged to the SAR.

10.13.2 Results

10.13.2.1 Evapotranspiration

ET for the entire Integrated SAR Model domain for Scenario 2c.6 is summarized in Figure 513. The change in ET for the entire model area, compared to baseline conditions, is show on Figure 514 while seasonal ET is shown on Figure 515. As shown, ET in the entire model area decreased by approximately 50 afy as compared to baseline (Scenario 2a) conditions. The majority of this decrease occurred in Prado Basin during the summer months as the result of reduced effluent discharge from WRCRWA. Elsewhere, ET is not significantly affected by the reduction in discharge. The total ET under Scenario 2c.6 conditions for Prado Basin is shown on Figure 516. Figures 517 and 518 show the change in ET in Prado, compared to baseline conditions, and seasonal ET in Prado, respectively.

10.13.2.2 Groundwater Levels

Groundwater level hydrographs for selected wells are provided in Appendix S. Consistent with the ET results above, groundwater levels under Scenario 2c.6 conditions did not show decreases in water level at target wells in Prado Basin. In other basins as well, hydrographs were coincident with Scenario 2a baseline groundwater levels.

10.13.2.3 Streamflow

Average streamflow at the main SAR gaging station locations (E St., MWD Crossing, and at Prado Dam) is shown on Figure 519 under baseline (Scenario 2a) and Scenario 2c.6 conditions. The monthly streamflow distributions at the three gaging stations along the SAR are shown on Figures 520 through 522 under Scenario 2a and Scenario 2c.6 conditions. Average annual streamflow is summarized in Table 19. No reductions or transfers of recycled water affect the MWD Crossing and E. St. gages, as the project only reduces discharge at the WRCRWA discharge in Chino Basin. Streamflow was reduced at Prado Dam by a total of 13 cfs (Figure 519, Table 19). The reduction in streamflow is also visible in the exceedance plot for Prado Dam in Figure 522.

10.13.2.4 Rising Water

The amount of rising water for the scenario runs is summarized in Table 20 and shown annually on Figure 523. As shown, rising water in Yucaipa and Riverside-Arlington Basins is unaffected by Scenario 2c.6. In Prado Basin, rising water under Scenario 2c.6 conditions decreases by 270 afy, compared to baseline (Scenario 2a) conditions.

10.13.2.5 Average Annual Water Budgets

Average annual water budgets under Scenario 2c.6 conditions are shown in Figures 524 through 530 for each groundwater basin and Prado (refer to area outlined on Figure 84). The reduction of discharge from WRCRWA in Chino Basin causes a reduction of streambed percolation, rising water, and ET. This corresponds to a decrease in groundwater storage in Chino Basin (90 afy compared to baseline conditions; Figure 528).

10.14 Scenario 2c.7: IEUA Baseflow Reduction Activities

10.14.1 HCP Covered Activities Implemented

Scenario 2c.7 implements all of the IEUA baseflow reduction activities, as summarized in Table 10-13 below. These activities are shown on Figure 531 and described in Table 17 and Section 10.2.

Table 10-13. HCP Activities (Scenario 2c.7)

Project ID	Activity	Type
IEUA.3.01	Cucamonga Creek Dry-Weather Flow Diversion to Regional Water Recycling Plant No. 1 Project	Dry-Weather Flow Capture
IEUA.3.02	Cucamonga Creek at Interstate 10 Dry-Weather Flow Diversion to Regional Water Recycling Plant No. 1 Project	Dry-Weather Flow Capture
IEUA.3.03	Chino Creek at Chino Hills Parkway Dry-Weather Flow Diversion to Carbon Canyon Water Recycling Facility Project	Dry-Weather Flow Capture
IEUA.3.04	Day Creek at Wineville Basin Outflow Diversion to Regional Water Recycling Plant No. 1 Project	Dry-Weather Flow Capture
IEUA.3.05	San Sevaine Creek Diversion to Regional Water Recycling Plant No. 1 Project	Dry-Weather Flow Capture
IEUA.3.06	Lower Deer Creek Diversion to Regional Water Recycling Plant No. 5 Project	Dry-Weather Flow Capture

Please note, the covered activity IEUA.4 (Inland Empire Utilities Agency Regional Wastewater Treatment Expansion) was developed later in the modeling process. As such, scenarios that were already completed (including Scenario 2c.7) were not rerun to incorporate this additional project.

10.14.1.1 Surface Water Diversion

No increases in stormwater diversion would occur under Scenario 2c.7 conditions. Dry-weather flows (1,800 afy) would be diverted during dry weather months to water recycling plants in Chino Basin and used in the recycled water system (Figure 532).

10.14.1.2 Artificial Recharge

No increases in artificial recharge would occur under Scenario 2c.7 conditions.

10.14.1.3 Surface Water Discharge

In Scenario 2c.7, only dry-weather flow diversions are implemented. No alteration to recycled water discharge is anticipated. Dry-weather flows will be diverted, treated, and reused in the recycled water system.

10.14.2 Results

10.14.2.1 Evapotranspiration

ET for the entire Integrated SAR Model domain for Scenario 2c.7 is summarized in Figure 533. The change in ET for the entire model area, compared to baseline conditions, is show on Figure 534 while seasonal ET is shown on Figure 535. As shown, ET in the entire model area decreased by approximately 10 afy as compared to baseline (Scenario 2a) conditions. The majority of this decrease occurred in Prado Basin during the summer months as the result of dry weather capture. ET for the first nine model years are coincident with that under baseline conditions. The total ET under Scenario 2c.7 conditions for Prado Basin is shown on Figure 536. Figures 537 and 538 show the change in ET in Prado, compared to baseline conditions, and seasonal ET in Prado, respectively.

10.14.2.2 Groundwater Levels

Water levels under Scenario 2c.7 conditions are provided in Appendix S. Water levels are shown alongside Scenario 2a baseline conditions for comparison. As shown, no increases or decreases occur upstream of the dry-weather flow activities in Chino Basin. Further, no increases or decreases in water levels at the wells shown in Chino Basin occurred either. Water levels were coincident with baseline conditions for Scenario 2c.7 hydrographs.

10.14.2.3 Streamflow

Average streamflow at the main SAR gaging station locations (E St., MWD Crossing, and at Prado Dam) is shown on Figure 539 under baseline (Scenario 2a) and Scenario 2c.7 conditions. The distributions of monthly streamflow in the SAR at E St., MWD Crossing, and Prado Dam under Scenario 2a and Scenario 2c.7 conditions are shown on Figures 540 through 542. Average annual streamflow is summarized in Table 19. Reductions in dry-weather flow in Chino Basin resulted in no changes upstream to average discharges at MWD Crossing and E St. At Prado Dam, streamflow decreased by 2 cfs (Figure 539, Table 19).

10.14.2.4 Rising Water

The amount of rising water for the scenario runs is summarized in Table 20 and shown annually on Figure 543. As shown, rising water in Yucaipa and Riverside-Arlington Basins is not significantly affected by Scenario 2c.7, which diverts flows downstream of these locations. In Prado Basin, rising water under Scenario 2c.7 conditions decreases very slightly by 10 afy, compared to baseline (Scenario 2a) conditions.

10.14.2.5 Average Annual Water Budgets

Average annual water budgets under Scenario 2c.7 conditions are shown in Figures 544 through 550 for each groundwater basin and Prado. Dry-weather capture in Chino Basin causes a negligible change in groundwater storage in Chino Basin (Figure 548).

10.15 Scenario 2c.8: IEUA Reduced Flow from Wastewater Treatment Plants

10.15.1 HCP Covered Activities Implemented

Scenario 2c.8 applies effluent discharge reduction at IEUA's WWTPs, as summarized in Table 10-14 below. This activity is shown on Figure 551 and described in Table 17 and Section 10.2.

Table 10-14. HCP Activities (Scenario 2c.8)

Project ID	Activity	Type
IEUA.4	Inland Empire Utilities Agency Regional Wastewater Treatment Expansion	Recycled Water

This HCP covered activity was developed later in the modeling process. As such, scenarios that were already completed were not rerun to incorporate this additional project. This includes Scenarios 2b.1, 2b.2, and 2b.3 (all project scenarios under varying hydrologic assumptions), Scenario 2c.7 (IEUA baseflow reduction activities), and Scenario 2e.2 (all IEUA activities).

10.15.1.1 Surface Water Diversion

No increases in stormwater or dry-weather flow diversion would occur under Scenario 2c.8 conditions.

10.15.1.2 Artificial Recharge

No increases in artificial recharge would occur under Scenario 2c.8 conditions.

10.15.1.3 Surface Water Discharge

In Scenario 2c.8, 13.8 cfs (7.4 mgd) of effluent flow (i.e., discharge) is reused within IEUA's service area – thereby reducing discharges from the treatment plants to Prado Lake, Chino Creek, and Cucamonga Creek during the cooler shoulder and winter months (i.e., November through March). Effluent is reduced by approximately 9,860 afy, as shown on Figure 552.

10.15.2 Results

10.15.2.1 Evapotranspiration

ET for the entire Integrated SAR Model domain for Scenario 2c.8 is summarized in Figure 553. The change in ET for the entire model area, compared to baseline conditions, is show on Figure 554 while seasonal ET is shown on Figure 555. As shown, ET in the entire model area decreased by approximately 10 afy as compared to baseline (Scenario 2a) conditions. All of this decrease occurred in Prado Basin during the colder months as the result of reduced discharges. The total ET under Scenario 2c.8 conditions for Prado Basin is shown on Figure 556. Figures 557 and 558 show the change in ET in Prado, compared to baseline conditions, and seasonal ET in Prado, respectively.

10.15.2.2 Groundwater Levels

Water levels under Scenario 2c.8 conditions are provided in Appendix S. Water levels are shown alongside Scenario 2a baseline conditions for comparison. As shown, no increases or decreases occur upstream of reduced discharge point locations in Chino Basin. Further, no increases or decreases in water levels at the wells shown in Chino Basin occurred either. Water levels were coincident with baseline conditions for Scenario 2c.8 hydrographs.

10.15.2.3 Streamflow

Average streamflow at the main SAR gaging station locations (E St., MWD Crossing, and at Prado Dam) is shown on Figure 559 under baseline (Scenario 2a) and Scenario 2c.8 conditions. The distributions of monthly streamflow in the SAR at E St., MWD Crossing, and Prado Dam under Scenario 2a and Scenario 2c.8 conditions are shown on Figures 560 through 562. Average annual streamflow is summarized in Table 19. Reductions in discharge in Chino Basin resulted in no changes upstream to average discharges at MWD Crossing and E St. At Prado Dam, streamflow decreased by 14 cfs (Figure 562, Table 19).

10.15.2.4 Rising Water

The amount of rising water for the scenario runs is summarized in Table 20 and shown annually on Figure 563. As shown, rising water in Yucaipa and Riverside-Arlington Basins is not significantly affected by Scenario 2c.8, which reduces flow downstream of these locations. In Prado Basin, rising water under Scenario 2c.8 conditions decreases by 180 afy, compared to baseline (Scenario 2a) conditions.

10.15.2.5 Average Annual Water Budgets

Average annual water budgets under Scenario 2c.8 conditions are shown in Figures 564 through 570 for each groundwater basin and Prado. Reduced discharge in Chino Basin causes a negligible change in groundwater storage in Chino Basin (Figure 568) and reduces groundwater storage in Prado Basin by approximately 40 acre-ft/yr (Figure 570).

10.16 Scenario 2d.1: Phase I Active Recharge Activities

10.16.1 General Assumptions

Scenario 2d runs implement various combinations of active recharge (stormwater capture) activities to assess the effects of each or combinations of projects. Project impacts were evaluated by comparing individual model runs (with operation of selected HCP Covered Activities) to results from the baseline model run (i.e., no HCP Covered Activities). The general assumptions for the Scenario 2d model runs are the same as those used for the Baseline Model Run (Scenario 2a; refer to Section 10.5). Differences from the baseline assumptions for each Scenario 2d run are discussed below.

10.16.2 HCP Covered Activities Implemented

Scenario 2d.1 implements Valley District's Phase I active recharge activities, which include improvements to existing basins. These projects are summarized in Table 10-15 below and shown on Figure 571. Additional project information is also provided in Table 17 and in Section 10.2.

Table 10-15. HCP Activities (Scenario 2d.1)

Project ID	Activity	Type
VD.2.03	Lytle Creek	Stormwater Capture
VD.2.07	Cajon-Vulcan 1	Stormwater Capture
VD.2.11	Devil Creek	Stormwater Capture
VD.2.12	Waterman Basin Spreading Grounds	Stormwater Capture
VD.2.13	Twin Creek Spreading Grounds	Stormwater Capture
CD.4	Mill Creek Diversion Project	Stormwater Capture

10.16.2.1 Surface Water Diversion

Improvements to existing recharge basins would increase diversion capacity of existing facilities, resulting in an additional average annual diversion of 18,710 afy (Figure 572).

10.16.2.2 Artificial Recharge

The annual change in artificial recharge from the baseline model (Scenario 2a) is also 18,710 afy (Figure 573). Stormwater diverted from Lytle Creek, Cajon Creek, Devil Creek, Waterman Creek, Twin Creek, and Mill Creek would be recharged in the associated recharge basins, so this volume corresponds with the additional volume diverted from SAR tributaries under Scenario 2d.1 conditions.

10.16.2.3 Surface Water Discharge

No effluent discharge reduction activities occur in Scenario 2d.1.

10.16.3 Results

10.16.3.1 Evapotranspiration

ET for the entire Integrated SAR Model domain for Scenario 2d.1 is summarized in Figure 574. The change in ET for the entire model area, compared to baseline conditions, is shown on Figure 575 while seasonal ET is shown on Figure 576. As shown, ET in the entire model area increased by approximately 210 afy as compared to baseline (Scenario 2a) conditions. The majority of this increase occurred in the SBBA as the result of additional stormwater recharge. Elsewhere, ET is not significantly affected. The total ET under Scenario 2d.1 conditions for Prado Basin is shown on Figure 577. Figures 578 and 579 show the change in ET in Prado, compared to baseline conditions, and seasonal ET in Prado, respectively.

10.16.3.2 Groundwater Levels

Groundwater level hydrographs for selected wells are provided in Appendix S. Water levels under Scenario 2d.1 conditions are slightly lower near the SAR in Rialto-Colton Basin. Elsewhere, at other monitoring locations presented, no changes in groundwater levels are observed in the groundwater level hydrographs. In Riverside-Arlington and Chino Basins, groundwater levels follow Scenario 2a baseline condition water levels.

10.16.3.3 Streamflow

Average streamflow at the main SAR gaging station locations (E St., MWD Crossing, and at Prado Dam) is shown on Figure 580 under baseline (Scenario 2a) and Scenario 2d.1 conditions. The distributions of monthly streamflow in the SAR at E St., MWD Crossing, and Prado Dam under Scenario 2a and Scenario 2d.1 conditions are shown on Figures 581 through 583. Differences in streamflow are evident at lower flows at E St. in the exceedance plots, and Table 19 shows a decline in average annual streamflow from 2 cfs to 4 cfs at E St., MWD Crossing, and Prado Dam (see also Figure 580).

10.16.3.4 Rising Water

The amount of rising water for the scenario runs is summarized in Table 20 and shown annually on Figure 584. Minimal decreases in rising water (approximately 20 afy at MWD Crossing and 10 afy at Prado) are observed for Scenario 2d.1 compared with the baseline condition.

10.16.3.5 Average Annual Water Budgets

Average annual water budgets under Scenario 2d.1 conditions are shown in Figures 585 through 591 for each groundwater basin and Prado. The development of Phase I Active Recharge Activities increases groundwater storage in the SBBA by nearly 5,400 afy in response to increased stormwater capture. The rise in groundwater and reduced streamflow in this area also leads to decreased streambed percolation and increased ET and underflow to Rialto-Colton Basin (Figure 587).

10.17 Scenario 2d.2: Phase II Active Recharge Facilities Along Lytle Creek

10.17.1 HCP Covered Activities Implemented

Scenario 2d.2 evaluates Valley District's Phase II active recharge activities, which include the construction of new recharge facilities, along Lytle Creek. This project is summarized in Table 10-16 below and shown in Figure 592. Additional project information is also provided in Table 17 and Section 10.2.

Table 10-16. HCP Activities (Scenario 2d.2)

Project ID	Activity	Type
VD.2.09	Lytle-Cajon	Stormwater Capture

10.17.1.1 Surface Water Diversion

Scenario 2d.2 evaluates the creation of a new in-channel recharge basin and associated stormwater diversion from Lytle Creek. Annual change in stormwater diversion, compared to the baseline, is shown on Figure 593. In the SBBA, stormwater diversion increases 2,910 afy over baseline diversion.

10.17.1.2 Artificial Recharge

The annual change in artificial recharge from the baseline model (Scenario 2a) is also 2,910 afy (Figure 594). Stormwater diverted from Lytle Creek would be recharged in the associated recharge basins, so this volume corresponds with the volume of diverted stormwater under Scenario 2d.2 conditions.

10.17.1.3 Surface Water Discharge

No effluent discharge reduction activities occur in Scenario 2d.2.

10.17.2 Results

10.17.2.1 Evapotranspiration

ET for the entire Integrated SAR Model domain for Scenario 2d.2 is summarized in Figure 595. The change in ET for the entire model area, compared to baseline conditions, is show on Figure 596 while seasonal ET is shown on Figure 597. As shown, ET in the entire model area increased only slightly (by 20 afy) as compared to baseline (Scenario 2a) conditions. This increase occurred in Riverside-Arlington Basin as the result of additional stormwater recharge along Lytle Creek. Elsewhere, ET is not significantly affected. The total ET under Scenario 2d.2 conditions for Prado Basin is shown on Figure 598. Figures 599 and 600 show the change in ET in Prado, compared to baseline conditions, and seasonal ET in Prado, respectively.

10.17.2.2 Groundwater Levels

Groundwater level hydrographs for selected wells are provided in Appendix S. Scenario 2d.2 groundwater levels are displayed with those calculated under baseline conditions for wells along the SAR. Groundwater levels are coincident with baseline condition water levels at the plotted wells along the SAR.

10.17.2.3 Streamflow

Average streamflow at the main SAR gaging station locations (E St., MWD Crossing, and at Prado Dam) is shown on Figure 601 under baseline (Scenario 2a) and Scenario 2d.2 conditions. The distributions of monthly streamflow in the SAR at E St., MWD Crossing, and Prado Dam under Scenario 2a and Scenario 2d.2 conditions are shown on Figures 602 through 603. Changes in streamflow are not evident in the exceedance plots at MWD Crossing or Prado Dam. The average annual flow is reduced very slightly by between 1 cfs and 2 cfs at MWD Crossing and Prado Dam, as shown in Figure 601 and Table 19.

10.17.2.4 Rising Water

The amount of rising water for the scenario runs is summarized in Table 20 and shown annually on Figure 605. Rising water is not influenced significantly by activities in Scenario 2d.2, compared to baseline (Scenario 2a) conditions.

10.17.2.5 Average Annual Water Budgets

Average annual water budgets under Scenario 2d.2 conditions are shown in Figures 606 through 612 for each groundwater basin and Prado. The development of Phase II Active Recharge Activities along Lytle Creek increases groundwater storage in the SBBA by approximately 900 afy in response to increased stormwater capture. The rise in groundwater and reduced streamflow in this area also leads to decreased streambed percolation and increased ET and underflow to Rialto-Colton Basin (Figure 608).

10.18 Scenario 2d.3: Phase II Active Recharge Facilities Along Cajon Creek and Cable Creek

10.18.1 HCP Covered Activities Implemented

Scenario 2d.3 evaluates Valley District's Phase II active recharge activities, which include the construction of new recharge facilities, along Cajon and Cable Creeks. These projects are summarized in Table 10-17 below and shown in Figure 613. Additional project information is also provided in Table 17 and in Section 10.2.

Table 10-17. HCP Activities (Scenario 2d.3)

Project ID	Activity	Type
VD.2.01	Cajon Creek	Stormwater Capture
VD.2.02	Cable Creek	Stormwater Capture
VD.2.08	Vulcan 2	Stormwater Capture

10.18.1.1 Surface Water Diversion

Scenario 2d.3 evaluates the creation of new recharge basins and associated stormwater diversion from Cajon Creek and Cable Creek. Annual change in stormwater diversion, compared to the baseline, is shown on Figure 614. In the SBBA, stormwater diversion increases by 5,990 afy.

10.18.1.2 Artificial Recharge

The annual change in artificial recharge from the baseline model (Scenario 2a) is 5,990 afy (Figure 615). Stormwater diverted from Cajon and Cable Creeks would be recharged in the associated recharge basins, so this volume corresponds with the volume of diverted stormwater under Scenario 2d.3 conditions.

10.18.1.3 Surface Water Discharge

No effluent discharge reduction activities occur in Scenario 2d.3.

10.18.2 Results

10.18.2.1 Evapotranspiration

ET for the entire Integrated SAR Model domain for Scenario 2d.3 is summarized in Figure 616. The change in ET for the entire model area, compared to baseline conditions, is show on Figure 617 while seasonal ET is shown on Figure 618. As shown, ET in the entire model area increased by approximately 160 afy as compared to baseline (Scenario 2a) conditions. The majority of this increase occurred in the SBBA as the result of additional stormwater recharge. Elsewhere, ET is not significantly affected. The total ET under

Scenario 2d.3 conditions for Prado Basin is shown on Figure 619. Figures 620 and 621 show the change in ET in Prado, compared to baseline conditions, and seasonal ET in Prado, respectively.

10.18.2.2 Groundwater Levels

Groundwater level hydrographs are provided for selected wells along the SAR in Appendix S. Groundwater levels at selected observation wells along the SAR were mostly unaffected by increases in stormwater capture in SBBA under Scenario 2d.3 conditions.

10.18.2.3 Streamflow

Average streamflow at the main SAR gaging station locations (E St., MWD Crossing, and at Prado Dam) is shown on Figure 622 under baseline (Scenario 2a) and Scenario 2d.3 conditions. The distributions of monthly streamflow in the SAR at E St., MWD Crossing, and Prado Dam under Scenario 2a and Scenario 2d.3 conditions are shown on Figures 623 through 625. Streamflow decreases slightly at MWD Crossing and Prado Dam by 3 cfs to 5 cfs (Figure 622, Table 19). Slight departures in the exceedance plots at higher flow rates are observed in Figures 624 and 625.

10.18.2.4 Rising Water

Rising water is shown in Table 20 for each scenario and baseline conditions and shown annually on Figure 626. No significant changes are observed in rising groundwater as a result of activities in Scenario 2d.3.

10.18.2.5 Average Annual Water Budgets

Average annual water budgets under Scenario 2d.3 conditions are shown in Figures 627 through 633 for each groundwater basin and Prado. The development of Phase II Active Recharge Activities along Cajon and Cable Creeks reflects an increase in artificial recharge of approximately 6,000 afy in the SBBA. However, this is offset by a decline in streambed percolation in the basin of around 5,400 afy. The remaining difference becomes an increase in groundwater storage in the SBBA and outflow to Rialto-Colton Basin. Water budgets in other groundwater basins shown minimal differences from baseline conditions.

10.19 Scenario 2d.4: Phase II Active Recharge Facilities Along City Creek, Plunge Creek, and Mill Creek

10.19.1 HCP Covered Activities Implemented

Scenario 2d.4 evaluates Valley District's Phase II active recharge activities, which include the construction of new recharge facilities, along City, Plunge, and Mill Creeks. These projects are summarized in Table 10-18 below and shown in Figure 634. Additional project information is also provided in Table 17 and in Section 10.2.

Table 10-18. HCP Activities (Scenario 2d.4)

Project ID	Activity	Type
VD.2.05	City Creek	Stormwater Capture
VD.2.06	Plunge Creek – Basin 1	Stormwater Capture
VD.2.10	Plunge Creek – Basin 2	Stormwater Capture

10.19.1.1 Surface Water Diversion

Scenario 2d.4 evaluates the creation of new recharge basins and associated stormwater diversion from City Creek and Plunge Creek. No new facilities are planned along Mill Creek. Annual change in stormwater diversion, compared to the baseline, is shown on Figure 635. In the SBBA, stormwater diversion increases 7,700 afy.

10.19.1.2 Artificial Recharge

The annual change in artificial recharge from the baseline model (Scenario 2a) is also 7,700 afy (Figure 636). Stormwater diverted from City and Plunge Creeks would be recharged in the associated recharge basins, so this volume corresponds with the volume of diverted stormwater under Scenario 2d.4 conditions.

10.19.1.3 Surface Water Discharge

No effluent discharge reduction activities occur in Scenario 2d.4.

10.19.2 Results

10.19.2.1 Evapotranspiration

ET for the entire Integrated SAR Model domain for Scenario 2d.4 is summarized in Figure 637. The change in ET for the entire model area, compared to baseline conditions, is shown on Figure 638 while seasonal ET is shown on Figure 639. As shown, ET in the entire model area increased by approximately 30 afy as compared to baseline (Scenario 2a) conditions. The majority of this increase occurred in the SBBA and Riverside-Arlington Basin as the result of additional stormwater recharge. Elsewhere, ET is not significantly affected. The total ET under Scenario 2d.4 conditions for Prado Basin is shown on Figure 640. Figures 641 and 642 show the change in ET in Prado, compared to baseline conditions, and seasonal ET in Prado, respectively.

10.19.2.2 Groundwater Levels

Groundwater level hydrographs for selected wells are provided in Appendix S. Minimal changes in groundwater levels are observed in the water level hydrographs along the SAR, as compared with baseline condition water levels.

10.19.2.3 Streamflow

Average streamflow at the main SAR gaging station locations (E St., MWD Crossing, and at Prado Dam) is shown on Figure 643 under baseline (Scenario 2a) and Scenario 2d.4 conditions. The distributions of monthly streamflow in the SAR at E St., MWD Crossing, and Prado Dam under Scenario 2a and Scenario 2d.4 conditions are shown on Figures 644 through 646. Average annual streamflow is summarized in Table 19. A reduction of between 5 cfs and 7 cfs is observed at E St., MWD Crossing, and Prado Dam (Figure 643, Table 19). Exceedance probability plots show decreases at E St. across a range of flows (Figure 644).

10.19.2.4 Rising Water

The amount of rising water for the scenario runs is summarized in Table 20 and shown annually on Figure 647. As shown, rising water in Riverside-Arlington, Yucaipa, and Prado Basins is relatively unaffected by Scenario 2d.4, as compared to Scenario 2a baseline conditions.

10.19.2.5 Average Annual Water Budgets

Average annual water budgets under Scenario 2d.4 conditions are shown in Figures 648 through 654 for each groundwater basin and Prado. The development of Phase II Active Recharge Activities along City Creek and Plunge Creek increases groundwater storage in the SBBA by over 1,300 afy in response to increased stormwater capture. The rise in groundwater and reduced streamflow in this area also leads to decreased streambed percolation and increased ET and underflow to Rialto-Colton Basin (Figure 650).

10.20 Scenario 2d.5: Enhanced Recharge Project

10.20.1 HCP Covered Activities Implemented

Scenario 2d.5 implements the Enhanced Recharge Project, as summarized in Table 10-19 below. The Enhanced Recharge Project location is shown in Figure 655 and is described in Table 17 and in Section 10.2.

Table 10-19. HCP Activities (Scenario 2d.5)

Project ID	Activity	Type
VD.3	Enhanced Recharge Project	Diversion/ Recharge Basin

10.20.1.1 Surface Water Diversion

The Enhanced Recharge Project is located on the SAR with diversion facilities downstream of Seven Oaks Dam (Figure 655). Baseline conditions were modeled with a diversion capacity of 195 cfs. Improvements and the construction of additional recharge basins would increase diversion capacity to 500 cfs. The annual change in stormwater diversion from the baseline model (Scenario 2a) is 3,720 afy (Figure 656). The diversion and recharge would occur in the SBBA downstream of Seven Oaks Dam.

10.20.1.2 Artificial Recharge

The annual change in artificial recharge from the baseline model (Scenario 2a) is 3,720 afy (Figure 657). Stormwater diverted from the SAR would be recharged into the SAR spreading basins groundwater basins, so this volume corresponds with the additional volume diverted from the SAR under Scenario 2c.5 conditions.

10.20.1.3 Surface Water Discharge

No effluent discharge reduction activities occur in Scenario 2d.5.

10.20.2 Results

10.20.2.1 Evapotranspiration

ET across the entire Integrated SAR Model area under Scenario 2d.5 conditions is summarized in Figure 658. The change in ET for the entire model area, compared to baseline conditions, is shown on Figure 659 while seasonal ET is shown on Figure 660. The total ET, change in ET, and seasonal ET for Prado Basin under Scenario 2d.5 conditions is shown on Figures 661, 662, and 663, respectively. ET was not significantly affected by the increase in capture below Seven Oaks Dam. Annual average ET in the model domain remained almost constant, changing from 29,240 afy under baseline conditions to 29,220 afy under Scenario 2d.5 conditions.

10.20.2.2 Groundwater Level

Groundwater level hydrographs for selected wells are provided in Appendix S. Water levels under Scenario 2c.3 conditions are displayed next to those calculated under baseline conditions for wells along the SAR. Water levels adjacent to the SAR in Rialto-Colton, Riverside-Arlington, and Chino Basins remained unaffected and were coincident with the baseline Scenario 2a water levels.

10.20.2.3 Streamflow

The distribution of monthly streamflow in the Santa Ana River at E St., MWD Crossing, and Prado Dam under Scenario 2a and Scenario 2d.5 is shown on Figures 664 through 667. The distribution plots are coincident at lower flows with baseline Scenario 2a, but diverge slightly at flows greater than 190 cfs. This is consistent with the increased diversion at higher streamflows in Scenario 2d.5 downstream of the Seven Oaks Dam. Average annual streamflow is tabulated in Table 19. Under Scenario 2d.5 conditions, streamflow at MWD Crossing decreased 8 cfs, from 103 to 95 cfs. Similar decreases were seen at Prado Dam.

10.20.2.4 Rising Water

The amount of rising water for the scenario runs is summarized in Table 20. As shown, rising water in Yucaipa and Prado Basins is unaffected by Scenario 2c.5. In the Riverside-Arlington Basin, rising water under Scenario 2c.5 conditions decreases by 10 afy, compared to baseline (Scenario 2a) conditions.

10.20.2.5 Average Annual Water Budgets

The annual water budgets for Scenario 2d.5 are shown on Figures 669 through 675 for each groundwater basin and Prado. In the SBBA, the increased artificial recharge of approximately 3,700 afy yielded an increase in groundwater storage of approximately 3,000 afy. Streambed percolation declined slightly, while underflow outflow to Rialto-Colton Basin increased. Water budgets in other basins were similar to Scenario 2a (Baseline).

10.21 Scenario 2d.6: Riverside North Aquifer Storage and Recovery Project

10.21.1 HCP Covered Activities Implemented

Scenario 2d.6 implements the Riverside North Aquifer Storage and Recovery (RNASR) Project, as summarized in Table 10-20 below. These activities are shown on Figure 676 and described in Table 17 and Section 10.2.

Table 10-20. HCP Activities (Scenario 2d.6)

Project ID	Activity	Type
RPU.5	Riverside North Aquifer Storage and Recovery Project	Stormwater Capture

10.21.1.1 Surface Water Diversion

Scenario 2d.6 evaluates the diversion of water from the SAR by an inflatable dam to in-channel and off-channel recharge basins. Annual change in stormwater diversion, compared to the baseline, is shown on Figure 677. Stormwater diversion increases 2,170 afy in Rialto-Colton Basin and by 3,780 afy in Riverside-Arlington Basin, for a total of 5,950 afy.

10.21.1.2 Artificial Recharge

The annual change in artificial recharge from the baseline model (Scenario 2a) is also 5,950 afy (Figure 678). Stormwater diverted from the SAR would be recharged in newly-constructed recharge basins, so this volume corresponds with the volume of diverted stormwater under Scenario 2d.6 conditions.

10.21.1.3 Surface Water Discharge

No effluent discharge reduction activities occur in Scenario 2d.6.

10.21.2 Results

10.21.2.1 Evapotranspiration

ET for the entire Integrated SAR Model domain for Scenario 2d.6 is summarized in Figure 679. The change in ET for the entire model area, compared to baseline conditions, is show on Figure 680 while seasonal ET is shown on Figure 681. As shown, ET in the entire model area increased by approximately 50 afy as compared to baseline (Scenario 2a) conditions. The majority of this increase occurred in the Riverside-Arlington Basin as the result of additional streamflow capture and recharge. ET remains similar to baseline conditions elsewhere in the model area. The total ET under Scenario 2d.6 conditions for Prado Basin is shown on Figure 682. Figures 683 and 684 show the change in ET in Prado, compared to baseline conditions, and seasonal ET in Prado, respectively.

10.21.2.2 Groundwater Levels

Groundwater levels at selected locations along the SAR are presented in Appendix S. The RNASR project increases groundwater levels in the vicinity of the project in Rialto-Colton Basin. Groundwater levels at other monitoring locations in Appendix S along the SAR show negligible change from Scenario 2a baseline conditions.

10.21.2.3 Streamflow

Average streamflow at the main SAR gaging station locations (E St., MWD Crossing, and at Prado Dam) is shown on Figure 685 under baseline (Scenario 2a) and Scenario 2d.6 conditions. The distributions of monthly streamflow in the SAR at E St., MWD Crossing, and Prado Dam under Scenario 2a and Scenario 2d.6 conditions are shown on Figures 686 through 688. A small reduction in average annual streamflow of 1 cfs and 3 cfs is observed at MWD Crossing and Prado under Scenario 2d.6 conditions, as shown in Figure 685 and Table 19.

10.21.2.4 Rising Water

Rising water for each scenario is tabulated in Table 20 and shown annually on Figure 689. Due to the increased recharge and slightly higher water levels, annual average rising water in Riverside-Arlington Basin increases slightly by 30 afy. Elsewhere in the model area, rising water is unaffected by Scenario 2d.6 activities.

10.21.2.5 Average Annual Water Budgets

Average annual water budgets under Scenario 2d.6 conditions are shown in Figures 690 through 696 for each groundwater basin and Prado. Operation of the RNASR Project increases groundwater storage in the Rialto-Colton Basin by nearly 700 afy in response to increased stormwater capture. The rise in groundwater and reduced streamflow in this area also leads to decreased streambed percolation and increased underflow to Riverside-Arlington Basin (Figure 693).

10.22 Scenario 2d.7: Evaluation of Valley District Stormwater Capture Program at Prado Dam

10.22.1 HCP Covered Activities Implemented

Scenario 2d.7 evaluates the cumulative impact of Valley District's stormwater capture program activities at Prado Dam. These activities are summarized in Table 10-21 below and shown on Figure 697. The individual projects are described in Table 17 and in Section 10.2 of this report.

Table 10-21. HCP Activities (Scenario 2d.7)

Project ID	Activity	Type
CD.4	Mill Creek Diversion Project	Diversion/ Recharge Basin
RPU.5/ VD.2.14	Riverside North Aquifer Storage and Recovery (RNASR) Project	In-Stream and Off-Stream Recharge
VD.2.01	Cajon Creek	Diversion/ Recharge Basin
VD.2.02	Cable Creek	Diversion/ Recharge Basin
VD.2.03	Lytle Creek	Diversion/ Recharge Basin
VD.2.05	City Creek	Diversion/ Recharge Basin
VD.2.06	Plunge Creek – Basin 1	Diversion/ Recharge Basin
VD.2.07	Cajon-Vulcan 1	Diversion/ Recharge Basin
VD.2.08	Vulcan 2	Recharge Basin
VD.2.09	Lytle-Cajon	In-Channel Recharge Basin
VD.2.10	Plunge Creek – Basin 2	Diversion/ Recharge Basin
VD.2.11	Devil Creek	Diversion/ Recharge Basin
VD.2.12	Waterman Basin Spreading Grounds	Recharge Basin
VD.2.13	Twin Creek Spreading Grounds	Recharge Basin
VD.3	Enhanced Recharge Project	Diversion/ Recharge Basin

10.22.1.1 Surface Water Diversion

Scenario 2d.7 evaluates the fifteen stormwater diversion and recharge projects listed above. Annual change in stormwater diversion, compared to the baseline, is shown on Figure 698. In the SBBA, stormwater diversion increases 39,030 afy. In Rialto-Colton, an additional 6,110 afy would be diverted. The total additional annual average stormwater diversion is 45,150 afy.

10.22.1.2 Artificial Recharge

Scenario 2d.7 activities recharge an additional total annual average of 45,150 afy of stormwater in the SBBA, Rialto-Colton, and Riverside-Arlington Basins (Figure 699). The additional annual average artificial recharge in the SBBA in Scenario 2d.7 is 37,650 afy. In Rialto-Colton, 3,950 afy additional artificial recharge occurs. In Riverside-Arlington, 3,550 afy additional artificial recharge occur. The total additional volume of artificial recharge is the same as the additional volume diverted from the SAR.

10.22.1.3 Surface Water Discharge

No effluent discharge reduction activities occur in Scenario 2d.7.

10.22.2 Results

10.22.2.1 Evapotranspiration

ET across the entire Integrated SAR Model area under Scenario 2d.7 conditions is summarized in Figure 700. The change in ET for the entire model area, compared to baseline conditions, is shown on Figure 701 while seasonal ET is shown on Figure 702. The total ET, change in ET, and seasonal ET for Prado Basin under Scenario 2d.7 conditions is shown on Figures 704, 705, and 706, respectively.

10.22.2.2 Groundwater Levels

Groundwater level hydrographs for selected wells are provided in Appendix S. Water levels under Scenario 2d.7 conditions are displayed next to those calculated under baseline conditions for wells along the SAR. In Rialto-Colton Basin, recharge from the Lytle-Cajon project and RNASR increased water levels. Elsewhere, downstream along the SAR, water levels were not affected greatly by the increase in stormwater capture.

10.22.2.3 Streamflow

The distribution of monthly streamflow in the Santa Ana River at E St., MWD Crossing, and Prado Dam under Scenario 2a and Scenario 2d.7 is shown on Figures 706 through 709. As shown on Figure 706, streamflow under Scenario 2d.7 conditions decreased at E St., as compared to the baseline. At MWD Crossing, the decrease in streamflow appeared in the exceedance plot at 80 cfs and above (Figure 708). At Prado Dam, decreases in streamflow were visible at the higher flow rates, but not lower in the plot (Figure 709). Average annual streamflow is summarized in Table 19. The mean annual streamflow decreased at E St., MWD Crossing, and Prado Dam by between 9 to 10 cfs.

10.22.2.4 Rising Water

The amount of rising water for the scenario runs is summarized in Table 20 and on Figure 710. As shown, rising water in Yucaipa Basin is relatively unaffected by Scenario 2d.7. In the Riverside-Arlington and Prado Basins, rising water under Scenario 2d.7 conditions increases by 20 afy and decreases by 20 afy, respectively, compared to baseline (Scenario 2a) conditions.

10.22.2.5 Average Annual Water Budgets

The annual water budgets for Scenario 2d.7 are shown in Figures 711 to 717 for each groundwater basin and Prado. The majority of the streamflow diversion and artificial recharge under Scenario 2d.7 conditions occurs in the SBBA. The increase in artificial recharge causes a decrease in streambed percolation, as streamflow is captured and recharged in basins instead (Figure 712). Streambed percolation decreases from 116,140 afy to 98,470 afy in the SBBA. Change in SBBA groundwater storage increases to 23,630 afy from 6,350 afy during the baseline Scenario 2a simulation. Underflow outflow to Rialto-Colton basin increases as well.

In Rialto-Colton, the increased artificial recharge causes a decrease in streambed percolation, an increase in underflow outflow to Riverside-Arlington, and an increase in groundwater storage by 1,600 afy (Figure 713). The increase in artificial recharge also results in a decrease in streambed percolation in Riverside-Arlington, along with an increase in underflow from Riverside-Arlington to Chino Basin, and less of a decline in Riverside-Arlington Basin groundwater storage.

In Chino Basin and Prado Basin, the water budgets remain very similar to Scenario 2a (Figures 715 and 717).

10.23 Scenario 2e.1: IEUA Stormflow Activities

10.23.1 General Assumptions

Scenario 2e runs implement various combinations of IEUA covered activities to assess the combined effects of the projects. Project impacts were evaluated by comparing individual model runs (with operation of selected HCP Covered Activities) to results from the baseline model run (i.e., no HCP Covered Activities). The general assumptions for the Scenario 2e model runs are the same as those used for the Baseline Model Run (Scenario 2a; refer to Section 10.5). Differences from the baseline assumptions for each Scenario 2e run are discussed below.

10.23.2 HCP Covered Activities Implemented

Scenario 2e.1 implements IEUA’s stormflow activities. These activities are shown on Figure 718 and summarized in Table 10-22 below. The activities are described in Table 17 and in Section 10.2.

Table 10-22. HCP Activities (Scenario 2e.1)

Project ID	Activity	Type
IEUA.1.01	Wineville Basin (2010 RMPU)	Stormwater Capture
IEUA.1.02	Lower Day Basin (2010 RMPU)	Stormwater Capture
IEUA.1.03	San Sevaine Basin Cells 1-5 (2013 RMPU)	Stormwater Capture
IEUA.1.04	Victoria Basin Improvements (2013 RMPU)	Stormwater Capture
IEUA.1.05	Montclair Basin Cells 1-4 (2013 RMPU)	Stormwater Capture
IEUA.1.06	Jurupa Basin (2010 RMPU)	Stormwater Capture
IEUA.1.07	Declez Basin (2010 RMPU)	Stormwater Capture
IEUA.1.08	CSI Basin (2010 RMPU)	Stormwater Capture
IEUA.1.09	Ely Basin (2010 RMPU)	Stormwater Capture
IEUA.1.10	RP3 Basin (2010 RMPU)	Stormwater Capture
IEUA.1.11	Turner Basin (2010 RMPU)	Stormwater Capture
IEUA.1.12	East Declez Basin	Stormwater Capture

RMPU = Recharge Master Plan Update (WEI, 2013)

10.23.2.1 Surface Water Diversion

Stormwater capture projects in Chino Basin would increase stormwater diversion by 6,860 afy. Stormwater diversion would occur along various tributaries to the SAR and artificially recharge diverted water in stormwater basins. The annual increase in stormwater capture is shown in Figure 719.

10.23.2.2 Artificial Recharge

The annual change in artificial recharge from the baseline model (Scenario 2a) is also 6,860 afy (Figure 720). Stormwater diverted from tributaries in Chino Basin would be recharged in the associated recharge basins, so this volume corresponds with the additional volume diverted from SAR tributaries above.

10.23.2.3 Surface Water Discharge

No effluent discharge reduction activities occur in Scenario 2e.1.

10.23.3 Results

10.23.3.1 Evapotranspiration

ET for the entire Integrated SAR Model domain for Scenario 2e.1 is summarized in Figure 721. The change in ET for the entire model area, compared to baseline conditions, is shown on Figure 722 while seasonal

ET is shown on Figure 723. As shown, ET in the entire model area increased by approximately 170 afy as compared to baseline (Scenario 2a) conditions. The majority of this increase occurred in Chino Basin (including Prado Basin) as the result of higher groundwater levels due to Scenario 2e.1 artificial recharge activities. ET remains similar to baseline conditions elsewhere in the model area. The total ET under Scenario 2e.1 conditions for Prado Basin is shown on Figure 724. Figures 725 and 726 show the change in ET in Prado, compared to baseline conditions, and seasonal ET in Prado, respectively. In Prado, the increased stormwater spreading led to an increase in evapotranspiration of approximately 110 afy.

10.23.3.2 Groundwater Levels

Groundwater level hydrographs for selected wells are provided in Appendix S. Water levels in Chino Basin depart from baseline conditions slowly, developing 1 to 2 ft higher water levels from artificial recharge activities. Water levels in other observation locations outside of Chino Basin are coincident with basin water levels under baseline conditions.

10.23.3.3 Streamflow

Average streamflow at the main SAR gaging station locations (E St., MWD Crossing, and at Prado Dam) is shown on Figure 727 under baseline (Scenario 2a) and Scenario 2e.1 conditions. The distributions of monthly streamflow in the SAR at E St., MWD Crossing, and Prado Dam under Scenario 2a and Scenario 2e.1 conditions are shown on Figures 728 through 730. Streamflow at Prado Dam is reduced by an annual average of 8 cfs (Figure 727, Table 19). The exceedance plot shows differences at higher stormflows in Figure 730.

10.23.3.4 Rising Water

The amount of rising water for the scenario runs is summarized in Table 20 and shown annually on Figure 731. Rising water increases slightly over baseline conditions by 20 afy in Riverside-Arlington Basin and by 30 afy in Prado Basin.

10.23.3.5 Average Annual Water Budgets

Average annual water budgets under Scenario 2e.1 conditions are shown in Figures 732 through 738 for each groundwater basin and Prado. IEUA stormwater activities increase groundwater storage in Chino Basin by nearly 4,900 afy in response to increased stormwater capture. The rise in groundwater and reduced streamflow in this area also leads to a slight decrease in streambed percolation as well as increased ET (Figure 736).

10.24 Scenario 2e.2: All IEUA Activities

10.24.1 HCP Covered Activities Implemented

Scenario 2e.1 implements all of IEUA's stormflow activities and dry-weather diversion activities. These activities are shown on Figure 739 and summarized in Table 10-22 below. The activities are described in Table 17 and in Section 10.2.

Table 10-23. HCP Activities (Scenario 2e.2)

Project ID	Activity	Type
IEUA.1.01	Wineville Basin (2010 RMPU)	Stormwater Capture
IEUA.1.02	Lower Day Basin (2010 RMPU)	Stormwater Capture
IEUA.1.03	San Sevaine Basin Cells 1-5 (2013 RMPU)	Stormwater Capture
IEUA.1.04	Victoria Basin Improvements (2013 RMPU)	Stormwater Capture
IEUA.1.05	Montclair Basin Cells 1-4 (2013 RMPU)	Stormwater Capture
IEUA.1.06	Jurupa Basin (2010 RMPU)	Stormwater Capture
IEUA.1.07	Declez Basin (2010 RMPU)	Stormwater Capture
IEUA.1.08	CSI Basin (2010 RMPU)	Stormwater Capture
IEUA.1.09	Ely Basin (2010 RMPU)	Stormwater Capture
IEUA.1.10	RP3 Basin (2010 RMPU)	Stormwater Capture
IEUA.1.11	Turner Basin (2010 RMPU)	Stormwater Capture
IEUA.1.12	East Declez Basin	Stormwater Capture
IEUA.3.01	Cucamonga Creek Dry-Weather Flow Diversion to Regional Water Recycling Plant No. 1 Project	Dry-Weather Flow Capture
IEUA.3.02	Cucamonga Creek at Interstate 10 Dry-Weather Flow Diversion to Regional Water Recycling Plant No. 1 Project	Dry-Weather Flow Capture
IEUA.3.03	Chino Creek at Chino Hills Parkway Dry-Weather Flow Diversion to Carbon Canyon Water Recycling Facility Project	Dry-Weather Flow Capture
IEUA.3.04	Day Creek at Wineville Basin Outflow Diversion to Regional Water Recycling Plant No. 1 Project	Dry-Weather Flow Capture
IEUA.3.05	San Sevaine Creek Diversion to Regional Water Recycling Plant No. 1 Project	Dry-Weather Flow Capture
IEUA.3.06	Lower Deer Creek Diversion to Regional Water Recycling Plant No. 5 Project	Dry-Weather Flow Capture

Please note, the covered activity IEUA.4 (Inland Empire Utilities Agency Regional Wastewater Treatment Expansion) was developed later in the modeling process. As such, scenarios that were already completed (including Scenario 2e.2) were not rerun to incorporate this additional project.

10.24.1.1 Surface Water Diversion

Stormwater and dry-weather capture projects in Chino Basin would increase surface water diversion by 8,660 afy. Stormwater diversion would occur along various tributaries to the SAR and artificially recharge diverted water in stormwater basins. Dry-weather flows would be diverted during dry months to water treatment facilities. The annual increase in stormwater capture and dry-weather flow diversion is shown in Figure 740.

10.24.1.2 Artificial Recharge

The annual change in artificial recharge from the baseline model (Scenario 2a) is 6,860 afy (Figure 741). Stormwater diverted from tributaries in Chino Basin would be recharged in the associated recharge basins, so this volume corresponds with the additional volume diverted from SAR tributaries above without dry-weather flow diversions (1,800 afy).

10.24.1.3 Surface Water Discharge

No effluent discharge reduction activities occur in Scenario 2e.2.

10.24.2 Results

10.24.2.1 Evapotranspiration

ET for the entire Integrated SAR Model domain for Scenario 2e.2 is summarized in Figure 742. The change in ET for the entire model area, compared to baseline conditions, is shown on Figure 743 while seasonal ET is shown on Figure 744. As shown, ET in the entire model area increased by approximately 170 afy as compared to baseline (Scenario 2a) conditions. The majority of this increase occurred in Chino Basin (including Prado Basin) as the result of higher groundwater levels due to Scenario 2e.2 artificial recharge activities. ET remains similar to baseline conditions elsewhere in the model area. The total ET under Scenario 2e.2 conditions for Prado Basin is shown on Figure 745. Figures 746 and 747 show the change in ET in Prado, compared to baseline conditions, and seasonal ET in Prado, respectively. In Prado, the increased stormwater spreading led to an increase in evapotranspiration of approximately 100 afy.

10.24.2.2 Groundwater Levels

Groundwater level hydrographs are presented in Appendix S. Groundwater levels for Scenario 2e.2 are compared to Scenario 2a groundwater levels for reference. Groundwater levels along the SAR from selected wells are shown. In Chino Basin, an increase in water levels is apparent at both monitoring locations. Similar to 2e.1, the water levels at these locations increases to 1 to 2 ft by the end of the simulation period due to additional recharge in Chino Basin.

10.24.2.3 Streamflow

Average streamflow at the main SAR gaging station locations (E St., MWD Crossing, and at Prado Dam) is shown on Figure 748 under baseline (Scenario 2a) and Scenario 2e.2 conditions. The distributions of monthly streamflow in the SAR at E St., MWD Crossing, and Prado Dam under Scenario 2a and Scenario 2e.2 conditions are shown on Figures 749 through 751. Streamflow decreases by 11 cfs from baseline conditions at Prado Dam (Figure 748, Table 19). Upstream, streamflow at MWD Crossing and E St. is not affected by Scenario 2e.2 activities.

10.24.2.4 Rising Water

The amount of rising water for the scenario runs is summarized in Table 20 and shown annually on Figure 752. Rising water increases slightly over baseline conditions by 30 afy in Riverside-Arlington Basin and by 20 afy in Prado Basin.

10.24.2.5 Average Annual Water Budgets

Average annual water budgets under Scenario 2e.2 conditions are shown in Figures 753 through 759 for each groundwater basin and Prado. IEUA stormwater and dry-weather capture activities increase groundwater storage in Chino Basin by nearly 4,900 afy in response to increased stormwater capture. The rise in groundwater and reduced streamflow in this area also leads to a slight decrease in streambed percolation as well as increased ET (Figure 757).

10.25 Scenario 2f: Western's Victoria Recharge Basin Project

10.25.1 HCP Covered Activities Implemented

Scenario 2f evaluates Western's Arlington Basin Water Quality Improvement Project (Victoria Recharge Basin Project). This project is summarized in Table 10-24 below and shown in Figure 760. Additional project information is also provided in Table 17 and Section 10.2.

Table 10-24. HCP Activities (Scenario 2f)

Project ID	Activity	Type
West.6*	Arlington Basin Water Quality Improvement Project	Stormwater Capture

* Surface hydrology not connected to main stem of the SAR, but need to evaluate habitat effect(s) for covered species.

The general assumptions for Scenario 2f are the same as those used for the Baseline Model Run (Scenario 2a). Differences from the baseline assumptions are discussed below.

10.25.1.1 Surface Water Diversion

Scenario 2f evaluates artificial recharge in Victoria Basin, part of which comes from diverted stormwater. Annual change in stormwater diversion, compared to the baseline, is shown on Figure 761. In Riverside-Arlington Basin, stormwater diversion increases 300 afy over baseline diversion.

10.25.1.2 Artificial Recharge

The annual change in artificial recharge from the baseline model (Scenario 2a) is 2,150 afy (Figure 762). A portion of this recharge comes from diverted stormwater (300 afy). The remaining 1,850 afy of recharge comes from other sources (imported or recycled water).

10.25.1.3 Surface Water Discharge

No effluent discharge reduction activities occur in Scenario 2f.

10.25.2 Results

10.25.2.1 Evapotranspiration

ET for the entire Integrated SAR Model domain for Scenario 2f is summarized in Figure 763. The change in ET for the entire model area, compared to baseline conditions, is shown on Figure 764 while seasonal ET is shown on Figure 765. As shown, ET in the entire model area increased slightly (by 30 afy) as compared to baseline (Scenario 2a) conditions. This increase occurred in Riverside-Arlington Basin as the result of additional recharge in Victoria Basin. Elsewhere, ET is not significantly affected. The total ET under Scenario 2f conditions for Prado Basin is shown on Figure 766. Figures 767 and 768 show the change in ET in Prado, compared to baseline conditions, and seasonal ET in Prado, respectively.

10.25.2.2 Groundwater Levels

Groundwater level hydrographs for selected wells are provided in Appendix S. Scenario 2f groundwater levels are displayed with those calculated under baseline conditions for wells along the SAR. Groundwater levels are coincident with baseline condition water levels at the plotted wells along the SAR.

10.25.2.3 Streamflow

Average streamflow at the main SAR gaging station locations (E St., MWD Crossing, and at Prado Dam) is shown on Figure 769 under baseline (Scenario 2a) and Scenario 2f conditions. The distributions of monthly streamflow in the SAR at E St., MWD Crossing, and Prado Dam under Scenario 2a and Scenario 2f conditions are shown on Figures 770 through 772. Changes in streamflow are not evident in the exceedance plots at E St., MWD Crossing, or Prado Dam. The average annual flow is increased very slightly by 1 cfs at MWD Crossing, as shown in Figure 769 and Table 19.

10.25.2.4 Rising Water

The amount of rising water for the scenario runs is summarized in Table 20 and shown annually on Figure 773. Rising water increases by 190 afy in Riverside-Arlington Basin under Scenario 2f conditions, compared to the baseline (Scenario 2a).

10.25.2.5 Average Annual Water Budgets

Average annual water budgets under Scenario 2f conditions are shown in Figures 774 through 780 for each groundwater basin and Prado. Artificial recharge in Victoria Basin increases groundwater storage in the Riverside-Arlington Basin by approximately 1,370 afy. The rise in groundwater and reduced streamflow in this area also leads to increased ET and rising water in Riverside-Arlington (Figure 777).

10.26 Scenario 2g: Clean Water Factory – 5 MGD from Clean Water Factory to Redlands Basins (CWF + SNRC)

10.26.1 HCP Covered Activities Implemented

Scenario 2g implements discharge of 5 MGD of water from City of San Bernardino Municipal Water Department's (SBMWD's) Clean Water Factory (CWF) to Redlands Basins, along with SNRC activities. These projects are summarized in Table 10-25 below and shown on Figure 781. Additional project information is also provided in Table 17 and a description is included in Section 10.2.

Table 10-25. HCP Activities (Scenario 2g)

Project ID	Activity	Type
WD.1	SBMWD Recycled Water Project	Recycled Water
EV.4.01 - 4.03	Sterling Natural Resource Center (SNRC)	Recycled Water

The general assumptions for Scenario 2g are the same as those used for the Baseline Model Run (Scenario 2a). Differences from the baseline assumptions are discussed below.

10.26.1.1 Surface Water Diversion

No increases in surface water diversions would occur under Scenario 2g conditions.

10.26.1.2 Artificial Recharge

The annual change in artificial recharge from the baseline model (Scenario 2a) is 7,120 afy, which includes 1,520 afy of water discharged to Redlands Basins from the SNRC and 5,600 acre-ft/yr of water discharged to Redlands Basins from the CWF (Figure 782). In addition, 7,150 afy of in-channel recharge occurs along City Creek from SNRC discharges.

10.26.1.3 Surface Water Discharge

Both the CWF and SNRC reduce surface water discharges from RIX in Riverside Basin. Under Scenario 2g conditions, surface water discharge from RIX is reduced by 5 MGD (5,600 afy) by the CWF (Figure 782). Discharge is reduced by an additional 9,400 afy by the SNRC. SNRC water is discharged to City Creek during low flow conditions to enhance recharge and is discharged to Redlands Basin during high flow conditions. Surface water discharge to City Creek is approximately 7,430 afy. Of this, 7,150 afy percolates in City Creek while approximately 280 afy of SNRC discharge reaches the SAR (Figure 782). However, since this section of the SAR is typically dry, discharge that flows into the SAR will likely percolate before it can contribute to streamflow.

10.26.2 Results

10.26.2.1 Evapotranspiration

ET for the entire Integrated SAR Model domain for Scenario 2g is summarized in Figure 783. The change in ET for the entire model area, compared to baseline conditions, is shown on Figure 784 while seasonal ET is shown on Figure 785. As shown, ET in the entire model area decreased by approximately 540 afy as compared to baseline (Scenario 2a) conditions. The majority of this decrease occurred in Riverside-

Arlington Basin as the result of reduced discharge from RIX. ET in the SBBA increased due to the relocation of discharge to this location. ET in Prado Basin decreased by approximately 40 afy under Scenario 2g conditions. Elsewhere, ET is not significantly affected. The total ET under Scenario 2g conditions for Prado Basin is shown on Figure 786. Figures 787 and 788 show the change in ET in Prado, compared to baseline conditions, and seasonal ET in Prado, respectively.

10.26.2.2 Groundwater Levels

Groundwater level hydrographs for selected wells are provided in Appendix S. Water levels under Scenario 2g conditions are slightly lower in Riverside-Arlington downgradient of RIX and higher in the vicinity of the proposed SNRC facility and Redlands Basin. Elsewhere, at other monitoring locations presented, no changes in groundwater levels are observed in the groundwater level hydrographs.

10.26.2.3 Streamflow

Average streamflow at the main SAR gaging station locations (E St., MWD Crossing, and at Prado Dam) is shown on Figure 789 under baseline (Scenario 2a) and Scenario 2g conditions. The distributions of monthly streamflow in the SAR at E St., MWD Crossing, and Prado Dam under Scenario 2a and Scenario 2g conditions are shown on Figures 790 through 792. Table 19 shows a decline in average annual streamflow of 16 cfs at MWD Crossing and Prado Dam (see also Figure 789).

10.26.2.4 Rising Water

The amount of rising water for the scenario runs is summarized in Table 20 and shown annually on Figure 793. Rising water at MWD Crossing decreases by approximately 1,210 afy for Scenario 2g compared with the baseline condition. A minimal decrease in rising water (approximately 10 afy) is also observed at Prado under Scenario 2g conditions.

10.26.2.5 Average Annual Water Budgets

Average annual water budgets under Scenario 2g conditions are shown in Figures 794 through 800 for each groundwater basin and Prado. The relocation of wastewater to the SBBA from Riverside-Arlington Basin increases groundwater storage in the SBBA by nearly 12,700 afy (Figure 795). In Riverside-Arlington Basin, reduced streambed percolation and recharge from RIX discharge leads to a decrease in groundwater storage of approximately 400 afy compared to baseline conditions (Figure 797).

10.27 Scenario 2h: RIX Operational Scenarios

10.27.1 HCP Covered Activities Implemented

Scenarios 2h.1 through 2h.4 evaluate RIX operational alternatives as part of SBMWD's Recycled Water Project. The 2h scenarios also assume operation of the SNRC. These projects are summarized in Table 10-26 below and detailed RIX operations are shown on Figure 801. Additional project information is also provided in Table 17 and Section 10.2.

Table 10-26. HCP Activities (Scenarios 2h.1-2h.4)

Project ID	Activity	Type
WD.1	SBMWD Recycled Water Project	Recycled Water
EV.4.01 - 4.03	Sterling Natural Resource Center	Effluent Discharge Reduction / Recharge

Note: Scenarios 2h.1 and 2h.2 evaluate conservation measure alternatives to WD.1.

The operational alternatives included under Scenario 2h are summarized in Table 21. Scenario 2h.1 and 2h.2 model short-term operational scenarios (i.e., High-Pulse Event and Extended RIX Shutdown). Since the Integrated SAR Model has monthly stress periods, daily changes such as the ones assumed in Scenarios 2h.1 and 2h.2 are not well resolved at a monthly resolution. However, the analysis of a daily operational change can be informed by the effects of the long-term operational Scenarios 2h.3 and 2h.4, since the results will be comparable – depending on RIX pumping assumptions. In Scenario 2h.3, 18.5 MGD is discharged from RIX, including a 2.8 MGD over-extraction. In Scenario 2h.4, 18.5 MGD is discharged, including a 6 MGD over-extraction.

10.27.1.1 Surface Water Discharge

Figure 802 shows the change in recycled water discharge from Riverside-Arlington at RIX to SBBA under Scenario 2h.3 conditions, as a result of the RIX assumptions shown in Table 21 (including SNRC and CWF assumptions). Figure 803 shows a similar transfer for Scenario 2h.4.

10.27.1.2 Pumping

The annual change in RIX operational assumptions is shown in Figure 804 for Scenario 2h.3 and in Figure 805 for Scenario 2h.4. In Scenario 2h.3, RIX plant production is 18.5 MGD compared to 30.2 MGD in the baseline run. Inflow to the plant is 15.7 MGD, so the 18.5 MGD plant production represents a 2.8 MGD over-extraction (Figure 804). In Scenario 2h.4, RIX plant production is 18.5, but inflow to the plant is 12.5 MGD, 6 MGD over-extraction (Figure 805).

10.27.2 Results

10.27.2.1 Evapotranspiration

Evapotranspiration results for Scenario 2h.3 are shown in Figures 806 through 811. Average annual ET is reduced from Scenario 2a: Baseline by 490 afy, from 29,650 afy to 29,160 afy. The reduction in ET primarily occurs in Riverside-Arlington Basin as a result of reductions in RIX discharge. In Scenario 2h.4 (Figures 812 through 817), with a 6 MGD over-extraction, ET is further reduced to 28,950 afy, a -670 afy reduction in Riverside-Arlington Basin (Figure 812). ET at Prado is reduced by 40 afy in both Scenarios 2h.3 and 2h.4 (Figures 809 and 815).

10.27.2.2 Groundwater Levels

Groundwater level hydrographs for selected wells are provided in Appendix S. Scenario 2h.3 and Scenario 2h.4 groundwater levels are displayed with those calculated under baseline conditions for wells along the SAR. Groundwater levels are coincident with baseline condition water levels at Prado Basin along the SAR. Upstream, at Airport No. 2 and 1S/4W20H03 water levels were slightly higher due to the change in recycled water discharge (SNRC and CWF) versus the baseline. At 28th St, water levels were slightly lower.

10.27.2.3 Streamflow

Average streamflow at the main SAR gaging station locations (E St., MWD Crossing, and at Prado Dam) is shown on Figure 818 and Figure 819 under baseline (Scenario 2a) and Scenarios 2h.3 and 2h.4 conditions, respectively. The distributions of monthly streamflow in the SAR at E St., MWD Crossing, and Prado Dam under Scenario 2a and Scenarios 2h.3 and 2h.4 conditions are shown on Figures 820 through 822 and Figures 823 through 825. Changes in streamflow are occur due to the alteration of recycled water discharge with the implementation of SNRC and CWF and changes to RIX operations. Streamflow is reduced at Prado from 269 cfs to 255 cfs and 252 cfs for 2h.3 and 2h.4 (Table 19). There is a 3 cfs difference between Scenario 2h.3 and Scenario 2h.4 at MWD Crossing and Prado due to the differences in the amount of over-extraction.

10.27.2.4 Rising Water

The amount of rising water for the scenario runs is summarized in Table 20 and shown annually on Figures 826 and 827. Rising water in Riverside-Arlington Basin decreases by approximately 1,100 afy and 1,300 afy due to activities in Scenario 2h.3 and 2h.4, respectively, as compared to baseline (Scenario 2a) conditions.

10.27.2.5 Average Annual Water Budgets

Average annual water budgets under Scenarios 2h.3 and 2h.4 conditions are shown in Figures 828 through 834 for each groundwater basin and Prado. The changes in RIX operations result in reduced rising water in Riverside-Arlington Basin, reduced ET, and reduced streamflow downstream of RIX. There is also additional recharge in the SBBA due to the implementation of the SNRC and CWF.

10.28 Scenarios 4.1 through 4.3: Management Scenarios under Average Climate Assumptions

10.28.1 General Scenario 4 Assumptions

The purpose of Scenario 4 is to evaluate the various upstream water supply projects and determine whether they could result in rejected recharge and optimize storage and recovery. To overcome any rejected recharge, projects could be phased, or pumping could be added in strategic locations to optimize storage and recovery. Major assumptions are summarized below.

This section presents strategies and management actions that may be necessary to address shallow groundwater during average hydrologic conditions or land subsidence during prolonged drought. Also, under different hydrologic regimes, different actions may be required to address decline in water levels in the vicinity of Western Judgment Index Wells and 1961 Decree Index Wells. These differences and management actions during varying hydrologic regimes indicate potential management alternatives.

Major assumptions for Scenario 4 management runs are summarized below in Table 10-27.

Table 10-27. Scenario 4 Management Assumptions

Scenario	Hydrology		Management Activities						
			Upstream Basins including SBBA, Rialto-Colton Basin, and Riverside-Arlington Basin					Chino Basin	
	Time Period	Climate	Optimized Use of SWP Recharge	SWP Recharge	All HCP Covered Activities	Phasing of HCP Covered Activities	Adjusted Groundwater Pumping	All HCP Covered Activities	Adjusted Groundwater Pumping
4.1	1966-1990 (25 years)	Average	X				X	X	X
4.2					X		X	X	X
4.3				X		X	X	X	X
4.4	1999-2016 (18 years)	Prolonged Drought	X				X	X	X
4.5					X		X	X	X
4.6				X		X	X	X	X

10.28.1.1 Hydrologic Assumptions

The hydrologic base period for Scenarios 4.1, 4.2, and 4.3 is the period from January 1966 through December 1990. This 25-year period was chosen because it is consistent with the base period previously identified by the HCP Hydrology TAC (HCP base period). This period includes wet, dry, and average hydrological conditions and the average precipitation during this period is approximately the same as the long-term average (Figure 59).

The hydrologic base period for Scenarios 4.4, 4.5, and 4.6 is the period from January 1999 through December 2016. This period was selected to simulate prolonged drought conditions (Figure 59). The average precipitation is below average, as indicated by a declining trend of the cumulative departure from mean precipitation throughout the period. This period was selected to evaluate assumptions identical to Scenarios 4.1-4.3, but under a period of prolonged drought to evaluate how management actions would shift between the average and drought conditions.

10.28.1 Implementation of HCP Covered Activities

In the SBBA and Rialto-Colton Basins, the goal of the proposed HCP Covered Activities is to increase water supply. However, if it is determined through modeling that implementing all of the HCP Covered Activities would result in rejected recharge, water agencies may choose to implement less projects initially or could choose to increase groundwater pumping in strategic areas. Scenarios 4.1 and 4.4 consider a situation in which none of the upstream HCP Covered Activities will be modeled under average (base period) and prolonged drought hydrology, respectively, while Scenarios 4.2 and 4.5 assume implementation of all HCP Covered Activities. Results from these model runs will help determine potential phasing for projects based on a cost-benefit analysis.

10.28.1.1 Management Assumptions

In Scenarios 4.1 and 4.4, imported water recharge in the SBBA and Rialto-Colton Basin is optimized based on the constraints discussed below to determine how much imported water – delivered in the upper watershed – would result in rejected recharge, if any. In Scenario 4.2 and 4.5, all of the HCP Covered Activities are implemented to determine if rejected recharge will occur. Changes in groundwater pumping, or recovery, in Rialto-Colton, Riverside-Arlington, and Chino Basins are used to reduce water levels and reduce rejected recharge where necessary.

10.28.1.1.1 Adjustment of Imported Water Recharge

Results from the modeling scenarios will provide insight into whether or not utilization of all of the available SWP supplies would result in rejected recharge and how much imported water is necessary given the proposed HCP Covered Activities.

10.28.1.1.2 Adjustment of Pumping

Due to the increased storage provided by the HCP Covered Activities, pumping in all of the groundwater basins will likely be altered to make use of the additional water. For example, the Riverside North Aquifer Storage and Recovery Project in Riverside Basin will also provide additional groundwater. Due to the age of the Gage and Flume wellfields, replacement wells will likely be installed that would increase the ability to extract groundwater in these areas. Pumping thresholds in each basin were developed through iterative model runs in order to meet necessary water level requirements (which are discussed in the following section). Geoscience also worked with representative agencies within the TAC to determine future pumping volumes, locations, and prioritization in response to increased storage from the HCP Covered Activities.

10.28.1.1.3 Criteria Used to Evaluate and Determine Management Activities

In addition to evaluating general water balance terms regarding each basin's inflow, outflow, and change in storage, criteria used to evaluate and determine management activities include compliance with Western Judgement, Rialto 1961 Decree, Chino Basin Optimum Basin Management Program (OBMP) and Peace Agreement, and other metrics developed for the SBBA and Chino Basin.

10.28.1.1.4 Western Judgment

According to the 1969 Western Judgment, extractions from the Colton Basin Area and Riverside Basin Area shall be limited so as to maintain water levels at or above fall 1963 water levels for three index wells (i.e., Johnson 1, Flume 2, and Flume 5; see Figure 835). If the average lowest static water levels in these wells fall below 822.04 ft amsl, extraction for the Colton and Riverside Basin Areas can be transferred to the SBBA to the extent necessary to restore water levels to fall 1963 levels. The Judgment also stipulates that Valley District may provide replenishment water for the SBBA to offset these extractions. Scenario 4 modeling tracked the average water level for each of the scenario runs.

In addition to the water level and replenishment requirements of the Western Judgment, performance metrics for the SBBA include:

- Avoiding potential for liquefaction (maintaining water levels at depths greater or equal to 50 feet below ground surface in the Pressure Zone area of the SBBA),
- Avoiding rejected recharge and flow out of basin, and
- Avoiding potential for land subsidence (maintaining water levels above land subsidence thresholds).

10.28.1.1.5 Rialto 1961 Decree

In Rialto Basin, pumping rates for all wells within the 1961 Decree boundary are dependent on the average spring-high water level elevation in Rialto Basin Index Wells (i.e., Rialto No. 4, WVWD No. 11, and WVWD No. 16) as follows:

1) Unlimited pumping if the average spring-high water level is above 1,002.3 ft amsl;
2) Pumping as imposed by 1961 Decree if the average spring-high water level is between 969.7 ft amsl and 1,002.3 ft amsl; and
3) Pumping reduced by 1% for every foot the average spring-high water level is below 969.7 ft amsl, to a maximum of 50% (County of San Bernardino Superior Court, 1961).

These index wells are also shown on Figure 836. Scenario 4 modeling tracked the average spring-high water level for each of the scenario runs. Reductions in groundwater pumping were then applied progressively in iterations based on the following rules that govern pumping in Rialto Basin within the Decree boundary.

10.28.1.1.6 OBMP and Peace Agreement

In Chino Basin, groundwater production, replenishment, recharge, and storage are managed under the OBMP and Peace Agreement so that total storage within the basin ranges from 5,300,000 acre-ft (equal to the Operational Storage Requirement, or OSR, of the basin) to 5,800,000 acre-ft (representing the safe storage of the basin) (WEI, 2018). The difference between these two storage thresholds, known as the Safe Storage Capacity (SSC), represents the volume available for Storage and Recovery Programs – like the proposed HCP Covered Activities. The storage level in the Chino Basin was therefore tracked for each of the modeling scenarios.

10.28.2 Results

10.28.2.1 Western Judgment

Initial Western Judgment Index water level was corrected for the over-simulation bias observed at the end of the calibration period in the calibrated model. The over-simulation bias in the Western Judgment Index wells was a result of both a time shift between the end of the calibration period and the most current water levels and an over-simulation during the last five years of the calibration period simulation. This bias was removed to match the current index water levels for this assessment.

Index water level during average hydrologic conditions and forecasted 2040 pumping conditions results in Western Judgment Index Well average water levels below 822.04 ft. Hydrograph results for the Western Judgment Index Wells are shown in Figure 837.

Reductions in forecasted 2040 pumping are necessary to comply with the Western Judgment in Colton and Riverside Basin areas in Scenario 4.1. In this management scenario, pumping was reduced in production wells in the vicinity of the Western Judgment Index wells (Figure 838). The reduction in pumping totals 1,790 afy and amounts to a 10% reduction in pumping from these wells. The resulting increase in water level in Western Judgment Index wells is seen in Figure 837. This pumping is transferred amongst agency wells in the SBBA. A summary of pumping volume is shown in Table 10-28 and 10-29 (Section 10.28.2.6) for Scenario 4.1 and 4.2. While this pumping is transferred to the SBBA, reduction in pumping to avoid additional land subsidence in the Pressure Zone is necessary. This corresponding feedback indicates that transferring additional pumping to wells in the SBBA may be complicated by land subsidence thresholds.

Reductions in forecasted 2040 pumping were also necessary to comply with the Western Judgment in Scenario 4.2 (Figure 839). The reduction in pumping due to the Western Judgment is slightly less than Scenario 4.1, at 1,700 afy. The location of pumping increases/decreases under Scenario 4.2 conditions is shown on Figure 840. Additional decreases in pumping to comply with the Western Judgment may be necessary in both Scenario 4.1 and Scenario 4.2 based on the Index Water Levels in Figures 837 and 839.

10.28.2.2 1961 Decree

Figure 841 shows the resulting hydrographs from the initial iteration and iteration with adjusted Decree pumping for Scenario 4.1. For Scenario 4.2, Figure 842 shows the resulting hydrographs from both iterations. The implementation of HCP activities, particularly the Riverside North Aquifer Storage and Recovery Project, increases water levels as compared to the Scenario 4.1 alternative without this project.

10.28.2.3 Shallow Water Levels (Less than 50 Feet below Land Surface)

Shallow water levels less than 50 ft below land surface present management concerns, and areas of shallow groundwater as a result of additional artificial recharge raise the prospect of rejected recharge, or recharge in excess of the storage capacity of different areas in the groundwater basin. Figures 843 through 846 show areas where groundwater was shallower than 50 ft bgs. A wet period (March 1983) was selected to evaluate this criterion. In Scenario 4.1, a small area of shallow groundwater in the SBBA in the vicinity of the SAR is visible. This area increases slightly under the implementation of HCP activities in Scenario 4.2.

10.28.2.4 Water Levels Below Land Subsidence Thresholds

Water levels below the land subsidence threshold were also assessed at the end of a dry hydrologic period (September 1990 hydrology). The results are also shown in Figures 843 through 846. As a result of evaluation of this criterion, pumping was reduced by 4,161 afy in the Pressure Zone area within the SBBA. A map showing the location of the pumping increases and reductions is shown in Figures 838 for Scenario 4.1 and Figure 840 for Scenario 4.2. During average hydrology in Scenario 4.1, small areas of water levels below land subsidence thresholds are present. During Scenario 4.2, no areas are visible. Competing optimization goals are present when the Western Judgment mandates pumping transfers to SBBA and land subsidence threshold shows a need for pumping reductions in SBBA. Herein, these competing goals have been met by shifting the location of pumping away from areas that show land subsidence risk. When this risk is more widespread in Scenarios 4.4 and 4.5 during drought hydrology, it is more difficult to accommodate the transfer of additional pumping to the SBBA without impacting the land subsidence threshold.

10.28.2.5 Projected Change in Storage in Chino Basin

Change in storage in Chino Basin for the Scenario 4 runs is presented in Figure 847. Declines in groundwater storage under Scenario 4 conditions are generally higher than Scenario 2a Baseline declines because of increased pumping under 2040 pumping assumptions. The average change in storage with the assumed 2040 pumping condition in Scenarios 4.1 and 4.2 is approximately -14,200 afy and 14,500 afy, respectively (Figure 847).

10.28.2.6 Average Annual Water Budgets

Average annual water budgets for Scenarios 4.1 and 4.2 are shown on Figures 848 through 854. Pumping adjustments for Scenarios 4.1 and 4.2 are summarized in Tables 10-28 and 10-29 below. Pumping was reduced in the SBBA, Rialto-Colton, and Riverside-Arlington Basins by a total of -7,632 afy due to constraints on pumping from the 1961 Decree, Western Judgment, and the applied optimization criteria in the Pressure Zone of the SBBA. A slight increase (approximately 700 afy) in underflow outflow is observed in the SBBA water budget as a result of all HCP activity recharge between Scenarios 4.1 and 4.2.

Table 10-28. Pumping Adjustments: Scenario 4.1

Groundwater Basin	Scenario 4.1		
	Original Pumping	Adjusted Pumping	Difference (Adjusted - Original)
	acre-ft/yr		
SBBA	203,518	199,357	-4,161
Rialto-Colton	24,046	21,761	-2,285
Riverside-Arlington	73,138	71,952	-1,186
Total	**300,702**	**293,070**	**-7,632**

Table 10-29. Pumping Adjustments: Scenario 4.2

Groundwater Basin	Scenario 4.2		
	Original Pumping	Adjusted Pumping	Difference (Adjusted - Original)
	acre-ft/yr		
SBBA	203,518	206,994	3,476
Rialto Colton	24,046	23,456	-590
Riverside-Arlington	73,138	72,012	-1,126
Total	**300,702**	**302,463**	**1,760**

Groundwater ET figures for Scenarios 4.1 and 4.2 are presented on Figures 855 through 866. Streamflow results are presented in Figures 867 to 874 while rising water is presented on Figures 875 and 876.

10.29 Scenarios 4.4 through 4.6: Management Scenarios under Prolonged Drought

10.29.1 General Assumptions

Assumptions for Scenarios 4.4 through 4.6 are the same as those described in Section 10.28.1 above. In Scenario 4.4, imported water recharge in the SBBA and Rialto-Colton is optimized based on the constraints outlined in Section 10.28.1.1, to determine how much imported water, delivered in the upper watershed, would result in rejected recharge – if any – during drought hydrology. In Scenario 4.5, all of the HCP Covered Activities are implemented to determine if rejected recharge will occur during drought hydrology. Changes in groundwater pumping, or recovery, in Rialto-Colton, Riverside-Arlington, and Chino Basins were used to reduce water levels and reduce rejected recharge where necessary.

10.29.2 Results

10.29.2.1 Western Judgment

Pumping volumes in the Colton and Riverside Basin areas were assessed within the context of the Western Judgment. The location of the Western Judgment Index Wells is shown in Figure 835. Index water level during average hydrologic conditions and forecasted 2040 pumping conditions results in Western Judgment Index Well average water levels below 822.04 feet. Hydrograph results for the Western Judgment Index Wells are shown in Figures 877 and 878 for Scenarios 4.4 and 4.5, respectively.

Reductions in forecasted 2040 pumping are necessary to comply with the Western Judgment in Colton and Riverside Basin areas in Scenarios 4.4 and 4.5. In these management scenarios, pumping is reduced in production wells in the vicinity of Western Judgment Index wells (Figure 879 and 880). The reduction in pumping totals approximately 1,790 afy and amounts to a 10% reduction in pumping from these wells.

A summary of pumping volume is shown in Tables 10-30 and 10-31 (Section 10.29.2.6) for Scenarios 4.4 and 4.5. While this pumping is transferred to the SBBA, reduction in pumping to avoid additional land subsidence in the Pressure Zone is necessary. Drought condition hydrology (1999-2016) causes a general widespread decline in water levels in the SBBA and in Index well water levels.

10.29.2.2 1961 Decree

Figures 881 and 882 show the resulting hydrographs from iteration runs to address compliance with the 1961 Decree. The location of pumping increases and reductions is shown in Figures 879 and 880. The implementation of HCP activities, particularly the Riverside North Aquifer Storage and Recovery Project, increases water levels in Scenario 4.5.

10.29.2.3 Shallow Water Levels (Less than 50 Feet below Land Surface)

Under drought hydrologic conditions, widespread shallow groundwater is not a management concern (Figures 883 through 886).

10.29.2.4 Water Levels Below Land Subsidence Thresholds

In both Scenarios 4.4 and 4.5, widespread water level decline results in water levels below land subsidence thresholds (Figures 883 through 886). Figures 883 and 885 show the initial results and Figures 884 and 886 show the result with pumping reduction applied to wells in the Pressure Zone of the SBBA. The location of pumping increases and reductions is shown in Figures 879 and 880.

10.29.2.5 Projected Change in Storage in Chino Basin

Change in storage in Chino Basin for Scenario 4 scenarios is presented in Figure 847. Declines in groundwater storage under Scenario 4 conditions are generally higher than Scenario 2a Baseline declines because of increased pumping under 2040 pumping assumptions. The average change in storage with the assumed 2040 pumping condition in Scenarios 4.4 and 4.5 is approximately -19,000 afy (Figure 847).

10.29.2.6 Average Annual Water Budgets

Average annual water budgets for Scenarios 4.4 and 4.5 are shown in Figures 848 through 854. Pumping adjustments for Scenarios 4.4 and 4.5 are summarized in Tables 10-30 and 10-31 below. Pumping was reduced in the SBBA, Rialto-Colton, and Riverside-Arlington Basins by a total of -39,896 afy due to constraints on pumping from the 1961 Decree, Western Judgment, and the land subsidence threshold criteria in the Pressure Zone of the SBBA. Less of a pumping decrease is necessary if all HCP Covered Activities are implemented (Scenario 4.5). The primary reductions were necessary to meet the land subsidence threshold criteria in the SBBA during drought conditions. The Western Judgment Index water levels fall during drought conditions, indicating a transfer of pumping to SBBA may be necessary. However, particularly during drought conditions and in the Pressure Zone, pumping is being otherwise reduced. This may indicate a need to transfer pumping to other wells in the SBBA.

Table 10-30. Pumping Adjustments: Scenario 4.4

Groundwater Basin	Scenario 4.4		
	Original Pumping	Adjusted Pumping	Difference (Adjusted - Original)
	acre-ft/yr		
SBBA	205,464	168,921	-36,544
Rialto Colton	22,626	20,460	-2,167
Riverside-Arlington	73,708	72,523	-1,186
Total	**301,799**	**261,903**	**-39,896**

Table 10-31. Pumping Adjustments: Scenario 4.5

Groundwater Basin	Scenario 4.5		
	Original Pumping	Adjusted Pumping	Difference (Adjusted - Original)
	acre-ft/yr		
SBBA	205,464	168,712	-36,753
Rialto Colton	22,626	20,776	-1,850
Riverside-Arlington	73,708	72,523	-1,186
Total	**301,799**	**262,010**	**-39,789**

Groundwater ET figures for Scenarios 4.4 and 4.5 are presented in Figures 887 to 898. Streamflow results are presented in Figures 899 to 906 while rising water is shown 907 and 908.

10.30 Scenario Summary

Model scenario runs are presented individually above and changes in fluxes compared to the Scenario 2a baseline are assessed. Different combinations of HCP Covered Activities have been implemented, and comparative analysis between different individual scenarios is also utilized to isolate the effects of individual activities and hydrologic assumptions. Different groups of activities include:

- Scenario 1: Flow in the SAR
- Scenario 2a: Baseline

- Scenario 2b: All Projects, Varying Climate
- Scenario 2c: Baseflow Reduction Activities
- Scenario 2d: Stormflow Activities
- Scenario 2e: IEUA Activities
- Scenario 2f: Western's Victoria Recharge Basin
- Scenario 2g: Clean Water Factory – 5 MGD to Redlands Basins (CWF + SNRC)
- Scenario 2h: RIX Operational Scenarios
- Scenario 4: Management Runs

Summary results for streamflow and rising water from all scenarios are shown in Tables 20 and 21, respectively. The summary results are a compendium of results from TMs 5a, 5b, and 5c. Project scenario results are in the process of being finalized based on review by the TAC. TMs 5a and 5b have been reviewed and in some cases, updates have been advised by the TAC. These updates have been incorporated into TM 5c modeling, but may not be reflected in TM 5a and 5b scenario results from previous draft TMs. Also, as of the writing of this draft Summary Report, draft TM 5c is currently out for review by the TAC. Results for these three TMs will be finalized in the final Summary Report and compiled into unified summary tables.

10.30.1 Streamflow

Average streamflow results for each scenario can be viewed against a baseline with no activities or against similar scenarios to isolate individual projects or assumptions. In addition, results can be compared to historical averages at the top of the table. Streamflow in Scenario 2a is higher than the same hydrologic period historically. For climate change scenarios, Scenario 2b streamflow results show a 5 to 9 cfs reduction in average streamflow at Prado Dam due to climate change (Scenarios 2b.2 and 2b.3, respectively) and a 63 cfs reduction under All HCP Covered Activities conditions. Exceedance probability plots can be used to identify under which flow regimes (e.g., low vs. high) the reductions occur.

Baseflow reduction activities reduce or relocate recycled water discharges along the SAR. Scenario 2c alternatives assess different combinations of baseflow reduction activities. Scenarios 2c.1 through 2c.4 assume different combinations of City of San Bernardino and Rialto Baseflow Reductions activities (SNRC, CWF, and Rialto). Reduction in streamflow at Prado Dam from SNRC and San Bernardino Baseflow Reduction Activities in Scenario 2c.2 is 26 cfs. Rialto Baseflow Reduction under Scenario 2c.3 reduces streamflow by approximately 5 cfs. SNRC only accounts for a 12 cfs reduction at Prado Dam based on the results of Scenario 2c.4 (SNRC only). IEUA Baseflow Reduction activities (Scenario 2c.7) slightly reduce streamflow, by approximately 2 cfs.

Various combinations of stormflow activities are implemented in the 2d scenarios. Phased implementation of Valley District stormflow activities are assessed in Scenarios 2d.1 through 2d.4. These scenarios show decreases in average streamflow at Prado varying from 2 cfs to 6 cfs for the various activities. IEUA Stormflow activities (Scenario 2e.1) results in an 8 cfs decline in streamflow at Prado. Exceedance probability charts show the affected flow regimes. Scenario 2f (Western's Victoria Recharge Project) does not influence flows along the main stem of the SAR. Scenario 4 alternatives include varying hydrologic and management assumptions. Reductions in streamflow at Prado from these scenario runs range from 34 cfs to 77 cfs under various assumptions of covered activities and hydrology.

10.30.2 Rising Water

Rising water, similar to streamflow, is documented in Table 20. The results tabulated in TM 5a, 5b, and 5c are compiled herein. Rising water is shown for three primary areas of historical rising water including Yucaipa, Riverside-Arlington, and Prado. The results are compared with baseline values of rising water.

Under Scenario 2c.1 (SNRC + San Bernardino baseflow reduction + Rialto baseflow reduction) and Scenario 2c.2 (SNRC + San Bernardino baseflow reduction), baseflow reduction activities reduce rising water in Riverside-Arlington by 1,240 afy to 1,320 afy, due to the transference of recycled water discharge upstream, from RIX to City Creek and Redlands Basin. Scenario 2c.4, which implements SNRC only, shows a reduction in rising water in Riverside-Arlington of 710 afy.

Climate change alternatives Scenarios 2b.2 and 2b.3 with All HCP Covered Activities show rising water reductions of 1,670 afy and 2,020 afy, respectively. Approximately 440 afy of this reduction in the 2030 climate change alternative (Scenario 2b.2) and 790 afy in the 2070 climate change alternative (Scenario 2b.3) is due to climate change – as determined by comparing the rising water results with those from All HCP Covered Activities with No Climate Change (Scenario 2b.1).

RIX Operational Alternatives in Scenario 2h result in a decrease of rising water in Riverside-Arlington Basin of approximately 1,100 afy to 1,300 afy. The rising water results are most influenced by baseflow reduction activities as opposed to stormflow activities, which reduce higher flow regimes.

11.0 USES AND LIMITATIONS

The Integrated SAR Model was constructed as a management tool for the Upper Santa Ana Valley Basin to assess the effects of various projects, including the Habitat Conservation Plan "Covered Activities." As a management tool, the model is intended to be used to inform the decision-making process. An understanding of the intended uses of the model and limitations and uncertainties associated with modeling results is key to interpreting modeling results and informing the decision-making process.

The Integrated SAR Model has combined previous modeling efforts and knowledge base in the Upper Santa Ana Valley Basin into one model. The Integrated SAR Model added key components to the unified numerical model that were absent or not contiguous in previous models to allow the simulation of streamflow and evapotranspiration for the purpose of assessing the effect of various projects on flows and riparian habitat in the Upper Santa Ana River. Calibration of the model was conducted with a focus on time-history matching of streamflow and groundwater levels in Upper Santa Ana River.

11.1 Model Uses

The calibrated Integrated SAR Model forms the basis for scenario analyses conducted for baseline model simulations and project condition model simulations. Model results from scenarios with and without "Covered Activities" were used to isolate the effects of the streamflow diversions, effluent discharge reductions, and recharge activities. The comparison of water level and water budget results from project condition simulations and the baseline simulation reduces some of the uncertainty associated with the absolute model predicted values of groundwater level and streamflow. The results of the modeling scenarios provided in this report are meant to serve as an indication of anticipated effects from proposed HCP covered activities and should be verified with field observations. As outlined in the Draft Final Upper Santa Ana River Wash Habitat Conservation Plan (ICF, 2019), the HCP includes a compliance monitoring and reporting program to measure and respond to potential project impacts.

11.2 Non-Intended Model Uses

The model is not intended to exactly predict water levels or streamflow beyond a level that could be reasonably anticipated from the residual statistics. The goal of the calibration process is to minimize the difference between observed and simulated water levels and streamflow. Minimization of these errors through calibration should not be interpreted as an absence of uncertainty or error. Model calibration was directed at addressing observed biases in the model-simulated water levels and streamflow, and additional focus was placed on areas of interest in the vicinity of the Santa Ana River.

One goal of this report is to characterize the magnitude, spatial, and temporal distribution of residuals in the model. This information can guide future applications of the model and indicate if additional calibration in a given area of interest is warranted. As the model is applied in different applications, an assessment of the calibration and suitability for the intended purpose should be conducted prior to using the model.

11.3 Sources of Uncertainty

Sources of uncertainty in model come from several factors. The largest source of uncertainty comes from estimations of major water budget components, as the largest components have the most influence on the overall water balance. Inflows to the groundwater basin, like mountain front runoff, areal recharge, return flow, and underflow, were estimated using various modeling techniques or assumptions correlated with hydrologic conditions. Outflows, like groundwater pumping, are subject to uncertainty due to measurement and recording error (Figure 909).

Uncertainty exists in the spatial characterization of groundwater hydraulic properties like hydraulic conductivity and storativity. Typically, hydraulic properties are estimated from pumping test data/aquifer performance tests at point locations in the model domain. These observations are not distributed evenly vertically in the aquifer or laterally in the model domain. As a result of the previous observation, there is greater geologic uncertainty with depth and away from existing wells/test data.

These uncertainties combine to make predictions of water levels at the margin of the model domain difficult and prone to larger residuals (Figure 910). Some observed water levels are significantly higher than regional groundwater levels due to locally higher groundwater conditions or perched groundwater conditions. In addition, while effort was made to simulate geologic structure (e.g., faulting) based on the geologic understanding presented in Section 3.0, much of the subsurface geology is unknown. Buried stratigraphic folds and eroded land surfaces can have significant effect on groundwater flow. In areas where the geologic understanding is weaker (such as those areas shown on Figure 910), the simulation of the model may be less accurate – especially at depth where hydrogeologic data from boreholes are limited or absent.

12.0 FUTURE WORK

The Integrated SAR Model is the first integration of pre-existing, individual numerical groundwater (MODFLOW) models in the Upper Santa Ana River Basin. Future work with the Integrated SAR Model on additional applications is anticipated and ongoing refinement and improvement of areas of interest throughout the model is expected. Improvements or additional work in specific areas of interest can be incorporated back into the Integrated SAR Model.

12.1 Individual Models

Development of individual basin models from the larger Integrated SAR Model is an important next step in the development process. Individual models will be generated along the original boundary with updated boundary conditions to represent the underflow simulated by the Integrated SAR Model between adjacent groundwater basins. Depending upon the simulation needs of the project, running a more localized version of the model may save development and modeling time. These needs can be assessed on a project-by-project basis. Streamflow and riparian ET simulation capabilities, as well as the ability to resolve underflow inflow across basin boundaries, are key benefits of using the Integrated SAR model. Some projects with a smaller geographic area of interest may benefit from using a smaller individual version of the model.

12.2 Development of Solute Transport Model

Solute transport modeling capability in the Integrated SAR Model would help identify and manage water quality (e.g., TDS and TIN) in the Upper SAR. Parties in Chino Basin have expressed concern about developing this capability in Chino Basin since other calibrated models are already being used for water quality management in this area. Elsewhere in the Upper SAR, however, the model could provide insight on fate and transport of nutrients and TDS throughout the upper groundwater basin. Additional work on characterization of porosity and parameters for the fate and transport model may be necessary to add solute transport modeling capability.

12.3 Additional Calibration in the Yucaipa Groundwater Basin

The Yucaipa Groundwater Basin has complex hydrogeologic conditions that make flow modeling prone to higher residuals. The range of observed water levels in the basin is much larger than other groundwater basins. Internal faulting subdivides the basin into compartments with different water levels. In addition, some uncertainty in aquifer extent and thickness along the boundary with the SBBA exists and influences the magnitude of underflow to the SBBA. Additional improvement of the model in this area is possible through future work.

12.4 Refinement/Standardization of Flux Terms

Methodologies for determining various boundary conditions (e.g., areal recharge, return flow, mountain front runoff) vary by individual groundwater basin based on original model development. Creating unified methodologies for the estimation of various inflows to the groundwater system in the future could potentially improve uncertainties and resolve differences in the estimation methodologies.

13.0 SUMMARY

The Integrated SAR Model has combined previous modeling efforts and knowledge base in the Upper Santa Ana Valley Basin into one model. Existing models were updated with the appropriate resolution, or cell size, and orientation to match that of the Integrated SAR Model and were updated with hydrologic data that cover the model calibration period from January 1966 through December 2016. A model for the Chino Basin area was also developed based on the approach outlined by the previous model report (WEI, 2015). Each updated model was rerun individually to ensure the modeling results were consistent with the original existing models. The updated existing models were then incorporated into the Integrated SAR Model domain by developing unified model layers across the groundwater basin, based on the lithologic model of the area and hydrogeologic conceptual understanding. The Integrated SAR Model added key components to the unified numerical model that were absent or not contiguous in previous models to allow the simulation of streamflow and evapotranspiration for the purpose of assessing the effect of various projects on flows and riparian habitat in the Upper SAR.

Calibration of the Integrated SAR Model was conducted with a focus on time-history matching of streamflow and groundwater levels in Upper Santa Ana River. The Integrated SAR Model was successfully calibrated through an initial condition simulation for 1966 and a transient calibration from 1966 through 2016 using monthly stress periods. The calibrated model has a mean residual of -0.98 ft and an RMSE of 64.54 ft. The acceptable model calibration is also reflected by a relative error of 2.2% for the initial condition simulation and 1.8% for the transient calibration. Common modeling practice is to consider a good fit between measured and model-calculated water levels if the relative error is below 10% (Spitz and Moreno, 1996). Calibration is further supported with an R^2 value of 0.99. Results of the flow model calibration indicate that:

- Some areas within the model domain exhibit more error than others. In general, under-simulation of water levels at basin boundaries is more likely due to uncertainty regarding boundary inflows, model layer thickness and hydraulic properties, and the presence of perched groundwater conditions.

- Water level residuals show a generally random distribution in space, with higher residuals in the SBBA and Yucaipa Basin.

- Overall, the calibration results indicate that the standard of calibration achieved in the Integrated SAR Model is suitable for the scale and purpose for which it was developed. Of approximately 108,500 observations, over 41,000 (38%) fell within +/- 20 ft of the observed water level while over 79,000 (73%) fell within +/- 60 ft. Errors were found to be generally randomly distributed in space and time, with the exception of the anomalies noted herein.

- In contrast to the previous individual groundwater models, the Integrated SAR Model explicitly simulates underflow between adjacent groundwater basins for the first time. Model-calculated underflow from Yucaipa Basin to the SBBA averaged 8,180 acre-ft/yr, underflow from Bunker Hill Basin to Rialto-Colton Basin averaged 3,660 acre-ft/yr, underflow from Lytle Basin to Rialto-Colton Basin averaged 13,250 acre-ft/yr, underflow from Rialto-Colton to Riverside Basin averaged 16,490 acre-ft/yr, and underflow from Riverside to Chino Basin averaged 17,280 acre-ft/yr.

- In general, the Integrated SAR Model is able to reproduce similar streamflow dynamics seen in observed measurements. At the E Street gaging station, there is some tendency for the model to over-estimate streamflow later in the calibration and the model appears to slightly under-estimate streamflow at MWD Crossing.

- Many of the basin areas respond to changes in hydrologic conditions (i.e., wet and dry periods cause rises and declines in groundwater storage, respectively). Basin response to hydrology is greatest in the SBBA, and generally diminishes in basins with increasing distance from mountain front recharge sources.

- The Integrated SAR Model tends to over-estimate groundwater declines in the SBBA during the latter part of the model simulation period, likely due to the large amount of underflow from Lytle Basin to the Rialto-Colton Basin. This over-estimation in cumulative storage decline can be corrected through future work on the model calibration.

Model scenarios were conducted to assess the hydrologic response of the Upper SAR to various project activities, including streamflow diversions, recharge basins (new basins and modifications), effluent reductions, and new discharge locations. Specifically, the Integrated SAR Model scenarios evaluate the effects of proposed HCP covered activities and other basin management strategies on riparian habitat, groundwater levels, and streamflow. The scenario runs simulate various project effects individually or in combination to assess hydrologic responses in comparison to a baseline (no project) scenario. For each scenario run, model-predicted flow and groundwater impacts were evaluated, including water level and water budgets for each groundwater basin (e.g., evapotranspiration and underflow across each groundwater basin). Scenario results were compared to a baseline, no project condition simulation to estimate impacts attributable to individual HCP Covered Activities or combinations of HCP Covered Activities. In addition, this information was provided to the Environmental Impact Report (EIR) team for them to establish thresholds of significance.

The Integrated SAR Model was constructed as a management tool for the Upper Santa Ana Valley Basin to assess the effects of various projects, including the Habitat Conservation Plan “Covered Activities.” As a management tool, the model is intended to be used to inform the decision-making process. An understanding of the intended uses of the model and limitations and uncertainties associated with modeling results is key to interpreting modeling results and informing the decision-making process.

14.0 REFERENCES

A.A. Webb (Albert A. Webb Associates), 2016. 2015 Urban Water Management Plan. Prepared for Jurupa Community Services District, dated June 27, 2016.

AQUA TERRA Consultants, 2005. Hydrologic Modeling of the Calleguas Creek Watershed with the U.S. EPA Hydrologic Simulation Program – FORTRAN (HSPF) Final Report. Prepared for Larry Walker Associates, Ventura County Watershed Protection District, and Calleguas Creek Watershed Management Plan. March 10, 2005.

ASTM (American Society for Testing and Materials), 1996. D 5981-96: Standard Guide for Calibrating a Ground-Water Flow Model Application.

ASTM, 1993. D 5447-93: Standard Guide for Application of a Ground-Water Flow Model to a Site-Specific Problem.

CGS (California Geological Survey), 2002. California Geomorphic Provinces. CGS Note 36.

CGS, 2015. Peninsular Ranges Geomorphic Province. Geological Gems of California State Parks, Special Report 230, GeoGem Note 46.

City of Chino, 2016. 2015 Urban Water Management Plan. Dated September 2016.

City of Chino Hills, 2016. City of Chino Hills Urban Water Management Plan – 2015.

City of Norco, 2016. City of Norco Urban Water Management Plan – 2015. Dated July 1, 2016.

CivilTec (CivilTec Engineering, Inc.), 2016. Cucamonga Valley Water District 2015 Urban Water Management Plan. Prepared for Cucamonga Valley Water District, dated June 2016.

CWE, 2018. Cactus Basin 4 and 5: Water Supply Benefit Calculation. Draft. Prepared for San Bernardino County Flood Control, dated August 2.

Danskin, W.R., K.R. McPherson, and L.R. Woolfenden, 2006. Hydrology, Description of Computer Models, and Evaluation of Selected Water-Management Alternatives in the San Bernardino Area, California. U.S. Geological Survey Open-File Report 2005-1278, in cooperation with San Bernardino Valley Municipal Water District.

Donigian, A.S. 2002. Watershed Model Calibration and Validation: The HSPF Experience. AQUA TERRA Consultants.

Dutcher, L.C. and A.A. Garrett, 1963. Geologic and Hydrologic Features of the San Bernardino Basin Area, California, with Special Reference to Underflow across the San Jacinto Fault. Prepared in cooperation with San Bernardino County Flood Control District. U.S. Geological Survey Water Supply Paper 1419. Washington, D.C.: USGS.

DWR (State of California Department of Water Resources), 1955. Santa Ana River Investigation. DWR Bulletin 15, dated February.

Engel, B., D. Storm, M. White, and J.G. Arnold. 2007. A Hydrologic/Water Quality Model Application Protocol. Journal American Water Resources Association.

Environmental Simulations, Inc., 1999. Guide to Using Groundwater Vistas - Version 2.4. pp. 251.

Flint, L.E. and A.L. Flint, 2014. California Basin Characterization Model: A Dataset of Historical and Future Hydrologic Response to Climate Change: U.S. Geological Survey Data Release. Prepared in cooperation with the California Water Science Center, Pepperwood Foundation, University of California at Davis, and Southwest Climate Science Center.

French, J.J., 1999. Ground-Water Outflow from Chino Basin, Upper Santa Ana Valley, Southern California. U.S. Geological Survey Water Supply Paper 1999-G.

Geo-Logic (Geo-Logic Associates), 2014. County of San Bernardino Solid Waste Management Division Remedial Action Plan – Yucaipa Disposal Site, Yucaipa, California. Prepared for the County of San Bernardino and submitted to the California Regional Water Quality Control Board, Santa Ana Region. Dated September.

GEOSCIENCE (GEOSCIENCE Support Services, Inc.), 2020a. Upper Santa Ana River Integrated Model – TM No. 3: Model Calibration. Prepared for San Bernardino Valley Municipal Water District, dated February 11.

GEOSCIENCE, 2020b. Upper Santa Ana River Integrated Model – TM No. 5c: Predictive Scenario Results, Part 3. Draft. Prepared for San Bernardino Valley Municipal Water District, dated April 10.

GEOSCIENCE, 2019a. Upper Santa Ana River Integrated Model – TM No. 4: Major Assumptions of Predictive Scenarios. Prepared for San Bernardino Valley Municipal Water District, dated February 8.

GEOSCIENCE, 2019b. Upper Santa Ana River Integrated Model – TM No. 4b: Major Assumptions of Management Scenarios that Will Reduce, or Eliminate, Rejected Recharge Upstream and Optimize

Storage and Recovery. Draft. Prepared for San Bernardino Valley Municipal Water District, dated August 1.

GEOSCIENCE, 2019c. Upper Santa Ana River Integrated Model – TM No. 5a: Predictive Scenario Results, Part 1. Draft. Prepared for San Bernardino Valley Municipal Water District, dated January 31.

GEOSCIENCE, 2019d. Upper Santa Ana River Integrated Model – TM No. 5b: Predictive Scenario Results, Part 2. Draft. Prepared for San Bernardino Valley Municipal Water District, dated June 28.

GEOSCIENCE, 2019e. Santa Ana River Waste Load Allocation Model Update – Summary Report. Prepared for the Santa Ana Watershed Project Authority, dated November 12.

GEOSCIENCE, 2018a. Upper Santa Ana River Integrated Model – TM No. 1: Model Integration. Draft. Prepared for San Bernardino Valley Municipal Water District, dated March 16.

GEOSCIENCE, 2018b. Upper Santa Ana River Integrated Model – TM No. 2: Flow Model Calibration Plan. Draft. Prepared for San Bernardino Valley Municipal Water District, dated January 29.

GEOSCIENCE, 2018c. Upper Santa Ana River Integrated Model – Database Plan. Prepared for San Bernardino Valley Municipal Water District, dated March 21.

GEOSCIENCE, 2017. Calculation of Annual Water Budgets and Validation of Annual Change in Storage Using the Yucaipa Watershed and Groundwater Models – TM1: Model Calibration. Draft. Prepared for Yucaipa Valley Water District, dated July 28.

GEOSCIENCE, 2016. Addendum to Stormwater Flow and Capture Analysis – Active Recharge Project for the Tributaries of the Santa Ana River, San Bernardino Valley, California. Draft. Prepared for San Bernardino Valley Municipal Water District, dated March 31.

GEOSCIENCE, 2015. Development of a Joint Groundwater Model for the Rialto-Colton Groundwater Basin. Prepared for the San Bernardino Valley Municipal Water District, dated December 1.

GEOSCIENCE, 2014. Determination of the Usable Capacity and Safe Yield for Each Sub-Basin within the Yucaipa Basin Area. Prepared for San Bernardino Valley Municipal Water District in partnership with City of Redlands, San Gorgonio Pass Water Agency, South Mesa Water Company, Western Heights Water Company, City of Yucaipa, and Yucaipa Valley Water District, dated April 17.

GEOSCIENCE, 2013. Calculate and Forecast New Conservation for the Western-San Bernardino Watermaster. Prepared for San Bernardino Valley Municipal Water District and Western Municipal Water District, dated August 1.

GEOSCIENCE, 2012. Geophysical Survey Investigation for the Proposed Santa Ana River Recharge Basins. Prepared for San Bernardino Valley Municipal Water District, dated August 13.

GEOSCIENCE, 2009. San Bernardino Basin Area Refined Basin Flow Model and Solute Transport Model. Prepared for the San Bernardino Valley Municipal Water District, dated September 30.

Halford K.J. and E.L. Kuniansky, 2002. Documentation of Spreadsheets for the Analysis of Aquifer-Test and Slug-Test Data. U.S. Geological Survey Open-File Report 02-197.

Harbaugh, A.W, 2005. MODFLOW-2005, the U.S. Geological Survey Modular Ground-Water Model – The Ground-Water Flow Process: U.S. Geological Survey Techniques and Methods 6-A16.

ICF, 2019. Draft Final: Upper Santa Ana River Wash Habitat Conservation Plan. Prepared for San Bernardino Valley Water Conservation District, dated May 2019.

K&S (Krieger & Stewart Engineering Consultants), 2016. 2015 Urban Water Management Plan. Prepared for Rubidoux Community Services District, dated July 2016.

Karen E. Johnson, Water Resources Planning, 2016. Chino Basin Desalter Authority 2015 Urban Water Management Plan. Prepared for Chino Basin Desalter Authority, dated June 2016.

Kendrick, K.J., D.M. Morton, S.G. Wells, and R.W. Simpson, 2002. Spatial and Temporal Deformation along the Northern San Jacinto Fault, Southern California: Implications for Slip Rates. Bulletin of the Seismological Society of America, Vol. 92, No 7, pp2783-2802, dated October.

Kenny, M., 2011. Near surface fault rupture, stratigraphy and structural evaluation for the proposed Santa Ana River Recharge Project, Southeastern San Bernardino Valley, San Bernardino County, California. Letter to GEOSCIENCE Support Services, Inc., dated September 1.

KWC Engineers, 2016. 2015 Urban Water Management Plan. Prepared for City of Corona, dated July 2016.

Langenheim, V.E., R.C. Jachens, J.C. Matti, E. Hauksson, D.M. Morton, A. Christensen, 2005. Geophysical evidence for wedging in the San Gorgonio Pass structural knot, southern San Andreas fault zone, southern California. GSA Bulletin; November/December 2005; v. 117; no. 11/12; p. 1554–1572; doi: 10.1130/B25760.1.

Maddock, T., III, K.J. Baird, R.T. Hanson, W. Schmid, and H. Ajami, 2012. RIP-ET: A riparian evapotranspiration package for MODFLOW-2005: U.S. Geological Survey Techniques and Methods 6-A39, 76 p.

Matti, J.C. and S.E. Carson, 1991. Liquefaction Susceptibility in the San Bernardino Valley and Vicinity, Southern California – A Regional Evaluation. U.S. Geological Survey Bulletin 1898.

Matti, J.C., D.M. Morton, and V.E. Langenheim, 2015. Geologic and Geophysical Maps of the El Casco 7.5′ Quadrangle, Riverside County, Southern California, with Accompanying Geologic-Map Database. U.S. Geological Survey Open File Report 2010-1274.

McDonald, M.G., and A.W. Harbaugh, 1988. A Modular Three-Dimensional Finite-Difference Ground-Water Flow Model: U.S. Geological Survey Techniques of Water-Resources Investigations Book 6, Chapter A1, 586 p.

Morton, D.M., and F.K. Miller, 2006. Geologic Map of the San Bernardino and Santa Ana 30′ x 60′ Quadrangles, California. U.S. Geological Survey Open-File Report 2006-1217.

MVWD (Monte Vista Water District), 2016. Monte Vista Water District 2015 Urban Water Management Plan. Dated June 2016.

Niswonger, R.G., S. Panday, and M. Ibaraki, 2011. MODFLOW-NWT, a Newton Formulation of MODFLOW-2005: U.S. Geological Survey Techniques and Methods 6-A37.

Ontario Municipal Utilities Company, 2016. 2015 Urban Water Management Plan – City of Ontario. Dated July 2016.

Paulinski, S., 2012. Structural, Hydrogeologic Framework, and Textural Model of the Rialto-Colton Basin and the Chino and North Riverside Area. M.S. Thesis, California State University, Sacramento.

PRISM Climate Group, 2017. 30-Year Normal Precipitation (1981-2010). Oregon State University. http://prism.oregonstate.edu.

Reilly, T.E., and A.W. Harbaugh, 2004. Guidelines for Evaluating Ground-Water Flow Models. Scientific Investigations Report 2004-5038. U.S. Geological Survey: Reston, Virginia.

RMC, 2016. Eastern Municipal Water District 2015 Urban Water Management Plan. Prepared for Eastern Municipal Water District, dated June 2016.

RMC, 2016. 2015 Urban Water Management Plan Update. Prepared for Western Municipal Water District, dated June 2016.

SCAG (Southern California Association of Governments), 2015a. 2012 Land Use Data. Revised 2015. Available at: http://gisdata-scag.opendata.arcgis.com/datasets?t=Land%20Use.

Scheevel Engineering, 2018. Riverside North Aquifer Storage & Recovery – Operation & Maintenance Model Technical Memorandum. Draft. Prepared for GEOSCIENCE Support Services, Inc., dated December 16.

Soil Survey Staff, Natural Resources Conservation Service, United States Department of Agriculture. Soil Survey Geographic (SSURGO) Database for Aliso-San Onofre Subbasin, CA. Available online at http://www.arcgis.com/apps/OnePane/basicviewer/index.html?appid=a23eb436f6ec4ad69820 00dbaddea5ea. Accessed 08/16/2011.

Spitz, K. and J. Moreno, 1996. *A Practical Guide to Groundwater and Solute Transport Modeling*. Oxford University Press, Inc.

Stephenson, W.J., J.K. Odum, R.A. Williams, and M.L. Anderson, 2002. Delineation of Faulting and Basin Geometry along a Seismic Reflection Transect in Urbanized San Bernardino Valley, California. Bulletin of the Seismological Society of America, Vol. 92, No. 6, pp. 2504–2520, dated August.

USEPA (United States Environmental Protection Agency). 2000. EPA BASINS Technical Note 6 – Estimating Hydrology and Hydraulic Parameters for HSPF. EPA-823-R00-012. July 2000.

WEI (Wildermuth Environmental, Inc.), 2018. Storage Framework Investigation Final Report. Prepared for Chino Basin Watermaster, dated October 2018.

WEI, 2017. Annual Report of the Prado Basin Habitat Sustainability Committee – Water Year 2015/2016. Prepared for Inland Empire Utilities Agency and Chino Basin Watermaster. Dated July.

WEI, 2015. 2013 Chino Basin Groundwater Model Update and Recalculation of Safe Yield Pursuant to the Peace Agreement. Prepared for the Chino Basin Watermaster, dated October.

WEI, 2009. 2008 Santa Ana River Wasteload Allocation Model Report – 2004 Basin Plan Amendment Required Monitoring and Analyses. Prepared for the Basin Monitoring Program Task Force, dated May.

West Yost (West Yost Associates), 2017. 2015 Urban Water Management Plan. Prepared for San Gabriel Valley Water Company Fontana Water Company Division, dated June 2016 (amended December 2017).

Woolfenden and Kadhim, 1997. Geohydrology and Water Chemistry in the Rialto-Colton Basin, San Bernardino County, California. U.S. Geological Survey Water-Resources Investigation Report 97-4012. Prepared in cooperation with San Bernardino Valley Municipal Water District.

WRIME, 2010. Riverside-Arlington Basins Numerical Groundwater Model and Groundwater Management Plans (GWMPs) Development – Numerical Model Calibration, Validation, and Sensitivity Analysis. Prepared for Riverside Public Utilities and Western Municipal Water District.

WSC (Water Systems Consulting, Inc.), 2016. 2015 San Bernardino Valley Regional Urban Water Management Plan. Prepared for San Bernardino Valley Municipal Water District, East Valley Water District, City of Loma Linda, City of Redlands, City of San Bernardino Municipal Water Department, West Valley Water District, Yucaipa Valley Water District, City of Colton, City of Rialto, and Riverside Highland Water Company, dated June 2016.

WSC, 2016. 2015 Urban Water Management Plan. Prepared for Riverside Public Utilities Water Division, dated June 2016.

Zheng, C., M.C. Hill, G. Cao, R. Ma, 2012. MT3DMS: Model Use, Calibration, and Validation. American Society of Agricultural and Biological Engineers Vol 55(4):1549-1559, dated July.

GEOSCIENCE

GEOSCIENCE Support Services, Inc. | P (909) 451-6650 | F (909) 451-6638

620 Arrow Highway, Suite 2000, La Verne, CA 91750 | Mailing: P.O. Box 220, Claremont, CA 91711